LECTURES IN ELEMENTARY FLUID DYNAMICS:

Physics, Mathematics and Applications

J. M. McDonough

Departments of Mechanical Engineering and Mathematics

University of Kentucky, Lexington, KY 40506-0503

Contents

List of Figures

Chapter 1

Introduction

It takes little more than a brief look around for us to recognize that fluid dynamics is one of the most important of all areas of physics—life as we know it would not exist without fluids, and without the behavior that fluids exhibit. The air we breathe and the water we drink (and which makes up most of our body mass) are fluids. Motion of air keeps us comfortable in a warm room, and air provides the oxygen we need to sustain life. Similarly, most of our (liquid) body fluids are water based. And proper motion of these fluids within our bodies, even down to the cellular level, is essential to good health. It is clear that fluids are completely necessary for the support of carbon-based life forms.

But the study of biological systems is only one (and a very recent one) possible application of a knowledge of fluid dynamics. Fluids occur, and often dominate the physical phenomena, on all macroscopic (non-quantum) length scales of the known universe—from the mega-parsecs of galactic structure down to the micro and even nanoscales of biological cell activity. In a more practical setting, we easily see that fluids greatly influence our comfort (or lack thereof); they are involved in our transportation systems in many ways; they have an effect on our recreation (*e.g.*, basketballs and footballs are inflated with air) and entertainment (the sound from the speakers of a TV would not reach our ears in the absence of air), and even on our sleep (water beds!).

From this it is fairly easy to see that engineers must have at least a working knowledge of fluid behavior to accurately analyze many, if not most, of the systems they will encounter. It is the goal of these lecture notes to help students in this process of gaining an understanding of, and an appreciation for, fluid motion—what can be done with it, what it might do to you, how to analyze and predict it. In this introductory chapter we will begin by further stressing the importance of fluid dynamics by providing specific examples from both the pure sciences and from technology in which knowledge of this field is essential to an understanding of the physical phenomena (and, hence, the beginnings of a predictive capability—*e.g.*, the weather) and/or the ability to design and control devices such as internal combustion engines. We then describe three main approaches to the study of fluid dynamics: *i)* theoretical, *ii)* experimental and *iii)* computational; and we note (and justify) that of these theory will be emphasized in the present lectures.

1.1   Importance of Fluids

We have already emphasized the overall importance of fluids in a general way, and here we will augment that with a number of specific examples. We will somewhat arbitrarily classify these in two main categories: *i)* physical and natural science, and *ii)* technology. Clearly, the second of these is often of more interest to an engineering student, but in the modern era of emphasis

on interdisciplinary studies, the more scientific and mathematical aspects of fluid phenomena are becoming increasingly important.

1.1.1 Fluids in the pure sciences

The following list, which is by no means all inclusive, provides some examples of fluid phenomena often studied by physicists, astronomers, biologists and others who do not necessarily deal in the design and analysis of devices. The accompanying figures highlight some of these areas.

1. Atmospheric sciences

    (a) global circulation: long-range weather prediction; analysis of climate change (global warming)
    (b) mesoscale weather patterns: short-range weather prediction; tornado and hurricane warnings; pollutant transport

2. Oceanography

    (a) ocean circulation patterns: causes of El Niño, effects of ocean currents on the weather
    (b) effects of pollution

3. Geophysics

    (a) convection (thermally-driven fluid motion) in the earth's mantle: understanding of plate tectonics, earthquakes, volcanoes
    (b) convection in earth's molten core: production of the magnetic field

4. Astrophysics

    (a) galactic structure and clustering
    (b) stellar evolution—from formation by gravitational collapse to death as a supernovae, from which the basic elements are distributed throughout the universe, all via fluid motion

5. Biological sciences

    (a) circulatory and respiratory systems in animals
    (b) cellular processes

1.1.2 Fluids in technology

As in the previous case, we do not intend this list of technologically important applications of fluid dynamics to be exhaustive, but mainly to be representative. It is easily recognized that a complete listing of fluid applications would be nearly impossible simply because the presence of fluids in technological devices is ubiquitous. The following provide some particularly interesting and important examples from an engineering standpoint.

1. Internal combustion engines—all types of transportation systems

2. Turbojet, scramjet, rocket engines—aerospace propulsion systems

3. Waste disposal

    (a) chemical treatment
    (b) incineration
    (c) sewage transport and treatment

4. Pollution dispersal—in the atmosphere (smog); in rivers and oceans

5. Steam and gas turbines, and hydroelectric facilities for electric power generation

6. Pipelines

    (a) crude oil and natural gas transferral
    (b) irrigation facilities
    (c) office building and household plumbing

7. Fluid/structure interaction

    (a) design of tall buildings
    (b) continental shelf oil-drilling rigs
    (c) dams, bridges, etc.
    (d) aircraft and launch vehicle airframes and control systems

8. Heating, ventilating and air-conditioning (HVAC) systems

9. Cooling systems for high-density electronic devices—digital computers from PCs to supercomputers

10. Solar heat and geothermal heat utilization

11. Artificial hearts, kidney dialysis machines, insulin pumps
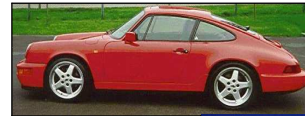
12. Manufacturing processes

   (a) spray painting automobiles, trucks, etc.
   (b) filling of containers, e.g., cans of soup, cartons of milk, plastic bottles of soda
   (c) operation of various hydraulic devices
   (d) chemical vapor deposition, drawing of synthetic fibers, wires, rods, etc.

1.2   The Study of Fluids

We begin by introducing the "intuitive notion" of what constitutes a fluid. As already indicated we are accustomed to being surrounded by fluids—both gases and liquids are fluids—and we deal with these in numerous forms on a daily basis. As a consequence, we have a fairly good intuition regarding what is, and is not, a fluid; in short we would probably simply say that a fluid is "anything that flows." This is actually a good practical view to take, most of the time. But we will later see that it leaves out some things that are fluids, and includes things that are not. So if we are to accurately analyze the behavior of fluids it will be necessary to have a more precise definition. This will be provided in the next chapter.

   It is interesting to note that the formal study of fluids began at least 500 hundred years ago with the work of Leonardo da Vinci, but obviously a basic practical understanding of the behavior of fluids was available much earlier, by the time of the ancient Egyptians; in fact, the homes of well-to-do Romans had flushing toilets not very different from those in modern 21st-Century houses, and the Roman aquaducts are still considered a tremendous engineering feat. Thus, already by the time of the Roman Empire enough practical information had been accumulated to permit quite sophisticated applications of fluid dynamics. The more modern understanding of fluid motion began several centuries ago with the work of L. Euler and the Bernoullis (father and son), and the equation we know as Bernoulli's equation (although this equation was probably deduced by someone other than a Bernoulli). The equations we will derive and study in these lectures were introduced by Navier in the 1820s, and the complete system of equations representing essentially all fluid motions were given by Stokes in the 1840s. These are now known as the *Navier–Stokes equations*, and they are of crucial importance in fluid dynamics.

   For most of the 19th and 20th Centuries there were two approaches to the study of fluid motion: theoretical and experimental. Many contributions to our understanding of fluid behavior were made through the years by both of these methods. But today, because of the power of modern digital computers, there is yet a third way to study fluid dynamics: computational fluid dynamics, or CFD for short. In modern industrial practice CFD is used more for fluid flow analyses than either theory or experiment. Most of what can be done theoretically has already been done, and experiments are generally difficult and expensive. As computing costs have continued to decrease, CFD has moved to the forefront in engineering analysis of fluid flow, and any student planning to work in the thermal-fluid sciences in an industrial setting must have an understanding of the basic practices of CFD if he/she is to be successful. But it is also important to understand that in order to do CFD one must have a fundamental understanding of fluid flow itself, from both the theoretical, mathematical side and from the practical, sometimes experimental, side. We will provide a brief introduction to each of these ways of studying fluid dynamics in the following subsections.

1.2.1   The theoretical approach

Theoretical studies of fluid dynamics generally require considerable simplifications of the equations of fluid motion discussed above. We present these equations here as a prelude to topics we will

consider in detail as the course proceeds. The version we give is somewhat simplified, but it is sufficient for our present purposes.

$$\nabla \cdot \boldsymbol{U} = 0\,,$$

$$\frac{D\boldsymbol{U}}{Dt} = -\nabla P + \frac{1}{Re}\nabla^2 \boldsymbol{U}\,.$$

These are the Navier–Stokes (N.–S.) equations of incompressible fluid flow. In these equations all quantities are dimensionless as we will discuss in detail later: $\boldsymbol{U} \equiv (u, v, w)^T$ is the velocity vector; P is pressure divided by (assumed constant) density, and Re is a dimensionless parameter known as the *Reynolds number*. We will later see that this is one of the most important parameters in fluid dynamics; indeed, considerable qualitative information about a flow field can be deduced by knowing its value.

In particular, one of the main efforts in theoretical analysis of fluid flow has always been to learn to predict changes in the qualitative nature of a flow as Re is increased. In general, this is a very difficult task far beyond the intended purpose of these lectures. But we mention it here to emphasize the importance of proficiency in applied mathematics in theoretical studies of fluid flow. From a physical point of view, with geometry of the flow situation fixed, a flow field generally becomes "more complicated" as Re increases. This is indicated by the accompanying time series of a velocity component for three different values of Re. In part (a) of the figure Re is low, and the flow ultimately becomes time independent. As the Reynolds number is increased to an intermediate value, the corresponding time series shown in part (b) of the figure is considerably complicated, but still with evidence of somewhat regular behavior. Finally, in part (c) is displayed the high-Re case in which the behavior appears to be random. We comment in passing that it is now known that this behavior is <u>not</u> random, but more appropriately termed *chaotic*.
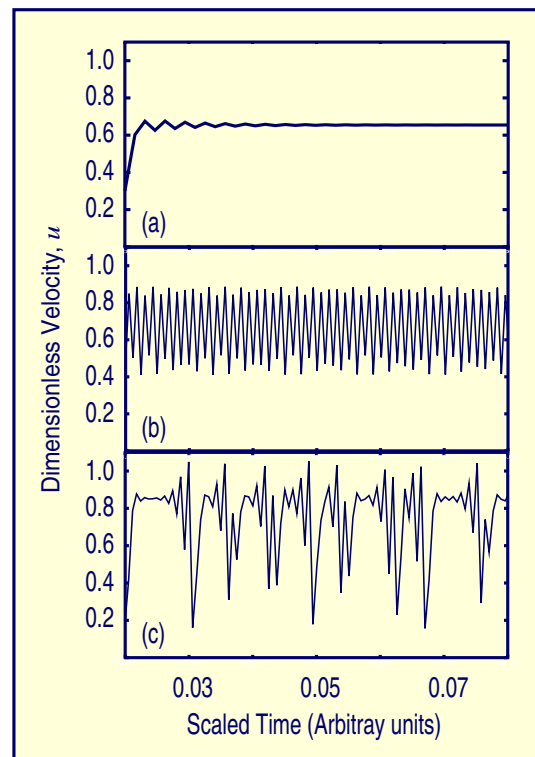
We also point out that the N.–S. equations are widely studied by mathematicians, and they are said to have been one of two main progenitors of 20th-Century mathematical analysis. (The other was the Schrödinger equation of quantum mechanics.) In the current era it is hoped that such mathematical analyses will shed some light on the problem of turbulent fluid flow, often termed "the last unsolved problem of classical mathematical physics." We will from time to time discuss turbulence in these lectures because most fluid flows are turbulent, and some understanding of it is essential for engineering analyses. But we will not attempt a rigorous treatment of this topic. Furthermore, it would not be be possible to employ the level of mathematics used by research mathematicians in their studies of the N.–S. equations. This is generally too difficult even for graduate students.

1.2.2   Experimental fluid dynamics

In a sense, experimental studies in fluid dynamics must be viewed as beginning when our earliest ancestors began to learn to swim, to use logs for transportation on rivers and later to develop a myriad assortment of containers, vessels, pottery, *etc.*, for storing liquids and later pouring and using them. Rather obviously, fluid experiments performed today in first-class fluids laboratories are far more sophisticated. Nevertheless, until only very recently the outcome of most fluids experiments was mainly a qualitative (and <u>not</u> quantitative) understanding of fluid motion. An indication of this is provided by the adjacent pictures of wind tunnel experiments.

In each of these we are able to discern quite detailed qualitative aspects of the flow over different prolate spheroids. Basic flow patterns are evident from colored streaks, even to the point of indications of flow "separation" and transition to turbulence. However, such diagnostics provide no information on actual flow velocity or pressure—the main quantities appearing in the theoretical equations.

There have long been methods for measuring pressure in a flow field, and these could be used simultaneously with the flow visualization of the above figures to gain some quantitative data. On the other hand, it has been possible to accurately measure flow velocity simultaneously over large areas of a flow field only recently. If point measurements are sufficient, then *hot-wire anemometry* (HWA) or *laser-doppler velocimetry* (LDV) can be used; but for field measurements it is necessary to employ some form of *particle image velocimetry* (PIV). The following figure shows an example of such a measurement for fluid between two co-axial cylinders with the inner one rotating.
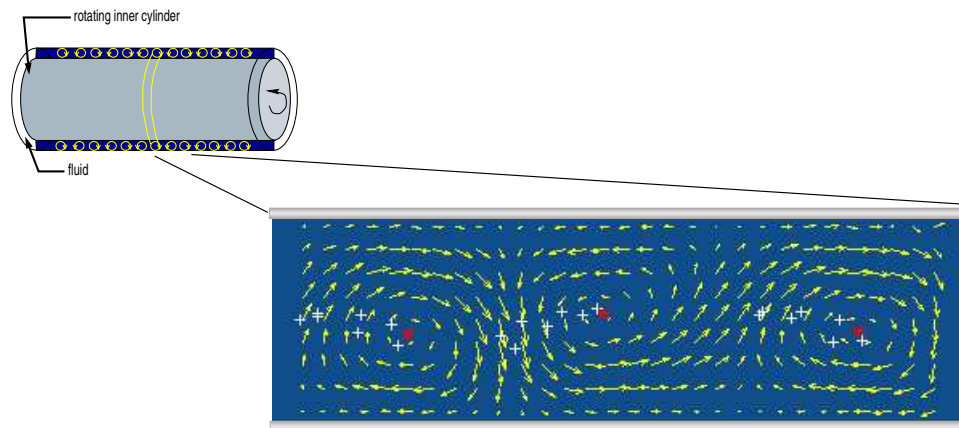
This corresponds to a two-dimensional slice through a long row of toroidally-shaped (donut-like) flow structures going into and coming out of the plane of the page. The arrows indicate flow direction in the plane; the red asterisks show the center of the "vortex," and the white pluses are locations at which detailed time series of flow velocity have been recorded. It is clear that this quantitative detail is far superior to the simple visualizations shown in the previous figures, and as a consequence PIV is rapidly becoming the preferred diagnostic in many flow situations.
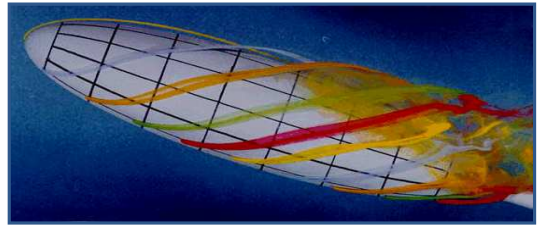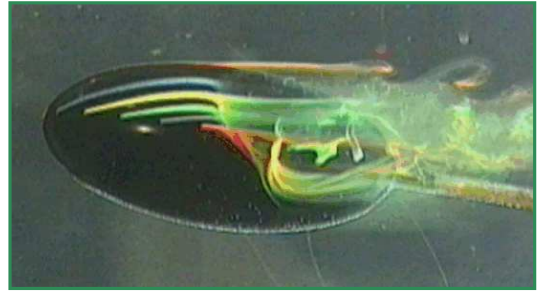
1.2.3   Computational fluid dynamics

We have already noted that CFD is rapidly becoming the dominant flow analysis technique, especially in industrial environments. The reader need only enter "CFD" in the search tool of any web browser to discover its prevalence. CFD codes are available from many commercial vendors and as "freeware" from government laboratories, and many of these codes can be implemented on anything from a PC to a parallel supercomputer. In fact, it is not difficult to find CFD codes that can be run over the internet from any typical browser. Here we display a few results produced by such codes to indicate the wide range of problems to which CFD has already been applied, and we will briefly describe some of the potential future areas for its use.

The figure in the lower left-hand corner provides a direct comparison with experimental results shown in an earlier figure. The computed flow patterns are very similar to those of the experiment, but in contrast to the experimental data the calculation provides not only visualization of qualitative flow features but also detailed quantitative output for all velocity component values and pressure, typically at on the order of 10^5 to 10^6 locations in the flow field. The upper left-hand figure displays predictions of the instantaneous flow field in the left ventricle of the human heart. Use of CFD in biomedical and bioengineering areas is still in its infancy, but there is little doubt that it will ultimately dominate all other analysis techniques in these areas because of its generality and flexibility.
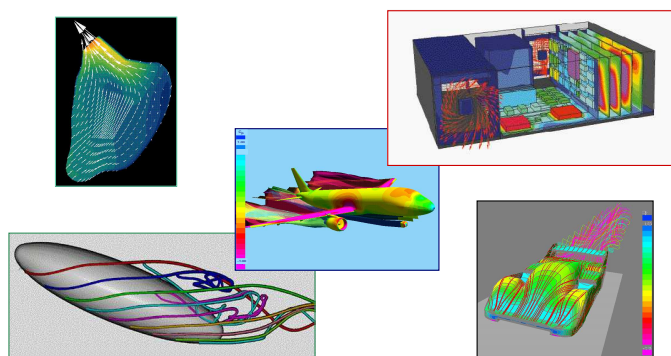
The center figure depicts the pressure field over the entire surface of an airliner (probably a Boeing 757) as obtained using CFD. It was the need to make such predictions for aircraft design that led to the development of CFD, initially in the U. S. aerospace industry and NASA laboratories, and CFD was the driving force behind the development of supercomputers. Calculations of the type shown here are routine today, but as recently as a decade ago they would have required months of CPU time.

The upper right-hand figure shows the temperature field and a portion (close to the fan) of the velocity field in a (not-so-modern) PC. This is a very important application of CFD simply because of the large number of PCs produced and sold every year worldwide. The basic design tradeoff is the following. For a given PC model it is necessary to employ a fan that can produce sufficient air flow to cool the computer by forced convection, maintaining temperatures within the operating limits of the various electronic devices throughout the PC. But effectiveness of forced convection cooling is strongly influenced by details of shape and arrangement of circuit boards, disk drives, *etc.* Moreover, power input to the fan(s), number of fans and their locations all are important design parameters that influence, among other things, the <u>unwanted noise</u> produced by the PC.

Finally, the lower right-hand figure shows pressure distribution and qualitative nature of the velocity field for flow over a race car, as computed using CFD. In recent years CFD has played an ever-increasing role in many areas of sports and athletics—from study and design of Olympic swimware to the design of a new type of golf ball providing significantly longer flight times, and thus driving distance (and currently banned by the PGA). The example of a race car also reflects current heavy use of CFD in numerous areas of automobile production ranging from the design of modern internal combustion engines exhibiting improved efficiency and reduced emissions to

various aspects of the manufacturing process, *per se*, including, for example, spray painting of the completed vehicles.

It is essential to recognize that a CFD computer code solves the Navier–Stokes equations, given earlier, and this is not a trivial undertaking—often even for seemingly easy physical problems. The user of such codes must understand the mathematics of these equations sufficiently well to be able to supply all required auxiliary data for any given problem, and he/she must have sufficient grasp of the basic physics of fluid flow to be able to assess the outcome of a calculation and decide, among other things, whether it is "physically reasonable"—and if not, what to do next.

1.3   Overview of Course

In this course mainly the theoretical aspects of fluid dynamics will be studied; it is simply not possible to cover all three facets of the subject of fluid dynamics in a single one-semester course meeting only three hours per week. At the same time, however, we will try at every opportunity to indicate how the theoretical topics we study impact both computational and experimental practice. Moreover, the approach to be taken in these lectures will be to emphasize the importance and utility of the "equations of fluid motion" (the Navier–Stokes equations). There has been a tendency in recent years to de-emphasize the use of these equations—at precisely a time when they should, instead, be emphasized. They are the underlying core of every CFD analysis tool, and failure to understand their physical origins and how to deal with their mathematical formulations will lead to serious deficiencies in a modern industrial setting where CFD is heavily used.

The equations of fluid motion (often simply termed "the governing equations") consist of a system of partial differential equations (as can be seen in an earlier section) which we will derive from basic physical and mathematical arguments very early in these lectures. Once we have these equations in hand, and understand the physics whence they came, we will be able to very efficiently attack a wide range of practical problems. But there is considerable physical and notational background needed before we can do this, and it is this material that will be emphasized in the second chapter of these lectures.

There are four main physical ideas that form the basis of fluid dynamics. These are: *i)* the continuum hypothesis, *ii)* conservation of mass, *iii)* balance of momentum (Newton's second law of motion) and *iv)* balance (conservation) of energy. The last of these is not needed in the description of some types of flows, as we will later see, and it will receive a less detailed treatment than items *ii)* and *iii)* which are crucial to all of what we will study in this course.

The remaining chapters of this set of lectures will contain the following material. In Chap. 2 we discuss the first of the main physical ideas noted above, provide a precise definition of a fluid, and then describe basic fluid properties, classifications and ways in which fluid flow can be visualized, *e.g.*, in laboratory experiments. Chapter 3 is devoted to a mathematical derivation of the Navier–Stokes equations starting from the fundamental physical laws given above. This is followed with further discussion of the physics embodied in these equations, but now in the context of a precise mathematical representation. We then consider "scaling" the N.–S. equations, *i.e.*, putting them in dimensionless form, and we study the corresponding dimensionless paramenters. Then in a final chapter we turn to applications, both "theoretical" and practical. In particular, we will study some of the simpler exact solutions to the N.–S. equations because these lead to deeper physical insights into the behavior of fluid motions, and we will also expend significant effort on such topics as engineering calculations of flow in pipes and ducts because of the practical importance of such analyses.

Chapter 2

Some Background: Basic Physics of Fluids

In the following sections we will begin with a discussion of the continuum hypothesis which is necessary to provide the framework in which essentially all analyses of fluids are conducted. We are then able to address the question of just what is a fluid, and how do fluids differ from things that are not fluids—solids, for example. We follow this with a section on fluid properties, and we then study ways by which fluid flows can be classified. Finally, we conclude the chapter with some discussions of flow visualization, *i.e.*, how we attempt to "see" fluid motion, either experimentally or computationally, in a way that will help us elucidate the physics associated with the fluid behavior.

2.1   The Continuum Hypothesis

As already indicated, in subsequent sections we will want to study various properties of fluids and details of their behavior. But before doing this we need to establish some underlying ideas that will allow our later developments to follow logically. In particular, we must be sure to understand, at a very fundamental level, just what we are working with when we analyze fluids (and also solids), because without this understanding it is easy to make very bad assumptions and approximations.

The most fundamental idea we will need is the *continuum hypothesis*. In simple terms this says that when dealing with fluids we can ignore the fact that they actually consist of billions of individual molecules (or atoms) in a rather small region, and instead treat the properties of that region as if it were a continuum. By appealing to this assumption we may treat any fluid property as varying continuously from one point to the next within the fluid; this clearly would not be possible without this hypothesis. We will state this more formally below after we have investigated in more detail just what are the implications of such an assumption.

Consider for example the velocity at a specific point in a fluid. If we forego the continuum hypothesis, the structure of the fluid consists of numerous atoms and/or molecules moving about more or less randomly; moreover, these will be relatively widely spaced, which we can quantify by the *mean free path*—the average distance a molecule travels between collisions with other molecules. In a gas at standard conditions, this distance is roughly 10 times greater than the distance between molecules, which is in turn about 10 times a molecular diameter. This is shown in Fig. 1(a). In Fig. 1(b) we show a small volume from this region containing a point at which we desire to know the velocity of the fluid. This volume is much smaller than the mean free path, and as a consequence it contains only a few molecules. Moreover, none is actually at the desired point, and they are all moving in different directions. It is clear that if we are to measure velocity (or any

other characteristic of the fluid) at the molecular scale we will obtain a result only at particular instances in time when a molecule is actually at the required location. Furthermore, it can be inferred from the figures that such measurements would exhibit a very erratic temporal behavior, and would likely be of little value for engineering analyses.
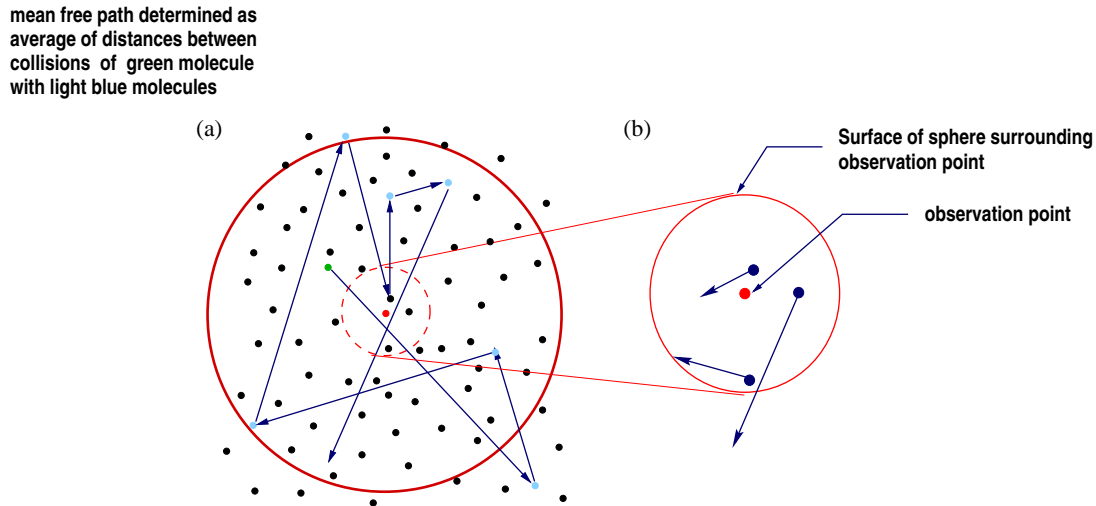
Figure 2.1: Mean Free Path and Requirements for Satisfaction of Continuum Hypothesis; (a) mean free path determined as average of distances between collisions; (b) a volume too small to permit averaging required for satisfaction of continuum hypothesis.

The remedy is to average the velocities of all molecules in a region surrounding the desired point, and use this result as the value at the point. But we know from the theory of statistical analysis that averaging over such a small sample as shown in Fig. 2.1(b) is not likely to provide a significant result. On the other hand, if we were to average over the volume contained in the large red sphere of Fig. 2.1(a) we would expect to obtain a representative value for the velocity at the desired point.

The conclusion we must draw from all this is that at a selected point, at any given instant, there will be no molecule, and consequently we have no way to define the velocity (or speed) of the fluid at that point. But if we can choose a neighborhood of the point that contains enough molecules to permit averaging (*i.e.*, its length scale is larger than the mean free path), and at the same time is small compared with the typical length scales of the problem under consideration, then the resulting average will be useful for engineering analyses. Furthermore, we can imagine continuously sliding this averaging volume through the fluid, thus obtaining a continuous function defined at every point for the velocity in particular, and in general for any flow properties to be treated in more detail in the sequel. This permits us to state the following general idea that we will employ throughout these lectures, often without specifically noting it.

Continuum Hypothesis. *We can associate with any volume of fluid, no matter how small (but greater than zero), those macroscopic properties (e.g., velocity, temperature, etc.) that we associate with the bulk fluid.*

This allows us to identify with each point a "fluid particle," or "fluid parcel," or "fluid element," (each with possibly its own set of properties, but which vary in a regular way, at least over short distances), and then consider the volume of fluid as a whole to be a continuous aggregation of these fluid particles.

To make this discussion more concrete we provide some specific examples. First, we consider air at standard sea-level temperature and pressure. In this situation, the number of molecules in a cubic meter is $\mathcal{O}(10^{25})$. If we consider a volume as small as a μm^3, *i.e.*, $(10^{-6}\text{m})^3 = 10^{-18}\,\text{m}^3$, there are still $\mathcal{O}(10^7)$ molecules in this region. Thus, meaningful averages can easily be computed. In fact, we can decrease the linear dimensions of our volume by nearly two orders of magnitude (nearly to nanoscales) before the number of molecules available for averaging would render the results unreliable. Thus, it is clear that sea-level air is a fluid satisfying the continuum hypothesis.

In contrast to this, consider a cube of volume $\mathcal{O}(10^{-6})$ cubic meters (*i.e.*, a centimeter on a side) at an altitude of 300 km. At any given instant there is only one chance in 10^8 of finding even a single molecule in this volume. Averaging of properties would be completely impossible even though the linear length scale is macroscopic, *viz.*, ~ 1 cm. Thus, in this case (low-Earth orbit altitudes) the continuum hypothesis is not valid.

It is interesting to note that while most analyses of fluid flow involve situations where the continuum hypothesis clearly is valid, there are cases for which it is not. Very high altitude, but suborbital, flight at altitudes to be accessed by the next generation of military aircraft is an example. But a more surprising one is flow on length scales in the micro and nano ranges. These are becoming increasingly important, and because the length scales of the devices being studied are only a few mean free paths of the fluids being used, the continuum hypothesis is often not valid. As a consequence, in these situations the analytical methods we will study in the present lectures must be drastically modified, or completely replaced.

2.2 Definition of a Fluid

We are now in a position to examine the physical behavior of fluids, and by so doing see how they differ from other forms of matter. This will lead us to a precise definition that does not suffer the deficiencies alluded to earlier.

2.2.1 Shear stress induced deformations

The characteristic that distinguishes a fluid from a solid is its inability to resist deformation under an applied shear stress (a tangential force per unit area). For example, if one were to impose a shear stress on a solid block of steel as depicted in Fig. 2.2(a), the block would not begin to change shape until an extreme amount of stress has been applied. But if we apply a shear stress to a fluid element, for example of water, we observe that no matter how small the stress, the fluid element deforms, as shown in Fig. 2.2(b) where the dashed lines indicate the vertical boundaries of the fluid element <u>before</u> application of the shear stress. Furthermore, the more stress that is applied, the
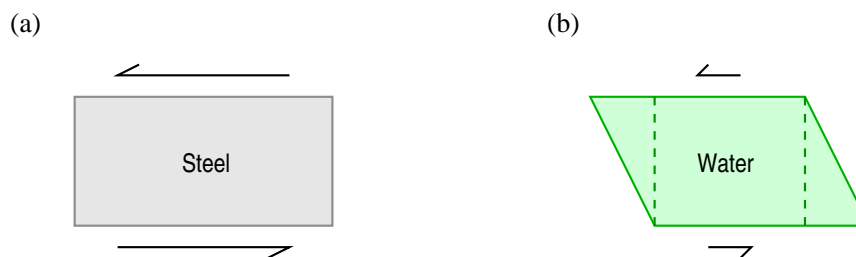
Figure 2.2: Comparison of deformation of solids and liquids under application of a shear stress; (a) solid, and (b) liquid.

more the fluid element will deform. This provides us with a characterizing feature of liquids (and gases—fluids, in general) that distinguishes them from other forms of matter, and we can thus give a formal definition.

Definition 2.1 *A _fluid_ is any substance that deforms continuously when subjected to a shear stress, no matter how small.*

We remark that continuous deformation under arbitrarily small shear stresses is <u>not</u> seen in a number of common substances that appear to "flow," for example, various household granular cooking ingredients such as sugar, salt, flour, many spices, *etc.* Clearly, any of these can be "poured," but their response to shear stress is very different from that of a fluid. To see this consider pouring a cup of sugar onto a table. If we do this carefully we will produce a pile of sugar having a nearly conical shape, as indicated in Fig. 2.3(a). If we were to analyze the outer surface

(b)   pool of coffee

(a)   pile of sugar
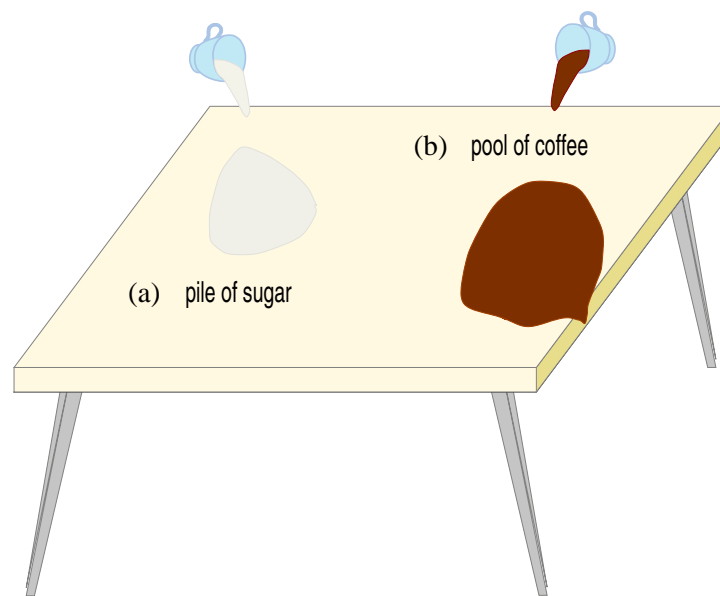
Figure 2.3: Behavior of things that "flow"; (a) granular sugar, and (b) coffee.

of this cone it would be seen that the grains of sugar on this surface must be supporting some shear stress induced by gravitational forces. But the shape of the pile is not changing—there is <u>no deformation</u>; hence, sugar is <u>not</u> a fluid, even though it flows.

By way of contrast, pour a cup of coffee onto the table. The coffee will spread across the surface of the table, as shown in Fig. 2.3(b), stopping only for somewhat detailed reasons we will be able to understand later. But in any case, it is clear that coffee cannot "pile up." The shear stresses induced by gravitational forces cannot be supported, and deformation occurs: coffee is a fluid.

We should note further that the "structure" of granular substances such as sugar is very different from that of fluids, as a little further investigation will show. Again, using sugar as a common example, it can be seen that there is a very different kind of interaction between pairs of small but <u>macroscopic</u> solid grains of sugar than occurs at microscopic levels for atoms and/or molecules (or even fluid parcels) of gases and liquids. In particular, among other differences is the very important one of sliding friction generated by the movement of grains of sugar past one another. This is the main reason such granular materials are able to support some shear stress without deforming.

2.2.2 More on shear stress

We will later need to be able to study forces acting on fluid elements, and shear stress will be very important in deriving the equations of fluid motion and later in the calculation of drag due to flow over submerged objects and flow resistance in pipes and ducts. Since shear stress is a (tangential) force per unit area, we can express this for a <u>finite</u> area A as

$$\bar{\tau} = \frac{F}{A} \, ,$$

where F is the applied tangential force. This is the *average shear stress* acting on the finite area A. But in the derivation and analysis of the differential equations describing fluid motion it is often necessary to consider shear stress <u>at a point</u>. The natural way to define this is

$$\tau = \lim_{\Delta A \to 0} \frac{\Delta F}{\Delta A} \, .$$

We note that this limit must be viewed in the context of the continuum hypothesis, and because of this the formal limit shown above must be replaced with $\Delta A \to \epsilon$, $\epsilon > 0$, where ϵ is sufficiently small to be negligible in comparison with macrosopic length scales squared.

2.3 Fluid Properties

Our next task is to consider various properties of fluids which to some extent permit us to distinguish one fluid from another, and they allow us to make estimates of physical behavior of any specific fluid. There are two main classes of properties to consider: transport properties and (other, general) physical properties. We will begin by considering three basic transport properties, namely viscosity, thermal conductivity and mass diffusivity; but we will not in these lectures place much emphasis on the latter two of these because they will not be needed. Following this, we will study basic physical properties such as density and pressure, both of which might also be viewed as thermodynamic properties, especially in the context of gases. Finally, we will briefly consider surface tension.

2.3.1 Viscosity

Our intuitive notion of viscosity should correspond to something like "internal friction." Viscous fluids tend to be gooey or sticky, indicating that fluid parcels do not slide past one another, or past solid surfaces, very readily. This can be an indication of some degree of internal molecular order, or possibly other effects on molecular scales; but in any case it implies a resistance to shear stresses. These observations lead us to the following definition.

Definition 2.2 *<u>Viscosity</u> is that fluid property by virtue of which a fluid offers resistance to shear stresses.*

At first glance this may seem to conflict with the earlier definition of a fluid (a substance that cannot resist deformation due to shear stresses), but resistance to shear stress, *per se*, simply implies that the <u>rate</u> of deformation may be limited. It does not mean that there is no deformation. In particular, we intuitively expect that water would deform more readily than honey if both were subjected to the same shear stress. Furthermore, our intuition would dictate that water and air would likely have relatively low viscosities while molasses and tar would exhibit rather large viscosity—at least if all were at standard temperature. Observations of this sort can be more precisely formulated in the following way.

Newton's Law of Viscosity. *For a given rate of angular deformation of a fluid, shear stress is directly proportional to viscosity.*

We remark that in some fluid mechanics texts this is stated as the definition of viscosity, but we will see later that there are fluids (termed "non-Newtonian") whose shear stress does not behave in this way.

The statement of Newton's law of viscosity may at first seem somewhat convoluted and difficult to relate to physical understanding of any of the quantities mentioned in it. We will attempt to remedy this by considering a specific physical situation that will permit a clear definition of "angular deformation rate" and physical intuition into how it is related to the other two quantities of this statement.

Flow Between Two Horizontal Plates with One in Motion

We consider flow between two horizontal parallel flat plates spaced a distance h apart, depicted in Fig. 2.4. We apply a tangential force F to the upper plate sufficient to move it at velocity U in the x direction, and study the resulting fluid motion between the plates.
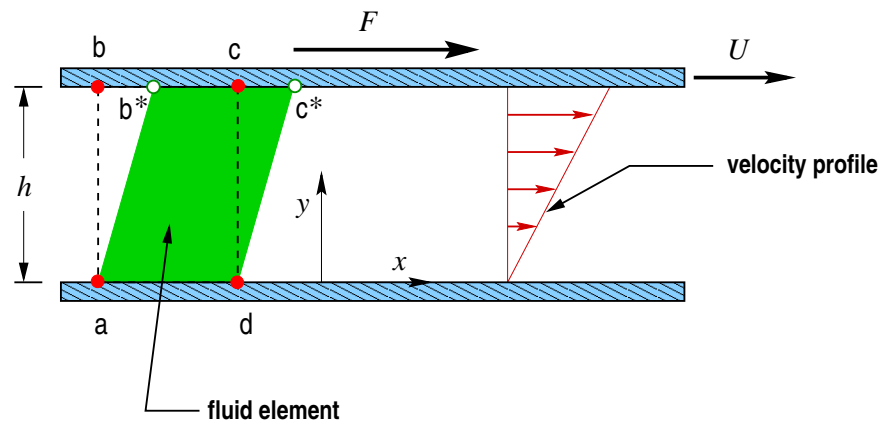
Figure 2.4: Flow between two horizontal, parallel plates with upper one moving with velocity U.

We first note the assumption that the plates are sufficiently large in the lateral extent that we can consider flow in the central region between the plates to be uneffected by "edge effects." We next consider the form of the *velocity profile* (the spatial distribution of velocity vectors) between the plates. At $y = 0$ the velocity is zero, and at $y = h$ it is U, the speed of the upper plate. The fact that it varies linearly at points in between the plates, as indicated in the figure, is not necessarily obvious and will be demonstrated in a later lecture. This detail is not crucial for the present discussion.

The first obvious question is "Why is the velocity zero at the stationary bottom plate, and equal to the speed of the moving top plate?" This is a consequence of what is called the *no-slip condition* for viscous fluids: it is an experimental observation that such fluids always take on the velocity of the surfaces to which they are adjacent. This is made plausible if we consider the detailed nature of <u>real surfaces</u> in contrast to perfectly-smooth ideal surfaces. Figure 2.5 presents a schematic of what is considered to be the physical situation. Real surfaces are actually very jagged on microscopic scales and, in fact, on scales sufficiently large to still accomodate the continuum hypothesis for typical fluids. In particular, this surface roughness permits parcels of fluid to be trapped and temporarily immobilized. Such a fluid parcel clearly has zero velocity with respect to
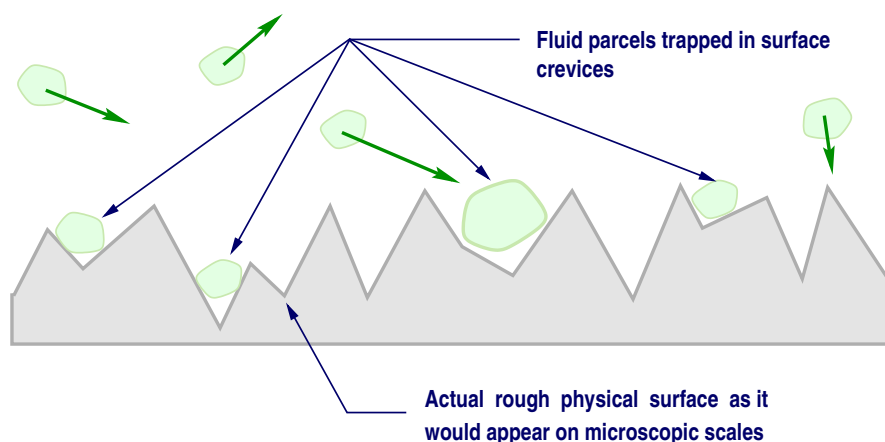
Figure 2.5: Physical situation giving rise to the no-slip condition.

the surface, but it is in this trapped state only momentarily before another fluid particle having sufficient momentum to dislodge it does so. It is then replaced by another fluid particle, which again has zero velocity with respect to the surface, and this constant exchange of fluid parcels at the solid surface gives rise to the zero surface velocity characterizing the no-slip condition.

Now that we have shown the top and bottom velocities to be plausible we can consider details of the shearing process caused by the moving upper plate. One interesting observation is that if when we apply the force F, the upper plate moves with a steady velocity no matter how small F is, we are guaranteed that the substance between the plates is a fluid (recall the definition of fluid). Referring back to Fig. 2.4, we see that the consequence of this is deformation of the region `abcd` to a new shape `ab*c*d` in a unit of time. Experiments show that the force needed to produce motion of the upper plate with speed U is proportional to the area of this plate, and to the speed U; furthermore, it is inversely proportional to the spacing between the plates, h. Thus,

$$F = \mu \frac{AU}{h} ,\tag{2.1}$$

with μ being the constant of proportionality.

Now recall that the (average) shear stress is defined by $\bar{\tau} = F/A$, so Eq. (2.1) becomes

$$\bar{\tau} = \mu \frac{U}{h} .$$

If we observe that U/h is the *angular velocity* of the line `ab` (check the units to see that this is the case) of Fig. 2.4, and hence the *rate of angular deformation* of the fluid, we see that this expression is a mathematical formulation of Newton's law of viscosity, with μ denoting viscosity.

It is also clear that if u is the velocity at any point in the fluid, as depicted in the velocity profile of Fig. 2.4, then

$$\frac{du}{dy} = \frac{U}{h} .$$

Hence, Newton's law of viscosity can be written in the more general, differential, form at any point of the fluid as

$$\tau = \mu \frac{du}{dy} .\tag{2.2}$$

It is important to note that Eq. (2.2) is not the most general one for shear stress, and we will encounter a more complete formulation later when deriving the Navier–Stokes equations.

Units of Viscosity

At this point it is useful to consider the units of viscosity. To do this we solve Eq. (2.1) for μ to obtain

$$\mu = \frac{Fh}{AU} \,.$$

We can now easily deduce the units of μ in terms of very common ones associated with force, distance, area and velocity.

We will usually employ "generalized" units in these lectures, leaving to the reader the task of translating these into a specific system, *e.g.*, the SI system of units. We will use the notation

$$
\begin{aligned}
T &\sim \ time \\
L &\sim \ length \\
F &\sim \ force \\
M &\sim \ mass \,.
\end{aligned}
$$

Now recall that velocity has units L/T in this formalism, so it follows that the units of viscosity are given by

$$\mu \sim \frac{F \cdot L}{L^2(L/T)} \sim \frac{F \cdot T}{L^2} \,.$$

In SI units this would be n·s/m^2; *i.e.*, Newton·seconds/square meter.

In many applications it is convenient to employ the combination viscosity/density, denoted ν:

$$\nu = \frac{\mu}{\rho} \,.$$

This is called the *kinematic* viscosity while μ is termed the *dynamic* viscosity. Since the (generalized) units for density are M/L^3, the units for kinematic viscosity are

$$\nu \sim \frac{F \cdot T/L^2}{M/L^3} \sim \frac{F \cdot T \cdot L}{M} \,.$$

But by Newton's second law of motion $F/M \sim acceleration \sim L/T^2$. Thus,

$$\nu \sim \frac{L^2}{T} \,,$$

or, again in SI units, m^2/s.

Physical Origins of Viscosity

Viscosity arises due to two main physical effects: intermolecular cohesion and transfer of molecular momentum. It should be expected that the former would be important (often dominant) in most liquids for which molecules are relatively densely packed, and the latter would be more important in gases in which the molecules are fairly far apart, but moving at high speed. These observations are useful in explaining the facts that the viscosity of a liquid <u>decreases</u> as temperature increases while that of a gas <u>increases</u> with increasing temperature.

First consider the liquid case, using water (H_2O) as an example. We know that the water molecule has a structure similar to that depicted in Fig. 2.6(a), *i.e.*, a polar molecule with weak intermolecular bonding due to the indicated charges. We also know that the kinetic energy and
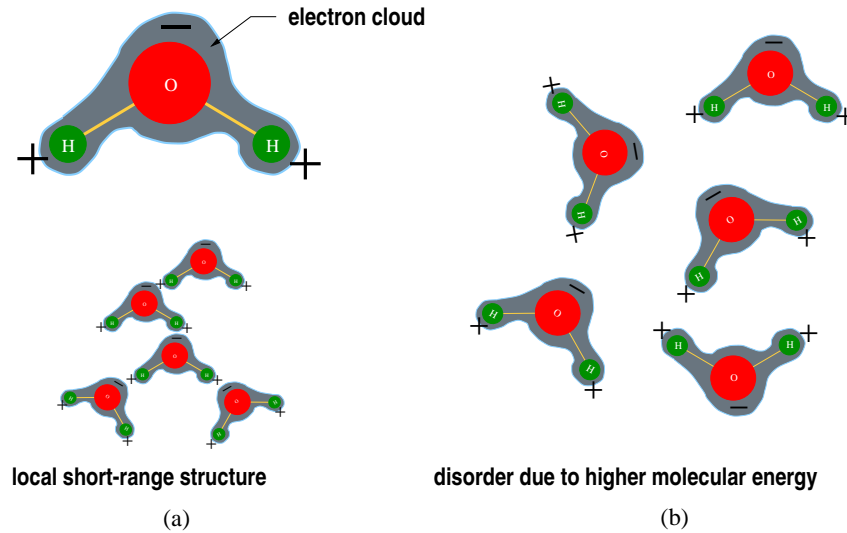
Figure 2.6: Structure of water molecule and effect of heating on short-range order in liquids; (a) low temperature, (b) higher temperature.

momentum increase with increasing temperature. Thus, at higher temperatures the forces available to break the polar bonds are much greater than at lower temperatures, and the local order shown in Fig. 2.6(a) is reduced (as indicated in Fig. 2.6(b)); so also is the "internal friction" reduced, and the liquid is then less viscous than at lower temperatures.

In the case of gases it is easiest to analyze a fixed-volume closed system as shown in Fig. 2.7. Figure 2.7(a) depicts the low-temperature situation, and from this it is easy to imagine that molecular collisions and hence, also intermolecular exchanges of momentum, are relatively infrequent. But increasing the temperature results in higher energy and momentum; moreover, because of the corresponding higher velocities any given molecule covers a greater distance, on average, in a unit of time, thus enhancing the probability of colliding with another molecule. Thus,
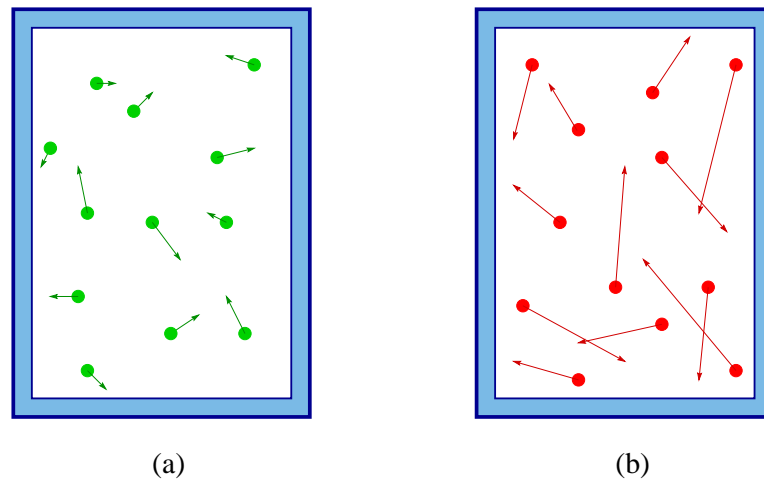
Figure 2.7: Effects of temperature on viscosity of gases; (a) low temperature, (b) higher temperature.

both the number of collisions and the momentum exchanged per collision increase with temperature in a gas, and it is known from the kinetic theory of gases that both of these factors result in increased viscosity.

Diffusion of Momentum

We know from basic physics that *diffusion* corresponds to "mixing" of two or more substances at the <u>molecular level</u>. For example, we can consider the (mass) diffusion of salt into fresh water and quantify the degree of mixing with the concentration of salt. But we can also analyze diffusion of energy and momentum in a similar way. We will later see, after we have derived the equations of fluid motion, that diffusion of momentum is one of the key physical processes taking place in fluid flow; moreover, it will be clear, mathematically, that viscosity is the transport property that mediates this process. Here we will provide a brief physical description of how this occurs.

We first note that by *diffusion of momentum* we simply mean mixing <u>on molecular scales</u> of a high-momentum portion of flow (and thus one of higher speed in the case of a single constant-temperature fluid) with a lower-momentum portion. The end result is a general "smoothing" of the velocity profiles such as were first shown in Fig. 2.4.

The physical description of this process is best understood by considering the initial transient leading to the velocity profile of that figure. In particular, let <u>both</u> plates in Fig. 2.4 have zero speed until time $t = 0^+$. Then at time $t = 0$ the fluid is motionless throughout the region between the plates. An instant later the top plate is impulsively set into motion with speed U, due to the tangential force F. At this instant the velocity profile will appear as in Fig. 2.8(a). The fluid
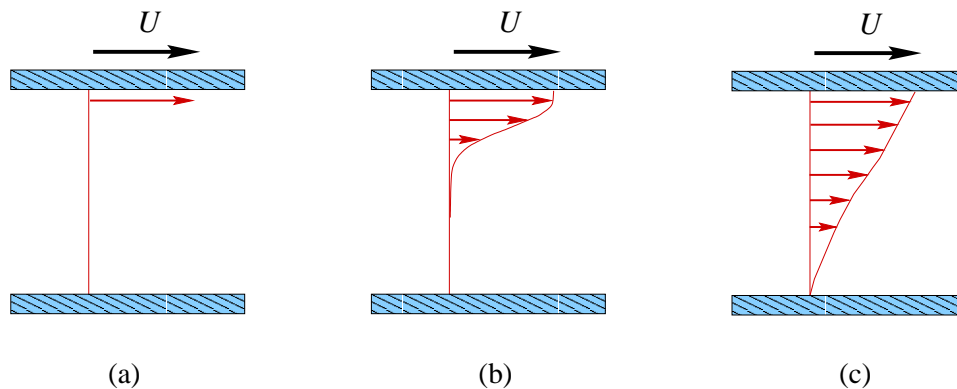
Figure 2.8: Diffusion of momentum—initial transient of flow between parallel plates; (a) very early transient, (b) intermediate time showing significant diffusion, (c) nearly steady-state profile.

velocity immediately adjacent to the top plate is that of the plate (by the no-slip condition), but it is zero at all other locations. (Notice that the velocity profile is very nonsmooth.) This does not, however, imply that the molecules making up the fluid have zero velocity, but only that when their velocities are averaged over a finite, but arbitrarily small, volume (continuum hypothesis, again!) this average is everywhere zero.

But high-momentum fluid parcels adjacent to the upper plate (recall Fig. 2.5) are colliding with zero-momentum parcels, and exchanging momentum with them. Thus, at a later time, but still quite soon after initiation of the motion, the velocity profile might appear as in Fig. 2.8(b). We see that high velocity (actually, momentum) has <u>diffused</u> away from the plate and into the interior of the fluid region. Figure 2.8(c) shows the continuation of this process at a still later time. Now

we can see that the velocity field is generally smooth and has nearly acquired the appearance of the linear profile of Fig. 2.4 except close to the bottom plate. When the flow attains its steady behavior the completely linear velocity profile will be seen.

There are still two main related questions that must be addressed with regard to diffusion of momentum. Namely, what exactly does all this have to do with viscosity, and are there observed differences in behavior between liquids and gases? We consider the first of these by again recalling our intuitive notion of viscosity—internal friction—and augmenting this with our new understanding of the physics of diffusion of momentum. We have seen that momentum diffuses due to interactions between molecules of relatively high-speed fluid parcels with those of relatively low-speed parcels, as depicted in Fig. 2.9. We should observe that in the context of this figure there is a velocity
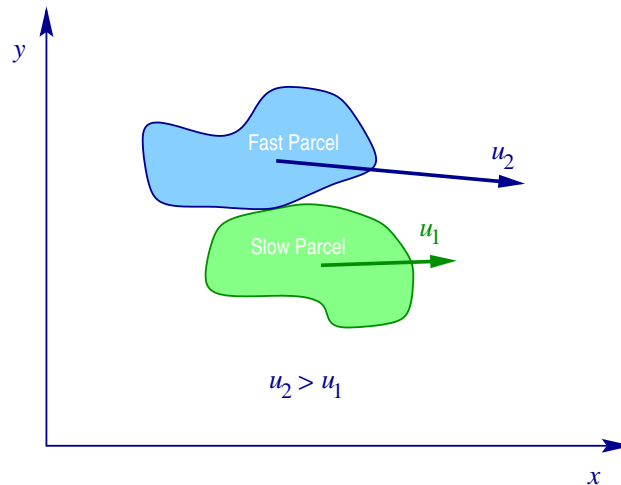
Figure 2.9: Interaction of high-speed and low-speed fluid parcels.

difference in the y direction since $u_2 > u_1$. Furthermore, at least a part of the momentum exchange between the two interacting parcels takes place in the tangential ($\sim x$) direction via a force generated by the shear stress.

Now we recall Newton's law of viscosity, Eq. (2.2),

$$\tau = \mu \frac{du}{dy} \, .$$

We can see that we have now "come full circle." We have shown that the shear stress associated with this formula is physically related to exchanges of momentum between fluid parcels "in contact" with one another, and thus exerting an internal frictional force. These parcels must be moving at different velocities to create the physical momentum exchange; at the same time this guarantees that the mathematical formulation embodied in Newton's law of viscosity has $du/dy \neq 0$, and thus $\tau \neq 0$. Also, we see that for fixed velocity difference $u_2 - u_1$, τ will increase with increasing viscosity μ, the constant of proportionality in Newton's law of viscosity.

Finally, we comment that the preceding discussion applies equally for all fluids—both liquids and gases, provided the continuum hypothesis has been satisfied. But at the same time, details of the behavior of μ will in fact differ, especially with respect to temperature, as we noted earlier.

Non-Newtonian Fluids

Before going on to a study of other properties of fluids it is worthwhile to note that not all fluids satisfy Newton's law of viscosity given in Eq. (2.2). In particular, in some fluids this simple linear relation must be replaced by a more complicated description. Some common examples are ketchup, various paints and polymers, blood and numerous others. It is beyond the intended scope of these lectures to treat such fluids in any detail, but the reader should be aware of their existence and the form of their representation.

It is common for the shear stress of non-Newtonian fluids to be expressed in terms of an empirical relation of the form

$$\tau = \mathcal{K} \left(\frac{du}{dy} \right)^n ,$$

where the exponent n is called the *flow behavior index*, and $\mathcal{K}$ is termed the *consistency index*. This representation is often called a "power law," and fluids whose shear stress can be accurately represented in this way are called *power-law fluids*. For more information on such fluids the reader is referred to more advanced texts and monographs on fluid dynamics.

2.3.2   Thermal conductivity

Thermal conductivity is the transport property that mediates the diffusion of heat through a substance in a manner analogous to that already discussed in considerable detail with respect to viscosity and momentum. We can associate heat with *thermal energy*, so thermal conductivity provides an indication of how quickly thermal energy diffuses through a medium. The basic formula representing this process is *Fourier's law of heat conduction* which is typically written in the form

$$q = -k \frac{dT}{dy} , \tag{2.3}$$

with q representing the heat flux (amount of heat per unit area per unit time), k is the thermal conductivity, and dT/dy is the component of the temperature gradient in the y direction—thus chosen to coincide with the velocity gradient component appearing in Newton's law of viscosity. It is evident that this formula is quite analogous to Newton's law of viscosity except for the minus sign; this sign convention is not necessary, but is widely used.

We remark that the behavior of k with respect to changes in temperature is very similar, at least qualitatively, to that of μ in the case of fluids; indeed, the underlying physics is the same for both properties. On the other hand, we do not consider viscosity of solids (until they become molten and then are no longer solid), but thermal conductivity in solids is an important property with rather different physical origins. We will not pursue this further in these lectures.

2.3.3   Mass diffusivity

The final transport property we introduce is the *mass diffusivity*. We alluded to this earlier in our discussion of salt diffusing into fresh water. As might by now be expected, the form of the mathematical expression and the underlying physics it represents are analogous to those already given for diffusion of momentum and thermal energy in the case of fluids. This is given by *Fick's law of diffusion*:

$$j_1 = -\rho \mathcal{D}_{12} \frac{dm_1}{dy} . \tag{2.4}$$

In this equation j_1 is the mass flux of species 1 whose mass fraction is m_1; ρ is density of the mixture of species 1 and 2, and $\mathcal{D}_{12}$ is the mass diffusivity of species 1 in species 2. As is the

case for thermal conductivity, mass diffusivity can be defined for all of liquids, gases and solids. Moreover, the physics of mass diffusion is significantly more complex than that of momentum diffusion, and we will not consider this herein.

2.3.4 Other fluid properties

In this section we will provide definitions and physical descriptions of various other fluid properties that are not transport properties. Essentially all of these should be at least somewhat familiar because they are all treated in elementary physics and thermodynamics courses. Thus, the discussions here will be considerably less detailed than was true for viscosity.

Density

We begin this section with the definition of *density*, ρ.

Definition 2.3 *The <u>density</u> of a fluid (or any other form of matter) is the amount of mass per unit volume.*

We first consider the average density of a <u>finite</u> volume of fluid, ΔV, and just as we did in the case of shear stress we apply a limit process in order to obtain the pointwise value of density. Hence, if Δm denotes the mass of the volume ΔV, the definition implies that

$$\bar{\rho} = \frac{\Delta m}{\Delta V} \, ,$$

and

$$\rho = \lim_{\Delta V \to 0} \frac{\Delta m}{\Delta V} \tag{2.5}$$

is the density <u>at a point</u> in the fluid. We again note that $\Delta V \to 0$ is formal and must be viewed within the context of the continuum hypothesis, as noted earlier.

In thermodynamics one often employs the *specific volume*, v, which is just the reciprocal of the density; hence, it is the volume occupied by a unit of mass. In this course we will seldom use this quantity and, in fact, the symbol v will usually denote the y-direction component of the velocity vector.

We close this section by recalling the units of density and specific volume. In the generalized unit notation introduced earlier these are

$$\rho \sim \frac{M}{L^3} \qquad \text{and} \qquad v \sim \frac{L^3}{M} \, ,$$

respectively.

Specific Weight and Specific Gravity

The two quantities we consider in this section are more often encountered in studies of fluid statics (often termed "hydrostatics") than in fluid dynamics. Nevertheless, for the sake of completeness we provide the following definitions and descriptions.

Definition 2.4 *The <u>specific weight</u>, γ, of a substance is its weight per unit volume.*

If we recall that weight is a force, equal to mass times acceleration, then it is clear that the definition implies

$$\gamma = \rho g \, , \tag{2.6}$$

where g is usually gravitational acceleration. But any acceleration could be used; for example, if it is required to analyze the behavior of propellants in orbiting spacecraft tanks during station-keeping maneuvers the factor g would be replaced by local acceleration induced by small thrusters of the spacecraft.

It is clear from the definition abd Eq. (2.6) that the generalized units of specific weight are

$$\gamma \sim \frac{F}{L^3}\,.$$

We also remark that Bernoulli's equation, to be studied later, is sometimes written in terms of specific weight. In addition, we note that the notation γ is often used in fluid dynamics for a very different quantity, the ratio of specific heats, c_p/c_v, usually denoted by k in thermodynamics texts. Nevertheless, the context of these symbols is usually clear, and no confusion results.

Definition 2.5 *The specific gravity, SG, of a substance is the ratio of its weight to that of an equal volume of water at a specified temperature, usually $4\,^{\circ}C$.*

Because SG is a ratio of weights, it is a dimensionless quantity and thus has no units.

Pressure and Surface Tension

In general, fluids exert both normal and tangential forces on surfaces with which they are in contact (*e.g.*, surfaces of containers and "surfaces" of adjacent fluid elements). We have already seen in our discussions of viscosity that tangential forces arise from shear stresses, which in turn are caused by relative motion of "layers of fluid." Pressure is the name given normal forces per unit area; *i.e.*,

Definition 2.6 *Pressure is the normal force per unit area in a fluid.*

As we have done with other fluid properties, we can define average pressure acting over a finite area ΔA as

$$\bar{p} = \frac{\Delta F_n}{\Delta A}\,,$$

where ΔF_n is the normal component of the force $\Delta \boldsymbol{F}$. Then the pressure at a point is given as

$$p = \lim_{\Delta A \to 0} \frac{\Delta F_n}{\Delta A}\,, \tag{2.7}$$

where, as usual, the limit process is viewed within the confines of the continuum hypothesis. It is clear from the definition that the units of pressure must be

$$p \sim \frac{F}{L^2}\,.$$

In Fig. 2.10 we display a qualitative summary of pressure and shear stress indicating their actions on the surface of a body submerged in a fluid flow. We note, however, that although the sketch is for flow over a surface and specifically shows pressure and shear stress at the surface, these same quantities are present everywhere in a fluid flow.

On molecular scales pressure arises from collisions of molecules with each other or with the walls of a container. From an engineering viewpoint we have seen in elementary physics classes that pressure results from the weight of fluid in a static situation (hydrostatics), but we will later see that fluid motion also leads to pressure—which should not be surprising since fluid motion
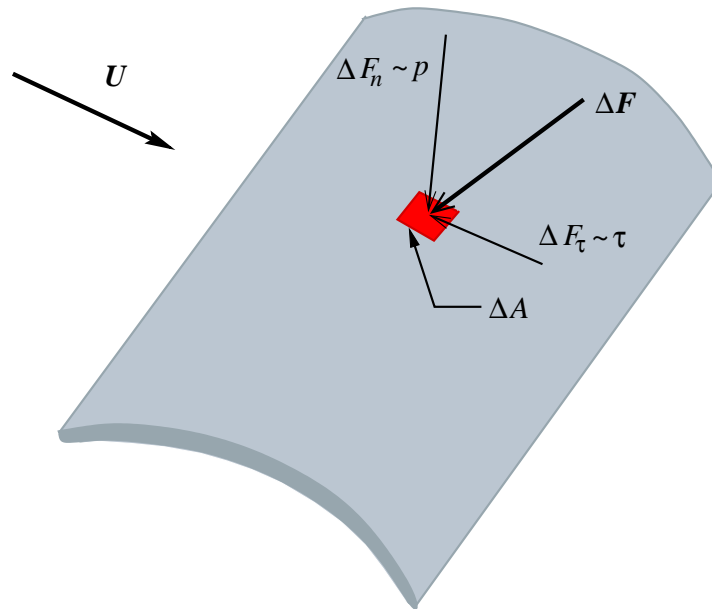
Figure 2.10: Pressure and shear stress.

is also required to produce shear stresses. We should also note that pressure in a gas always corresponds to a <u>compressive</u> force. On the other hand, while liquids are capable of sustaining very high compressive <u>normal</u> forces, they can also support weak tensile forces. Thus, in a gas pressure is always positive, but in a liquid it is possible for it to be negative. (We remark that this is another manifestation of intermolecular cohesive forces in liquids.)

The ability of liquids to support weak tensile forces is observed in fluid phenomena associated with *surface tension*. Surface tension arises at liquid-solid and liquid-gas interfaces, and in general at the interface between any two immiscible fluids. Although the detailed physics of surface tension is rather complicated, the basic notion is that at the interface what was a three-dimensional liquid (molecular) structure is disrupted and becomes a two-dimensional one. Thus, the molecular forces that are elsewhere distributed over three directions become concentrated into two directions at the interface, leading to an increase in pressure (which, by definition, is associated with area rather than volume).

Indeed, if we consider an idealized spherical droplet of, say water, in air shown in Fig. 2.11, we recognize from a force balance that without surface tension producing an increased pressure, the droplet would lose its shape. That is, the pressure of the liquid in the interior of the droplet (in mechanical equilibrium) would exactly equal the outer pressure of the air, and there would be no force opposing flattening of the droplet. But in the presence of surface tension the internal pressure at the surface is increased, and the droplet maintains its shape. This force balance leads to a simple formula relating the change in pressure across the interface to the surface tension:

$$\Delta p = \frac{2\sigma}{r} \, , \tag{2.8}$$

where σ is the surface tension. It is clear that the dimensions of surface tension are F/L. We note that Eq. (2.8) is valid only for spherical shapes; a slightly more complicated formula, which we shall not present here, is required for more general situations.
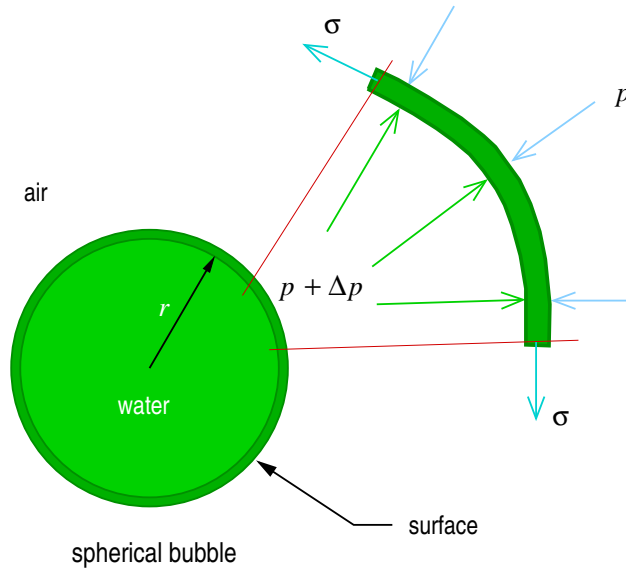
Figure 2.11: Surface tension in spherical water droplet.

An interesting example of the effects of surface tension can be found in wet sand. It is common experience that we cannot walk on water. But is also difficult to walk on dry sand. However, when we wet sand with water sufficiently to "activate" surface tension effects we can easily walk on the mixture.

Another surface tension effect is *capillarity*. The manifestation of this is the curved shape of liquid surfaces near the walls if a container having sufficiently small radius to make surface tension forces non-negligible. Fig. 2.12 displays this effect for two different cases. Details of the physics of
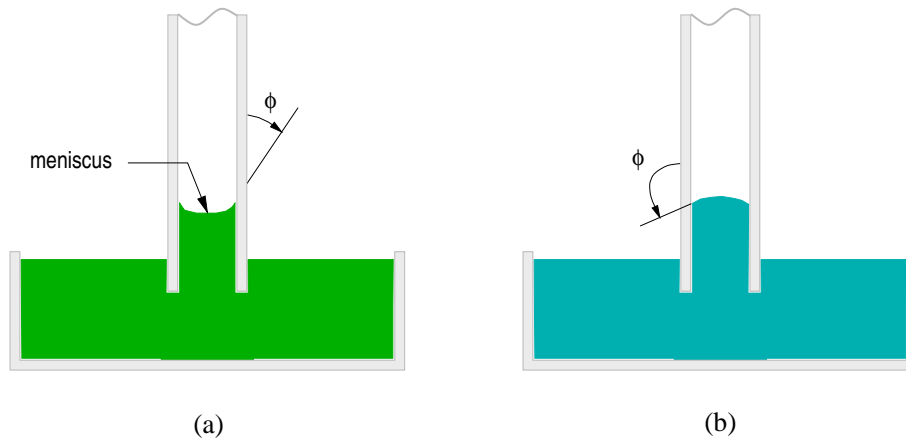
Figure 2.12: Capillarity for two different liquids.

capillarity, like that of surface tension, are rather complicated, and a rigorous treatment is beyond the scope of these lectures. But the basic idea is fairly simple. We see from Fig. 2.11 that surface tension acts in a direction parallel to the surface of the interface. Now the interaction of the gas-liquid interface is altered at the solid wall—one can imagine that this is caused by a combination

of liquid molecular structure (including size of molecules) and details of the wall surface structure (recall Fig. 2.5). This interaction causes the interface to make a generally nonzero angle ϕ with the solid boundary as shown in Fig. 2.12. This altered interface is called a *meniscus*, and the angle ϕ is termed the *contact angle*.

The important point to note here is that unless $\phi = 90°$ there will be a vertical component of force arising from surface tension. In Fig. 2.12(a) $\phi < 90°$ holds, and the surface tension force tends to pull the liquid up into the tube along the wall. (Assume for simplicity that the tube is open to the atmosphere.) By way of contrast, Fig. 2.12(b) displays a case of $\phi > 90°$ for which the surface tension force acts downward.

Temperature

Temperature is, of course, a property of all matter. Our intuitive notion of temperature is simply "how hot or cold an object feels." For solid matter temperature arises from molecular vibrations, while for gases it is associated with molecular translational motion. In particular, we have the following definition for the gaseous case of fluids.

Definition 2.7 *The temperature of gases is directly related to the average translational energy of the molecules of the gas via the following formula:*

$$T = \frac{\frac{1}{2}m\overline{U^2}}{\frac{3}{2}k} \tag{2.9}$$

It is clear that the numerator of this expression is the mean molecular kinetic energy with m being molecular mass (not molecular weight!) and U the molecular speed. In the denominator k is Boltzmann's constant.

For liquids temperature must be viewed as arising from a combination of the above two effects, and as we have already implied in our discussion of temperature dependence of viscosity of liquids, they can possess considerable (at least short-range) structure causing their properties to behave somewhat more like those of solids than of gases.

Equation of State

We now have in hand all of the properties we will need for the subsequent lectures, and for gases these can be related through various *equations of state* as studied in thermodynamics. This is also true of liquids, but the state equations are far less general and much more complex. For gases at moderate to high temperature and low to moderate pressure the equation of state for an *ideal gas* is usually employed to relate the properties pressure, temperature and density. This is expressed as

$$p = \rho \mathcal{R} T, \tag{2.10}$$

where $\mathcal{R}$ is the *specific gas constant* for the gas under consideration. We recall that this is related to the *universal gas constant* $\mathcal{R}_0$ via

$$\mathcal{R} = \mathcal{R}_0/W \tag{2.11}$$

with W being the average molecular weight.

We mention here that Eq. (2.10) is usually termed the equation of state for a "thermally-perfect" gas in the context of fluid dynamics, and especially in the study of gas dynamics.

2.4 Classification of Flow Phenomena

There are many ways in which fluid flows can be classified. In this section we will present and discuss a number of these that will be of particular relevance as we proceed through these lectures. We will begin with some classifications that are quite intuitive, such as whether a flow is steady or unsteady, proceed to ones requiring quite specific mathematical definitions, such as rotational and irrotational flows, and finally describe classifications requiring additional physical insights as in distinguishing between laminar and turbulent flows. It is important to bear in mind throughout these discussions that the classifications we are considering are concerned with the <u>flow</u>, and not with the fluid itself. For example, we will later distinguish between compressible and incompressible flows, and we will see that even though gases are generally very compressible substances, it is often very accurate to treat the flow of gases as incompressible.

2.4.1 Steady and unsteady flows

One of the most important, and often easiest to recognize, distinctions is that of *steady* and *unsteady* flow. In the most general case all flow properties depend on time; for example the functional dependence of pressure at any point (x, y, z) at any instant might be given as $p(x, y, z, t)$. This leads to the following:

Definition 2.8 *If all properties of a flow are independent of time, then the flow is <u>steady</u>; otherwise, it is <u>unsteady</u>.*

Real physical flows essentially always exhibit some degree of unsteadiness, but in many situations the time dependence may be sufficiently weak to justify a steady-state analysis, which in such a case would often be termed a *quasi-steady* analysis. It is also worth mentioning that the term *transient* arises often in fluid dynamics, just as it does in many other branches of the physical sciences. Clearly, a transient flow is time dependent, but the converse is <u>not</u> necessarily true. Transient behavior does not persist for "long times." In particular, a flow may exhibit a certain type of behavior, say oscillatory, for a few seconds, after which it might become steady. On the other hand, time-dependent (unsteady) behavior is generally persistent, but it may be generically similar for all time; *i.e.*, the qualitative nature of the behavior may be fixed even though the detailed motion changes with time. Such a flow is often termed *stationary*. Examples of these flow situations are depicted in Fig. 2.13.

We note, for the sake of clarification, that in some branches of engineering (particularly electrical) some of the flows we here call stationary would be considered steady. Electrical engineers have a tendency to refer to anything after the initial transient has died away as "steady." For example, a periodic flow following some possibly irregular initial transient would be called steady. But this contradicts our basic definition because a periodic behavior clearly depends on time.

2.4.2 Flow dimensionality

Dimensionality of a flow field is a concept that often causes considerable confusion, but it is actually a very simple notion. The first thing to note is that it is not necessarily true that dimensionality of the flow field equals the geometric dimension of the container of the fluid. But at the same time we must recognize that all <u>physical</u> flows are really three dimensional (3D). Nevertheless, it is often
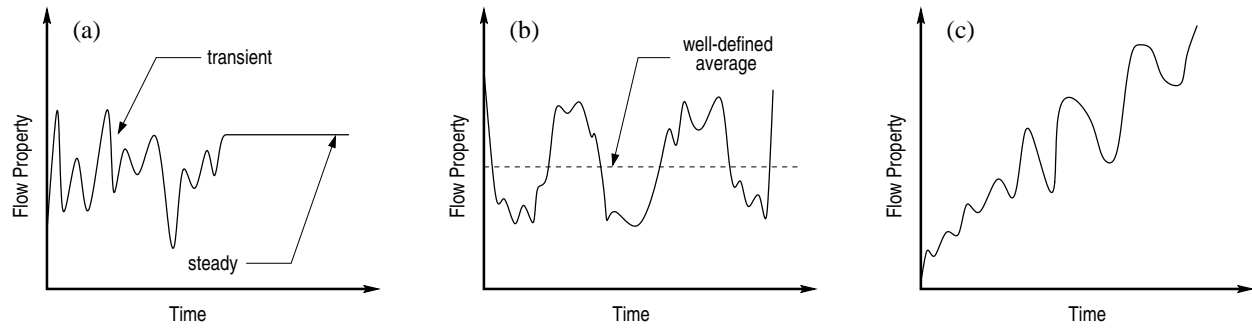
Figure 2.13: Different types of time-dependent flows; (a) transient followed by steady state, (b) unsteady, but stationary, flow, (c) unsteady.

convenient, and sometimes quite accurate, to view them as being of a lower dimensionality, *e.g.*, 1D or 2D. We will start with the following mathematical definition of dimension, and then provide some examples that will hopefully clarify these ideas.

Definition 2.9 *The dimensionality of a flow field corresponds to the number of spatial coordinates needed to describe all properties of the flow.*

We remark that the typical confusion arises because of our tendency to associate dimension with the number of nonzero components of the velocity field; often, coincidentally, this turns out to be correct. But it is not the correct definition.

   We have already seen an example of 1-D flow in our discussions of viscosity. Namely, the flow between two horizontal parallel plates of "infinite" extent in the x and z directions. A similar flow, but now between plates of finite extent in the x direction, is shown in Fig. 2.14(a).
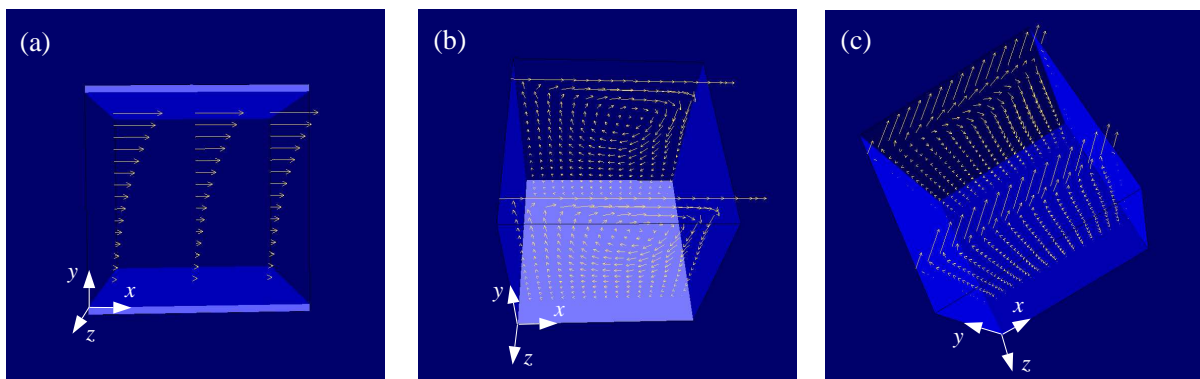
Figure 2.14: Flow dimensionality; (a) 1-D flow between horizontal plates, (b) 2-D flow in a 3-D box, (c) 3-D flow in a 3-D box.

   It should be clear that if we associate u with the x direction, v with the y direction and w with the z direction, then the v and w velocity components do not depend on any coordinates; they are constant and equal to zero in Fig. 2.14(a). At the same time, u depends only on y. If we now assume density and temperature are constant (*i.e.*, do not depend on any spatial coordinate) then at least for a gas it is easily argued that the pressure p must also be constant. Thus, all of the

main flow field variables can be completely specified by the single coordinate y, and the flow is 1D. We remark that the one-dimensionality did <u>not</u> arise from the fact that there was only one nonzero component of velocity. Indeed, in principle, v and w could both also depend only on y in the same manner as does u (or, possibly in a different manner); then all three components of the velocity field would be nonzero, but the flow would still be only 1D.

In Fig. 2.14(b) is displayed a 2-D flow. The physical situation is that of a box of fluid that is infinite only in the z direction, the top of the box is moving in the x direction, and it is transparent so that we can view the flow field. There are two key observations to be made. First, each of the planes of velocity vectors indicate motion that varies with both the x and y directions; hence, the flow is at least two dimensional. But we also see that the two planes of vectors are exactly alike—they do not change in the z direction. Thus, the flow is 2D.

Finally, the 3-D case is presented in Fig. 2.14(c) which represents a box containing fluid with the upper (solid) surface moved diagonally with respect to the x and $(-)z$ directions. We again show two planes of velocity vectors; but unlike the previous case, they differ significantly from one another, indicating a z dependence of the u and v components as well as the obvious x and y dependence. In addition, it should be clear that for this case the z component of velocity, w, is nonzero and also varies with x, y and z.

2.4.3   Uniform and non-uniform flows

We often encounter situations in which a significant simplification can be had if we are able to make an assumption of *uniform flow*. We begin by giving a precise definition of this useful concept, and we then provide some examples of uniform and non-uniform flows.

Definition 2.10 *A <u>uniform flow</u> is one in which all velocity vectors are identical (in both direction and magnitude) at every point of the flow for any given instant of time. Flows for which this is not true are said to be <u>nonuniform</u>.*

This definition can be expressed by the following mathematical formulation:

$$\frac{\partial \boldsymbol{U}}{\partial \boldsymbol{s}} \equiv \left[\begin{array}{c} \frac{\partial u}{\partial \boldsymbol{s}} \\ \frac{\partial v}{\partial \boldsymbol{s}} \\ \frac{\partial w}{\partial \boldsymbol{s}} \end{array} \right] = \left[\begin{array}{c} 0 \\ 0 \\ 0 \end{array} \right]. \tag{2.12}$$

Here, $\boldsymbol{U}$ is the velocity vector, and $\boldsymbol{s}$ is an arbitrary vector indicating the direction with respect to which differentiation will be performed. For example, $\boldsymbol{s}$ might be in any one of the coordinate directions, or in any other direction. But no matter what the direction is, the derivative with respect to that direction must be everywhere zero for the flow to be uniform. It should also be observed that the above definition implies that a uniform flow must be of <u>zero</u> dimension—it is everywhere constant, and thus does not depend on any spatial coordinates. From this we see that none of the examples in Fig. 2.14 correspond to a uniform flow.

Figure 2.15 provides some examples of uniform and non-uniform flow fields. Part (a) of the figure clearly is in accord with the definition. All velocity vectors have the same length and the same direction. Part (b) of Fig. 2.15 contains a particularly important case that we will often encounter later in the course. From the definition we see that this is a non-uniform flow; the velocity vectors have different magnitudes as we move in the flow direction. On the other hand, at any given x location they all have the same magnitude. This is usually termed *locally uniform*. Figure 2.15(c) shows a case closer to actual flow physics, and it is nonuniform. In fact, most actual flows are nonuniform, but we will see that especially local uniformity will be an important, and often quite accurate, simplification.
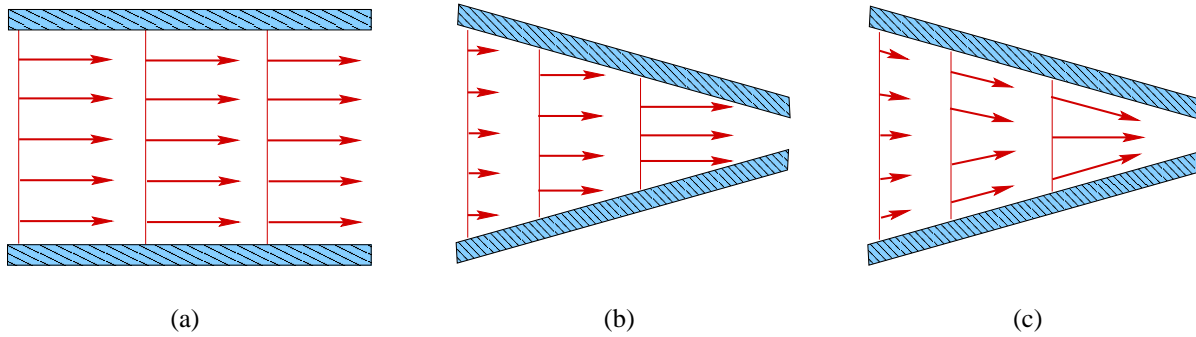
Figure 2.15: Uniform and non-uniform flows; (a) uniform flow, (b) non-uniform, but "locally uniform" flow, (c) non-uniform flow.

2.4.4 Rotational and irrotational flows

Intuitively, we can think of rotational flows as those containing many "swirls" or "vortices;" *i.e.*, the fluid elements are rotating. Conversely, fluids not exhibiting such effects might be considered to be irrotational. But we will see from the precise definition, and some examples that follow, that these simple intuitive notions can sometimes be quite inaccurate and misleading. It thus is preferable to rely on the rigorous mathematical definition.

Definition 2.11 *A flow field with velocity vector U is said to be <u>rotational</u> if* $\mathrm{curl}\, U \neq 0$*; otherwise, it is <u>irrotational</u>.*

To understand this definition, and even more to be able to use it for calculations, we need to consider some details of the curl of a vector field; this is given by the following.

Definition 2.12 *The <u>curl</u> of any (3-D) vector field $F = F(x, y, z)$ is given by*

$$\mathrm{curl}\, \boldsymbol{F} = \nabla \times \boldsymbol{F} = \left(\frac{\partial}{\partial x}, \frac{\partial}{\partial y}, \frac{\partial}{\partial z} \right) \times (\boldsymbol{F}_1(x, y, z), \boldsymbol{F}_2(x, y, z), \boldsymbol{F}_3(x, y, z)) \, . \qquad (2.13)$$

We next need to see how to use this definition for practical calculations. In the case that is of interest in this course, the vector field will be the velocity field

$$\boldsymbol{U}(x, y, z) = (u(x, y, z), v(x, y, z), w(x, y, z))^T \, ,$$

and $\mathrm{curl}\, \boldsymbol{U}$ is called *vorticity*, denoted $\boldsymbol{\omega}$. Thus,

$$\boldsymbol{\omega} \equiv \nabla \times \boldsymbol{U} \, , \qquad (2.14)$$

and if $\boldsymbol{\omega} \neq 0$ the corresponding flow field is rotational. In Cartesian coordinate systems $\boldsymbol{\omega}$ is easily calculated from the following formula:

$$\begin{aligned} \boldsymbol{\omega} &= \begin{vmatrix} \boldsymbol{e}_1 & \boldsymbol{e}_2 & \boldsymbol{e}_3 \\ \frac{\partial}{\partial x} & \frac{\partial}{\partial y} & \frac{\partial}{\partial z} \\ u & v & w \end{vmatrix} \\ &= \left(\frac{\partial w}{\partial y} - \frac{\partial v}{\partial z} \right) \boldsymbol{e}_1 + \left(\frac{\partial u}{\partial z} - \frac{\partial w}{\partial x} \right) \boldsymbol{e}_2 + \left(\frac{\partial v}{\partial x} - \frac{\partial u}{\partial y} \right) \boldsymbol{e}_3 \, . \qquad (2.15) \end{aligned}$$

In this expression the e_i , $i = 1, 2, 3$ are the *unit basis vectors* for the three-dimensional Euclidean space $\mathbb{R}^3$. It is clear that, in general, vorticity is a vector field of the same dimension as the velocity field. But we note that for a 2-D velocity field with one component, say w, identically constant, vorticity collapses to a scalar; it will, however, still depend on the same two spatial coordinates as does the velocity field.

We will often (in fact, most of the time) throughout these lectures employ a short-hand notation for partial differentiation in the form, *e.g.*,

$$\frac{\partial u}{\partial x} = u_x \,, \qquad \frac{\partial v}{\partial z} = v_z \,, \quad etc.$$

Hence, the above formula for vorticity can be written more concisely as

$$\boldsymbol{\omega} = ((w_y - v_z), (u_z - w_x), (v_x - u_y))^T \,.$$

We can now re-examine consequences of the definition of rotational in the context of this formula for vorticity. First, we note that any uniform flow is automatically irrotational because from Eq. (2.12) it is easily seen that all components of $\boldsymbol{\omega}$ must be identically zero. But we should also observe that there is another manner in which a flow can be irrotational. Namely, if we set

$$
\begin{aligned}
w_y &= v_z \\
u_z &= w_x \\
v_x &= u_y \,,
\end{aligned}
\qquad (2.16)
$$

then we see from Eq. (2.15) that the vorticity vector is again identically zero; but in this case we have not required velocity gradient components to be identically zero (as was true for uniform flows), so the flow field can be considerably more complex, yet still irrotational.

In the following subsections we provide some specific physical examples of flows that are either rotational or irrotational.

1-D Shear Flows

If we recall Figs. 2.4 and 2.14(a) we see that the only nonzero velocity component is u and that it varies only with the coordinate y. As a consequence, all velocity derivatives are identically zero except for u_y. From this we see that the third component of the vorticity vector must be nonzero. Hence, these simple 1-D flows are rotational. It should be noted that there is no indication of swirl (*i.e.*, vortices) but, on the other hand as indicated in Fig. 2.4, there is rotation of fluid elements. It is also interesting to note that the direction of vorticity in these cases is pointing out of the plane of the figures—the z direction—even though the velocity field is confined to x-y planes. Even so, this does not change our assessment of the dimensionality of the flow field: vorticity is a property of the flow, and it is pointing in the z direction; but it is changing only in the y direction (in fact, in Fig. 2.4 it is constant).

2-D Shear Flow Over a Step

In this section we present a flow field that is two dimensional, and in this case it contains a very prominent vortex. This is displayed in Fig. 2.16 in which red denotes high magnitude, but negative, vorticity, and blue corresponds to positive high magnitude vorticity. The large areas of green color have nearly zero vorticity. The black lines represent paths followed by fluid elements,
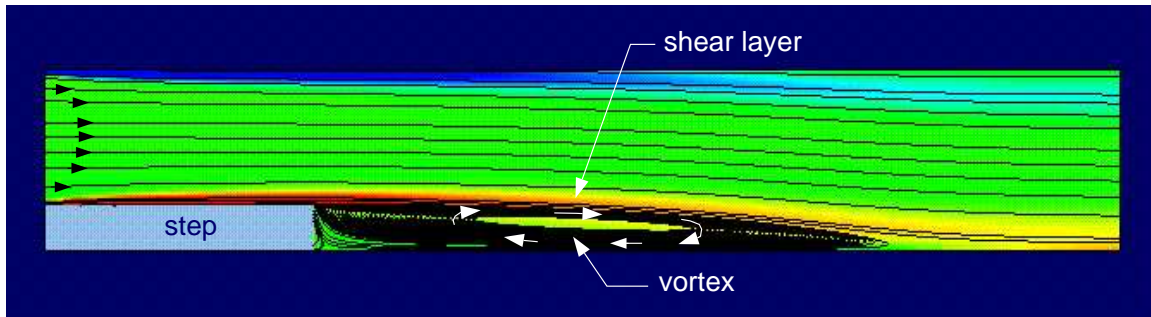
Figure 2.16: 2-D vortex from flow over a step.

and the flow is from left to right. What is interesting about this particular flow is that the vortex itself is for the most part in a region of relatively low vorticity. The high magnitudes are found near the upper boundary, along the top surface of the step, and in the "shear layer" behind the step where the vortex meets the oncoming flow.

We should observe that for such a flow, except in the vicinity of the vortex, the main flow direction will be from left to right so that the velocity vectors have large u components and relatively small v components. If we now recall that in 2D the only component of the vorticity vector is

$$\omega_3 = v_x - u_y \,,$$

we can easily see why the vorticity is negative along the upper surface of the step, and positive along the upper boundary. In particular, since v is very small, we do not expect much contribution to ω_3 from v_x. At the same time, along the top of the step the u component of velocity is increasing with y as it goes from a zero value on the step (due to the no-slip condition) out to the speed of the oncoming flow farther away from the step. Hence, $u_y > 0$ holds; but this term has a minus sign in the formula for vorticity. A similar argument holds for the vorticity at the upper boundary.

3-D Shear Flow in a Box

Figure 2.17 provides an image indicating some of the qualitative features of vorticity associated with the 3-D flow of Fig. 2.14(c). The colors represent magnitude of vorticity, $|\boldsymbol{\omega}|$, with blue being large values and red indicating values near zero. This is a flow field of a fluid confined to a cubic box with shear induced at the top by moving the solid lid in a diagonal direction as indicated by the arrows of the figure. The main points of interest in this figure are: first, the extreme variability in a three-dimensional sense of the magnitude of vorticity throughout the flow field; second, the complicated structure of the lines indicating motion of fluid parcels; and three, particularly the vortical shape near the top of the box. It is worthwhile to recall at this point the discussion of effects of viscosity given earlier and especially how the combination of the no-slip condition and diffusion of momentum can be expected to set up such a flow field.

The Potential Vortex

Up to this point we have seen examples of flows that have vorticity, but no apparent vortex, and flows that have both vorticity and a vortex. We have also noted the case of uniform flow which exhibits neither vorticity nor an observable vortex. In this section we will briefly introduce the one remaining possibility: a flow containing a vortex, but for which the vorticity is identically zero.
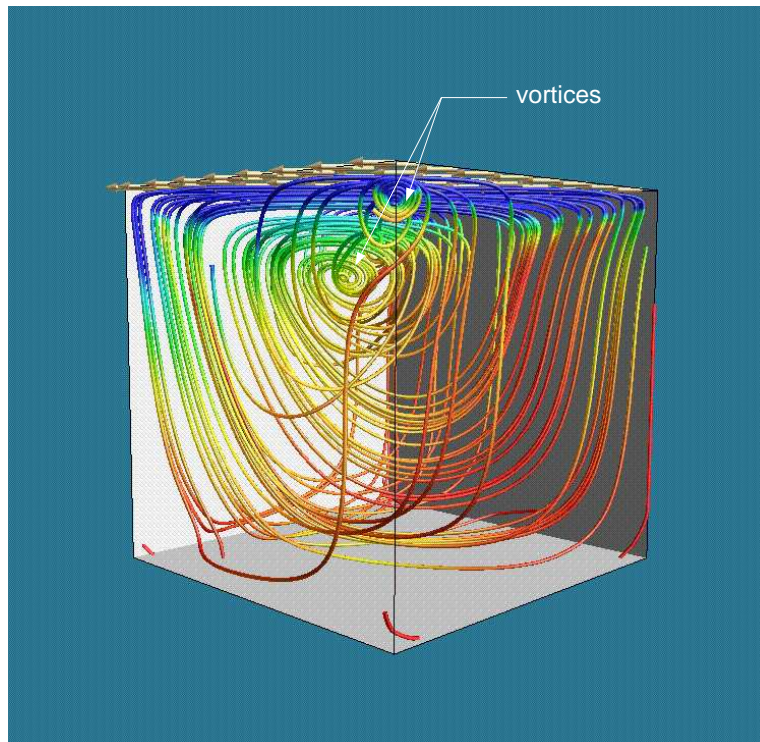
Figure 2.17: 3-D vortical flow of fluid in a box.

Potential flows are a class of flows that were once studied in great detail because in many cases it was possible to obtain exact solutions to their corresponding equation(s). They are, by definition, irrotational; but they are not necessarily trivial as is true for uniform flow. The study of such flows in modern fluid dynamics has been relegated to brief introductions, primarily due to the effectiveness of CFD in calculating general flow fields for which few assumptions need be made; but they once formed the basis of most incompressible aerodynamics analyses. We will not provide a detailed description of the potential flow we are considering here because it will not be of particular use in our later studies. On the other hand, it does provide a final example associated with vorticity that we should be aware of.

Figure 2.18 provides a sketch of the *potential vortex* flow field. It is important to examine the orientation of the fluid elements shown in this figure and compare this with what would occur in "rigid-body rotation" of the same fluid. Potential vortex flow is one-dimensional and is represented in polar coordinates. Its radial velocity component u is identically zero, as is the z (into the paper) component; its azimuthal component is given by

$$v = \frac{K}{r}\,,$$

where K is a constant. This can be shown to satisfy $\nabla \times \boldsymbol{U} = 0$ in polar coordinates, and thus the flow is irrotational.

It should be noted that the motion of any particular fluid element does not correspond to rigid-body rotation—which does not lead to zero vorticity. In fact, we see from the figure that as the fluid element moves in the θ direction it maintains the same face perpendicular to the radial direction (as would happen for rigid-body rotation); but it is distorted in such a way that originally
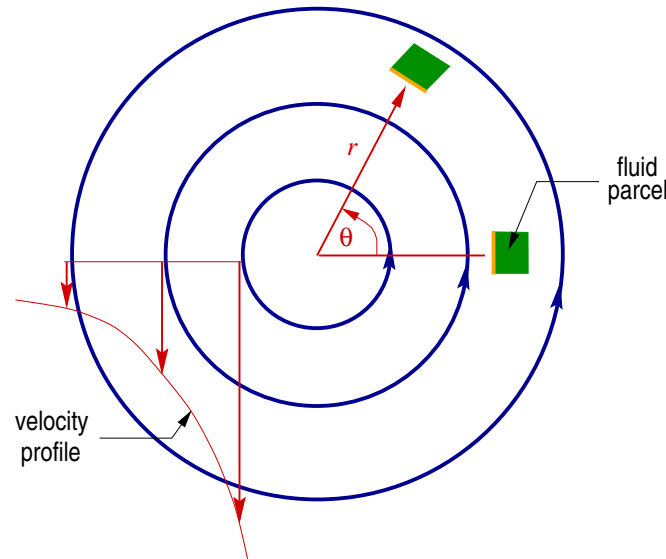
Figure 2.18: Potential Vortex.

perpendicular faces are distorted in opposite directions, leaving the net rotation of the fluid element at zero. Thus, we see that (net) rotation of fluid elements is required for nonzero vorticity. Indeed, it is possible to provide a completely physically-based derivation of rotation, the outcome of which shows that vorticity as defined above is just twice the rotation.

2.4.5   Viscous and inviscid flows

It is a physical fact that all fluids possess the property of viscosity which we have already treated in some detail. But in some flow situations it turns out that the forces on fluid elements that arise from viscosity are small compared with other forces. Understanding such cases will be easier after we have before us the complete equations of fluid motion from which we will be able to identify appropriate terms and estimate their sizes. But for now it is sufficient to consider a case in which viscosity is small (such as a gas flow at low temperature); hence, the shear stress will be reasonably small (recall Eq. (2.2)) and, in turn, the corresponding shear forces will be small. Assume further that pressure forces are large by comparison with the shear forces. In this situation it might be appropriate to treat the flow as *inviscid* and ignore the effects of viscosity. Clearly, in situations where viscous effects are important, they must not be neglected, and the flow is said to be *viscous*.

2.4.6   Incompressible and compressible flows

As we have stressed previously, and as was also the case for the previous classification, it is the flow that is being considered in this case, and not the fluid. We mentioned earlier the fact that gases are, in general, quite compressible; yet flows of gases can often be treated as incompressible flows. A simple, and quite important, example of this is flow of air in air-conditioning ducts. For our purposes in this course, a flow will be considered as *incompressible* if its density is constant. This will often be the case in the problems treated here. But we note that there are some flows exhibiting variable density, and which can still be analyzed accurately as incompressible. We will later give a more technical description of incompressible flow, but the present discussion will suffice for most of these lectures.

2.4.7   Laminar and turbulent flows

From the standpoint of analysis of fluid flow, the distinction between laminar and turbulent is one of the most important. With the power of present-day computers essentially any laminar flow can be <u>predicted</u> with better accuracy than can be achieved with laboratory measurements. But for turbulent flow this is not the case. At present, except for the very simplest of flow situations, it is not possible to predict turbulent fluid motion. In fact, it is sometimes said that we do not even actually know what turbulence is. But certainly, at least from a qualitative perspective, we can readily recognize it, and on this basis it is clear that <u>most flows</u> of engineering importance <u>are turbulent</u>. It is our purpose in the present section to present some examples that will help provide intuition regarding the differences between laminar and turbulent flows.

Probably our most common experience with the distinction between laminar and turbulent flow comes from observing the flow of water from a faucet as we increase the flow rate. We depict this in Fig. 2.19. Part (a) of the figure displays a laminar (and steady) flow in which the trajectories

| (a) | (b) | (c) |
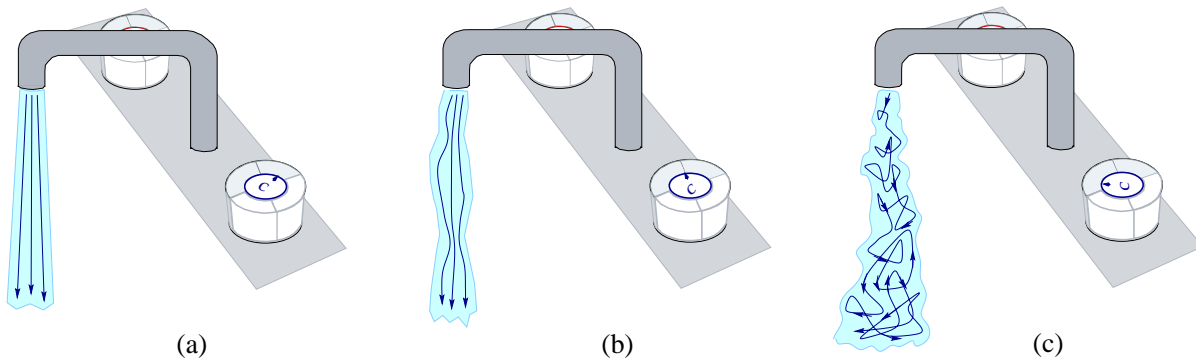
Figure 2.19: Laminar and turbulent flow of water from a faucet; (a) steady laminar, (b) periodic, wavy laminar, (c) turbulent.

followed by fluid parcels are very regular and smooth; furthermore, there is no indication that these trajectories might cross one another. In part (b) of the figure we present a flow that is still laminar, but one that results as we open the faucet more than in the previous case permitting a higher flow speed. In such a case the surface of the stream of water begins to exhibit waves, and these will change in time (basically in a periodic way). Thus the flow has become time dependent, but there is still no apparent intermingling of trajectories. Finally, in part (c) of the figure we show a turbulent flow corresponding to much higher flow speed. We see that the paths followed by fluid parcels are now quite complicated and entangled indicating a high degree of mixing (in this case only of momentum). Such flows are three dimensional and time dependent, and very difficult to predict in detail.

The most important single point to observe from the above figure and discussion is that as flow speed increases, details of the flow become more complicated and ultimately there is a "transition" from laminar to turbulent flow.

Identification of turbulence as a class of fluid flow was first made by Leonardo da Vinci more than 500 years ago, as indicated by his now famous sketches one of which we present here in Fig. 2.20. In fact, da Vinci was evidently the first to use the word "turbulence" to describe this type of flow behavior. Despite this early recognition of turbulence, little formal investigation was carried out until the late 19th Century when experimental facilities were first becoming sufficiently sophisticated to permit such studies. The work of Osbourne Reynolds in the 1880s and 1890s is still

Figure 2.20: da Vinci sketch depicting turbulent flow.

widely used today, and in some sense little progress has been made over the past 100 years. In Fig. 2.21 we display a rendition of Reynolds' original experiments that indicated in a semi-quantitative way the transition to turbulence of flow in a pipe as the flow speed is increased. What is evident
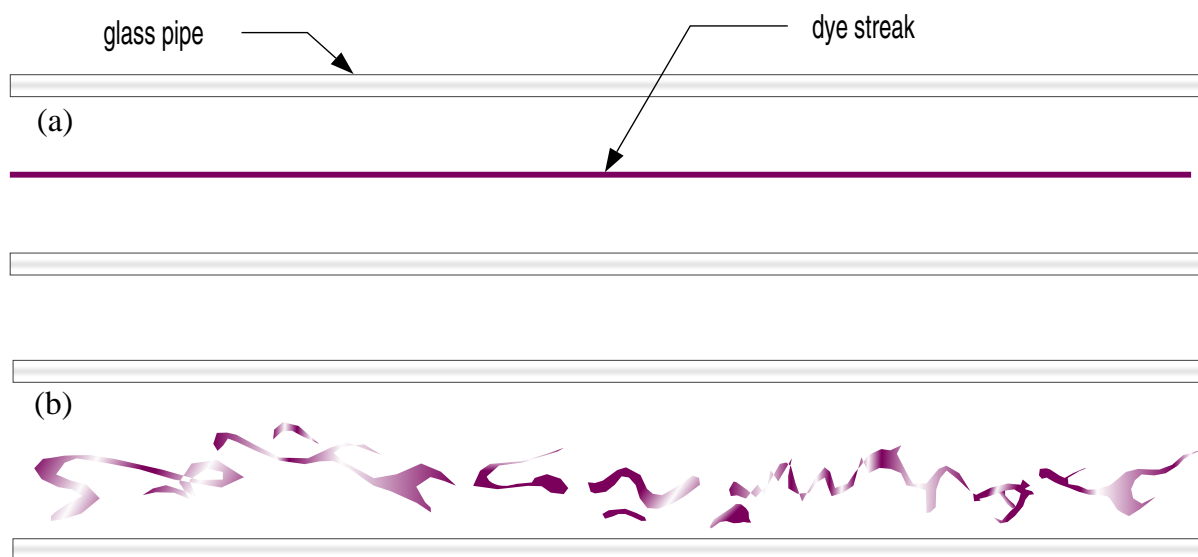
Figure 2.21: Reynolds' experiment using water in a pipe to study transition to turbulence; (a) low-speed flow, (b) higher-speed flow.

from this figure is analogous to what we have already seen with flow from a faucet, but now in the context of an actual experiment; namely, as long as the flow speed is low the flow will be laminar, but as soon as it is fast enough turbulent flow will occur.

The details as to how and why this happens are not completely understood and still constitute a major area of research in fluid dynamics, despite the fact that the problem has been recognized for five centuries and has been the subject of intense investigation for the past 120 years.

A similar transition can also take place as a flow evolves spatially, as indicated in Fig. 2.22 (and

also in da Vinci's sketch). As the flow moves from left to right we see the path of the dye streak
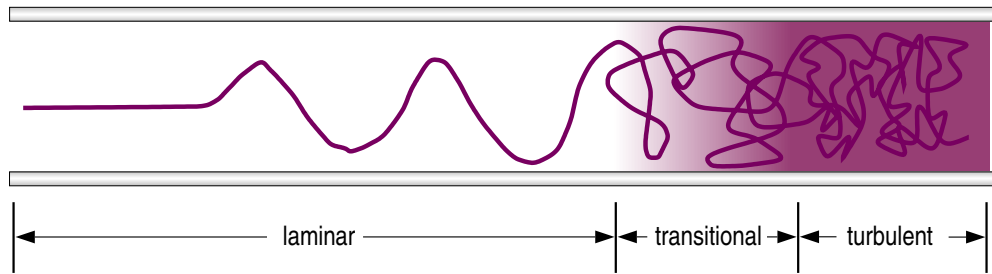
Figure 2.22: Transition to turbulence in spatially-evolving flow.

become more complicated and irregular as transition begins. Only a little farther down stream the
flow is turbulent leading to complete mixing of the dye and water if the flow speed is sufficiently
high.

   In these lectures we will not study turbulence to any extent except in our analyses of pipe
flow in which it will be necessary to assess whether a given flow is turbulent and then employ the
appropriate (laminar or turbulent) "friction factor." Nevertheless, it is important to recognize that
most flows encountered in engineering practice are turbulent, and the main tool available is CFD.
It is widely accepted that the Navier–Stokes equations are capable of exhibiting turbulent solutions
and, as we have noted earlier, these equations are the basis for essentially all CFD codes. But even
with such tools we are still far from being able to reliably predict turbulent flow behavior. This is
still the subject of much research throughout the world.

2.4.8   Separated and unseparated flows

The term "separated flow" may at first seem to be a rather inappropriate description of flow
phenomena, and it does not mean exactly what it might seem to imply—in particular, separated
does not mean that there is no fluid adjacent to the surface from which the flow is said to be
separated. On the other hand, we will recognize that this is a quite apt description once we
understand the physics associated with it. We first observe that flow behind a backward-facing
step displayed earlier in Fig. 2.16 is one of the best-known examples of separated flow. This type
of behavior is encountered often in devices of engineering importance (e.g., in interior cooling-air
circuits of aircraft engine turbine blades), so it is worthwhile to attempt to understand why and
how such a flow field occurs.

   It is easiest to first consider a flow situation in which separation does not occur. Suppose
we examine what happens with a very slow-moving fluid in a geometric setting similar to that
of Fig. 2.16. For example, assume the fluid is pancake syrup that has been removed from the
refrigerator only moments before the start of our experiment. Figure 2.23(a) provides a sketch of
the approximate flow behavior as the syrup oozes along the top of the step and then encounters
the corner. As the flow reaches the corner its momentum is very low due to its low speed, and it
exhibits no tendency to "overshoot" the corner; thus, it oozes around the corner, flows down the
vertical face of the step and continues on its way. Fluid initially in the vicinity of the solid surface
remains close to it, even when making a 90 degree turn—i.e., the flow remains "attached" to the
surface.

   Now consider the same experiment but with a less viscous fluid and/or a higher-speed flow.
Figure 2.23(b) presents this case. Now the flow momentum is high, and it is difficult for the fluid to
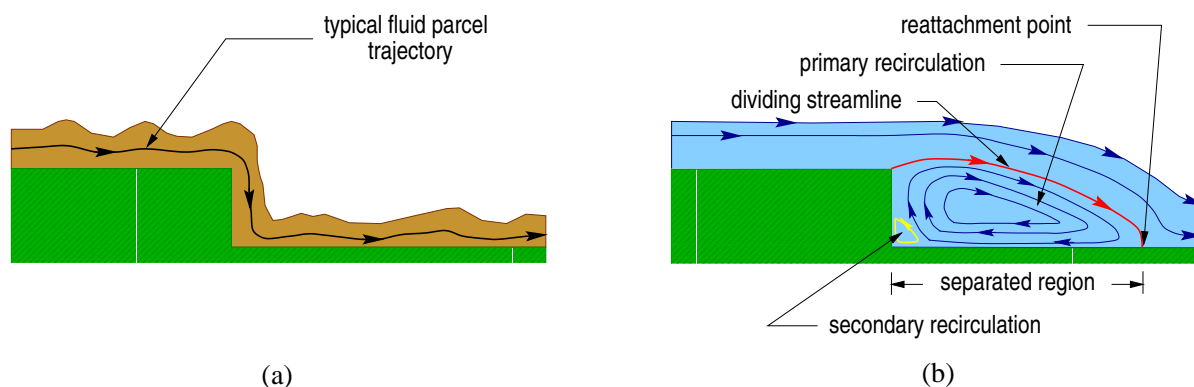
Figure 2.23: (a) unseparated flow, (b) separated flow.

turn the sharp corner without part of it overshooting. This high-speed fluid then shears the fluid immediately beneath it at the same time the lower portions of this region begin to move toward the step to fill the void caused, in the first place, by the overshooting fluid coming off the step. The immediate consequence of this combination of physical events is the *primary recirculation* region indicated in Fig. 2.23(b). (This is just alternative terminology for the vortex shown previously in Fig. 2.16.) Such vortices, or recirculation zones, are common features of essentially all separated flows.

We have also indicated several other features found in separated flows. The *dividing streamline* is shown in red. This is a flow path such that the flow on one side does not mix with flow on the other side (except in turbulent flows). In some flow situations, such as the present one, the flow is quite different in nature, qualitatively, on opposite sides of the dividing streamline, but in other situations we will encounter later, the flow behavior is identical on both sides. Also shown in the figure is the location of the *reattachment point*. This is the point where the dividing streamline again attaches to the solid surface. Finally, in the lower corner of the step we have pictured a "secondary" recirculation region. This is caused when the reversed flow of the primary vortex is unable to follow the abrupt turn at the lower corner. It then separates from the lower surface, leading to the secondary recirculation. This can occur in very high speed flows for which the speed in the primary recirculation zone, itself, is large.

It should further be noted that an abrupt change in direction induced by geometry (like the corner of the step) is not the only manner in which a flow can be caused to separate. We will see in our later studies that flow is impeded by increases in pressure in the flow direction. With sufficient increases the flow can separate in this case as well, even when the surface is quite smooth. This can occur for airfoils at high angles of attack, resulting in "stalling" of the wing and loss of lift. Thus, an understanding of this mechanism for separation is also very important.

2.5 Flow Visualization

In the context of laboratory experiments flow visualization is an absolute necessity, and it was within this context that the techniques we will treat here were first introduced. It is worth noting that even for theoretical analyses much can often be learned from a well-constructed sketch that emphasizes the key features of the flow physics in a situation of interest. But, even more important, is the fact that now CFD can produce details of 3-D, time-dependent fluid flows that simply could not previously have been obtained. So visualization is all the more important in this

context. The visualization techniques we will describe in this section are very standard (and there are others); they are: streamlines, pathlines and streaklines. We will devote a subsection to a brief discussion of each of these, introducing their mathematical representations and their physical interpretations. Before beginning this we note one especially important connection amongst these three representations of a flow field: they are all equivalent for steady flows.

2.5.1   Streamlines

We have already seen some examples of streamlines; the curves appearing in Figs. 2.16 and 2.17, which we called trajectories of fluid elements, were actually streamlines, and in the preceding sub-section we introduced the notion of a dividing streamline—without saying exactly what a streamline is. We remedy these omissions with the following definition.

Definition 2.13 *A streamline is a continuous line within a fluid such that the tangent at each point is the direction of the velocity vector at that point.*

One can check that Figs. 2.16 and 2.23 are drawn in this manner; Fig. 2.24 provides more detail. In this figure we consider a 2-D case because it is more easily visualized, but all of the ideas we present work equally well in three space dimensions. The figure shows an isolated portion of a velocity field obtained either via laboratory experiments (*e.g.*, particle image velocimetry mentioned in Chap. 1) or from a CFD calculation. We first recall from basic physics that the
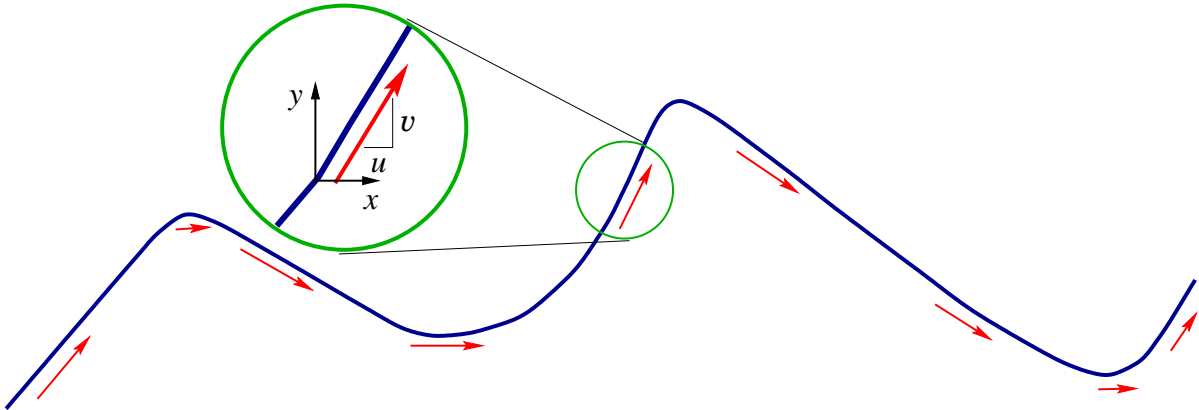
Figure 2.24: Geometry of streamlines.

velocity components are given by

$$u = \frac{dx}{dt} \qquad \text{and} \qquad v = \frac{dy}{dt}. \tag{2.17}$$

It is then clear from the figure that the local slope of the velocity vector is simply v/u. Thus,

$$\frac{v}{u} = \frac{dy/dt}{dx/dt},$$

or

$$\frac{dx}{u} = \frac{dy}{v} \quad \left(= \frac{dz}{w} \quad \text{in 3D} \right). \tag{2.18}$$

Equations (2.18) are often viewed as the defining relations for a streamline. The fact (given in the definition) that a streamline is everywhere tangent to the velocity field is especially clear if we write these as (in 2D)

$$\frac{dy}{dx} = \frac{v}{u}\,. \tag{2.19}$$

Furthermore, if the velocity field $(u, v)^T$ is known (as would be the case with PIV data or CFD simulations), streamlines can be constructed by solving the differential equation (2.19). We note, however, that for either of these types of data velocity is known at only a set of discrete points; so interpolations are need to actually carry out the integrations corresponding to solution of the differential equation. On the other hand, if formulas are known for u and v it may be possible to solve this equation analytically for the function $y(x)$ representing the streamline.

We should next consider some physical attributes of streamlines. The first thing to note is that streamlines display a snapshot of the entire flow field (or some selected portion of it) at a single instant in time with each streamline starting from a different selected point in the flow field. Thus, in a time-dependent flow a visualization based on streamlines will be constantly changing, possibly in a rather drastic manner. A second property of streamlines is that they cannot cross. This follows from their definition; *viz.*, they are in the direction of the velocity vector, and if they were to cross at any point in a flow field there would have to be two velocity vectors at the same point. Hence, the velocity would not be well defined. It is worth mentioning that the "entangled" fluid particle trajectories described earlier in our discussions of turbulent flow either cannot be viewed as streamlines, or the associated figures (Figs. 2.19 and 2.22) must be taken in a 3-D context so that apparently crossing streamlines do not actually cross. Finally, we note that in flows bounded by solid walls or surfaces, the wall (or surface) can be defined to be a streamline. This is because flow cannot penetrate a solid boundary, implying that the only nonzero component(s) of the velocity vector very close to the surface is (are) the tangential one(s)—*i.e.*, those in the direction of the streamlines.

2.5.2 Pathlines

We have already been exposed to pathlines in an informal way through our earlier discussions of "fluid parcel trajectories." Here, we begin with a more formal definition.

Definition 2.14 *A* pathline *(or particle path) is the trajectory of an individual element of fluid.*

It should first be noted that the basic equations already presented for streamlines still hold in the pathline case, but they must be used and interpreted somewhat differently. We can write either of Eqs. (2.17) in the form, *e.g.*,

$$dx = u\,dt\,. \tag{2.20}$$

It is clear that if the velocity field is independent of time this is equivalent to the formulation for streamlines; but if it is time dependent the result will be different, as we have sketched in Fig. 2.25. One should first recognize from this figure that, in contrast to a streamline, a pathline is a time-evolving visualization method. Even for steady flows the individual fluid parcel whose trajectory we consider gets longer as time goes on. In the case of a time dependent flow shown in the figure, the velocity field encountered by the fluid parcel changes with time, so its trajectory must respond to this. At the top of this figure is displayed an instantaneous streamline for comparison purposes. The second velocity field at a later time $t_1 > t_0$ is different from the first, and although the fluid parcel started at the same time and place as in the streamline case, the change in the velocity field has caused the location of the fluid parcel to differ from what would have been the case in the in-
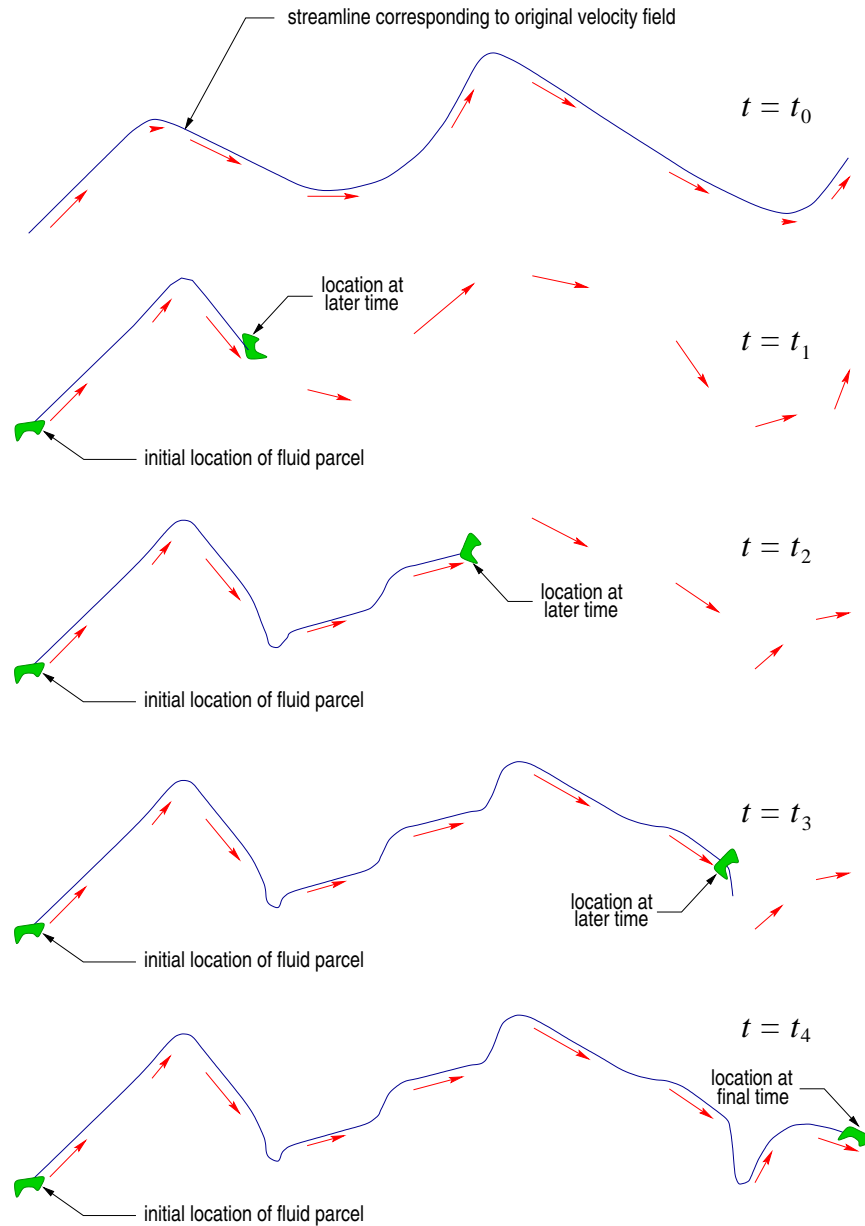
Figure 2.25: Temporal development of a pathline.

stantaneous streamline case. But once the fluid parcel has traveled a portion of its trajectory that portion is fixed; *i.e.*, we see in the third velocity field that approximately the first one third of the pathline is the same as that in the previous part of the figure. But the velocity field has changed, so the remainder of the pathline will be different from what it would have been if the velocity field had stayed constant. This is continued for two more steps in the figure, and from this it is easily seen that the pathline obtained during this evolution is quite different in detail from the streamline.

We should also note that if we were to now make a streamline at this final time it would also differ from the pathline. In particular, although we have not drawn the figure to display this, the velocity field adjacent to the older part of the pathline is not actually the one shown, in general.

(We have frozen the velocities at each new location of the fluid parcel to make them look consistent with the pathline but, in fact, these too are constantly changing.) We emphasize that what the velocity field does after passage of the fluid parcel under consideration is of no consequence to the pathline. This can be seen easily from the mathematical formulation. If we integrate Eq. (2.20) between times t_0 and t_1, we obtain

$$x_1 = x_0 + \int_{t_0}^{t_1} u(x(t), y(t), t)dt$$

as the x coordinate of the fluid parcel at $t = t_1$, with a similar expression for the y coordinate. Now we can repeat this process to get to time $t = t_2$:

$$x_2 = x_1 + \int_{t_1}^{t_2} u(x(t), y(t), t)dt$$

What we see, just as we have indicated schematically in the figure, is that the coordinates of the pathline between times t_1 and t_2 do not explicitly depend on the velocity field at locations visited by the fluid parcel prior to time t_1. On the other hand, if an instantaneous streamline were constructed at, say $t = t_2$, it would depend on all locations within the flow field at that instant.

2.5.3 Streaklines

Especially for unsteady flows the streakline is the closest of the three visualization techniques considered here to what is usually produced in a laboratory experiment. We begin with the definition.

Definition 2.15 *A streakline is the locus of all fluid elements that have previously passed through a given point.*

In comparing this with the case of pathlines we observe that the definition of a pathline involved only a single fluid element; but the current definition for a streakline concerns, evidently, a large number. Thus, in a sense, a streakline combines properties of streamlines and pathlines: it is made up of many pathlines (actually, fluid parcels each of which could produce a pathline), but all of these are observed simultaneously just as is a streamline traversing an entire flow field. The equations satisfied by the motion of these fluid elements are exactly the same as those for streamlines and pathlines; but now they must be solved for a large number of fluid parcels, all starting from the same spatial location at different times. This implies that in a time-dependent flow field each fluid element considered will have its trajectory determined not only by the velocity changes it encounters in traversing the flow field (as happened in the case of a pathline) but also by the changes in initial conditions at its point of origin. It is quite difficult to sketch such behavior except in very simple cases, and we shall not attempt to do so here. But we note that the dye injection technique used in the Reynolds experiment sketched in Fig. 2.21 results in a streakline: the figure shows an instantaneous snapshot (of the entire flow field) with dye being continuously injected.

Streamlines and pathlines are often compared by noting that the former corresponds to continuous injection of marker particles and instantaneous observation of them, whereas the pathline is formed by instantaneous injection and continuous observation.

2.6 Summary

In this chapter we have attempted to provide an introduction to the basic physics of fluid flow. We began with the continuum hypothesis, an important foundation for logical presentation of much

of the subsequent material and continued by noting the differences between fluids and other forms of matter and by giving a rigorous definition of a fluid in terms of response to shear stresses. We then introduced Newton's law of viscosity and presented a fairly detailed description of viscosity, including its physical origins and behavior as the mediator of diffusion of momentum. It is important to note that viscosity is one property that is not shared by nonfluids. We then briefly discussed various other fluid properties, most of which should already be familiar from elementary physics and thermodynamics courses. We next described numerous ways by means of which fluid flows can be classified and emphasized that for essentially all of these it is the <u>flow</u>, and not the fluid, that is being categorized. Then in the preceding section we provided an introduction to flow visualization by briefly describing three classic visualization techniques.

Chapter 3

The Equations of Fluid Motion

In this chapter we will derive the basic equations of motion for a viscous, incompressible fluid. As we noted earlier, there are <u>two</u> main physical principles involved: *i)* conservation of mass and *ii)* Newton's second law of motion, the latter of which leads to a system of equations expressing the balance of momentum. In addition, we will utilize Newton's law of viscosity in the guise of what will be termed a "constitutive relation" and, of course, all of this will be done within the confines of the continuum hypothesis. We should also note that Newton's second law of motion formally applies to point masses, *i.e.*, discrete particles, making its application to fluid flow seem difficult at best. But we will see that because we can define fluid particles (via the continuum hypothesis), the difficulties are not actually so great.

We will begin with a brief discussion of the two types coordinate systems widely used in the study of fluid motion, and provide a mathematical operator that relates these. We then review some additional mathematical constructs that will be needed in the subsequent derivations. Once this groundwork has been completed we will derive the "continuity" equation which expresses the law of conservation of mass for a moving fluid, and we will consider some of its practical consequences. We then provide a similar analysis leading to the momentum equations, thus arriving at the complete set of equations known as the Navier–Stokes (N.–S.) equations. These equations are believed to represent <u>all fluid motion</u> within the confines of the continuum hypothesis. We will provide qualitative discussions of the physical importance of each of their various terms, and we will close the chapter with a treatment of dimensional analysis and similitude, first based on the equations of motion, and then via the more standard engineering approach—use of the *Buckingham* Π *Theorem*.

3.1   Lagrangian & Eulerian Systems; the Substantial Derivative

In the study of fluid motion there are two main approaches to describing what is happening. The first is known as the *Lagrangian* viewpoint which involves watching the movement of each individual fluid parcel as it moves from some initial location, often described as "placing a coordinate system on each fluid parcel" and "riding on that parcel as it travels through the fluid." At each instant in time the fluid particle(s) being studied will have a different set of coordinates within some global coordinate system, but each particle will be associated with a specific initial set of coordinates. The alternative is the *Eulerian* description. This corresponds to a coordinate system fixed in space, and in which fluid properties are studied as functions of time as the flow passes fixed spatial locations.

3.1.1   The Lagrangian viewpoint

Use of Lagrangian-coordinate formulations for the equations of fluid motion is very natural in light of the fact that Newton's second law applies to point masses, and it is reasonable to view a fluid parcel as such. The equations of motion that arise from this approach are relatively simple because they result from direct application of Newton's second law. But their solutions consist merely of the fluid particle <u>spatial location</u> at each instant of time, as depicted in Fig. 3.1. This figure shows two different fluid particles and their particle paths for a short period of time. Notice that it is the location of the fluid parcel at each time that is given, and this can be obtained directly by
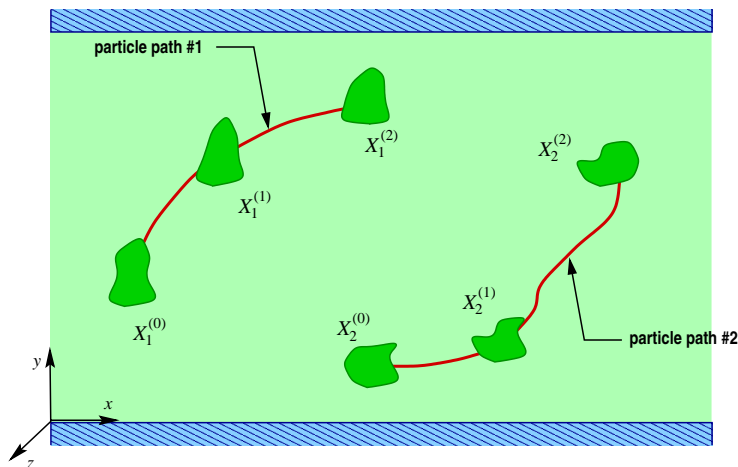
Figure 3.1: Fluid particles and trajectories in Lagrangian view of fluid motion.

solving the corresponding equations. The notation $X_1^{(0)}$ represents particle #1 at time $t = 0$, with X denoting the position vector $(x, y, z)^T$.

There are several important features of this representation requiring some explanation. First, it can be seen that the fluid parcel does not necessarily retain its size and shape during its motion. Later, when we derive the equation for mass conservation we will require that the mass of the fluid element remain fixed; hence, if the density is changing, which might well be the case, the volume must also change. Second, we can think of the changes in shape as having arisen due to interactions with neighboring fluid elements (not shown); we will treat this in more detail when we derive the momentum equations. We next observe that although the velocity is not directly calculated, it is easily deduced since, *e.g.*,

$$\frac{dx}{dt} = u \, .$$

Thus, if a sequence of locations of the fluid parcel is known for a period of time, it is easy to calculate its velocity (and acceleration) during this same period. Furthermore, we can think about obtaining values of any other fluid property (*e.g.*, temperature or pressure) at this sequence of locations by simply "measuring" them as we ride through the fluid on the fluid parcel. Finally, it must be emphasized that in order to obtain a complete description of the flow field using this approach it is necessary to track a very large number of fluid parcels. From a practical standpoint, either experimentally or computationally, this can present a significant burden. Furthermore, it is rather typical in engineering applications to need to know fluid properties and behavior at specific points in a flow field. In the context of a Lagrangian description it is difficult to specify, *a priori*, which fluid parcel to follow in order to obtain the desired information at some later time.

3.1.2 The Eulerian viewpoint

An alternative to the Lagrangian representation is the Eulerian view of a flowing fluid. This corresponds to a coordinate system fixed in space, and within which fluid properties are monitored as functions of time as the flow passes <u>fixed</u> spatial locations. Figure 3.2 is a simple representation of this situation. It is evident that in this case we need not be explicitly concerned with individual
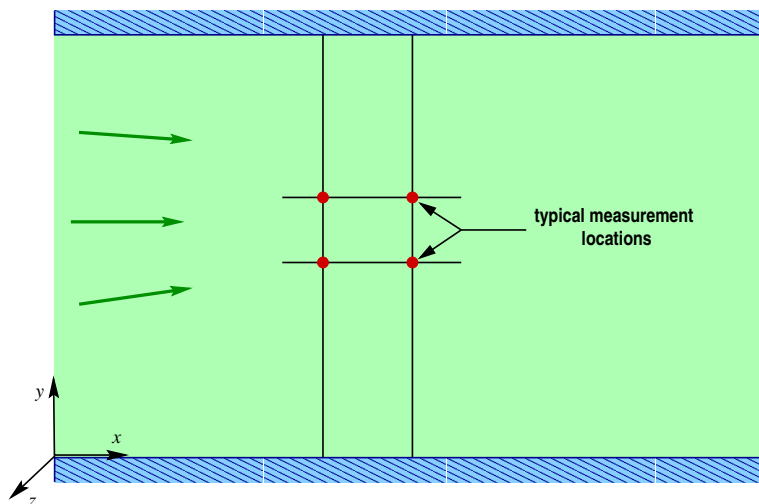
Figure 3.2: Eulerian view of fluid motion.

fluid parcels or their trajectories. Moreover, the flow velocity will now be measured directly at these locations rather than being deduced from the time rate-of-change of fluid parcel location in a neighborhood of the desired measurement points. It is fairly clear that this approach is more suitable for practical purposes, and essentially all engineering analyses of fluid flow are conducted in this manner. On the other hand, such a viewpoint does not produce "total" acceleration along the direction of motion of fluid parcels as needed for use of Newton's second law. It is worth noting that, because of this, physicists still typically employ a Lagrangian approach.

3.1.3 The substantial derivative

The disadvantage of use of an Eulerian "reference frame," especially in the context of deriving the equations of fluid motion, is the difficulty of obtaining acceleration at a point. In the case of the Lagrangian formulation, heuristically, one need only attach an accelerometer to a fluid parcel and record the results. But when taking measurements at a single (or a few, possibly, widely-spaced) points as in the Eulerian approach, it is more difficult to produce a formula for acceleration (and for velocity as well) in the direction of motion of fluid elements. With respect to the mathematical treatment of the equations of motion, this difficulty is overcome by expressing accelerations in an Eulerian reference frame in terms of those in a Lagrangian system. This can be done via a particular differential operator known as the *substantial* (or *material*) *derivative* which can be derived by enforcing an equivalence of motion in the two types of reference frames. We first state the formal definition of this operator after which we will consider some of the physical and mathematical details.

Definition 3.1 *The <u>substantial derivative</u> of any fluid property $f(x, y, z, t)$ in a flow field with*

velocity vector $\boldsymbol{U} = (u, v, w)^T$ *is given by*

$$
\begin{aligned}
\frac{Df}{Dt} &\equiv \frac{\partial f}{\partial t} + u\frac{\partial f}{\partial x} + v\frac{\partial f}{\partial y} + w\frac{\partial f}{\partial z} \\[2mm]
&= \frac{\partial f}{\partial t} + \boldsymbol{U} \cdot \nabla f\,.
\end{aligned}
\tag{3.1}
$$

We again recall that the operator ∇ is a vector differential operator defined as $\nabla \equiv (\partial/\partial x, \partial/\partial y, \partial/\partial z)^T$, so that in our subscript notation used earlier $\nabla f = (f_x, f_y, f_z)^T$.

It is worthwhile to consider some details regarding the substantial derivative. First, it is easily derived via a straightforward application of the chain rule and use of the definitions of the velocity components. For example, for a general function f which might represent an arbitrary fluid property we can write

$$
f(x, y, z) = f(x(t), y(t), z(t))
$$

if we recall that in a Lagrangian system the spatial coordinates of fluid particles are functions of time—so, any property associated with that fluid particle would also, in general, change with time. Now differentiate f with respect to t using the chain rule:

$$
\begin{aligned}
\frac{df}{dt} &= \frac{\partial f}{\partial x}\frac{dx}{dt} + \frac{\partial f}{\partial y}\frac{dy}{dt} + \frac{\partial f}{\partial z}\frac{dz}{dt} + \frac{\partial f}{\partial t}\frac{dt}{dt} \\[2mm]
&= \frac{\partial f}{\partial t} + u\frac{\partial f}{\partial x} + v\frac{\partial f}{\partial y} + w\frac{\partial f}{\partial z}\,,
\end{aligned}
$$

where the last line is obtained using definitions of velocity components given earlier in our discussion of streamlines (Chap. 2) and is identical to Eq. (3.1) except for notation on the left-hand side.

We again emphasize that the substantial derivative of any property is simply an Eulerian-coordinate representation of the Lagrangian derivative of that property. Thus, in the case of velocity components the substantial derivative is the *Lagrangian acceleration.* This terminology is often used, but the term *Eulerian acceleration* is also sometimes employed with the same meaning. It is also important to observe that the D/Dt notation of Eq. (3.1), although the single most common one, is not found universally; in fact, the simple d/dt is also quite often employed, and sometimes termed "total acceleration."

If we take $f = u$, the x component of velocity, the substantial derivative given in Eq. (3.1) is

$$
\frac{Du}{Dt} = \underbrace{\frac{\partial u}{\partial t}}_{\text{local accel.}} + \underbrace{u\frac{\partial u}{\partial x} + v\frac{\partial u}{\partial y} + w\frac{\partial u}{\partial z}}_{\text{convective acceleration}}\,,
\tag{3.2}
$$

and this represents the x-direction (Lagrangian, or total) acceleration, a_x, of a fluid parcel expressed in an Eulerian reference frame. We see that this consists of two contributions. The first of these is the *local acceleration* which would be present if we were to attempt to calculate the acceleration only with respect to the Eulerian coordinates; it is simply the time rate-of-change of the velocity component u at any specified spatial location. The second is the set of terms,

$$
\boldsymbol{U} \cdot \nabla u = u\frac{\partial u}{\partial x} + v\frac{\partial u}{\partial y} + w\frac{\partial u}{\partial z}\,,
$$

known as the *convective acceleration.* This quantity depends on both the local (in the same sense as above—point of evaluation) velocity and local velocity gradients, and it is the part of the total acceleration that arises specifically from the fact that the substantial derivative provides a Lagrangian

description. In particular, it represents spatial changes in velocity (or any other fluid property) due to motion of a fluid parcel being carried (convected) by the flow field $(u, v, w)^T$. It is important to observe that this contribution to the acceleration implies that fluid parcels may be accelerating even in a steady (time-independent) flow field, a result that might at first seem counterintuitive.

Consider steady flow in a convergent-divergent nozzle shown in Fig. 3.3. As always, flow speed
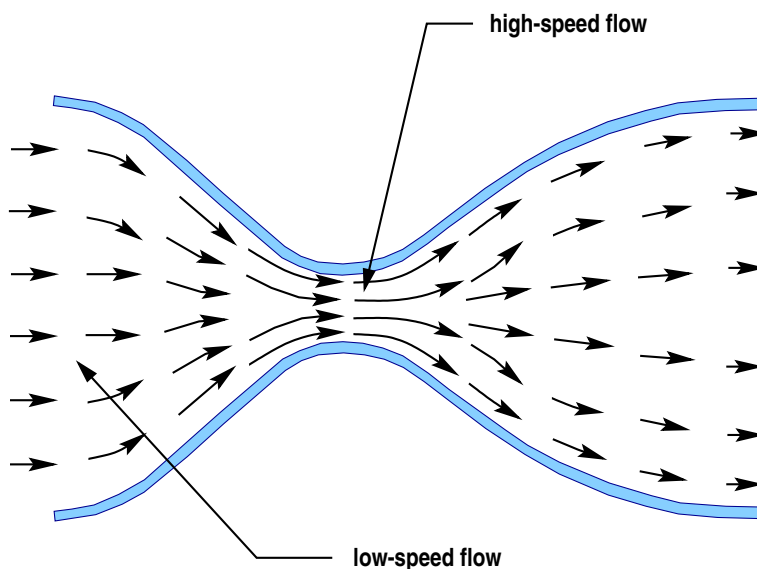
Figure 3.3: Steady accelerating flow in a nozzle.

is indicated by the length of the velocity vectors, and from this we see that the flow is experiencing an increase in speed as it enters the converging section of the nozzle. Our intuition should suggest that this is likely to occur, and we will later be able to show, analytically, that this must be the behavior of incompressible fluids. The main point here, however, is the fact that the flow velocity is changing spatially even though it is everywhere independent of time. This in turn implies that the convective acceleration must be nonzero, and hence the total acceleration given by the substantial derivative is also nonzero:

$$\frac{Du}{Dt} = uu_x + vu_y \neq 0\,,$$

and similarly,

$$\frac{Dv}{Dt} = uv_x + vv_y \neq 0\,,$$

for this 2-D case. That is, we have demonstrated acceleration in a steady flow.

We now consider a simple example to demonstrate calculating Lagrangian, or total, acceleration for a given velocity field.

EXAMPLE 3.1 Let the velocity field $\boldsymbol{U}$ have the components

$$u = x + y + z + t\,, \qquad v = x^2 y^3 z t\,, \qquad w = \exp(xyzt)\,.$$

Find the components of the Lagrangian acceleration.

The first thing to note when starting this calculation is that since the velocity field has three components, we should expect the acceleration to also be a vector with three components. In

particular, although we can concisely express Lagrangian acceleration in the form

$$\frac{D\boldsymbol{U}}{Dt} = \frac{\partial \boldsymbol{U}}{\partial t} + \boldsymbol{U} \cdot \nabla \boldsymbol{U} \,,$$

it is generally far simpler to work with the individual components. For example, the x-direction acceleration, which we shall denote as a_x, is given by

$$a_x \equiv \frac{Du}{Dt} = \frac{\partial u}{\partial t} + \boldsymbol{U} \cdot \nabla u \,,$$

or

$$a_x = u_t + u u_x + v u_y + w u_z \,,$$

with analogous expressions holding for the other two components:

$$
\begin{aligned}
a_y &= v_t + u v_x + v v_y + w v_z \,, \\
a_z &= w_t + u w_x + v w_y + w w_z \,.
\end{aligned}
$$

At this point, all that is required is carry out the indicated partial differentiations and substitute the results into the formulas. We have

$$u_t = 1 \,, \qquad u_x = 1 \,, \qquad u_y = 1 \,, \qquad u_z = 1 \,,$$

$$v_t = x^2 y^3 z \,, \qquad v_x = 2xy^3 zt \,, \qquad v_y = 3x^2 y^2 zt \,, \qquad v_z = x^2 y^3 t \,,$$

and

$$w_t = xyz \exp(xyzt) \,, \qquad w_x = yzt \exp(xyzt) \,, \qquad w_y = xzt \exp(xyzt) \,, \qquad w_z = xyt \exp(xyzt) \,.$$

It then follows from the above equations that

$$
\begin{aligned}
a_x &= 1 + (x + y + z + t) \cdot (1) + x^2 y^3 zt \cdot (1) + \exp(xyzt) \cdot (1) \,, \\
a_y &= x^2 y^3 z + (x + y + z + t) \cdot (2xy^3 zt) + (x^2 y^3 zt) \cdot (2xy^3 zt) + \exp(xyzt) \cdot (x^2 y^3 t) \,, \\
a_z &= xyz \exp(xyzt) + (x + y + z + t) \cdot (yzt \exp(xyzt)) + (x^2 y^3 zt) \cdot (xyt \exp(xyzt)) \,.
\end{aligned}
$$

3.2   Review of Pertinent Vector Calculus

In this section we will briefly review the parts of vector calculus that will be needed for deriving the equations of fluid motion. There are two main theorems from which essentially everything else we will need can be derived: Gauss's theorem and the general transport theorem. The first of these is usually encountered in elementary physics classes, but we will provide a fairly detailed (but non-rigorous) treatment here. The second is rather obscure and occurs mainly only in fluid dynamics; but it is very important, and it is quite directly related to an elementary integration formula due to Leibnitz.

3.2.1   Gauss's theorem

Gauss's theorem corresponds to a quite simple and rather intuitive idea: the integral of a derivative equals the net value of the function (whose derivative is being integrated) over the boundary of the domain of integration. In one space dimension this is precisely the *fundamental theorem of calculus*:

$$\int_a^b f(x)dx = F(b) - F(a) \,, \tag{3.3}$$

where $F(x)$ is a function such that $F'(x) = f(x)$; *i.e.*, F is the *antiderivative* or *primitive* of f. Thus, in keeping with our original statement, Eq. (3.3) can be expressed as

$$\int_a^b F'(x)dx = F(b) - F(a) \,. \tag{3.4}$$

The Divergence Theorem

This basic idea contained in Eq. (3.4) generalizes to two dimensions in the form of Gauss's theorem and the related Stokes' theorem and to three dimensions as Gauss's theorem, which is also known as the *divergence theorem*. It is this last form that will be of particular use in our later derivations.

Theorem 3.1 *(Gauss, or divergence) For any smooth vector field $\boldsymbol{F}$ over a region $\mathcal{R} \subset \mathbb{R}^3$ with a smooth boundary $\mathcal{S}$*

$$\int_{\mathcal{R}} \nabla \cdot \boldsymbol{F} \, dV = \int_{\mathcal{S}} \boldsymbol{F} \cdot \boldsymbol{n} \, dA. \tag{3.5}$$

We shall not prove this theorem here, but we will comment on some of the terminology and provide a physical interpretation.

We first remark that the similarities between the 1-D and 3-D cases should be obvious. For both of these (Eq. (3.4) and Eq. (3.5), respectvely) the left-hand side integral is over a region (an interval in the first case, and a volume in the second), and the integrand is a derivative—a simple, ordinary derivative in the 1-D case, and a divergence in the 3-D case. Furthermore, the right-hand side in both cases is an evaluation over the surface of the region (simply the endpoints of an interval in the 1-D case) of the function whose derivative appears in the integrand on the left-hand side.

We next need to provide some detail regarding terminology. The term *smooth* simply means "sufficiently differentiable that any desired operation associated with differentiation or integration can be easily justified." A *vector field* is a vector whose components are functions of the spatial coordinates, and possibly also time. Thus, the formal representation of a vector field $\boldsymbol{F}$ is

$$\boldsymbol{F}(x, y, z) = (F_1(x, y, z), F_2(x, y, z), F_3(x, y, z))^T \,.$$

We have already encountered velocity fields, and these will be our most-often used examples of vector fields in this course. The general time-dependent version of a 3-D velocity field is

$$\boldsymbol{U}(x, y, z, t) = (u(x, y, z, t), v(x, y, z, t), w(x, y, z, t))^T \,.$$

The integrands of both the volume and surface integrals of Gauss's theorem also need some explanation. The operation $\nabla \cdot \boldsymbol{F}$ is called the *divergence* of $\boldsymbol{F}$. We will say more about its physical interpretation later and here focus on the mathematics. Its form should be reminiscent of the "dot product" of two vectors, and that is essentially what it is. But recall that in forming the dot product of two vectors we <u>multiply</u> corresponding components of the two vectors, and then sum the results—thus producing a scalar quantity. In constructing the divergence of a vector field we carry out the same basic set of operations except that multiplication must be viewed in a more abstract way; *viz.*, operation on a component of a vector field by a differential operator is viewed, abstractly, as multiplication. Thus, we can write

$$\begin{aligned}
\nabla \cdot \boldsymbol{F} &= \left(\frac{\partial}{\partial x}, \frac{\partial}{\partial y}, \frac{\partial}{\partial z} \right) \cdot (F_1, F_2, F_3)^T \\
&= \frac{\partial F_1}{\partial x} + \frac{\partial F_2}{\partial y} + \frac{\partial F_3}{\partial z} \,.
\end{aligned} \tag{3.6}$$

The analogy with the vector dot product should be clear, and in particular we see that the divergence of a vector field is a <u>scalar</u> function.

An interesting point here is that integration of scalar functions over volumes is generally not particularly difficult, while integration of vectors over surfaces can be considerably less straightforward. Thus, among its other uses, Gauss's theorem provides a way to transform potentially complicated integrations over surfaces to much less complicated ones over volumes. But, sometimes just the opposite may be true (and we will later encounter cases of this).

To aid the understanding of the right-hand side surface integral in Gauss's theorem we provide Fig. 3.4. This figure displays the geometry of surface integration, showing the vector field $\boldsymbol{F}$ over
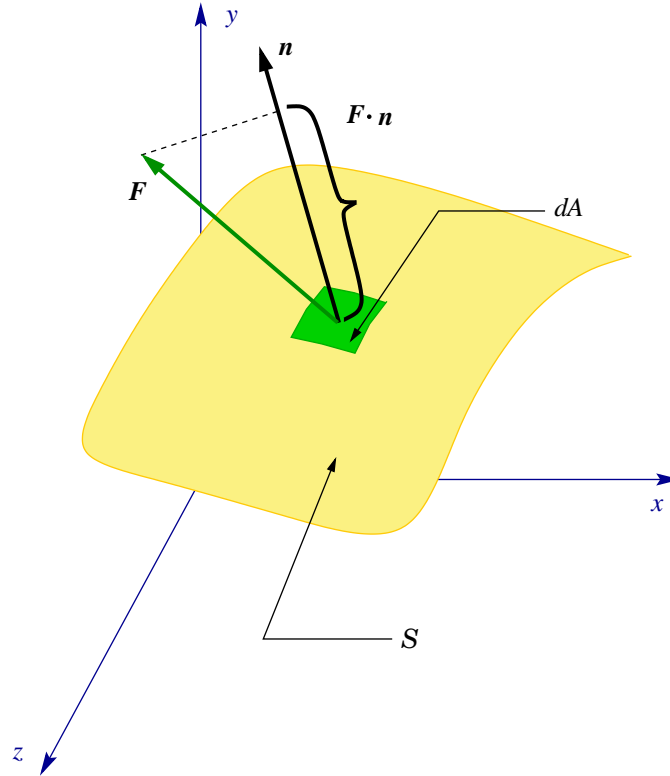
Figure 3.4: Integration of a vector field over a surface.

a differential element of surface dA. Also shown are the outward unit normal vector $\boldsymbol{n}$ and the projection of $\boldsymbol{F}$ onto $\boldsymbol{n}$, $\boldsymbol{F} \cdot \boldsymbol{n}$. This latter quantity is the amount of $\boldsymbol{F}$ actually going through the surface at that point (any component tangent to the surface cannot penetrate the surface). Then the integral over $\mathcal{S}$ is just the sum of these projections multiplied by their corresponding differential areas, in the limit of the area patches approaching zero.

Finally we note that Gauss's theorem is usually given the following "physical" interpretation. Since the divergence of a vector field at a point is said to indicate the tendency of the field to "radiate outward" from that point, the left-hand side of Eq. (3.5) provides a measure of the expansive tendencies of the vector function within the region $\mathcal{R}$. On the right-hand side $\boldsymbol{F} \cdot \boldsymbol{n} \, dA$ is the component of $\boldsymbol{F}$ crossing through the area element dA, as already noted. Thus, the right-hand side integral in Eq. (3.5) is related to the flux of $\boldsymbol{F}$ through the surface $\mathcal{S}$. Thus, we might express Gauss's theorem verbally as: the radiation of a quantity from a volume equals the flux of the quantity coming through the surface of the volume.

Application of Gauss's Theorem to a Scalar Function

It is sometimes useful to be able to apply a result of the form of Gauss's theorem to scalar functions, but it is quite clear from the form of the divergence operator on the left-hand side of Eq. (3.5) that this cannot be done directly. On the other hand, suppose we consider a vector field $\boldsymbol{F}$ that can be expressed as

$$\boldsymbol{F} = f\boldsymbol{b} \,,$$

where f is a scalar function, and $\boldsymbol{b}$ is an arbitrary (but nonzero) <u>constant</u> vector. Then we can correctly write Eq. (3.5) as

$$\int_{\mathcal{R}} \nabla \cdot f\boldsymbol{b} \, dV = \int_{\mathcal{S}} f\boldsymbol{b} \cdot \boldsymbol{n} \, dA \,.$$

Now we apply product-rule differentiation to the divergence in the left-hand side integral to obtain

$$\begin{aligned} \nabla \cdot f\boldsymbol{b} &= \boldsymbol{b} \cdot \nabla f + f\nabla \cdot \boldsymbol{b} \\ &= \boldsymbol{b} \cdot \nabla f \,, \end{aligned}$$

because $\boldsymbol{b} \equiv const.$ We remind the reader that the simplest way to apply the product rule for vector differential operators is to first "think about" applying it as if only scalars were involved, and then use the appropriate vector differential operators in each term to maintain a consistent order (*e.g.*, scalar, vector, matrix) for all terms in the equation. It is easily checked that all terms in the above expression are scalars—as divergence of a vector must be, from its definition.

We can now write

$$\int_{\mathcal{R}} \boldsymbol{b} \cdot \nabla f \, dV = \int_{\mathcal{S}} f\boldsymbol{b} \cdot \boldsymbol{n} \, dA \,,$$

which implies

$$\boldsymbol{b} \cdot \left[\int_{\mathcal{R}} \nabla f \, dV - \int_{\mathcal{S}} f\boldsymbol{n} \, dA \right] = 0 \,,$$

and since $\boldsymbol{b} \neq 0$ we have for Gauss's theorem

$$\int_{\mathcal{R}} \nabla f \, dV = \int_{\mathcal{S}} f\boldsymbol{n} \, dA \,. \tag{3.7}$$

Thus, the integral of the gradient of a scalar function f over a volume $\mathcal{R}$ equals the integral of f over the surface $\mathcal{S}$. Observe that the order is maintained across the equal sign since ∇f is a vector, and $f\boldsymbol{n}$ is also a vector. (From an "operational" standpoint, it is preferable to consider $\boldsymbol{n}dA$ as the vector on the right-hand side in this case because the outward unit normal vector $\boldsymbol{n}$ must be constructed so as to be perpendicular to the tangent plane of $\mathcal{S}$ in a neighborhood of dA.)

3.2.2 General transport theorem

As was mentioned earlier, the main uses of transport theorems come in deriving the equations of fluid dynamics, and other transport phenomena. We will follow an approach in this section similar to that emloyed in the discussion of Gauss's theorem; namely, we will first consider a 1-D example on the real line $\mathbb{R}$ to introduce the basic notions, and then extend these in a mainly heuristic way to multi-dimensional cases such as we will need in the present lectures. Thus, we will begin with an integration formula on the real line known as Leibnitz's formula; we then generalize this to 3-D (but it will work in any number of dimensions), and we conclude by providing a special case known as the Reynolds transport theorem. The basic problem being treated in all these cases is moving differentiation of an integral into the integrand when the limits of integration depend on the parameter with respect to which differentiation is being performed.

<div align="center">**Leibnitz's Formula**</div>

The simplest application of this type is *Leibnitz's formula* which, as we have already noted, applies on the real line. This takes the form

$$\frac{d}{dt}\int_{a(t)}^{b(t)} f(x,t)dx = \int_{a(t)}^{b(t)} \frac{\partial f}{\partial t}dx + \frac{\partial b}{\partial t}f(b,t) - \frac{\partial a}{\partial t}f(a,t), \tag{3.8}$$

where we have denoted the parameter by t since our applications of transport theorems will be in the context of time-dependent problems. Clearly this formula gives us a means by which to exchange integration and differentiation in cases where it would not be correct to simply move the differential operator through the integral sign and just differentiate the integrand.

It is of interest to consider the qualitative implications of this formula because they will be the same for all other integration formulas introduced in this section. Namely, Leibnitz's formula implies that the time-rate of change of a quantity f in a region (interval in this case) $[a(t), b(t)]$ that is changing in time is the rate of change of f within the region plus the net amount of f crossing the boundary of the region due to movement of the boundary. In particular, note that $\partial a/\partial t$ and $\partial b/\partial t$ are the speeds with which the respective boundary points are moving.

<div align="center">**The General Transport Theorem**</div>

Just as was true for the fundamental theorem of calculus, Leibnitz's formula possesses higher-dimensional analogues. In particular, in three dimensions we have the following.

Theorem 3.2 *(General Transport Theorem) Let $\boldsymbol{F}$ be a smooth vector (or scalar) field on a region $\mathcal{R}(t)$ whose boundary is $\mathcal{S}(t)$, and let $\boldsymbol{W}$ be the velocity field of the time-dependent movement of $\mathcal{S}(t)$. Then*

$$\frac{d}{dt}\int_{\mathcal{R}(t)} \boldsymbol{F}(\boldsymbol{x},t)\, dV = \int_{\mathcal{R}(t)} \frac{\partial \boldsymbol{F}}{\partial t}\, dV + \int_{\mathcal{S}(t)} \boldsymbol{F}\boldsymbol{W}\cdot\boldsymbol{n}\, dA. \tag{3.9}$$

The formula Eq. (3.9) is called the *general transport theorem*, and certain specific cases of it will be widely used in the sequel.

Before going on to this, however, it is worthwhile to again check whether the indicated vector operations are consistent from term to term in this equation. It should be clear, independent of the order of $\boldsymbol{F}$, that the first term on the right-hand side is consistent with that on the left-hand side since they differ only with respect to differentiation by a <u>scalar</u> parameter. It is the second term on the right that must be examined with more care. First, consider the case when $\boldsymbol{F}$ is a vector field, say of dimension three for definiteness. Then the first integral on the right is acting also on a 3-D vector field. We will assume that the velocity field $\boldsymbol{W}$ is also 3D (although this is not strictly necessary), and that the region $\mathcal{R}(t)$ is spatially 3D. Then the question is "What is the order of the integrand of this second integral?" But it is easy to see that the dot product of $\boldsymbol{W}$ and $\boldsymbol{n}$ leads to a <u>scalar</u>, a number—maybe different at each point of $\mathcal{S}(t)$, but nevertheless, a scalar; and a scalar times a vector is a vector. Hence, we obtain the correct order.

Now suppose $\boldsymbol{F}$ is replaced with a scalar function F. Then clearly the left-hand side and the first term on the right-hand side of Eq. (3.9) are scalars. But now this is also true of the second integral because, as before, the dot product of $\boldsymbol{W}$ and $\boldsymbol{n}$ produces a scalar, and this now multiplies the <u>scalar</u> F. In fact, it should be clear that $\boldsymbol{F}$ could be a matrix (often called a "tensor" in fluid dynamics), and the formula would still work.

Reynolds Transport Theorem

The most widely-encountered corollary of the general transport theorem, at least in fluid dynamics, is the following.

Theorem 3.3 *Let* $\mathbf{\Phi}$ *be any smooth vector (or scalar) field, and suppose* $\mathcal{R}(t)$ *is a* <u>*fluid element*</u> *with surface* $\mathcal{S}(t)$ *traveling at the flow velocity* $\boldsymbol{U}$. *Then*

$$\frac{D}{Dt} \int_{\mathcal{R}(t)} \mathbf{\Phi} \, dV = \int_{\mathcal{R}(t)} \frac{\partial \mathbf{\Phi}}{\partial t} \, dV \int_{\mathcal{S}(t)} \mathbf{\Phi} \boldsymbol{U} \cdot \boldsymbol{n} \, dA \,. \tag{3.10}$$

This formula is called the *Reynolds transport theorem*, and just as was the case for $\boldsymbol{F}$ in the general transport theorem, $\mathbf{\Phi}$ can have any order. But we will deal mainly with the scalar case in the sequel. There are two important things to notice in comparing this special case with the general formula. The first is that the integral on the left-hand side is now being differentiated with respect to the <u>substantial derivative</u>, and the second is that the velocity field in the second integral on the right is now $\boldsymbol{U}$, which is taken to be the velocity of an arbitrary fluid parcel. These restrictions will play a crucial role in later derivations.

Equation (3.10) follows immediately from the general transport theorem using these two restrictions and the chain rule for differentiation. We demonstrate this for the scalar case, and leave the vector case to ambitious readers. We begin by defining

$$F(x(t), y(t), z(t)) \equiv \int_{\mathcal{R}(t)} \Phi \, dV \tag{3.11}$$

with $\mathcal{R}(t)$ taken to be a <u>fluid element</u> (and hence the (x, y, z)-dependence of F). Now the general transport theorem applied to the scalar Φ is

$$\frac{d}{dt} \int_{\mathcal{R}(t)} \Phi \, dV = \int_{\mathcal{R}(t)} \frac{\partial \Phi}{\partial t} \, dV + \int_{\mathcal{S}(t)} \Phi \boldsymbol{W} \cdot \boldsymbol{n} \, dA \,,$$

but since $\mathcal{R}(t)$ is a fluid element we can replace $\boldsymbol{W}$ in the above equation with $\boldsymbol{U}$ to obtain

$$\frac{d}{dt} \int_{\mathcal{R}(t)} \Phi \, dV = \int_{\mathcal{R}(t)} \frac{\partial \Phi}{\partial t} \, dV + \int_{\mathcal{S}(t)} \Phi \boldsymbol{U} \cdot \boldsymbol{n} \, dA \,. \tag{3.12}$$

We next use the definition of the function F to write

$$\frac{d}{dt} \int_{\mathcal{R}(t)} \Phi \, dV = \frac{dF}{dt} \,,$$

and now we apply chain-rule differentiation to the right-hand side (just as we did earlier in "deriving" the substantial derivative). We obtain

$$\begin{aligned} \frac{dF}{dt} &= \frac{\partial F}{\partial t} \frac{dt}{dt} + \frac{\partial F}{\partial x} \frac{dx}{dt} + \frac{\partial F}{\partial y} \frac{dy}{dt} + \frac{\partial F}{\partial z} \frac{dz}{dt} \\ &= \frac{\partial F}{\partial t} + u \frac{\partial F}{\partial x} + v \frac{\partial F}{\partial y} + w \frac{\partial F}{\partial z} \\ &\equiv \frac{DF}{Dt} \,. \end{aligned} \tag{3.13}$$

This permits us to replace the ordinary derivative on the left-hand side of Eq. (3.12) with the substantial derivative (but only because $\mathcal{R}(t)$ is a fluid element traveling with velocity $(u, v, w)^T$), completing the derivation of Eq. (3.10) for the scalar case.

3.3   Conservation of Mass—the continuity equation

In this section we will derive the partial differential equation representing conservation of mass in a fluid flow, the so-called *continuity equation*. We will then, in a sense, "work backwards" to recover an integral form, often called the "control-volume" form, that can be applied to engineering calculations in an approximate, but very useful, way. We will then consider some specific examples of employing this equation.

3.3.1   Derivation of the continuity equation

We begin this section with the general statement of conservation of mass, and arrive at the differential form of the continuity equation via a straightforward analysis involving application of the general transport theorem and Gauss's theorem, both of which have been discussed in the previous section.

Conservation of Mass

We start by considering a fixed mass m of fluid contained in an arbitrary region $\mathcal{R}(t)$. As we have already hinted, we can identify this region with a fluid element, but in some cases we will choose to associate this with a macroscopic domain. In either case, the boundary $\mathcal{S}(t)$ of $\mathcal{R}(t)$ can in general move with time. Any such region is often termed a *system*, especially in thermodynamics contexts, and it might be either *open* or *closed*. From our point of view it is only important that it have <u>fixed mass</u>; it does not matter whether it is the same mass at all times—only that the amount is the same.

It is convenient for our purposes to relate the mass of the system to the density of the fluid comprising it via

$$m = \int_{\mathcal{R}(t)} \rho \, dV \, . \tag{3.14}$$

We emphasize that $\mathcal{R}(t)$ and ρ may both change with time, but they must do so in a way that leaves m unchanged if we are to have conservation of mass. An example of this might be a balloon filled with hot air surrounded by cooler air. As heat is transferred from the balloon to its surroundings, the temperature of the air inside the balloon will decrease, and the density will increase (equation of state for a perfect gas). At the same time the size of the balloon will shrink, corresponding to a change in $\mathcal{R}(t)$.

We can express this mathematically as

$$\frac{dm}{dt} = \frac{d}{dt} \int_{\mathcal{R}(t)} \rho \, dV = 0 \, . \tag{3.15}$$

That is, conservation of mass simply means that the time rate of change of mass of a system must be zero.

Application of General Transport Theorem

In order to proceed further toward our goal of obtaining a differential equation expressing mass conservation, we apply the general transport theorem to obtain

$$\int_{\mathcal{R}(t)} \frac{\partial \rho}{\partial t} \, dV + \int_{\mathcal{S}(t)} \rho \boldsymbol{W} \cdot \boldsymbol{n} \, dA = 0 \, . \tag{3.16}$$

In fluid systems it is often useful to take the velocity field $\boldsymbol{W}$ to be that of the flowing fluid, which corresponds to locally viewing $\mathcal{R}(t)$ as an arbitrary fluid element. When this is done Eq. (3.16) becomes

$$\int_{\mathcal{R}(t)} \frac{\partial \rho}{\partial t}\, dV + \int_{\mathcal{S}(t)} \rho \boldsymbol{U} \cdot \boldsymbol{n}\, dA = 0\,. \tag{3.17}$$

Use of Gauss's Theorem

At this point we recognize that our form of conservation of mass contains physical fluid properties that are useful for engineering analyses, namely the flow velocity $\boldsymbol{U}$ and the fluid density ρ. But the form of Eq. (3.17) is still somewhat complicated. In particular, it contains separate integrals over the fluid element's volume and over its surface. Our next step is to convert the surface integral to a volume integral by means of Gauss's theorem: recall that the form of this theorem will give, in the present case,

$$\int_{\mathcal{S}(t)} \rho \boldsymbol{U} \cdot \boldsymbol{n}\, dA = \int_{\mathcal{R}(t)} \nabla \cdot \rho \boldsymbol{U}\, dV\,,$$

and substitution of this into Eq. (3.17) leads to

$$\int_{\mathcal{R}(t)} \frac{\partial \rho}{\partial t} + \nabla \cdot \rho \boldsymbol{U}\, dV = 0\,. \tag{3.18}$$

The Differential Continuity Equation

We now recall that the region $\mathcal{R}(t)$ was arbitrary (*i.e.*, it can be made arbitrarily small—within the confines of the continuum hypothesis), and this implies that the integrand must be zero everywhere within $\mathcal{R}(t)$. If this were not so (*e.g.*, the integral is zero because there are positive and negative contributions that cancel), we could subdivide $\mathcal{R}(t)$ into smaller regions over which the integral was either positive or negative, and hence violating the fact that it is actually zero. Thus, we conclude that

$$\frac{\partial \rho}{\partial t} + \nabla \cdot \rho \boldsymbol{U} = 0\,. \tag{3.19}$$

This is the *differential form* of the continuity equation, the expression for mass conservation in a flowing system.

3.3.2 Other Forms of the Differential Continuity Equation

In this section we will write Eq. (3.19) in some alternative forms that will aid in understanding its mathematical structure and in applying it in specific physical situations. We first carry out the differentiations indicated by the divergence operator to obtain the equivalent form

$$\frac{\partial \rho}{\partial t} + \frac{\partial}{\partial x}(\rho u) + \frac{\partial}{\partial y}(\rho v) + \frac{\partial}{\partial z}(\rho w) = 0\,, \tag{3.20}$$

or in short-hand notation

$$\rho_t + (\rho u)_x + (\rho v)_y + (\rho w)_z = 0\,.$$

If we now apply the product rule for each of the spatial differentiations and use the definition of the substantial derivative, we find that

$$\frac{D\rho}{Dt} + \rho \nabla \cdot \boldsymbol{U} = 0\,,$$

which provides yet another equivalent alternative to the original form Eq. (3.19).

An important simplification of Eq. (3.19) occurs when the density is <u>constant</u>, for then $\partial\rho/\partial t = 0$, and we see from Eq. (3.20) that division by ρ leads to

$$\nabla \cdot \boldsymbol{U} = 0\,,$$

or, again, in our short-hand notation for partial differentiation

$$u_x + v_y + w_z = 0\,. \tag{3.21}$$

This is the continuity equation for <u>incompressible flow</u>. It corresponds to divergence of the velocity field being identically zero leading to the terminology "divergence free" (or, sometimes, "solenoidal") for incompressible flows. It expresses the law of mass conservation for such flows and, as we shall discuss in more detail later, it is the equation that sets the pressure field in an incompressible flow.

3.3.3   Simple application of the continuity equation

It is apparent from Eqs. (3.20) and (3.21) that if we somehow know the functional form of the velocity field and, in the case of (3.20) also the density distribution, we can determine from a direct calculation whether mass is being conserved, and thus whether the given flow is <u>physically possible</u>. We demonstrate this with the following example.

EXAMPLE 3.2 Consider a steady incompressible flow with velocity field

$$u(x,y,z) = 2x + y + z\,, \qquad v(x,y,z) = -y\,, \qquad w(x,y,z) = -z\,.$$

Then

$$u_x = 2\,, \qquad v_y = -1\,, \qquad w_z = -1\,,$$

and substitution into Eq. (3.21) gives

$$2 + (-1) + (-1) = 0\,.$$

Hence, mass is conserved, and this flow field is a "physically possible" one. We mention here that once a flow field and the density distribution are known it is always possible to check mass conservation at any point in the flow, and if we find that the continuity equation is not satisfied, it must be the case that the flow field, the density (or both), is (are) invalid. This test is essentially always performed for computational results, and it is now becoming possible to also do this with laboratory measurements obtained via PIV.

It is important to recognize that solving the continuity equation in the form of either (3.20) or (3.21) is nontrivial. These are partial differential equations (PDEs) and, moreover, the single continuity equation contains more than a single unknown. Hence, additional equations to be derived later are needed before solution can be considered. But even when there is a sufficient number of equations to match the number of unknowns, analytical solutions can seldom be derived. Most results must be computed with CFD techniques.

3.3.4   Control volume (integral) analysis of the continuity equation

We will now introduce a much simpler approach than attempting to solve the PDE that is the continuity equation. We will see that this can often be carried out analytically and, although it does not always produce exact results, what is obtained is often surprisingly accurate, and thus

quite useful for engineering analyses. We first derive the control-volume continuity equation from the differential equation, and we then apply this to several examples.

In such practical applications it is sometimes helpful to deal with <u>finite</u> volumes, often called *control volumes*, having bounding surfaces called *control surfaces*. Control volumes and their associated control surfaces are selected (defined) for convenience in solving any given problem, and while there usually is not a unique way to define the control volume the ease with which any particular problem might be solved can depend very strongly on that choice. Furthermore, it is important to note that a control volume does not necessarily coincide with the "system" defined earlier, as will be apparent as we proceed.

Derivation of Control-Volume Continuity Equation

Since Eq. (3.19) must hold at <u>every</u> point in a fluid, if we now take $\mathcal{R}$ to be a control volume (rather than a fluid element as done earlier) we can write

$$\int_{\mathcal{R}} \frac{\partial \rho}{\partial t} + \nabla \cdot \rho \boldsymbol{U} \, dV = 0 \,,$$

which is the same as Eq. (3.19) except that our interpretation of $\mathcal{R}$ has changed. We next use Gauss's theorem "in reverse" to convert the second term back to a surface integral. This leads to

$$\int_{\mathcal{R}(t)} \frac{\partial \rho}{\partial t} \, dV + \int_{\mathcal{S}(t)} \rho \boldsymbol{U} \cdot \boldsymbol{n} \, dA = 0 \,.$$

Finally, we apply the transport theorem, Eq. (3.9) with $\boldsymbol{F} = F = \rho$ to obtain

$$\frac{d}{dt} \int_{\mathcal{R}(t)} \rho dV = -\int_{\mathcal{S}(t)} \rho \boldsymbol{U} \cdot \boldsymbol{n} \, dA + \int_{\mathcal{S}(t)} \rho \boldsymbol{W} \cdot \boldsymbol{n} \, dA \,,$$

or

$$\frac{d}{dt} \int_{\mathcal{R}(t)} \rho dV + \int_{\mathcal{S}(t)} \rho (\boldsymbol{U} - \boldsymbol{W}) \cdot \boldsymbol{n} \, dA = 0 \,. \tag{3.22}$$

It is worthwhile to note that $\boldsymbol{U}$ is the flow velocity in the control volume $\mathcal{R}(t)$, and $\boldsymbol{W}$ is the velocity of the control surface $\mathcal{S}(t)$. Furthermore, as already indicated by Eq. (3.15), the first term is just the time-rate of change of mass in the control volume $\mathcal{R}(t)$.

In Eq. (3.22) it is useful to divide the control surface area into three distinct parts:

  i) $\mathcal{S}_e(t)$, the area of entrances and exits through which fluid may enter or leave the control volume;

  ii) $\mathcal{S}_m(t)$, the area of solid moving surfaces; and

  iii) $\mathcal{S}_f(t)$, the area of solid <u>fixed</u> surfaces.

Observe that any, or all, of these can in principle change with time. Figure 3.5 provides an example showing these different contributions to the control surface $\mathcal{S}$.

In this figure we see that the valves of the piston make up the parts of $\mathcal{S}$ corresponding to entrances and exits and are labeled $\mathcal{S}_e$. The head of the head and sidewalls of the cylinder are fixed and denoted by $\mathcal{S}_f$; but it should be noted that the actual area corresponding to the surface of the control volume $\mathcal{R}(t)$ is changing with time; and it is mainly the exposed area of the sidewalls that comprises this. Finally, the moving piston surface contributes and area $\mathcal{S}_m$. In the present case this area is moving but constant in value. Our intuition would suggest from all this that it is
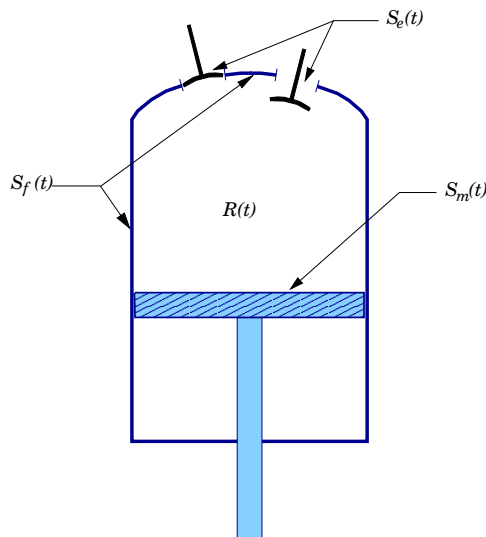
Figure 3.5: Contributions to a control surface.

only the surfaces corresponding to $\mathcal{S}_e(t)$ that can contribute to changes to the mass of the control volume since it is only through these areas that mass can enter or leave. We will now provide a detailed demonstration of why this must be true, strictly in a mathematical sense.

We can now express the second term in Eq. (3.22) as

$$\int_{\mathcal{S}(t)} \rho(\boldsymbol{U} - \boldsymbol{W}) \cdot \boldsymbol{n}\, dA = \int_{\mathcal{S}_e(t)} \rho(\boldsymbol{U} - \boldsymbol{W}) \cdot \boldsymbol{n}\, dA + \int_{\mathcal{S}_m(t)} \rho(\boldsymbol{U} - \boldsymbol{W}) \cdot \boldsymbol{n}\, dA + \int_{\mathcal{S}_f(t)} \rho(\boldsymbol{U} - \boldsymbol{W}) \cdot \boldsymbol{n}\, dA\,.$$

Now observe that on fixed surfaces $\mathcal{S}_f$, $\boldsymbol{U} \cdot \boldsymbol{n} = \boldsymbol{W} \cdot \boldsymbol{n} = 0$, and on moving surfaces $\mathcal{S}_m$, $\boldsymbol{U} \cdot \boldsymbol{n} = \boldsymbol{W} \cdot \boldsymbol{n}$, implying that $(\boldsymbol{U} - \boldsymbol{W}) \cdot \boldsymbol{n} = 0$ for both of these surface contributions. Thus, (3.22) collapses to

$$\frac{d}{dt} \int_{\mathcal{R}(t)} \rho\, dV + \int_{\mathcal{S}_e(t)} \rho(\boldsymbol{U} - \boldsymbol{W}) \cdot \boldsymbol{n}\, dA = 0\,. \tag{3.23}$$

It is clear from this equation that the only parts of the control surface that are actually important are those portions through which mass can either enter or leave the control volume. In words, Eq. (3.23) expresses the fairly obvious fact that

$$\left\{ \begin{array}{c} \text{time rate of increase} \\ \text{of control volume mass} \end{array} \right\} = \left\{ \begin{array}{c} \text{mass flux into} \\ \text{control volume} \end{array} \right\} - \left\{ \begin{array}{c} \text{mass flux out of} \\ \text{control volume} \end{array} \right\}\,.$$

We note that the flux of anything is

$$\textit{Flux} \sim \textit{Amount/Unit Area/Unit Time.}$$

Thus, if the mass flux out of the control volume is greater than that into it, the rate of increase of mass is negative, *i.e.*, the mass in the control volume is decreasing. In particular, it should be emphasized that this "word equation" and Eq. (3.23) which it represents imply that the mass in $\mathcal{R}(t)$ is <u>not</u> conserved (compare with Eq. (3.15)). Equation (3.23) is a *mass balance*.

Applications of Control-Volume Continuity Equation

We now apply Eq. (3.23) to some particular examples, some of which will be extremely simple, and some a bit more elaborate.

EXAMPLE 3.3 In this first example we assume the control volume $\mathcal{R}$ is fixed in space, and that it does not depend on time. Furthermore, we assume the entrance and exit are also fixed in both space and time and that the fluid density is independent of time but may possibly vary in space. Figure 3.6 depicts such a situation. Since $\mathcal{R}$ and $\mathcal{S}_e$ are no longer functions of time we can write
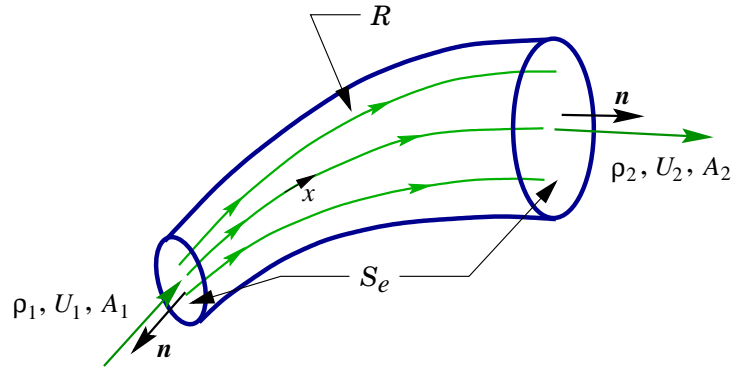
Figure 3.6: Simple control volume corresponding to flow through an expanding pipe.

Eq. (3.23) as

$$\int_{\mathcal{R}} \frac{\partial \rho}{\partial t}\, dV + \int_{\mathcal{S}_e} \rho \boldsymbol{U} \cdot \boldsymbol{n}\, dA = 0$$

because with the control volume fixed in space and the control surface also independent of time, it must be that $\boldsymbol{W} \equiv 0$. Then, since ρ is independent of time (but not necessarily constant in space) the first term on the left-hand side above is zero, and we are left with

$$\int_{\mathcal{S}_e} \rho \boldsymbol{U} \cdot \boldsymbol{n}\, dA = 0\,.$$

We now observe that in this case $\mathcal{S}_e$ consists of <u>two</u> pieces of area: A_1 (the entrance) and A_2 (the exit), as depicted in Fig. 3.6. If we now suppose that flow properties are uniform across each cross section (*i.e.*, we assume averaged one-dimensional flow), we have

$$\int_{\mathcal{S}_e} \rho \boldsymbol{U} \cdot \boldsymbol{n}\, dA = \underbrace{-\rho_1 U_1 A_1}_{\text{entrance}} + \underbrace{\rho_2 U_2 A_2}_{\text{exit}} = 0\,,$$

or

$$\rho_1 U_1 A_1 = \rho_2 U_2 A_2\,. \tag{3.24}$$

We should note that the minus sign in the first term on the right-hand side of the preceding equation arises because the flow direction and the outward unit normal are opposite at location 1, as shown in Fig. 3.6. This results in the form of Eq. (3.24), the steady, one-dimensional continuity equation.

If we now assume the flow to be incompressible so that $\rho_1 = \rho_2$, we see that

$$U_1 = U_2 \frac{A_2}{A_1}\,,$$

and since from Fig. 3.6 $A_2 > A_1$, it follows that $U_1 > U_2$. Thus, a steady incompressible flow must speed up when going through a constriction and slow down in an expansion, simply due to conservation of mass. Moreover, if we recall Fig. 3.3 and the fact that streamlines are everywhere tangent to the velocity field, we can deduce that the closer together are the streamlines, the faster the flow is moving.

It is easily checked that the units in Eq. (3.24) correspond to mass per unit time, and we call this the *mass flow rate*, denoted $\dot{m}$. In the present case of assumed uniform flow in each cross section we have

$$\dot{m} = \rho U A, \tag{3.25}$$

and in general we define the mass flow rate as

$$\dot{m} \equiv \int_{\mathcal{S}_e(t)} \rho \boldsymbol{U} \cdot \boldsymbol{n} \, dA \tag{3.26}$$

for any given surface $\mathcal{S}_e$. Finally, we should note that in the steady-state condition represented by Eq. (3.24) we can express this simply as

$$\dot{m}_{in} = \dot{m}_{out}.$$

A useful related concept is the *volume flow rate*, sometimes called the "discharge," usually denoted by Q and defined in our simple 1-D case by

$$Q = UA. \tag{3.27}$$

As with the mass flow rate, there is a more general definition,

$$Q \equiv \int_{\mathcal{S}_e(t)} \boldsymbol{U} \cdot \boldsymbol{n} \, dA,$$

which reduces to (3.27) if $\boldsymbol{U}$ is constant across the given cross section corresponding to $\mathcal{S}_e$. This formula shows that if the volume flow rate through a given area is known, we can immediately calculate the average velocity as

$$\overline{U} = \frac{Q}{A}.$$

The preceding example has shown that in a steady flow the mass flow rates must be constant from point to point, and if ρ is constant the volume flow rates must also be constant. The next example will demonstrate application of the control-volume continuity equation in an unsteady case.

EXAMPLE 3.4 Figure 3.7 displays a tank that is being simultaneously filled and drained with an incompressible fluid such as liquid kerosene. It is desired to determine the net rate of increase of volume of the fluid within the tank. The cross-sectional area of the inflowing liquid jet has been measured to be A_1 at a location where the (average over the cross section) velocity has magnitude U_1 and similarly, the outflow area is A_2 with corresponding velocity magnitude U_2. There are at least several different control volumes that might be defined to treat this problem; the one displayed with a dashed line is believed to be one of the simpler ones. It is to be noted that it contains all of the tank so that as the tank fills the new fluid will still be within the control volume. Furthermore, it isolates the jet of incoming liquid starting at a point where geometry and flow behavior are known. Moreover, the control surface is placed outside any regions where details of flow behavior are in doubt. Finally, we observe that although the control volume, itself, is changing with time the entrance and exit have been chosen to be independent of time, and in addition they
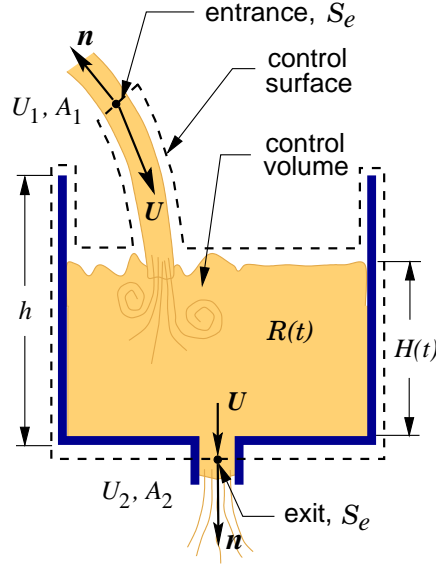
Figure 3.7: Time-dependent control volume for simultaneously filling and draining a tank.

are aligned perpendicular to the presumed flow direction at each of these, thus providing some further simplification.

Now the integral form of the continuity equation for this case is

$$\frac{d}{dt} \int_{\mathcal{R}(t)} \rho \, dV + \int_{\mathcal{S}_e} \rho \, (\boldsymbol{U} - \boldsymbol{W}) \cdot \boldsymbol{n} \, dA = 0 \,.$$

But the density ρ is constant corresponding to flow of an incompressible fluid. Furthermore, the flow velocity is one dimensional, varying only in the flow direction, and the entrance and exit are independent of time, implying that $\boldsymbol{W} = 0$. Thus, the above reduces to

$$\frac{d}{dt} \int_{\mathcal{R}(t)} dV + \int_{\mathcal{S}_e} U \boldsymbol{e}_1 \cdot \boldsymbol{n} \, dA = 0 \,,$$

where $\boldsymbol{e}_1$ is a local basis vector oriented in the flow direction.

We next denote the time-rate of change of volume of fluid by

$$\dot{V} \equiv \frac{d}{dt} \int_{\mathcal{R}(t)} dV \,,$$

and we can now write the integral continuity equation as

$$\dot{V} - U_1 A_1 + U_2 A_2 = 0 \,,$$

using the same sign conventions employed in the preceding example; thus

$$\dot{V} = Q_1 - Q_2 = Q_{in} - Q_{out} \,.$$

We should notice that when this equation is multiplied by ρ it provides an explicit example of the general physical principle stated after Eq. (3.23). Also observe that once $\dot{V}$ is known it can be used to find the time-rate of change of any appropriate physical dimension associated with the volume

of fluid; in particular, for any length scale L we have $\dot{V} = (\dot{L^3})$ from which we obtain $\dot{L} = \dot{V}/(3L^2)$. Thus, for example, if the geometry is known in say two of three directions corresponding to the volume of fluid, the time-rate of change of the third direction can be directly calculated. We leave as an exercise to the reader the task of applying this to determine the rate of change of $H(t)$, the height of fluid, in the above example.

As a final example in applying the control-volume continuity equation we will consider a case in which the entrances and exits are in motion but do not undergo changes of area.

EXAMPLE 3.5 Consider a jet plane in steady straight-and-level flight through still air at a speed U_p. We wish to determine $\dot{m}_{fuel}$, the fuel mass flow rate of one engine assuming the air density, ρ_i, engine intake area, A_i, engine exhaust nozzle area, velocity and density, A_e, U_e, ρ_e, respectively, are all known. Both U_p and U_e are speeds given with respect to a stationary observer on the ground. A sketch sufficient for analyzing this situation is provided in Fig. 3.8 We have not explicity pictured
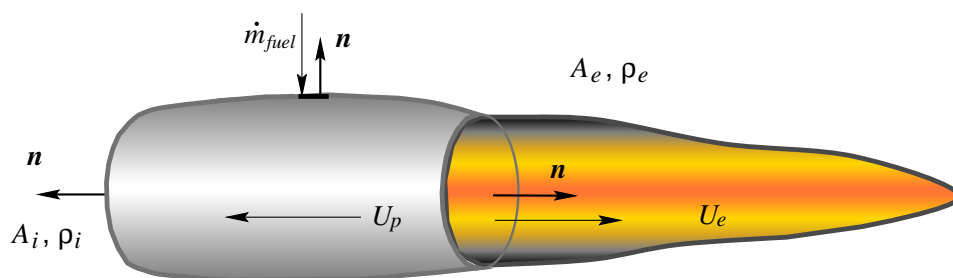
Figure 3.8: Calculation of fuel flow rate for jet aircraft engine.

the control volume for this problem because the natural one includes the entire engine, as is fairly obvious.

In this case since the only fluids involved are the incoming air, the fuel and the exhaust combustion gases, only a very crude model is needed to determine the mass flow rate of fuel. In particular, it is not necessary to deal with the individual engine components through which the various fluids pass as long as we can assume that no leaks of any fluid occur. The basic equation is the same as in the previous cases, *i.e.*, the control-volume continuity equation:

$$\frac{d}{dt} \int_{\mathcal{R}(t)} \rho \, dV + \int_{\mathcal{S}_e(t)} \rho \, (\boldsymbol{U} - \boldsymbol{W}) \cdot \boldsymbol{n} \, dA = 0 \,.$$

Since we are considering steady-state conditions $\mathcal{R}$ and $\mathcal{S}_e$ are independent of time. But it will be important to recognize that both the inlet plane and the exhaust plane of the engine are moving with respect to the air. We also note, as indicated above, that the jet exhaust velocity is taken with respect to a fixed coordinate system on the ground.

The first step in the analysis is to use time independence to write

$$\frac{d}{dt} \int_{\mathcal{R}} \rho \, dV = 0 \,.$$

We are then left with

$$\int_{\mathcal{S}_e} \rho \, (\boldsymbol{U} - \boldsymbol{W}) \cdot \boldsymbol{n} \, dA = 0 \,,$$

and we will next split this into three integrals—one for each of the entrances and/or exits of the control volume. Thus, we write

$$\int_{\mathcal{S}_{intake}} \rho\,(\boldsymbol{U} - \boldsymbol{W}) \cdot \boldsymbol{n}\,dA + \int_{\mathcal{S}_{fuel\,inlet}} \rho\,(\boldsymbol{U} - \boldsymbol{W}) \cdot \boldsymbol{n}\,dA + \int_{\mathcal{S}_{exhaust}} \rho\,(\boldsymbol{U} - \boldsymbol{W}) \cdot \boldsymbol{n}\,dA = 0\,,$$

and consider each of these integrals individually. We will invoke an assumption of uniform flow in each cross section and express the first integral, associated with the air intake, as

$$\int_{\mathcal{S}_{intake}} \rho\,(\boldsymbol{U} - \boldsymbol{W}) \cdot \boldsymbol{n}\,dA = \rho_i(U_i - U_p)\boldsymbol{e}_1 \cdot \boldsymbol{n}A_i = -\rho_i U_p A_i\,.$$

To obtain this result we have used the fact that the air is considered to be still (with respect to a fixed observer), implying $U_i = 0$, and that the plane (and its engine(s)) are moving with speed U_p. The outward normal vector at the intake is in the direction of the motion of the engine; hence the sign on the U_p-term remains negative.

The next integral is

$$\int_{\mathcal{S}_{fuel\,inlet}} \rho\,(\boldsymbol{U} - \boldsymbol{W}) \cdot \boldsymbol{n}\,dA\,,$$

and unlike the previous case we have no specific information with which to evaluate it. But what we should notice is first that velocity of the fuel inlet area is parallel to U_p; *i.e.*, there is no component of engine motion in the direction normal to the plane through which fuel must flow. Hence, it follows that $\boldsymbol{W} \cdot \boldsymbol{n} = 0$, and if we now compare what remains with Eq. (3.26) we see that this is precisely the fuel mass flow rate that we are to determine. That is, we have

$$\int_{\mathcal{S}_{fuel\,inlet}} \rho\,(\boldsymbol{U} - \boldsymbol{W}) \cdot \boldsymbol{n}\,dA = \int_{\mathcal{S}_{fuel\,inlet}} \rho\,\boldsymbol{U} \cdot \boldsymbol{n}\,dA = \dot{m}_{fuel}\,,$$

with $\boldsymbol{U} = U_{fuel}$. Now we do not know the value for this latter quantity, or of ρ_{fuel} or A_{fuel} (although, in principle, these would be available in an actual engineering problem), but we will see that we do not need to know this information. In fact, we would be able to find any one of these from the desired solution to the present problem. On the other hand, it is useful to formally evaluate the above integral in order to obtain the correct sign for this contribution. We note from Fig. 3.8 that the outward unit normal vector at the fuel inlet is in the opposite direction of the fuel flow; thus, it follows that $\dot{m}_{fuel}$ must have a minus sign when substituted into the overall control-volume continuity equation.

The final integral to consider is that over the engine exhaust plane $\mathcal{S}_{exhaust}$. The area, gas density and flow velocity are all given for this location. We remark that in practice the area A_e might be a desired quantity to determine during a design optimization phase, but for any specific analysis it would be considered known. The gas density would be somewhat more difficult to determine but in principle could be found from a detailed analysis of the combustion process taking place inside the combustors of the engine. Thus, we can express this integral as

$$\begin{aligned} \int_{\mathcal{S}_{exhaust}} \rho\,(\boldsymbol{U} - \boldsymbol{W}) \cdot \boldsymbol{n}\,dA &= \rho_e\,(U_e - U_p) \cdot \boldsymbol{n}A_e \\ &= \rho_e U_e A_e + \rho_e U_p A_e\,, \end{aligned}$$

where the plus sign on U_p arises from the fact that the airplane is flying in the direction opposite to the direction of the outward unit normal vector for $\mathcal{S}_{exhaust}$. Furthermore, since the exhaust

velocity was specified with respect to a fixed coordinate system, it can be entered directly as we have done here.

The previous results obtained for each of the individual integrals in the control-volume formulation can now be combined to produce

$$-\rho_i U_p A_i - \dot{m}_{fuel} + \rho_e \left(U_e + U_p \right) A_e = 0 \,,$$

or

$$\dot{m}_{fuel} = -\rho_i U_p A_i + \rho_e \left(U_e + U_p \right) A_e \,.$$

We observe that now $\dot{m}_{fuel}$ is positive because we have already accounted for the sign in the solution process. Finally, we should point out that in this steady-state case we could have simply used $\dot{m}_{in} = \dot{m}_{out}$, but we would have to exercise some caution when evaluating $\dot{m}_{out}$ to account for the fact that the airplane is moving with speed U_p. By using the formal analysis procedure presented here, we have automatically accounted for such details.

3.4   Momentum Balance—the Navier–Stokes Equations

In this section we will derive the equations of motion for incompressible fluid flows, *i.e.*, the Navier–Stokes (N.–S.) equations. We begin by stating a general force balance consistent with Newton's second law of motion, and then formulate this specifically for a control volume consisting of a fluid element. Following this we will employ the Reynolds transport theorem which we have already discussed, and an argument analogous to that used in deriving the continuity equation to obtain the differential form of the momentum equations. We then develop a multi-dimensional form of Newton's law of viscosity to evaluate surface forces appearing in this equation and finally arrive at the N.–S. equations.

3.4.1   A basic force balance; Newton's second law of motion

We begin by recalling that because we cannot readily view fluids as consisting of point masses, it is not appropriate to apply Newton's second law of motion in the usual form $F = ma$. Instead, we will use a more general form expressed in words as

$$\left\{ \begin{array}{c} \text{time rate of change of momentum} \\ \text{of a material region} \end{array} \right\} = \left\{ \begin{array}{c} \text{sum of forces acting} \\ \text{on the material region} \end{array} \right\} \,.$$

The somewhat vague terminology "material region" is widely used, and herein it will usually be simply a fluid element. But later when we develop the control-volume momentum equation the material region will be any region of interest in a given flow problem. We also remark that we are employing the actual version of Newton's second law instead of the one usually presented in elementary physics. Namely, if we recall that momentum is mass times velocity, *e.g.*, mu in 1D, then the general statement of Newton's second law is

$$F = \frac{d(mu)}{dt} \,,$$

which collapses to the usual $F = ma$ in the case of point masses that are independent of time.

At this point it is worthwhile to recall the equation for conservation of mass, Eq. (3.20), which we write here in the abbreviated form

$$\rho_t + (\rho u)_x + (\rho v)_y + (\rho w)_z = 0 \,,$$

containing the dependent variables ρ, u, v and w. It will be convenient to express the momentum equations in terms of these same variables, and to this end we first observe that the product, *e.g.*, ρu, is momentum per unit volume (since ρ is mass per unit volume). Thus, yet another alternative expression of Newton's second law is

$$F/V = \frac{d}{dt}(\rho u)\,,$$

or force per unit volume is equal to time-rate of change of momentum <u>per unit volume</u>. We are now prepared to develop formulas for the left- and right-hand sides of the word formula given above.

Time-Rate of Change of Momentum

As was the case in deriving the differential equation representing conservation of mass, it will again be convenient here to choose a fluid region corresponding to a fluid element. In contrast to what was done earlier, we will restrict our region $\mathcal{R}(t)$ to be a fluid element from the start. If, in addition, we utilize an Eulerian view of the fluid flow we recognize that the substantial derivative should be employed to represent acceleration or, in our present case, to calculate the time-rate of change of momentum. As noted above, it is convenient for later purposes to consider the momentum per unit volume, rather than the momentum itself; so for the x component of this we would have

$$\frac{D}{Dt} \int_{\mathcal{R}(t)} \rho u \, dV\,,$$

the equivalent of mass × acceleration. Then for the complete velocity vector $\boldsymbol{U}$ we can write

$$\frac{D}{Dt} \int_{\mathcal{R}(t)} \rho \boldsymbol{U} \, dV \equiv \left\{ \begin{array}{c} \text{time rate of change of} \\ \text{momentum vector} \end{array} \right\}\,. \tag{3.28}$$

We remind the reader that application of the substantial derivative operator to a vector is accomplished by applying it to each component individually, so the above expression actually contains three components, each of the form of that for x momentum.

Sum of Forces

We next consider the general form of the right-hand side of the word equation given earlier, *viz.*, the sum of forces acting on the material region (fluid element in the present case). There are two main types of forces to analyze:

i) <u>body forces</u> acting on the entire region $\mathcal{R}(t)$, denoted

$$\int_{\mathcal{R}(t)} \boldsymbol{F}_B \, dV\,, \qquad \text{and}$$

ii) <u>surface forces</u>,

$$\int_{\mathcal{S}(t)} \boldsymbol{F}_S \, dA\,,$$

acting only on the surface $\mathcal{S}(t)$ of $\mathcal{R}(t)$.

It is useful to view the surface $\mathcal{S}(t)$ as dividing the fluid into two distinct regions: one that is interior to $\mathcal{S}(t)$, *i.e.*, $\mathcal{R}(t)$, and one that is on the outside of $\mathcal{S}(t)$. This implies that when we focus attention on $\mathcal{R}(t)$ alone, as it will be convenient to do, we must somehow account for the fact that we have discarded the outside—which interacts with $\mathcal{R}(t)$. We do this by representing these effects as surface forces acting on $\mathcal{S}(t)$.

The Momentum Equations of Fluid Flow

We can now produce a preliminary version of the momentum equations from which we will derive the equations of fluid motion, the Navier–Stokes equations:

$$\frac{D}{Dt}\int_{\mathcal{R}(t)}\rho \boldsymbol{U}\,dV = \int_{\mathcal{R}(t)}\boldsymbol{F}_B\,dV + \int_{\mathcal{S}(t)}\boldsymbol{F}_S\,dA\,. \tag{3.29}$$

Just as was the case for the continuity equation treated earlier, this general form is not very convenient for practical use; it contains both volume and surface integrals, and it is not expressed entirely in terms of the typical dependent variables that are usually needed for engineering calculations. Thus, it will be necessary to introduce physical descriptions of the body and surface forces in terms of convenient variables and to manipulate the equation to obtain a form in which only a volume integral appears.

We first note that the body forces are generally easy to treat without much further consideration. In particular, the most common such force arising in practice is a buoyancy force due to gravitational acceleration; *i.e.*, typically $\boldsymbol{F}_B = \rho \boldsymbol{g}$ where $\boldsymbol{g}$ is gravitational acceleration, often taken as constant. We note in passing that numerous other body forces are possible, including electromagnetic and rotational effects. We shall not be concerned with these in the present lectures.

The surface forces require considerable effort for their treatment, and we will delay this until after we have further simplified Eq. (3.29) by moving differentiation inside the integral as we did earlier in deriving the equation representing conservation of mass. As should be expected we will employ a transport theorem to accomplish this. But in contrast to our analysis of the continuity equation we will use the *Reynolds transport theorem*, Eq. (3.10), which we repeat here for easy reference:

$$\frac{D}{Dt}\int_{\mathcal{R}(t)}\boldsymbol{\Phi}\,dV = \int_{\mathcal{R}(t)}\frac{\partial \boldsymbol{\Phi}}{\partial t}\,dV \int_{\mathcal{S}(t)}\boldsymbol{\Phi}\boldsymbol{U}\cdot\boldsymbol{n}\,dA\,. \tag{3.30}$$

Recall that $\boldsymbol{\Phi}$ is in general a vector field, but here we will work with only a single component at a time, so we can replace this with the scalar Φ, and for the present discussions set $\Phi = \rho u$, the x component of momentum per unit volume. Substitution of this into Eq. (3.30) results in

$$\frac{D}{Dt}\int_{\mathcal{R}(t)}\rho u\,dV = \int_{\mathcal{R}(t)}\frac{\partial \rho u}{\partial t}\,dV + \int_{\mathcal{S}(t)}\rho u\boldsymbol{U}\cdot\boldsymbol{n}\,dA\,,$$

and applying Gauss's theorem to the surface integral yields

$$\int_{\mathcal{R}(t)}\frac{\partial \rho u}{\partial t} + \nabla\cdot(\rho u\boldsymbol{U})\,dV \tag{3.31}$$

in the right-hand side of the above expression.

We next simplify the second term in the integrand of (3.31). First apply product-rule differentiation to obtain

$$\nabla\cdot(\rho u\boldsymbol{U}) = \boldsymbol{U}\cdot\nabla(\rho u) + \rho u\nabla\cdot\boldsymbol{U}\,.$$

Now we make use of the divergence-free condition of incompressible flow (*i.e.*, $\nabla\cdot\boldsymbol{U} = 0$) and constant density ρ to write

$$\nabla\cdot(\rho u\boldsymbol{U}) = \rho\boldsymbol{U}\cdot\nabla u\,.$$

Substitution of this result into Eq. (3.31) shows that

$$\begin{aligned}
\frac{D}{Dt}\int_{\mathcal{R}(t)}\rho u\,dV &= \int_{\mathcal{R}(t)}\rho\frac{\partial u}{\partial t} + \rho\boldsymbol{U}\cdot\nabla u\,dV \\[2mm]
&= \int_{\mathcal{R}(t)}\rho\frac{Du}{Dt}\,dV\,.
\end{aligned} \tag{3.32}$$

Thus, we have succeeded in interchanging differentiation with integration over the fluid element $\mathcal{R}(t)$.

We remark that the assumption of incompressible flow used above is not actually needed to obtain this result; but it simplifies the derivation, and we will be making use of it in the sequel in any case. We leave as an exercise to the reader the task of obtaining Eq. (3.32) <u>without</u> the incompressibility assumption as well as deriving analogous formulas for the other two components of momentum.

Substitution of (3.32) (and analogous results for y and z momentum) into Eq. (3.29) permits us to write the latter equation as

$$\int_{\mathcal{R}(t)} \rho \frac{D\boldsymbol{U}}{Dt}\, dV = \int_{\mathcal{R}(t)} \boldsymbol{F}_B\, dV + \int_{\mathcal{S}(t)} \boldsymbol{F}_S\, dA\,. \tag{3.33}$$

There are two main steps needed to complete the derivation. The first is analogous to what was done in the case of the continuity equation; namely, we need to convert the integral equation to a differential equation. The second is treatment of the surface forces. We will first provide a preliminary mathematical characterization of these forces that will lead to the differential equation. Details of the surface forces will be given in a separate section.

Preliminaries on Surface Forces

It is important to first understand the mathematical structure of the surface forces. This will not only aid in required manipulations of the equation, but it will also provide further insight into how these forces should be represented. We begin by noting that $\boldsymbol{F}_S$ must be a vector (because $\rho\boldsymbol{U}$ and $\boldsymbol{F}_B$ are vectors), and this suggests that there must be a matrix, say $\boldsymbol{\mathcal{T}}$, such that

$$\boldsymbol{F}_S = \boldsymbol{\mathcal{T}} \cdot \boldsymbol{n}\,,$$

where, as usual, $\boldsymbol{n}$ is the outward unit normal vector to the surface $\mathcal{S}(t)$. This is actually a completely trivial observation; but as will become more clear as we proceed, it is very important. Furthermore, it will also be important to recognize that the physics represented by the vector $\boldsymbol{F}_S$ must somehow be incorporated into the elements of the matrix $\boldsymbol{\mathcal{T}}$ since $\boldsymbol{n}$ is purely geometric.

Basic Form of Differential Momentum Equation

The above expression for $\boldsymbol{F}_S$ allows us to write Eq. (3.33) as

$$\int_{\mathcal{R}(t)} \rho \frac{D\boldsymbol{U}}{Dt}\, dV = \int_{\mathcal{R}(t)} \boldsymbol{F}_B\, dV + \int_{\mathcal{S}(t)} \boldsymbol{\mathcal{T}} \cdot \boldsymbol{n}\, dA\,,$$

and application of Gauss's theorem to the surface integral, followed by rearrangement, yields

$$\int_{\mathcal{R}(t)} \rho \frac{D\boldsymbol{U}}{Dt} - \boldsymbol{F}_B - \nabla \cdot \boldsymbol{\mathcal{T}}\, dV = 0\,. \tag{3.34}$$

Now recall that $\mathcal{R}(t)$ is an arbitrary fluid element that can be chosen to be arbitrarily small; hence, it follows from arguments used in an analogous situation while deriving the continuity equation that

$$\rho \frac{D\boldsymbol{U}}{Dt} - \boldsymbol{F}_B - \nabla \cdot \boldsymbol{\mathcal{T}} = 0\,. \tag{3.35}$$

This provides a fundamental, and very general, momentum balance that is valid at <u>all points</u> of <u>any</u> fluid flow (within the confines of the continuum hypothesis).

3.4.2 Treatment of surface forces

We can now complete the derivation of the Navier–Stokes equations by considering the details of the matrix $\mathcal{T}$ which must contain the information associated with surface forces. We again recall that $\mathcal{T}$ is a matrix, and $\boldsymbol{F}_S$ is a 3-D vector. Thus, $\mathcal{T}$ must be a 3×3 matrix having a total of nine elements. Since, as already noted, these must carry the same information found in the components of the surface force vector $\boldsymbol{F}_S$, we know from earlier discussions of shear stress and pressure that both of these must be represented in the elements of $\mathcal{T}$. That is, these elements must be associated with two types of forces:

    i) normal forces, and

    ii) tangential forces.

Figure 3.9 provides a detailed schematic of these various forces (and/or any associated stresses) in the context of an arbitrary (but geometrically simple) fluid element. We will first provide a detailed
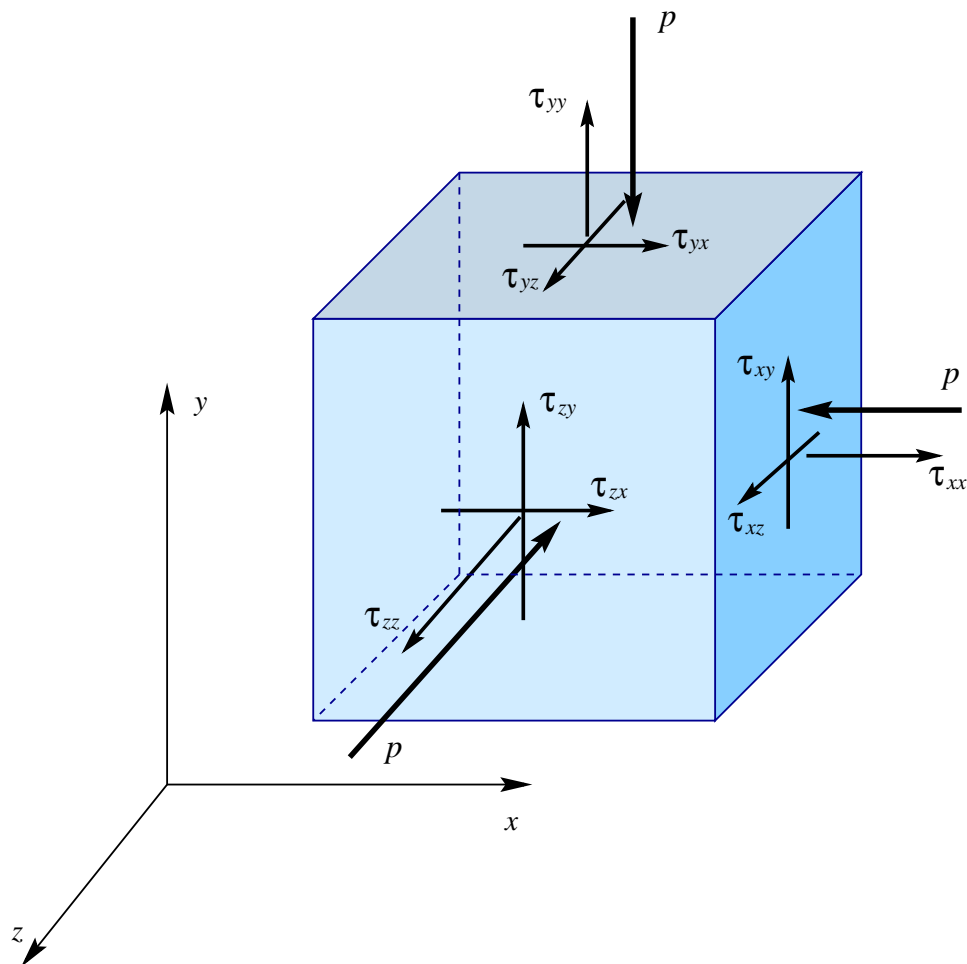
Figure 3.9: Schematic of pressure and viscous stresses acting on a fluid element.

discussion of the shear stresses that result from tangential forces, and then consider the normal forces and stresses in somewhat less detail.

Shear Stresses

We observe that there are six different shear stresses shown on this figure, and we need to consider some details of these. The first thing to note is that the subscript notation being employed here does <u>not</u> imply partial differentiation as has been the case in all other uses of such subscripts. Instead, the first subscript indicates the face of the cube on which the stress is acting (labeled according to the direction of its associated normal vector), and the second denotes the direction of the stress. In particular, for the τ_{xy} component, *e.g.*, the x subscript implies that we are considering a component acting on a face <u>perpendicular to the x axis</u>, and the y subscript indicates that this stress is in the y direction. It is clear from the figure that there must be two components of shear stress on each face because there are two tangential directions on each face. It is less clear what physics leads to these individual stresses, and thus what should be their mathematical representations. We will treat this in some detail at this time.

It is important to recall Newton's law of viscosity, which we earlier expressed in the mathematical form

$$\tau = \mu \frac{du}{dy}$$

for a one dimensional flow in the x direction. We now must generalize this formula to the present multi-dimensional situation.

If we imagine another fluid element in contact with the one of Fig. 3.9 and just above it so that it is sliding past the top y plane in the x direction, then we see that the above formulation of Newton's law of viscosity is associated with (but as we shall see below, <u>not</u> equal to) the 3-D shear stress component τ_{yx}. Similarly, if we were to imagine another fluid element sliding past the x face of the cube in the y direction, we would expect this to generate x-direction changes in the v component of velocity; hence, it follows that τ_{xy} is associated with $\mu \partial v / \partial x$. The partial derivatives (instead of ordinary ones) are now necessary because the flow is no longer 1D, and specific indication of this will be required for later developments.

We next note that it can be proven from basic physical considerations that the various components of the shear stress shown in Fig. 3.9 are related as follows:

$$\tau_{xy} = \tau_{yx}, \qquad \tau_{xz} = \tau_{zx}, \qquad \tau_{yz} = \tau_{zy}. \tag{3.36}$$

The interested reader is referred to more advanced treatments of fluid dynamics for such a proof; here we will provide an heuristic mathematical argument. In particular, if we consider the two shear stress components described above and imagine shrinking the fluid element depicted in Fig. 3.9 to a very small size we would see that in order to avoid discontinuities (in the mathematical sense) of τ along the edge of the cube between the x and y faces it would be necessary to require $\tau_{xy} = \tau_{yx}$, and similarly for the other components listed in Eq. (3.36) along the various other edges. But, in fact, this cubic representation is just a pictorial and should be viewed as a local projection of a more complicated shape. Hence, we can argue that there are such "edges" everywhere on an actual fluid element, and as we allow the size of such an element to become arbitrarily small, we must have the equalities shown in Eq. (3.36) over the entire surface of the fluid element.

We next need to consider the consequences of this. We see that on an x face we have

$$\tau_{xy} \sim \mu \frac{\partial v}{\partial x},$$

while on the y face that adjoins this we have

$$\tau_{yx} \sim \mu \frac{\partial u}{\partial y}\,.$$

But these two stresses must actually be equal, as noted above. It is completely unreasonable to expect that

$$\frac{\partial u}{\partial y} = \frac{\partial v}{\partial x}$$

in general, for this would imply an irrotational flow (recall Eqs. (2.16)), and most flows are not irrotational. The simplest way around this difficulty is to define the shear stresses acting on the surface of a 3-D fluid element as follows:

$$\tau_{xy} = \mu \left(\frac{\partial u}{\partial y} + \frac{\partial v}{\partial x} \right) = \tau_{yx}\,, \tag{3.37a}$$

$$\tau_{xz} = \mu \left(\frac{\partial u}{\partial z} + \frac{\partial w}{\partial x} \right) = \tau_{zx}\,, \tag{3.37b}$$

$$\tau_{yz} = \mu \left(\frac{\partial v}{\partial z} + \frac{\partial w}{\partial y} \right) = \tau_{zy}\,. \tag{3.37c}$$

We will often use the short-hand notations employed earlier for partial derivatives to express these as, $e.g.$,

$$\tau_{xy} = \mu(u_y + v_x)\,, \qquad \tau_{xz} = \mu(u_z + w_x)\,, \qquad \tau_{yz} = \mu(v_z + w_y)\,.$$

These provide the generalizations of Newton's law of viscosity alluded to earlier.

We can also provide a simple, physical argument for the form of these stresses. To understand the physics of the multi-dimensional shear stresses we again appeal to Newton's law of viscosity by recalling that it relates shear stress to rate of angular deformation through the viscosity. Thus, we need to seek the sources of angular deformation for each face of our fluid element. We will specifically consider only one of the x faces, but the argument we use will apply to any of the faces.

Figure 3.10 provides a schematic of the deformation caused by x- and y-direction motions of this face, viewed edgewise, both of which contribute to τ_{xy}. In particular, in the left figure we see that changes of the v component of velocity in the x direction will tend to distort the fluid element by moving the x face in a generally counter-clockwise direction. This change of v with respect to x corresponds to an angular deformation rate $\partial v/\partial x$. Similarly, in the right-hand figure we depict the effects of changes in u with respect to y, and hence the angular deformation rate $\partial u/\partial y$, also producing a distortion generally in the counter-clockwise direction. We note that it is not necessary that $\partial v/\partial x$ and $\partial u/\partial y$ both produce counter-clockwise distortions (or clockwise ones), but only that these occur in the xy plane. It is clear from Fig. 3.9 that this is the plane on which τ_{xy} acts, and the preceding physical argument shows that both $\partial v/\partial x$ and $\partial u/\partial y$ contribute to this component of shear stress as we have previously argued on purely mathematical grounds. We leave as an exercise to the reader to produce a physical argument analogous to that given here showing that $\partial v/\partial x$ and $\partial u/\partial y$ are the contributions to τ_{yx} on the y face of the fluid element shown in Fig. 3.9, thus suggesting that $\tau_{yx} = \tau_{xy}$.

Normal Viscous Stresses and Pressure

We remark here that there are actually two separate contributions to the normal force: one involves pressure, as would be expected; but there is a second type of normal force of viscous
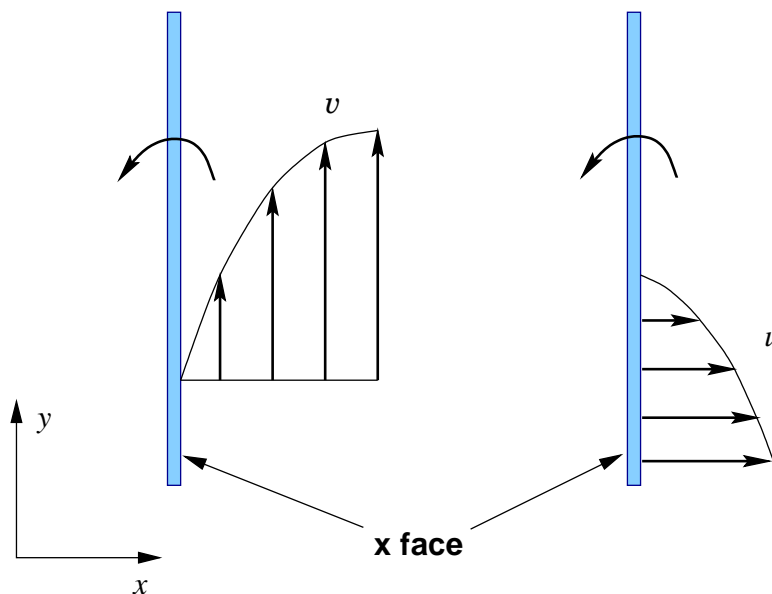
Figure 3.10: Sources of angular deformation of face of fluid element.

origin. We can see evidence of this when pouring very viscous fluids such as molasses or cold pancake syrup. Although they flow, they do so very slowly because the normal viscous forces are able to support considerable tensile stresses arising from gravitational force on the falling liquid. (We note that surface tension, discussed in Chap. 2, is also a factor here, but not the only one.) This can be further recognized if we consider dropping a solid object having the same density as molasses, *e.g.*, at the same time we begin to pour the latter. We would see that the solid object would fall to the floor much more quickly, retarded only by drag from the surrounding air (also of viscous origin, but not nearly as effective in slowing motion as are the internal viscous normal stresses in this case). Finally, we observe that viscous normal stresses also occur in flow of gases, but they must be compressive because gases cannot support tensile stresses.

As indicated in Fig. 3.9, the normal stresses are different from pressure (which is always compressive, as the figure indicates), and they are denoted τ_{xx}, τ_{yy} and τ_{zz}. We should expect, by analogy with the shear stresses, that, *e.g.*, τ_{xx} acts in the x direction, and on the x face of the fluid element. This combination requires that (again, by analogy with the form of shear stress)

$$\tau_{xx} = \mu \left(\frac{\partial u}{\partial x} + \frac{\partial u}{\partial x} \right) = 2\mu u_x \,, \tag{3.38a}$$

$$\tau_{yy} = \mu \left(\frac{\partial v}{\partial y} + \frac{\partial v}{\partial y} \right) = 2\mu v_y \,, \tag{3.38b}$$

$$\tau_{zz} = \mu \left(\frac{\partial w}{\partial z} + \frac{\partial w}{\partial z} \right) = 2\mu w_z \,. \tag{3.38c}$$

The factor of two in these equations does, in fact, have a physical origin. If we consider the right-hand side sketch in Fig. 3.10 we recognize that not only will there be an angular deformation, but also an x-direction distortion—all acting in the xy plane. Furthermore, both of these deformations are associated with the velocity gradient component $\partial u/\partial x$, *i.e.*, the component contributing to the normal viscous stress. While this contribution is acting in the xy plane as depicted in the figure,

there is yet a second contribution associated with motions in the xz plane, not shown. These both arise from the same component of velocity gradient, and the factor of two permits account to be taken of effects in both planes of the fluid element. As with the shear stresses, the same arguments apply for the other normal stresses acting on their respective faces of the fluid element.

Construction of the Matrix $\mathcal{T}$

We now again recall that the matrix $\mathcal{T}$ must carry the same information as does the surface force vector $\boldsymbol{F}_S$. We have not previously given much detail of this except to note that $\boldsymbol{F}_S$ could be resolved into normal and tangential forces. But we can see from Eq. (3.33) that this vector must also be viewed in terms of its separate components each of which is acting as the force in a momentum balance for the corresponding individual velocity components. Furthermore, we see from Eq. (3.35) that these force contributions come from taking the divergence of $\mathcal{T}$, implying that the first column of $\mathcal{T}$ should provide the force to balance the time-rate of change of momentum associated with the u component of velocity (*i.e.*, the x-direction velocity), *etc.* Thus, if we recall Fig. 3.9 we see that the information in the first column of $\mathcal{T}$ should consist of τ_{xx}, τ_{yx}, τ_{zx} and the contribution of pressure p acting on the x face.

With regard to the last of these we note that pressure is a scalar quantity, and as such it has no direction dependence. On the other hand, changes in pressure can be different in the different directions, and we will soon see that it is, in fact, only changes in pressure that enter the equations of motion. Moreover, we view the associated forces as compressive, as indicated in Fig. 3.9; *viz.*, they act in directions opposite the respective outward unit normals to the fluid element. Hence, all such terms will have minus signs in the formulas to follow.

The arguments given above for the first column of the matrix $\mathcal{T}$ apply without change to the remaining two columns, so we arrive at the following:

$$
\begin{aligned}
\mathcal{T} \;&=\; \begin{bmatrix} -p + \tau_{xx} & \tau_{xy} & \tau_{xz} \\ \tau_{yx} & -p + \tau_{yy} & \tau_{yz} \\ \tau_{zx} & \tau_{zy} & -p + \tau_{zz} \end{bmatrix} \\[2mm]
&=\; -p \begin{bmatrix} 1 & 0 & 0 \\ 0 & 1 & 0 \\ 0 & 0 & 1 \end{bmatrix} + \begin{bmatrix} \tau_{xx} & \tau_{xy} & \tau_{xz} \\ \tau_{xy} & \tau_{yy} & \tau_{yz} \\ \tau_{xz} & \tau_{yz} & \tau_{zz} \end{bmatrix} \qquad (3.39) \\[2mm]
&=\; -p\boldsymbol{I} + \boldsymbol{\tau} \, .
\end{aligned}
$$

In this equation $\boldsymbol{I}$ is the identity matrix, and $\boldsymbol{\tau}$ is often termed the *viscous stress tensor* in which we have used Eqs. (3.37) to equate τ_{xy} with τ_{yx}, *etc.*, to emphasize the <u>symmetry</u> of this matrix.

3.4.3   The Navier–Stokes equations

We are now prepared to calculate $\nabla \cdot \mathcal{T}$ appearing in Eq. (3.35) thus completing our derivation of the N.–S. equations. Recall that the symbolism $\nabla\cdot$ denotes a vector differential operation consisting of forming a "dot product" of the vector of operators $(\partial/\partial x, \partial/\partial y, \partial/\partial z)$ with whatever follows the "$\cdot$". In the present case this is a matrix which we should view as three column vectors to each of which $\nabla\cdot$ can be applied separately, with each application yielding a component of a vector, as is

needed to maintain the order of Eq. (3.35). Thus, we obtain

$$
\nabla \cdot \boldsymbol{\mathcal{T}} = \left(-\frac{\partial p}{\partial x} + \frac{\partial \tau_{xx}}{\partial x} + \frac{\partial \tau_{yx}}{\partial y} + \frac{\partial \tau_{zx}}{\partial z} \right) \boldsymbol{e}_1 \ +
$$
$$
\left(-\frac{\partial p}{\partial y} + \frac{\partial \tau_{xy}}{\partial x} + \frac{\partial \tau_{yy}}{\partial y} + \frac{\partial \tau_{zy}}{\partial z} \right) \boldsymbol{e}_2 \ + \tag{3.40}
$$
$$
\left(-\frac{\partial p}{\partial z} + \frac{\partial \tau_{xz}}{\partial x} + \frac{\partial \tau_{yz}}{\partial y} + \frac{\partial \tau_{zz}}{\partial z} \right) \boldsymbol{e}_3 \ \ ,
$$

where the $\boldsymbol{e}_i$s, $i = 1, 2, 3$, are the usual Euclidean basis vectors $(1, 0, 0)^T$, *etc.*

Next, we substitute Eq. (3.40) for $\nabla \cdot \boldsymbol{\mathcal{T}}$ in Eq. (3.35). We will carry out the details for the x component and leave treatment of the other two components as an exercise for the reader. We have after slight rearrangement

$$
\rho \frac{Du}{Dt} = -\frac{\partial p}{\partial x} + \frac{\partial \tau_{xx}}{\partial x} + \frac{\partial \tau_{yx}}{\partial y} + \frac{\partial \tau_{zx}}{\partial z} + F_{B,1} \,, \tag{3.41}
$$

where $F_{B,1}$ denotes the x component of the body force vector $\boldsymbol{F}_B$. Now recall that the multi-dimensional form of Newton's law of viscosity provides the following "constitutive relations" for the viscous stress components (Eqs. (3.37), (3.38)):

$$
\tau_{xx} = 2\mu u_x \,, \qquad \tau_{yx} = \mu(u_y + v_x) \,, \qquad \tau_{zx} = \mu(u_z + w_x) \,. \tag{3.42}
$$

Substitution of these into the second, third and fourth terms on the right-hand side of Eq. (3.41), and assuming viscosity is constant, yields the following expression:

$$
2\mu u_{xx} + \mu(u_y + v_x)_y + \mu(u_z + w_x)_z \,,
$$

which can be rearranged to the form

$$
\mu(u_{xx} + u_{yy} + u_{zz}) + \mu(u_{xx} + v_{xy} + w_{xz}) \,.
$$

The second term in this expression can be further rearranged, resulting in

$$
\mu(u_{xx} + v_{xy} + w_{xz}) = \mu(u_x + v_y + w_z)_x \,,
$$

under the assumption that the velocity components are sufficiently smooth to permit interchange of the order of partial differentiation. But if we now recall the divergence-free condition for incompressible flow, we see that the right-hand side of this expression is zero. Thus, the viscous stress terms in Eq. (3.41) collapse to simply

$$
\mu(u_{xx} + u_{yy} + u_{zz}) \,.
$$

Analogous results can be obtained for the y and z components of momentum, and we can write the complete system of equations representing momentum balance in an incompressible flow as

$$
\rho \frac{Du}{Dt} = -p_x + \mu(u_{xx} + u_{yy} + u_{zz}) + F_{B,1} \,,
$$
$$
\rho \frac{Dv}{Dt} = -p_y + \mu(v_{xx} + v_{yy} + v_{zz}) + F_{B,2} \,,
$$
$$
\rho \frac{Dw}{Dt} = -p_z + \mu(w_{xx} + w_{yy} + w_{zz}) + F_{B,3} \,.
$$

It is common to divide these equations by ρ (since it is constant), and express them as

$$u_t + uu_x + vu_y + wu_z = -\frac{1}{\rho}\,p_x + \nu\Delta u + \frac{1}{\rho}\,F_{B,1}\,, \tag{3.43a}$$

$$v_t + uv_x + vv_y + wv_z = -\frac{1}{\rho}\,p_y + \nu\Delta v + \frac{1}{\rho}\,F_{B,2}\,, \tag{3.43b}$$

$$w_t + uw_x + vw_y + ww_z = -\frac{1}{\rho}\,p_z + \nu\Delta w + \frac{1}{\rho}\,F_{B,3}\,. \tag{3.43c}$$

Here, ν is *kinematic viscosity*, the ratio of viscosity μ to density ρ, as given earlier in Chap. 2, and Δ is the second-order partial differential operator (given here in Cartesian coordinates)

$$\Delta = \frac{\partial^2}{\partial x^2} + \frac{\partial^2}{\partial y^2} + \frac{\partial^2}{\partial z^2}$$

known as the *Laplacian* or *Laplace operator*, and which is usually denoted by ∇^2 in the engineering and physics literature.

These equations are called the *Navier–Stokes equations*, and they provide a pointwise description of essentially any time-dependent incompressible fluid flow. But it is important to recall the assumptions under which they have been derived. First, the continuum hypothesis has been used repeatedly to permit pointwise definitions of various flow properties and to allow definition of fluid elements. Second, we have assumed constant density ρ, and corresponding to this a divergence-free velocity field; *i.e.*, $\nabla \cdot \boldsymbol{U} = 0$. In addition, we have invoked Newton's law of viscosity to provide a formulation for shear stresses, and tacitly assumed an analogous result could be used to define normal viscous stresses; furthermore, we have taken the viscosity to be constant. Finally, from a mathematical perspective, we are implicitly assuming the velocity and pressure fields are sufficiently smooth to permit the indicated differentiations.

While the composite of these assumptions may seem quite restrictive, in fact they are satisfied by many physical flows, and we will not in these lectures dwell much on the cases in which they may fail. But we note that at least for relatively low-speed flows all of the above assumptions essentially always hold to a good approximation. As the flow speed increases, constant density (and, consequently, also the divergence-free condition) fails as we move into compressible flow regimes, but in general this occurs only for gaseous flows. Constant viscosity is an extremely good assumption provided temperature is nearly constant, and for flows of gases it is generally a good approximation until the flows become compressible. The mathematical smoothness assumption is possibly the most likely to be violated, but from an engineering perspective this is usually not a major concern.

3.5   Analysis of the Navier–Stokes Equations

In this section we will first provide a brief introduction to the mathematical structure of Eqs. (3.43) which is particularly important when employing CFD codes to solve problems in fluid dynamics. We will then proceed to a term-by-term analysis of the physical interpretation of each of the sets of terms in the N.–S. equations. This will yield a better understanding of the overall behavior of solutions to these equations and the beginnings of being able to recognize the flow situations in which the equations can be simplified in order to more easily obtain solutions.

3.5.1 Mathematical structure

As we pointed out in Chap. 1, the N.–S. equations in the form of Eqs. (3.43) have been known for more than a century and a half, and during that time considerable effort has been devoted to their understanding and solution. In large part they have resisted this, and now that we have them before us we can begin to understand the difficulties. It should first be noted again that Eqs. (3.43) comprise a 3-D, time-dependent system of <u>nonlinear</u> partial differential equations (PDEs). (Terms such as uu_x are nonlinear in the dependent variable u.) The unknown dependent variables are the three velocity components u, v and w, and the pressure p. Hence, there are four unknown <u>functions</u> required for a solution, and only three differential equations. The remedy for this is to explicitly invoke conservation of mass, which in the case of incompressible flow implies that

$$u_x + v_y + w_z = 0\,. \tag{3.44}$$

It is of interest to note that the three momentum equations (3.43) can be viewed as the respective equations for the three velocity components, implying that the divergence-free condition (3.44) must be solved for pressure. This is particularly difficult because pressure does not even appear explicitly in this equation. In the context of computational fluid dynamics, other approaches are usually used for finding pressure and guaranteeing mass conservation, but discussion of these is beyond the intended scope of these lectures.

But we should note that in addition to the requirement to solve a system of nonlinear PDEs is the related one of supplying boundary and initial conditions needed to produce *particular solutions* corresponding to the physics of specific problems of interest. It is an unfortunate fact that often what seem to be perfectly reasonable physical conditions may be inadequate or simply incorrect, and it is important to have at least an elementary understanding of the structure of PDEs and their solutions to avoid this problem—especially when utilizing commercial CFD codes that have been written to provide an answer almost independent of the validity (or lack thereof) of the problem formulation. In the next chapter we will derive some well-known simple exact solutions to the N.–S. equations to demonstrate the combination of physical and mathematical reasoning that must be employed to successfully solve these equations.

3.5.2 Physical interpretation

At this point it is worthwhile to consider the N.–S. equations term-by-term and ascribe specific physical meaning to each of these terms. This will be of importance later when it is desired to simplify the equations to treat specific physical flow situations. Then, by knowing the physics represented by each (group of) term(s) and what physics is not included in a problem under consideration, we can readily determine which terms can be omitted from the equations to simplify the analysis. We will carry this out only for the x-momentum equation, but it will be clear that the same analysis can be used for the other two equations as well.

$$\underbrace{\underbrace{u_t}_{\substack{local \\ accel}} + \underbrace{uu_x + vu_y + wu_z}_{\substack{convective \\ accel}}}_{total\ acceleration} = \overbrace{-\frac{1}{\rho}p_x}^{\substack{pressure \\ forces}} + \overbrace{\nu\Delta u}^{\substack{viscous \\ forces}} + \overbrace{\frac{1}{\rho}F_{B,1}}^{\substack{body \\ forces}}\,.$$

Inertial Terms

The left-hand side of this equation is the substantial derivative of the u component of velocity, and as such is the total, or Lagrangian, acceleration treated earlier. These terms are often called

the "inertial terms" in the context of the N.–S. equations, and we recall that they consist of two main contributions: local acceleration and convective acceleration. Previously we attributed the latter of these to "Lagrangian effects," but it is also useful to view them simply as accelerations resulting from spatial changes in the velocity field for it is clear that in a uniform flow this part of the acceleration would be identically zero. It is of interest to note that while all of these terms represent acceleration, as indicated, they can also be viewed as time-rate of change of momentum per unit mass. This is particularly evident in the case of the local acceleration where it follows immediately from the definition of momentum.

Pressure Forces

The first term on the right-hand side of the above equation represents normal surface forces due to pressure, but in the present form this is actually a force per unit mass as it must be to be consistent with time-rate of change of momentum per unit mass on the left-hand side. We can easily check this in generalized units:

$$p \sim F/L^2 \quad \Rightarrow \quad p_x \sim F/L^3 \,,$$

and $\rho \sim M/L^3$. Thus,

$$\frac{1}{\rho} p_x \sim F/M \,,$$

as required. But we should also notice that by Newton's second law of motion this is just acceleration, as it must be.

Viscous Forces

The terms associated with the viscous forces deserve considerable attention. We earlier presented a quite lengthy treatment of viscosity while noting that this is the one fluid property that is not shared by nonfluids. Similarly, to understand the behavior of solutions to the N.–S. equations it is essential to thoroughly treat the unique phenomena arising from the viscous terms. These terms are

$$\nu \Delta u = \nu(u_{xx} + u_{yy} + u_{zz}) \,.$$

We leave as an exercise to the reader the task of demonstrating that the units of these terms are consistent with those of the rest of the above equation, namely force/unit mass (*i.e.*, acceleration).

In Chap. 2 we noted that viscosity arises at the molecular level, and the terms given above are associated with molecular transport (*i.e.*, diffusion) of momentum. In general, second derivative terms in a differential equation are usually associated with diffusion, and in both physical and mathematical contexts this represents a smearing, or smoothing, or mixing process. It is of interest to compare the effects of this for high- and low-viscosity fluids as depicted in Fig. 3.11. In part (a) of this figure we present a velocity profile corresponding to a case of relatively high fluid viscosity. It can be seen that this profile varies smoothly coming away from zero velocity at the wall, and reaching a maximum velocity in the center of the duct. The core region of high-speed flow is relatively small, and the outer (near the wall) regions of low speed flow are fairly large. This occurs because large viscosity is able to mediate diffusion of viscous forces (time-rate of change of momentum) arising from high shear stress near the solid surfaces far into the flow field, thus smoothing the entire velocity profile.

In contrast to this is the low viscosity case depicted in part (b) of Fig. 3.11. In this flow we see a quite narrow region of low-speed flow near the solid boundaries and a wide region of nearly
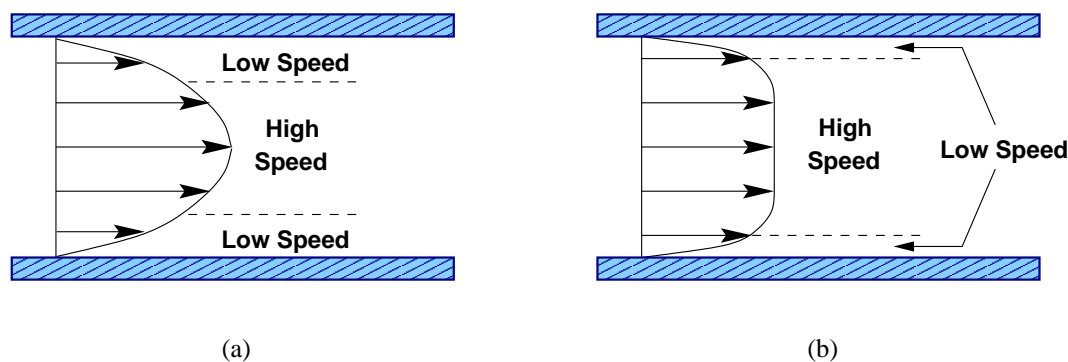
Figure 3.11: Comparison of velocity profiles in duct flow for cases of (a) high viscosity, and (b) low viscosity.

constant velocity flow in the central region of the duct. We should also note that the speed in this latter region is lower (for the same mass flow rate) than would be the speed on the centerline for the high viscosity case. This is because the low momentum fluid near the wall does not diffuse away into the central flow region; the speed of this region is nearly uniform, so for a given mass flow rate it must be lower.

In both of these cases it is important to note that diffusive action of the viscosity dissipates mechanical energy, ultimately converting it to thermal energy. In turn, this results in entropy increases and loss of usable energy. Thus, we see that the viscous terms in the momentum equations render them nonconservative, and appreciable pressure, shearing or body forces must be applied continuously to preserve the fluid motion.

3.6 Scaling and Dimensional Analysis

The equations of fluid motion presented in the preceding section are, in general, difficult to solve. As noted there, they comprise a nonlinear system of partial differential equations, and in many situations it is not yet possible even to rigorously prove that solutions exist. (As mentioned in Chap. 1, the N.–S. equations, or more particularly the attempts to solve them, played a significant role in the development of modern mathematical analysis throughout the 20th Century, and they continue to do so today.) At least in part because of these difficulties, until only very recently (with the advent of modern high-speed computers and CFD codes) much of the practical work in fluid dynamics required laboratory experiments. For example, flows about ships, trains and aircraft—and even tall buildings—were studied experimentally using wind tunnels and water tow tanks. Clearly, in any of these cases it could be prohibitively expensive to build a succession of full-scale models (often termed "prototypes") for testing and subsequent modification until a proper configuration was found.

This fact led to wind tunnel testing of much smaller scale models that were relatively inexpensive to build compared to the prototypes, and this immediately raises the question, "Under what circumstances will the flow field about a scale model be the same as that about the actual full-size object?" It is this question, along with some of its consequences from the standpoint of analysis, that will be addressed in the present section where we will show that the basic answer is: geometric and dynamic similarity must be maintained between scale model and prototype if data obtained from a model are to be applicable to the full-size object.

We begin with a subsection in which we discuss these two key ingredients to scaling analysis, without which utilizing such analyses would be impossible, *viz.*, geometric and dynamic similarity. We then provide a subsection that details scaling analysis of the N.–S. equations, followed by a subsection describing the Buckingham Π theorem widely used in developing correlations of experimental data. Finally, we describe physical interpretations of various dimensionless parameters that result from scaling the governing equations and/or applying the Buckingham Π theorem.

3.6.1   Geometric and dynamic similarity

Here we begin with a definition and discussion of a very intuitive idea, geometric similarity. We then introduce the very important concept of dynamic similarity and indicate how it is used to interpret results from studies of small-scale models in order to apply these to analysis of corresponding full-scale objects.

Geometric Similarity

The requirement of geometric similarity is an intuitively rather obvious one; we would not expect to obtain very useful information regarding lift of an airfoil by studying flow around a scale model of the Empire State Building being pulled through a water tow tank. While this (counter) example is rather extreme, it nevertheless hints at the necessity to consider some not-so-obvious details. These are stated in the following definition.

Definition 3.2 *Two objects are said to be <u>geometrically similar</u> if all linear length scales of one object are a fixed ratio of all corresponding length scales of the second object.*

This immediately implies that the two objects are of the same general shape, for otherwise there could be no "corresponding" linear length scales. To clarify this idea we present the following example.

EXAMPLE 3.6 In Fig. 3.12 we show an axisymmetric ogive that represents a typical shape for missile nose cones. The external tank of the space shuttle, for example, has a nose cone of this shape.

(a)   (b)
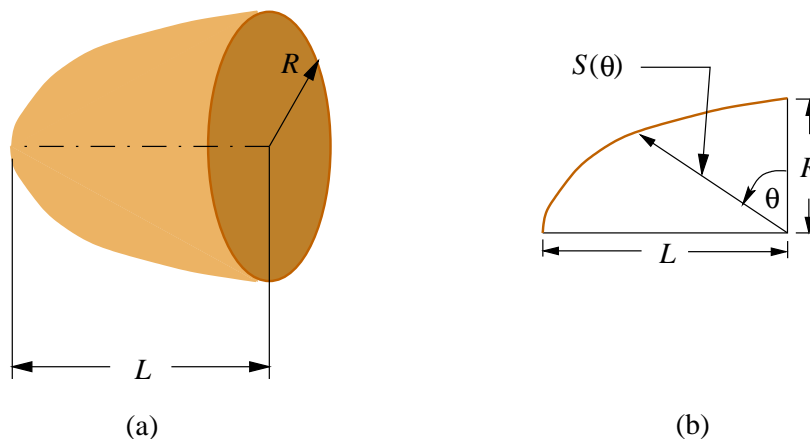
Figure 3.12: Missile nose cone ogive (a) physical 3-D figure, and (b) cross section indicating linear lengths.

In this simple example there is actually only <u>one</u> linear length scale: the distance $S(\theta)$ from the base of the ogive to the ogive surface. We can see this because $S(\theta) = R$ when $\theta = 0$, and $S(\theta) = L$ when $\theta = \pi/2$. So both of the obvious scales are covered by the distance to the surface, $S(\theta)$.

Now suppose we wish to design a wind tunnel model of this nose cone in order to understand details of the flow field around the actual prototype. We will require that the wind tunnel model have a base radius r with $r \ll R$ in order for it to fit into the wind tunnel. Then we have $r/R = \alpha$ with $\alpha \ll 1$, and by the definition of geometric similarity we must require that

$$\frac{s(\theta)}{S(\theta)} = \alpha \qquad \text{for all} \quad \theta \in [0, \pi/2] \,.$$

In particular, $\ell/L = \alpha$, where ℓ is the axial length of the model nose cone; $s(\theta)$ in the above equation is distance from the base to the surface of the model.

It should be clear that the surface areas and volume ratios of the model to the actual object will scale as α^2 and α^3, respectively. For example, consider the area of any cross section. For the prototype nose cone the area of the base is πR^2, and for the scale model it is $\pi r^2 = \pi (\alpha R)^2 = \alpha^2 \pi R^2$. Hence, the ratio is α^2, as indicated.

Dynamic Similarity

We will begin our treatment of dynamic similarity with a formal definition.

Definition 3.3 *Two geometrically similar objects are said to be <u>dynamically similar</u> if the forces acting at corresponding locations on the two objects are everywhere in the same ratio.*

We note that in the definition used here, we require geometric similarity in order to even consider dynamic similarity; some treatments relax this requirement, but such approaches are typically non-intuitive and sometimes not even self consistent.

We begin by observing that the specific requirements of the above definition are not easily checked, and we will demonstrate that all that is actually needed is equality of <u>all</u> dimensionless parameters associated with the flow in, or around, the two objects.

There are two ways by means of which we can determine the dimensionless parameters, and thus requirements for dynamic similarity, in any given physical situation. In cases for which governing equations are known, straightforward scaling of these equations will lead to the requirements needed to satisfy the above definition. On the other hand, when the governing equations are not known, the standard procedure is to employ the Buckingham Π Theorem.

We will introduce each of these approaches in the following two subsections, but we note at the outset that in the case of fluid dynamics the governing equations <u>are known</u>—they are the Navier–Stokes equations derived in the preceding sections. Thus, we would expect to usually make direct application of scaling procedures. Nevertheless, in the context of analyzing experimental data it is sometimes useful to apply the Buckingham Π theorem in order to obtain a better collapse of data from a range of experiments.

3.6.2   Scaling the governing equations

Although in most elementary fluid dynamics texts considerable emphasis is placed on use of the Buckingham Π theorem, as we have already noted, when the governing equations are known it is more straightforward to use them directly to determine the important dimensionless parameters for any particular physical situation. The approach for doing this will be demonstrated in the current section.

We begin by observing that from the definition of dynamic similarity we see that it is the ratios of forces at various corresponding locations in two (or more) flow fields that are of interest. Now if we could somehow arrange the equations of motion (via scaling) so that their solutions would be the same in each of the flow fields of interest, then obviously the ratios of forces would be the same everywhere in the two flow fields—trivially. In light of this, our goal should be to attempt to cast the Navier–Stokes equations in a form that would yield exactly the same solution for two geometrically similar objects, via scaling. Then, although the "unscaled" solutions would be different, they would differ in a systematic way related to the geometric similarity.

It is important to note that the form of the N.–S. equations given in (3.43) does not possess this property because we could change either ρ or ν (or both) in these equations thus producing different coefficients on pressure and viscous force terms, and the equations would have different solutions for the two flow fields, even for flows about geometrically similar objects.

The method we will employ to achieve the desired form of the equations of motion is usually called *scaling*, or sometimes *dimensional analysis*; but we will use the latter term to describe a specific procedure to be studied in the next section. Independent of the terminology, the goal of such an analysis is to identify the set of <u>dimensionless</u> parameters associated with a given physical situation (in the present case fluid flow, represented by the N.–S. equations) which completely characterizes behavior of the system (*i.e.*, solutions to the equations). The first step in this process is identification of independent and dependent variables, and parameters, that fully describe the system. Once this has been done, we introduce "typical values" of independent and dependent variables in such a way as to render the system dimensionless. Then, usually after some rearrangement of the equations, the dimensionless parameters that characterize solutions will be evident, and it is these that must be matched between flows about two geometrically similar objects to guarantee dynamic similarity.

We will demonstrate the scaling procedure using the 2-D incompressible continuity and N.–S. equations:

$$u_x + v_y = 0 \,, \tag{3.45a}$$

$$u_t + u u_x + v u_y = -\frac{1}{\rho} p_x + \nu(u_{xx} + u_{yy}) \,, \tag{3.45b}$$

$$v_t + u v_x + v v_y = -\frac{1}{\rho} p_y + \nu(v_{xx} + v_{yy}) - g \,. \tag{3.45c}$$

The independent variables of this system are x, y and t; the dependent variables are u, v and p, and the parameters are g, the gravitational acceleration in the y direction (taken as constant), density ρ and viscosity ν (or, alternatively, g, ρ and μ). In general, there must be boundary and initial conditions associated with Eqs. (3.45); but these will not introduce new independent or dependent variables, and usually will not lead to additional parameters. Thus, in the present analysis we will not consider these.

We next introduce the "typical" values of independent and dependent variables needed to make the equations dimensionless. These values must be chosen by the analyst, and experience is often important in arriving at a good scaling of the equations. Here we will demonstrate the approach with a simple flow in a duct as depicted in Fig. 3.13. In this case we have indicated a typical length scale to be the height H of the duct, and we have taken the velocity scale to be the centerline speed U_c (which is the maximum for these types of flows). This provides sufficient information to scale the spatial coordinates x and y as well as the velocity components u and v. But we still must scale time and pressure.

It is often (but not always) the case that the correct time scale can be obtained by combining
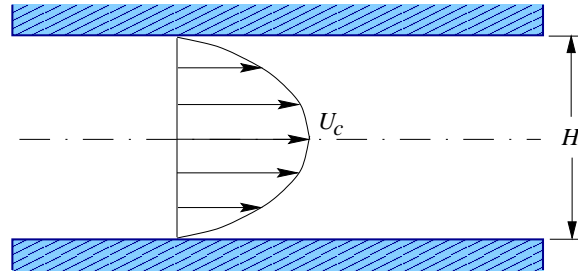
Figure 3.13: 2-D flow in a duct.

the length and velocity scales: using generalized units we see that

$$u \sim \frac{L}{T} \quad \Rightarrow \quad t_s = \frac{H}{U_c} \, .$$

We will use this in the current analysis. We will not attempt to specify a pressure scale at this point, but instead simply introduce the notation P_s for this quantity. We can now formally scale all independent and dependent variables:

$$x^* = x/H \, , \qquad y^* = y/H \, , \qquad t^* = t/t_s \, ,$$

and

$$u^* = u/U_c \, , \qquad v^* = v/U_c \, , \qquad p^* = p/P_s \, .$$

Notice that the "*" quantities are all dimensionless.

We next "solve" these expressions for the dimensional quantities that appear in the governing equations, and substitute the result. We begin with the continuity equation for which the necessary variables are

$$x = Hx^* \, , \qquad y = Hy^* \, , \qquad \text{and} \qquad u = U_c u^* \, , \qquad v = U_c v^* \, .$$

Substitution of the dependent variables into Eq. (3.45a) and noting that U_c is constant yield

$$U_c \frac{\partial u^*}{\partial x} + U_c \frac{\partial v^*}{\partial y} = 0 \quad \Rightarrow \quad \frac{\partial u^*}{\partial x} + \frac{\partial v^*}{\partial y} = 0 \, .$$

We now introduce the scaled independent variables by first observing that, *e.g.*,

$$\frac{\partial}{\partial x} = \frac{\partial}{\partial (Hx^*)} = \frac{1}{H} \frac{\partial}{\partial x^*} \, ,$$

which holds because H is constant and sifts through the (partial) differential in the denominator. This permits us to write the scaled continuity equation as

$$\frac{1}{H} \frac{\partial u^*}{\partial x^*} + \frac{1}{H} \frac{\partial v^*}{\partial y^*} = 0 \quad \Rightarrow \quad \frac{\partial u^*}{\partial x^*} + \frac{\partial v^*}{\partial y^*} = 0 \, . \tag{3.46}$$

We see from this that the scaled continuity equation is identical in form to the unscaled one, Eq. (3.45a). This is often, but not always, the case and, in fact, it is usually one of the things we attempt to achieve during the scaling process since conservation of mass is so fundamental.

We can now apply the same procedure to the x-momentum equation. Analogous to what we have just done, we begin by substituting

$$u = U_c u^* \,, \qquad v = U_c v^* \,, \qquad \text{and} \qquad p = P_s p^*$$

into Eq. (3.45b) to obtain

$$U_c \frac{\partial u^*}{\partial t} + U_c^2 u^* \frac{\partial u^*}{\partial x} + U_c^2 v^* \frac{\partial u^*}{\partial y} = -\frac{P_s}{\rho} \frac{\partial p^*}{\partial x} + \nu U_c \left(\frac{\partial^2 u^*}{\partial x^2} + \frac{\partial^2 u^*}{\partial y^2} \right) \,.$$

Next, we introduce scalings of the independent variables by first noting that the second-derivative terms associated with viscous forces can be treated as follows:

$$\frac{\partial^2}{\partial x^2} = \frac{\partial}{\partial x} \left(\frac{\partial}{\partial x} \right) = \frac{\partial}{\partial H x^*} \left(\frac{\partial}{\partial H x^*} \right) = \frac{1}{H^2} \frac{\partial^2}{\partial x^{*2}} \,,$$

with an analogous result for $\partial^2 / \partial y^2$. Then the partially-scaled result above takes the form

$$\frac{U_c}{t_s} \frac{\partial u^*}{\partial t^*} + \frac{U_c^2}{H} u^* \frac{\partial u^*}{\partial x^*} + \frac{U_c^2}{H} v^* \frac{\partial u^*}{\partial y^*} = -\frac{P_s}{\rho H} \frac{\partial p^*}{\partial x^*} + \frac{\nu U_c}{H^2} \left(\frac{\partial^2 u^*}{\partial x^{*2}} + \frac{\partial^2 u^*}{\partial y^{*2}} \right) \,.$$

But since $t_s = H/U_c$, we can write this as

$$\frac{U_c^2}{H} \left(\frac{\partial u^*}{\partial t^*} + u^* \frac{\partial u^*}{\partial x^*} + v^* \frac{\partial u^*}{\partial y^*} \right) = -\frac{P_s}{\rho H} \frac{\partial p^*}{\partial x^*} + \frac{\nu U_c}{H^2} \left(\frac{\partial^2 u^*}{\partial x^{*2}} + \frac{\partial^2 u^*}{\partial y^{*2}} \right) \,,$$

and we see that division by U_c^2/H will leave the left-hand side in the original form of Eq. (3.45b). This, like the situation with the continuity equation, occurs quite frequently at least in part because the left-hand side contains no physical parameters.

We can now write the above as

$$\frac{\partial u^*}{\partial t^*} + u^* \frac{\partial u^*}{\partial x^*} + v^* \frac{\partial u^*}{\partial y^*} = -\frac{P_s}{\rho U_c^2} \frac{\partial p^*}{\partial x^*} + \frac{\nu}{U_c H} \left(\frac{\partial^2 u^*}{\partial x^{*2}} + \frac{\partial^2 u^*}{\partial y^{*2}} \right) \,. \tag{3.47}$$

It should first be observed that all quantities on the left-hand side of this equation are dimensionless, as are all derivative terms on the right-hand side. This implies that it should be the case that $P_s/(\rho U_c^2)$ and $\nu/(U_c H)$ are also dimensionless. We will demonstrate this for the first of these, and leave a similar calculation for the second as an exercise for the reader. We have in generalized units

$$\rho U_c^2 \quad \sim \quad \frac{M}{L^3} \left(\frac{L}{T} \right)^2 \sim \frac{M}{L^2} \frac{L}{T^2}$$

$$\sim \quad \frac{\text{mass} \cdot \text{acceleration}}{\text{area}} \sim \frac{\text{force}}{\text{area}} \sim \text{pressure} \,.$$

We recall that P_s is an as yet to be determined pressure scale; hence, it must have dimensions of pressure, so the ratio $P_s/(\rho U_c^2)$ is dimensionless, as required. Moreover, we see that if we set $P_s = \rho U_c^2$ the coefficient on the pressure-gradient term in Eq. (3.47) is unity, a convenient notational simplification.

The quantity ρU_c^2 occurs widely in fluid dynamics; it is two times what is termed the *dynamic pressure*, denoted p_d: that is,

$$p_d = \frac{1}{2} \rho U^2 \,, \tag{3.48}$$

where we have suppressed the "*c*" subscript for generality. We will encounter dynamic pressure later in our studies of Bernoulli's equation, and elsewhere.

The final quantity in Eq. (3.47) with which we must deal is $\nu/(U_c H)$. This dimensionless group, or actually its reciprocal, is probably the single most important parameter in all of fluid dynamics. It is called the *Reynolds number* after Osbourne Reynolds who identified it as a key parameter in his early studies of transition to turbulence. In general we express the Reynolds number as

$$Re = \frac{UL}{\nu}, \tag{3.49}$$

where U and L are, respectively, velocity and length scales; ν, as usual, denotes the kinematic viscosity. It is interesting to note that this single dimensionless parameter contains two fluid property parameters, ρ and μ (since $\nu = \mu/\rho$), a characteristic flow speed U, and a characteristic geometric parameter, the length scale L. Since time and pressure scales can be readily derived from these, it is seen that this single parameter completely characterizes many fluid flows.

If we now suppress the "*" notation we can express Eqs. (3.45) in dimensionless form as

$$u_x + v_y = 0, \tag{3.50a}$$

$$u_t + uu_x + vu_y = -p_x + \frac{1}{Re}(u_{xx} + u_{yy}), \tag{3.50b}$$

$$v_t + uv_x + vv_y = -p_y + \frac{1}{Re}(v_{xx} + v_{yy}) - \frac{1}{Fr^2}, \tag{3.50c}$$

where Fr is the Froude number, defined as

$$Fr = \frac{U}{\sqrt{gH}}.$$

This dimensionless group arises naturally in the scaling analysis of the y-momentum equation carried out in a manner analogous to what we have just completed for the x-momentum equation. We leave these calculations as an exercise for the reader.

Equations (3.50) are dimensionless, and their solutions now depend only on the parameters Re and Fr. In particular, if two geometrically similar flow fields have the same Reynolds and Froude numbers, then they have the same scaled velocity and pressure fields. In turn, it is easily seen from the equations of motion that this implies that they will exhibit the same scaled forces at all locations in the flow. Then, in light of the geometric similarity, the unscaled forces will be in a constant ratio at all points of the flow field, and dynamic simlarity will have been achieved. We demonstrate the details of this with the following example.

EXAMPLE 3.7 Consider the two airfoils shown in Fig. 3.14. The one on the left can be considered to be a full-scale portion of an actual aircraft wing while the one on the right is a small wind tunnel model. We assume incompressible flow so that the equations derived earlier apply, and we also assume that no body forces are significant. It then follows from Eqs. (3.50) that the only dimensionless parameter required to completely set the flow behavior is the Reynolds number. As the figure implies, these airfoils are considered to be geometrically similar, and we wish to demonstrate that if the flow Reynolds numbers are the same for flow over the two airfoils, then the forces acting on these will exhibit a constant ratio between any two corresponding locations on the two airfoils. In this example we will examine only the forces due to pressure. We leave as an exercise to the reader demonstration that the same results to be obtained here also hold for the viscous forces.
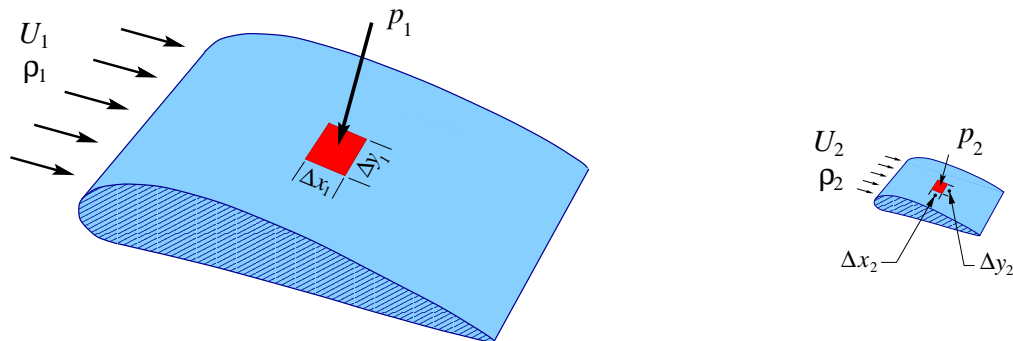
Figure 3.14: Prototype and model airfoils demonstrating dynamic similarity requirements.

We first observe that by geometric similarity we must have

$$\Delta x_1 = \alpha \Delta x_2 \qquad \text{and} \qquad \Delta y_1 = \alpha \Delta y_2$$

with the same value of α in both expressions. Now we can define pressure scales for the two flows as

$$P_{s,1} = \rho_1 U_1^2 \qquad \text{and} \qquad P_{s,2} = \rho_2 U_2^2\,,$$

which implies that the actual pressures acting on the respective elements of surface area shown in the figure must be

$$p_1 = p_1^* \rho_1 U_1^2\,, \qquad \text{and} \qquad p_2 = p_2^* \rho_2 U_2^2\,.$$

Here, the p_i^* are dimensionless pressures that arise as solutions to the governing equations. As such, they depend only on the dimensionless parameter values used for the solution, as we have discussed earlier.

Next, recall that the forces due to pressure acting on an element of surface area are given by

$$F = pA = p\Delta x \Delta y\,,$$

and it follows that

$$F_1 = p_1^* \rho_1 U_1^2 \Delta x_1 \Delta y_1\,, \qquad \text{and} \qquad F_2 = p_2^* \rho_1 U_2^2 \Delta x_2 \Delta y_2\,.$$

We can now check whether the forces F_1 and F_2 have a constant ratio at corresponding points over the entire surface of the airfoils. We have that

$$\frac{F_1}{F_2} = \frac{p_1^* \rho_1 U_1^2 \Delta x_1 \Delta y_1}{p_2^* \rho_2 U_2^2 \Delta x_2 \Delta y_2} = \frac{\rho_1 U_1^2}{\rho_2 U_2^2}\alpha^2\,.$$

Now observe that the second equality holds because if Re is the same in both flows it must be that the scaled pressures satisfy $p_1^* = p_2^*$; furthermore, since ρ_1, ρ_2, U_1 and U_2 are all constants, the far right-hand side must be a constant. Thus, we have shown that

$$\frac{F_1}{F_2} = \text{constant}\,,$$

and this has been done for a completely arbitrary element of surface on which pressure is acting. In particular, this must hold for all points on the surface, and we see that dynamic similarity holds

provided the dimensionless parameter(s) (Reynolds number in this case) and geometric similarity hold.

While the preceding example is quite straightforward, it does not indicate some of the inherent difficulties in conducting laboratory experiments in a manner suitable for obtaining useful data. We previously indicated, without much emphasis, that in order to satisfy the dynamic similarity requirement <u>all</u> dimensionless parameters must be matched between the actual and model flows. The example above has only a single parameter, the Reynolds number, and sometimes even this can be diffifcult to match. For example, even for the situation considered in the example, we can recognize that if the size of the model is very much smaller than that of the prototype (which we would expect to usually be the case), in order to have the Reynolds numbers equal in the two flows, the flow speed over the model would need to be much <u>higher</u> that that over the prototype—a somewhat counter-intuitive requirement.

But even worse is the situation in which more than a single parameter is needed to characterize the physical phenomena. Then matching one parameter may make it difficult, or even impossible, to match a second one. This, in fact, often occurs for buoyancy-driven flows under the Froude number scaling introduced above. In such situations, it is standard practice to match the two, or more, parameters as closely as possible, but not exactly, or in some cases to try to judge which is (are) the more important parameter(s) and match only that one. In either approach, the validity of the data for the desired prototype application is compromised to some extent.

3.6.3 Dimensional analysis via the Buckingham Π theorem

Dimensional analysis is a powerful technique that can be used for several purposes. It is typically first encountered for checking "dimensional consistency" of any given computational formula—the units of each separate term of the formula must be the same. Second is its application in "deriving" expressions for otherwise unknown dimensional quantities based only on the required dimension of the result. An example of this can be found in our choice of scaling parameters given earlier: recall that when we needed a time scale, we recognized that length/velocity has the correct dimensions and thus provides such a scale. But these uses are nearly trivial and automatic. Of much more importance is application of dimensional analysis to identify the dimensionless physical parameters needed to fully characterize a given physical phenomenon, either for correlating experimental (or even computational) data, or for assessing which terms might be neglected in the equations of fluid motion for a particular flow situation. Finally, as we have seen from the last example of the preceding section, such ideas can be useful in designing experiments so as to guarantee that data being collected for a scale model will be of use in predicting behavior of a corresponding (geometrically similar) full-scale object.

We must, however, emphasize from the start that use of the techniques to be presented in this section is most valuable in the context of analyzing data for which no governing equations are *a priori* known. Applications of the Buckingham Π theorem to be stated below are heavily emphasized in essentially all engineering elementary fluid dynamics texts but, in fact, in most cases we already know the governing equations—the N.–S. equations; as a consequence, it is usually more appropriate to apply the scaling analyses of the preceding section. We provide the information of the present section mainly for the sake of completeness.

We will begin by stating the Buckingham Π theorem and explaining the various terms contained in it. We will then provide a detailed example consisting of a relatively simple and easy-to-understand case, and complete the section by demonstrating application of this to curve fitting experimental data.

Determining Dimensionless Parameters in Absence of Governing Equations

    As alluded to above, the approach to doing this is well known and widely used. It is contained in a result known as the *Buckingham* Π *theorem* published in 1915.

Theorem 3.4 *For any given physical problem, the number of dimensionless parameters, N_p, needed to correlate associated data is N_d less than the total number of variables, N_v, where N_d is the number of independent dimensions needed to describe the problem. That is,*

$$N_p = N_v - N_d \,. \tag{3.51}$$

Moreover, for any dimensional quantity Q, we have

$$[Q] = [Q_0] \prod_{i=1}^{N_p-1} [P_i]^{a_i} \,, \tag{3.52}$$

where $[\,\cdot\,]$ denotes "dimension of."

We observe that Q_0 has the same dimensions as Q, and the remaining P_is are dimensionless. The a_is must be determined via the techniques to be presented in the example to follow. Finally, we note that the P_is are often called "π factors," and the name of the theorem arises from the capital Π symbol that indicates a product.

    Application of this theorem is relatively straightforward once the details of the required technique are understood. However, there is more needed than is obvious from the statement of the theorem alone, and we will treat this in the example of the next section. Before proceeding to this we outline the steps that will be required to complete a Buckingham Π theorem analysis. These are as follows:

1. determine all physical quantities associated with the problem;

2. find the dimensions (*i.e.*, units) of each physical quantity, and thus determine the total number of dimensions;

3. invoke the Buckingham Π theorem to determine the number of dimensionless parameters that are needed to characterize the problem, namely $N_p = N_v - N_d$;

4. express dimensions of one physical variable as a product of powers of dimensions of all other physical variables, for example,
$$[V_1] = [V_2]^{a_1} [V_3]^{a_2} \,,$$
   with V_is being variables of interest;

5. substitute all corresponding dimensions;

6. develop system of linear equations to be solved for the powers in the above expression by requiring powers of each dimension to be the same on both sides of the equation;

7. solve these equations for the powers, and substitute these back into the expression in 4. above;

8. rearrange this to the form of Eq. (3.52), and read off the desired dimensionless parameters.

Detailed Example of Applying Buckingham Π theorem

We will demontrate the above ideas with the following example.

EXAMPLE 3.8 We wish to obtain a correlation of data associated with the force exerted on the surface of a sphere of diameter D immersed in a fluid flowing with speed U. We will ignore all possible body forces acting on the sphere itself; in particular, we can imagine that the sphere is supported by a sting in a wind tunnel as depicted in Fig. 3.15 and instrumented so as to allow measurement of pressure and shear stresses at various points over its surface, and/or the forces exerted on the sting supporting the model. The fluid would probably be air (but could be nitrogen
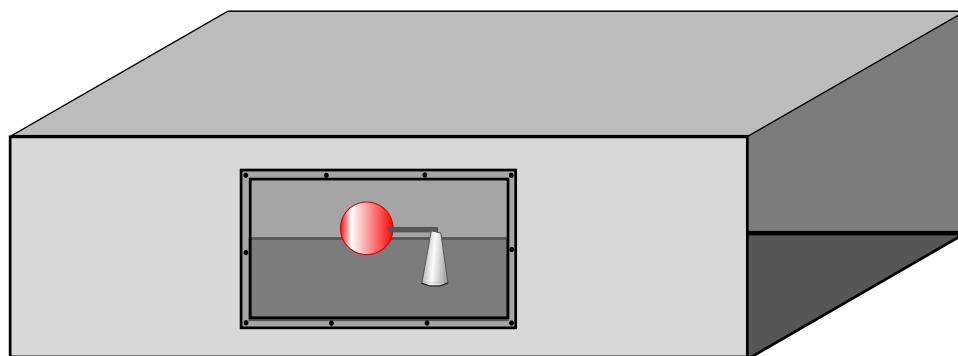
Figure 3.15: Wind tunnel measurement of forces on sphere.

or helium) at a known pressure and temperature. We will apply the Buckingham Π theorem to determine the dimensionless parameters to be employed in the data correlation.

As indicated in the preceding list of steps, the first task is to determine all important physical variables associated with this problem. In general, this must be done based on experience and basic understanding of physics. In the present problem our goal is to produce a correlation of the force acting on the sphere, so obviously force is one of the required physical variables. From our everyday experience, we would probably expect this force to in some way be proportional to the flow speed past the sphere. As a child you may have held your arm out the window of a moving automobile and felt a force acting to move your arm backwards; if you were perceptive, you might have noticed that the faster the automobile was traveling, the greater the force on your arm. Thus, the wind tunnel flow speed is expected to be an important parameter.

If we did not already have the equations of fluid motion in hand, the remaining physical parameters would be considerably less obvious. But in light of these equations we would certainly expect that viscosity and density of the fluid in the wind tunnel would be important. Finally, we would probably expect that the size of the sphere should be important in setting the force acting on it—a very small sphere would have little surface area with which to interact with the oncoming fluid, and conversely. We have thus identified the following set of five physical variables: force F, sphere diameter D, wind tunnel flow speed U, fluid density ρ and viscosity μ.

One might reasonably question why pressure was not included in this list. But recall that pressure is <u>force</u> per unit area, and we have already included force as well as the diameter which leads to area. Thus, pressure would be a redundant entry in the list of variables, but as we will later see, could be used in place of force.

The next step is to determine the number of independent dimensions associated with the physical situation. This is straightforward; we simply need to determine the generalized units (dimensions)

of each of the physical variables, and then count the number of different such dimensions. Thus, we have

$$
\begin{aligned}
F &\sim M\frac{L}{T^2} \\
D &\sim L \\
U &\sim \frac{L}{T} \\
\rho &\sim \frac{M}{L^3} \\
\mu &\sim \frac{M}{LT}\,,
\end{aligned}
$$

where as usual $M \sim$ mass, $L \sim$ length and $T \sim$ time.

As might have been expected, there are three dimensions, and we can now apply the first part of the Buckingham Π theorem; namely, we have found five (5) physical variables and three (3) distinct dimensions. It follows that there must be <u>two</u> (2) dimensionless parameters needed to completely describe the force acting on the sphere as a result of flow moving passed it. Our task now is to find these two parameters.

Our earlier discussion indicates that the initial step in this process is to express the dimensions of one of the variables (in this case, the force that is of key importance) as a product of powers of the dimensions of the other physical variables. This results in

$$[F] = [\mu]^{a_1}[\rho]^{a_2}[U]^{a_3}[D]^{a_4}\,, \tag{3.53}$$

where the a_is are unknown and must be determined. To do this we first substitute the dimensions of each of the physical quantities to obtain

$$\frac{ML}{T^2} = \left(\frac{M}{LT}\right)^{a_1}\left(\frac{M}{L^3}\right)^{a_2}\left(\frac{L}{T}\right)^{a_3}(L)^{a_4}\,, \tag{3.54}$$

or

$$
\begin{aligned}
MLT^{-2} &= M^{a_1}L^{-a_1}T^{-a_1}M^{a_2}L^{-3a_2}L^{a_3}T^{-a_3}L^{a_4} \\
&= M^{a_1+a_2}L^{-a_1-3a_2+a_3+a_4}T^{-a_1-a_3}\,. \tag{3.55}
\end{aligned}
$$

Now in order for this expression to be *dimensionally consistent* (*i.e.*, dimensions are the same on both sides of the equation), the power of each of the individual dimensions must match from one side of (3.55) to the other. This requirement leads to a system of linear equations for the powers, a_i, first appearing in Eq. (3.53):

$$a_1 + a_2 = 1\,, \tag{3.56a}$$
$$-a_1 - 3a_2 + a_3 + a_4 = 1\,, \tag{3.56b}$$
$$-a_1 - a_3 = -2\,, \tag{3.56c}$$

respectively, by considering first the mass M, then length L and finally time T.

We immediately observe from Eqs. (3.56) that there are four unknowns and only three equations. This is rather typical in applications of the Buckingham Π theorem: in particular, usually the number of unknowns will exceed the number of equations by one less than the number of dimensionless parameters to be found. This is the case here, and we will see below that it does not

present any problem with regard to determining the required parameters. (We note that there are occasional exceptions to this, but in this introductory treatment we will ignore such cases.)

Next we must solve Eqs. (3.56) for the a_is. Since there is an extra unknown in comparison with the number of equations, the best strategy is to solve for each of the other unknowns in terms of this additional one. In the present case it turns out that it is convenient to express each of a_1, a_2 and a_4 in terms of a_3. Starting with the first equation in the system (3.56) we see that

$$a_2 = 1 - a_1 \,,$$

and the third equation yields

$$a_1 = 2 - a_3 \,.$$

Thus, we have expressed a_1 in terms of a_3, and substitution of this into the expression for a_2 provides a relationship between a_2 and a_3:

$$a_2 = 1 - (2 - a_3) = a_3 - 1 \,.$$

Finally, we can insert both of these results into the third equation to obtain

$$-(2 - a_3) - 3(a_3 - 1) + a_3 + a_4 = 1 \,,$$

from which it follows that

$$a_4 = a_3 \,.$$

This is all that can be accomplished with regard to solving the system of equations (3.56). Clearly, there is an infinity of solutions—a different solution for each possible choice of a_3. But this will not prevent us from finding the desired dimensionless parameters, as we will now show.

The next step is to substitute these results back into Eq. (3.53); this yields

$$[F] = [\mu]^{2-a_3}[\rho]^{a_3-1}[U]^{a_3}[D]^{a_3} \,. \tag{3.57}$$

We now regroup the factors of this expression so as to combine all those involving some power including a_3 and, separately, those that do not. (Recall that the Buckingham Π theorem has indicated there are <u>two</u> dimensionless parameters, so such a grouping is natural.) This leads to

$$[F] = \left[\frac{\mu^2}{\rho}\right] \left[\frac{\rho\,U D}{\mu}\right]^{a_3} \,. \tag{3.58}$$

We should recognize that this is in the form of Eq. (3.52) given in the statement of the Π theorem if we set

$$Q_0 = F_0 \equiv \frac{\mu^2}{\rho} \,,$$

and

$$P_1 = \frac{\rho\,U D}{\mu} \,.$$

In particular, since $N_p = 2$ there can be only one factor in the Π product, *i.e.*, P_1.

Now recall that in the statement of the theorem Q_0 has the same dimensions as Q (which implies that their ratio will produce one dimensionless parameter). Thus, in the present case F_0 should have the dimensions of force; we check that this is true and find

$$\frac{\mu^2}{\rho} \sim \frac{(M/LT)^2}{M/L^3} \sim \frac{ML}{T^2} \quad (\sim \text{mass} \times \text{acceleration}) \sim F \,,$$

as required. Thus, one of the two dimensionless parameters (also sometimes termed "dimensionless groups") is

$$P_0 \equiv \frac{F}{F_0} = \frac{\rho F}{\mu^2} \, .$$

The second dimensionless parameter is, of course, P_1 which we immediately recognize as the Reynolds number (because $\rho/\mu = 1/\nu$) from our earlier scaling analysis of the equations of motion. Indeed, we should have expected from the start that this parameter would have to occur.

Application to Data Analysis

At this point it is worthwhile to consider how the preceding results can actually be used. As we have indicated earlier, one of the main applications of this approach is correlation of data from laboratory (and, now, computer) experiments. In particular, it is important to "collapse" data from a range of related experiments as much as possible before attempting a correlation, and this is precisely what can be accomplished with properly-chosen dimensionless parameters. (We comment that this can be foreseen from the scaling analysis of the governing equations in light of the fact that these must always produce the <u>same</u> solution for a given set dimensionless parameters, independent of the physical parameter values that led to these.)

In the present case we have found that only two dimensionless variables are needed to completely characterize data associated with the forces acting on a sphere immersed in a fluid flow, *viz.*, a dimensionless force defined as $\rho F/\mu^2$ and the Reynolds number, $Re = \rho U D/\mu$. This implies that we can in advance choose a fluid and the temperature at which the experiments are to be run (thereby setting ρ and μ), select a diameter D of the sphere that will fit into the wind tunnel (or tow tank) being used, and then run the experiments over a range of Re by simply varying the flow speed U. For each such run of the experiment we measure the force F and nondimensionalize it with the scaling ρ/μ^2 (which is fixed once the temperature is set). Figure 3.16 provides a plot of such data.

We can observe two distinct flow regimes indicated by the data, and a possible transitional regime between the two—not unlike our earlier intuitive description of the transition to turbulence (recall Fig. 2.22). In the first of these (Re less than approximately 20) the dimensionless force varies linearly with Reynolds number (a fact that can be derived analytically). In the last regime (Re greater than about 200) the force depends on the square of Re. In this case we would expect that

$$\frac{\rho F}{\mu^2} \Big/ Re^2$$

should be approximately constant. That is,

$$\frac{\rho F}{\mu^2} \Big/ \left(\frac{\rho U D}{\mu} \right)^2 = \frac{F}{\rho U^2 D^2} \sim \text{const.}$$

This suggests a different, but related, parameter by means of which to analyze the data. Namely, recall that pressure is force per unit area; so we have $F/D^2 \sim p$, and it follows that we might also correlate data using the quantity

$$\frac{p}{\rho U^2}$$

as the dimensionless parameter. It is of interest to note that this is precisely the scaled pressure arising in our earlier analysis of the Navier–Stokes equations. In practice, it is more common to
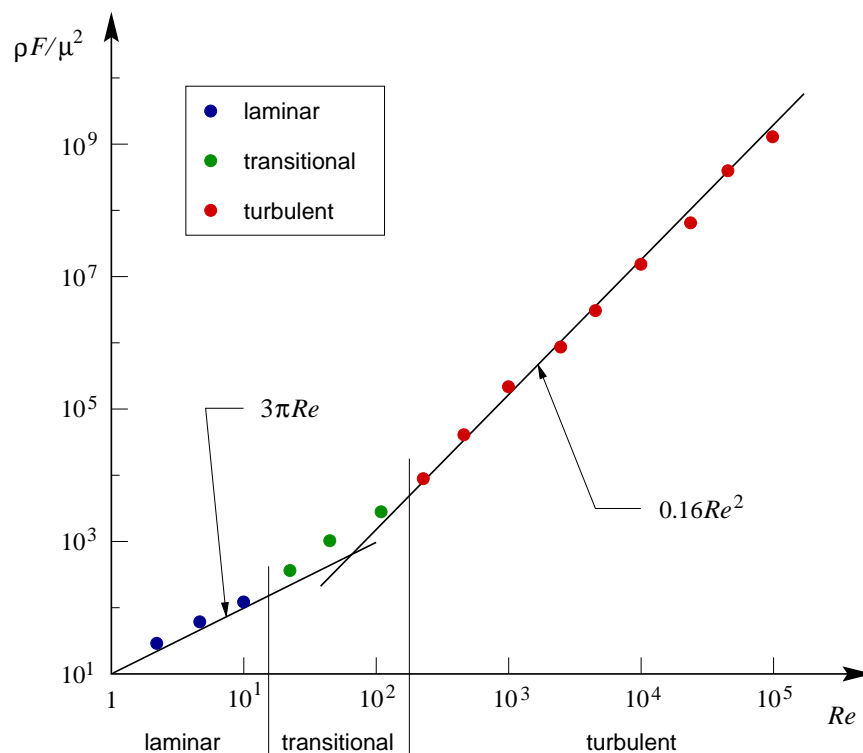
Figure 3.16: Dimensionless force on a sphere as function of Re; plotted points are experimental data, lines are theory (laminar) and curve fit (turbulent).

utilize a reference pressure, often denoted p_∞, and define the dimensionless *pressure coefficient* as

$$C_p \equiv \frac{p - p_\infty}{\frac{1}{2}\rho U_\infty^2} \,. \tag{3.59}$$

Then the above plot can also be presented as C_p *vs.* Re, a common practice in fluid dynamics.

3.6.4 Physical description of important dimensionless parameters

In the preceding sections we have encountered the dimensionless parameters Re, Fr and C_p. The first two of these were shown to completely characterize the nature of solutions to the N.–S. equations in a wide range of physical circumstances involving incompressible flow. The last appeared as a quantity useful for data correlations associated with force on an object due to fluid flow around it, as a function of Re. In the present section we will treat these in somewhat more detail, especially with regard to their physical interpretations, and we will introduce a few other widely-encountered dimensionless parameters.

Reynolds Number

The Reynolds number, Re, can be described as a ratio of inertial to viscous forces. A simple way to see this is to recall Eqs. (3.50) and note that if Re is large the diffusive terms (viscous force terms) will be small; hence, flow behavior will be dominated by the inertial forces (and possibly also pressure and body forces). A more precise way to obtain this characterization is to note that the

inertial forces are associated with accelerations and thus come from $F_{inertial} = ma$. Now observe that

$$m = \rho L^3 , \qquad \text{and} \qquad a \sim L/T^2 \sim U/T .$$

From this it follows that

$$ma \sim \frac{\rho L^3 U}{T} \sim \rho U^2 L^2 \sim \text{ inertial force} .$$

On the other hand, we can estimate the viscous forces based on Newton's law of viscosity:

$$\text{viscous force} \quad = \quad \tau A \simeq \mu \frac{\partial u}{\partial y} A$$

$$\sim \quad \mu \frac{U}{L} \cdot L^2 \sim \mu\, U L .$$

From this it follows that

$$\frac{\text{inertial force}}{\text{viscous force}} = \frac{\rho U^2 L^2}{\mu\, U L} = \frac{\rho\, U L}{\mu} = Re .$$

Froude Number

In a similar manner we can argue that the Froude number, Fr, represents the ratio of inertial forces to gravitational forces. In particular, recalling that $\rho \boldsymbol{g}$ is gravitational force per unit volume and using the expression just obtained for inertial force, we have

$$\frac{\text{inertial force}}{\text{gravitational force}} = \frac{\rho U^2 L^2}{\rho g L^3} = \frac{U^2}{gL} = Fr^2 .$$

Pressure Coefficient

We next recall the pressure coefficient given earlier in Eq. (3.59). It is easily checked that this is actually a ratio of pressure force to inertial force. If we consider the force that would result from a pressure difference such as

$$\Delta p \equiv p - p_\infty ,$$

we have

$$\frac{\text{pressure force}}{\text{inertial force}} = \frac{\Delta p L^2}{\rho U^2 L^2} = \frac{\Delta p}{\rho U^2} = \frac{1}{2} C_p ,$$

which is equivalent to Eq. (3.59).

Other Dimensionless Parameters

There are many other dimensionless parameters that arise in in fluid dynamics although most are associated with very specific flow situations. One that is more general than most others is the Mach number, M, that arises in the study of compressible flows, especially in aerodynamic applications. The Mach number is defined as

$$M \equiv \frac{\text{flow speed}}{\text{sound speed}} = \frac{U}{c} .$$

We can use this to somewhat more precisely define what we mean by an incompressible flow. Recall that we have previously viewed a flow as incompressible if its density is constant. But it is sometimes

preferable, especially in studies of combustion, to use a different approach. In particular, it can be shown that if the Mach number is less than approximately 0.3, no more than an approximately 10% error will be incurred by treating the flow as incompressible and, in particular, invoking the divergence-free condition. Thus, a "rule of thumb" is that flow can be considered incompressible if $M \leq 0.3$, and otherwise it must be treated as compressible. It turns out that in many combusting flows M is very low, but at the same time the density is changing quite rapidly. Our first thought in analyzing such flows is that they cannot be incompressible because of the variable density. But the Mach number rule of thumb indicates that we can treat the flow as divergence free. We leave as an exercise to the reader demonstration that this is not inconsistent with using the compressible continuity equation to handle the variable density.

The final dimensionless parameter we will mention here is the Weber number, denoted We. This is the ratio of inertial forces to surface tension forces and is given by

$$\frac{\text{inertial force}}{\text{surface tension force}} = \frac{\rho U^2 L}{\sigma} = We \,,$$

where σ is surface tension. As would be expected, this number is important for flows having a free surface such as occur at liquid-gas interfaces, but in the present lectures we will not be providing any further treatment of these.

Despite the emphasis we have placed on finding dimensionless parameters and writing governing equations in dimensionless form, we feel it is essential to remark that, especially in constructing modern CFD codes, such an approach is seldom, if ever, taken. There is a very fundamental reason for this stemming from the extreme generality of the Navier–Stokes equations. In particular, these equations represent essentially all possible fluid motions, and the physical details may differ drastically from one situation to the next. In turn, this implies that the specific dimensionless parameters needed for a complete description of the flow also will vary widely. Thus, it is basically not possible to account for this in a general CFD code in any way other than by writing the code for the original <u>unscaled</u> physical equations.

3.7 Summary

We conclude this chapter with a brief recap of the topics we have treated. We began with a discussion in which Lagrangian and Eulerian reference frames were compared, and we noted that the former is more consistent with application of Newton's second law of motion while the latter provided formulations in terms of variables more useful in engineering practice. We then introduced the substantial derivative that permits expressing Lagrangian motions in terms of an Eulerian reference frame. We next provided a brief review of the parts of vector calculus that are crucial to derivation of the equations of motion, namely Gauss's theorem and the transport theorems; we then proceeded to derive the equations of motion. The first step was to obtain the so-called "continuity" equation which represents mass conservation. The differential form of this was derived, and then by basically working backwards we produced a control-volume formulation that is valuable for "back-of-the-envelope" engineering calculations.

We next began derivation of the differential form of the equations of momentum balance—the Navier–Stokes equations. This began by stating a more general form of Newton's second law— one more appropriate for application to fluid elements, as needed for describing fluid flows. We expressed this in terms of acceleration (times mass per unit volume) and a sum of body and surface forces acting on an isolated fluid element. Then we treated the surface terms in detail, ultimately

employing Newton's law of viscosity to obtain formulas for the viscous stresses that generate most (except for pressure) of the surface forces. This led to the final form of the equations of motion, and we then discussed some of the basic mathematics and physics of these equations on a term-by-term basis.

The final section of the chapter was devoted to treatment of scaling and dimensional analysis of the governing equations in order to determine the important dimensionless parameters for any given flow situation. One of the prime uses of such information is to allow application of data obtained from small scale models to make predictions regarding flow in or around a full-scale object, and we emphasized that geometric and dynamic similarity must be enforced to do this reliably. A second important use of dimensionless parameters is to collapse experimental data to obtain more meaningful correlation formulas from curve-fitting procedures. Finding such parameters was approached in two distinct ways, one involving direct use of the equations and the other employing the Buckingham Π theorem. We noted that the former should essentially always be used when the equations governing the physics are known, while the latter must be used if this is not the case.

Chapter 4

Applications of the Navier–Stokes Equations

In this chapter we will treat a variety of applications of the equations of fluid motion, the Navier–Stokes (N.–S.) equations, derived in the preceding chapter. These applications will, in general, be of two types: those involving the derivation of exact solutions to the equations of motion, and those in which these and other results are used to solve practical problems. It will be seen that at least in some cases there will be considerable overlap between these types, and we will not attempt to subsection the chapter in terms of this classification. Rather, we will start with the simplest possible application, fluid statics. We will use the N.–S. equations to obtain the equation of fluid statics—an almost trivial process, and we will present several practical uses of this equation. We will then proceed to the next simplest case, derivation of Bernoulli's equation, and follow the same general approach in its treatment. We will follow this with a very brief treatment of the control-volume momentum equation, analogous to the control-volume continuity equation of the previous chapter, and we will then derive two classical exact solutions to the N.–S. equations, *viz.*, Couette flow and plane Poiseuille flow. We then conclude the chapter with a quite thorough treatment of pipe flow, including both the Hagen–Poiseuille exact solution to the N.–S. equations and treatment of various practical applications.

4.1 Fluid Statics

Fluid statics is an almost trivial application of the equations of fluid motion for it corresponds to the study of fluids <u>at rest</u>. There are two main topics within this area: *i)* determination of the pressure field and *ii)* analysis of forces and moments (arising from the pressure field) on submerged (and partially submerged) objects. We will emphasize the former in these lectures, while the only aspect of the latter to be treated will consist of a brief introduction to buoyancy. We will begin by deriving the equations of fluid statics from the N.–S. equations, and then provide some examples that lend themselves to introduction of important terminolgy associated with pressure. In addition we state Pascal's law that has a number of practical applications, and demonstrate one of these in an example. We then consider Archimedes' principle, a statement of the effects of buoyancy in a static fluid, and we provide a specific example that shows how to use this principle in calculations.

4.1.1   Equations of fluid statics

The equations of fluid statics are usually derived by a simple force balance under the assumption of mechanical equilibrium (pressure independent of time) for the fluid system. Here, however, we will obtain them as a special case of the N.–S. equations; this is actually much easier, and now that we have these equations available such an approach, among other things, emphasizes the unity of fluid mechanics in general as embodied in the N.–S. equations.

Thus, we begin by writing the 3-D incompressible N.–S. equations in a Cartesian coordinate system with the positive z direction opposite the direction of gravitational acceleration. This gives

$$u_x + v_y + w_z = 0\,, \tag{4.1a}$$

$$u_t + uu_x + vu_y + wu_z = -\frac{1}{\rho}p_x + \nu\Delta u\,, \tag{4.1b}$$

$$v_t + uv_x + vv_y + wv_z = -\frac{1}{\rho}p_y + \nu\Delta v\,, \tag{4.1c}$$

$$w_t + uw_x + vw_y + ww_z = -\frac{1}{\rho}p_z + \nu\Delta w - g\,. \tag{4.1d}$$

Now because the fluid is assumed to be motionless, we have $u = v = w \equiv 0$, implying that <u>all</u> derivatives of velocity components also are zero. In particular, there can be no viscous forces in a static fluid. Clearly, the continuity equation is satisfied trivially, and the momentum equations collapse to

$$p_x = 0\,, \tag{4.2a}$$

$$p_y = 0\,, \tag{4.2b}$$

$$p_z = -\rho g = -\gamma\,, \tag{4.2c}$$

where γ is the specific weight defined in Chap. 2.

The first two of these equations imply that in a static fluid the pressure is constant throughout planes aligned perpendicular to the gravitational acceleration vector; *i.e.*, $p_x = 0$ implies p is not a function of x, and similarly for y. We now integrate Eq. (4.2c) to formally obtain

$$p(x, y, z) = -\gamma z + C(x, y)\,,$$

where $C(x, y)$ is an integration <u>function</u>. (When integrating a partial differential equation we obtain integration functions instead of integration constants.) But we have already noted that Eqs. (4.2a) and (4.2b) imply that p cannot be a function of either x or y; so in this special case C is a constant, and we then have

$$p(z) = -\gamma z + C\,. \tag{4.3}$$

We remark here that the first liquid considered in this context was water, and as a result the contribution $\gamma z = \rho g z$ to the pressure in a static fluid is often termed the *hydrostatic pressure*.

The value of C must now be determined by assigning a value to p, say p_0, at some reference height $z = h_0$. This leads to

$$p_0 = p(h_0) = -\gamma h_0 + C \qquad \Rightarrow \quad C = p_0 + \gamma h_0\,,$$

and from this it follows that

$$p(z) = p_0 + \gamma(h_0 - z)\,. \tag{4.4}$$

This actually represents the solution to a simple *boundary-value problem* consisting of the first-order differential equation (4.2c) and the boundary condition $p(h_0) = p_0$, and we will emphasize this viewpoint in the sequel as we introduce several examples to demonstrate use of the equations of fluid statics.

Pascal's Law

One of the first results learned about fluid statics in high school physics classes is *Pascal's law*. We will state this, provide physical and mathematical explanations of it, and consider an important application.

Pascal's Law. *In any closed, static fluid system, a pressure change at any one point is transmitted <u>undiminished</u> throughout the system.*

We first observe that from Eqs. (4.2a) and (4.2b) it follows that for any xy plane in which a pressure change is introduced, pressure throughout that plane must be the new value because these equations require that the pressure be the same everywhere in any such plane. But if we now view Eq. (4.2c) as part of the boundary-value problem described above, we see that this new pressure will provide a new boundary condition which we denote here as $p_0 + \Delta p$ with Δp being the change in pressure. Then we see from Eq. (4.4) that this same <u>change</u> in pressure occurs at every height z in the fluid. In particular, we have

$$p(z) = p_0 + \Delta p + \gamma(h_0 - z).$$

This property of a static fluid serves as the basis of operation of many hydraulic devices, probably the simplest of which is the hydraulic jack. The purpose of any type of jack is usually to lift (or, in general, move) heavy objects by applying a minimal amount of force. Hydraulic devices are very effective in accomplishing this as indicated in the following example.

EXAMPLE 4.1 Consider the action of a hydraulic jack, depicted in Fig. 4.1, such as would be found in an automobile service center . A pressure change Δp_1 is applied to the left-hand cylinder
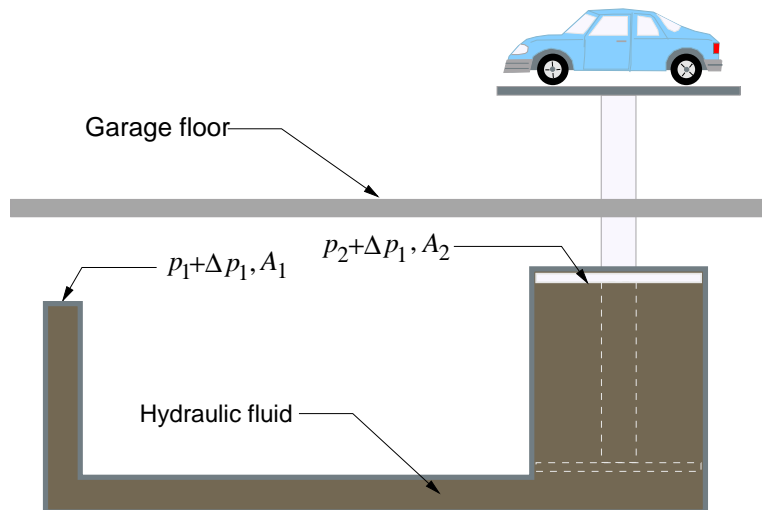
Figure 4.1: Hydraulic jack used to lift automobile.

that has area A_1. By Pascal's law this change is transmitted throughout the hydraulic fluid, and in

particular the pressure at the piston in the upper part of the right-hand cylinder is now $p_2 + \Delta p_1$. But the area, A_2, of this cylinder is far greater than A_1, so the force delivered to the piston is very large compared with that associated with the area of the left-hand cylinder. Thus, a relatively small amount of force applied on the left side is amplified due to the larger area of the right-side cylinder and the physical behavior of pressure in a static fluid. As a result, only moderate pressures are needed to lift quite heavy objects such as automobiles.

Analysis of Barometers and Manometers

In this section we will briefly analyze the fluid-static behavior associated with barometers and manometers. The main reason for presenting these simple analyses is that they motivate some important and widely-used terminology which we will also introduce at this time. We will provide one example related to each of these pressure measurement devices.

EXAMPLE 4.2 In Fig. 4.2 we display a sketch of a simple barometer such as might be used to measure atmospheric (or other ambient) pressure. This consists of a tube, such as a test tube, placed upside down in a container of fluid that is open to the ambient environment for which the pressure is to be measured. We will show that the height attained by the fluid in the tube is directly
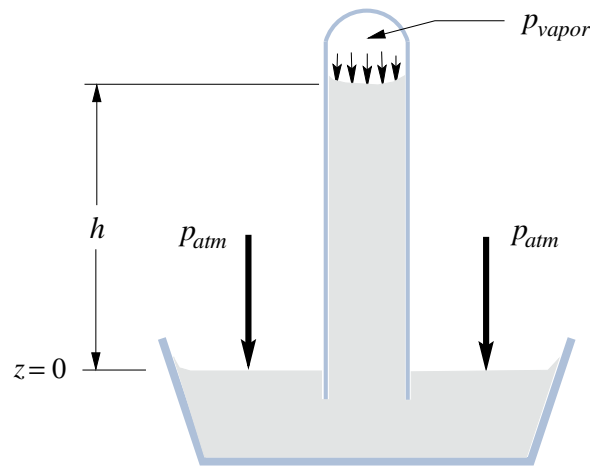
Figure 4.2: Schematic of a simple barometer.

proportional to the ambient pressure. We observe that such a measurement technique was long used for measuring atmospheric pressure, and hence the notation we have employed. We also note that mercury, Hg, was essentially always used as the barometer fluid until it was recognized that mercury vapor is a health hazard. This use led to the custom of quoting atmospheric pressure in inches or millimeters of mercury, a rather counter-intuitive nomenclature since length is not the correct unit for pressure. Nevertheless, this is still practiced today, at least in the atmospheric sciences.

The physical situation depicted in the figure can be analyzed using Eq. (4.2c). We have

$$\frac{\partial p}{\partial z} = -\rho g \,,$$

where ρ is density of the fluid <u>in the barometer</u>. The boundary condition required to solve this equation is

$$p(h) = p_{vapor} \,,$$

the vapor pressure of the barometer fluid (assumed known since the fluid is known).

Integration of the differential equation gives

$$p(z) = -\rho gz + C\,,$$

where C is an integration constant that must be determined using the boundary condition. We do this as follows:

$$p(h) = -\rho gh + C = p_{vapor}\,,$$

so

$$C = p_{vapor} + \rho gh\,.$$

But the fluids used in barometers are usually chosen to have very small vapor pressure under normal conditions, implying that

$$C \simeq \rho gh\,.$$

Thus, as the solution to the boundary-value problem we obtain

$$p(z) = \rho g(h - z).$$

Now the pressure that we wish to measure in this case occurs at $z = 0$, so the above yields

$$p_{atm} = p(0) = \rho gh\,,$$

where h is the height of the column of fluid in the test tube. As indicated at the start, a simple measurement of the height directly gives the desired pressure. We remark that atmospheric pressure is an *absolute pressure* measured with respect to the vacuum of outer space in which the Earth travels. Thus, we see that barometers measure <u>absolute</u> pressure.

We now perform a similar analysis for a manometer. Such devices were once essentially the only means of simultaneously measuring pressures at numerous locations on objects being tested in wind tunnels, although today quite sophisticated electronic pressure transducers are more often used. Nevertheless, manometers are still employed in some situations, so it is worthwhile to understand how they can be analyzed. The following example demonstrates this.

EXAMPLE 4.3 In this example we will demonstrate how a manometer can be used to measure pressures other than ambient. We consider a tank of fluid having density ρ_2 whose pressure we wish to measure. We connect a manometer containing a fluid of density ρ_1 to the outlet of the tank as shown in the figure and leave the downstream end of the manometer open to the atmosphere (whose pressure we assume is known—we could measure it with a barometer, if necessary). Observe that the densities must satisfy $\rho_1 > \rho_2$, and the two fluids must be *immiscible, i.e.,* they are incapable of mixing, in order for the manometer to function. Usually, fluid 1 will be a liquid and fluid 2 a gas; so the density requirement is easily satisfied. It is also typically the case that in static situations as we are treating here, mixing of gases with a liquid is negligible unless pressures are extremely high. We will assume this is not the case in the present example.

Our task is to calculate the pressure p_2 using the measured values of height h_i, $i = 1, 2, 3$, given in the figure under the assumption that the densities are also known. We will further assume that the measurement is being done at sea level, and at a known temperature, so that both p_{atm} and the gravitational acceleration g are specified. To determine p_2 we will first write the equation of fluid statics for each of the separate fluids. We note that this should be expected because the height of
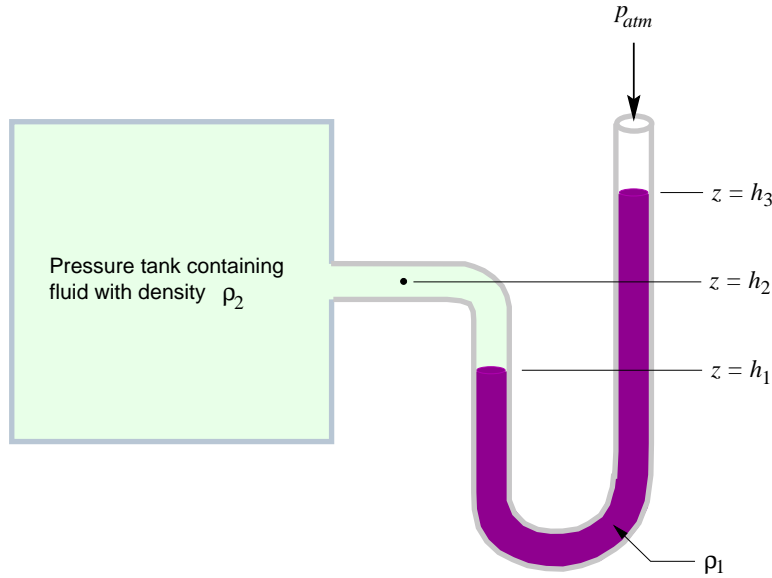
Figure 4.3: Schematic of pressure measurement using a manometer.

the first fluid in the manometer will be determined mainly by pressure in the second fluid. Thus, we write

$$\frac{\partial p_1}{\partial z} = -\rho_1 g \,,$$

$$\frac{\partial p_2}{\partial z} = -\rho_2 g \,.$$

In order to solve these we must specify boundary conditions. It is clear from the figure and the above discussion that the boundary condition for the first equation should be

$$p_1(h_3) = p_{atm} \,.$$

Furthermore, we must always require that pressure be continuous across an interface between two static fluids, for if it were not continuous there would be unbalanced forces (neglecting surface tension) at the interface tending to move it until the forces balanced. Continuity of pressure provides the boundary condition needed to solve the second equation, and it leads to coupling of the equations that is necessary for the height of fluid 1 to yield information on the pressure of fluid 2. The interface between the two fluids is at $z = h_1$, and continuity of pressure at this location implies

$$p_2(h_1) = p_1(h_1) \,.$$

We are now prepared to solve the two equations. Integration of each of these yields

$$p_1(z) = -\rho_1 g z + C_1 \,,$$

and

$$p_2(z) = -\rho_2 g z + C_2 \,.$$

We can find the integration constant C_1 by imposing the first boundary condition; we have:

$$p_{atm} = p_1(h_3) = -\rho_1 g h_3 + C_1 \qquad \Rightarrow \qquad C_1 = p_{atm} + \rho_1 g h_3 \,.$$

Thus, the complete (*particular*) solution to the first equation is

$$p_1(z) = p_{atm} + \rho_1 g(h_3 - z) \,.$$

At this point we recognize that evaluation of this at $z = h_1$ will provide the boundary condition needed for the second equation via continuity of pressure across the interface between the two fluids; we obtain

$$p_1(h_1) = p_{atm} + \rho_1 g(h_3 - h_1) = p_2(h_1) \,,$$

with the last equality coming from the second boundary condition. We can now determine C_2 by evaluating the equation for $p_2(z)$ above at h_1 and using the result just obtained. Thus, we have

$$p_2(h_1) = -\rho_2 g h_1 + C_2 = p_1(h_1) = p_{atm} + \rho_1 g(h_3 - h_1) \,.$$

The only unknown in this sequence of equalities is C_2, so we can solve for it by equating the second and last of the above expressions:

$$-\rho_2 g h_1 + C_2 = p_{atm} + \rho_1 g(h_3 - h_1) \,,$$

which results in

$$C_2 = p_{atm} + \rho_1 g(h_3 - h_1) + \rho_2 g h_1 \,.$$

This, in turn, leads to an expression for pressure in the tank, the desired result; after substitution of the above into the equation for $p_2(z)$ followed by some rearrangement, we obtain

$$p_2(z) = p_{atm} + \rho_1 g(h_3 - h_1) + \rho_2 g(h_1 - z) \,.$$

All that remains is to evaluate this at the height $z = h_2$ corresponding to the entrance to the pressurized tank. This yields

$$p_2(h_2) = p_{atm} + \rho_1 g(h_3 - h_1) + \rho_2 g(h_1 - h_2) \,,$$

as the desired pressure.

We should first observe that since we have assumed that the fluid in the tank is a gas, unless the tank is extremely tall (in the z direction) there will be little effect from the third term in the above equation. In particular, the choice of h_2 as the height at which to attach the manometer has little influence because the pressure will be essentially uniform within the tank. At the same time, it is important to note that this is not the case for liquids. If we recall Eq. (4.4) we see that if $\gamma = \rho g$ is significant, as is the case with liquids, then differences in height can easily lead to contributions in the second term of (4.4) that are as large as, or larger than, p_0 and cannot be neglected.

We also note that the direction of integration is important in analysis of multi-fluid problems such as the above. In particular, we have tacitly assumed in this example that integration is carried out in the positive z direction. But if for some reason this is not the case, then the signs must be changed to correctly account for this.

In the above equation for $p_2(z)$, once the fluids are prescribed so their densities are known the pressure at any height can be obtained directly by measuring the height; *i.e.*, it could be read from a scale, or gage. Thus, we can write that equation as

$$p_2(z) = p_{atm} + p_{gage} \,,$$

or

$$p_{gage} = p_2(z) - p_{atm} \,. \tag{4.5}$$

Once one has had the experience of reading pressure gages in laboratory experiments it is easy to remember this relationship. Namely, the experiments will usually be taking place in a laboratory that is, itself, at atmospheric pressure. Furthermore, before the experiment is started, the pressure gages will all read zero even though they are exposed to atmospheric pressure. (In fact, they will probably have been calibrated to do so.) As the experiment proceeds the gages will show different pressure values, and these values are the "gage" pressures. But to obtain the absolute pressure alluded to earlier it is necessary to add the atmospheric (or some other appropriate reference) pressure to the gage pressure. Thus, we have the general relationship amongst these pressures given by

$$p_{abs} = p_{gage} + p_{ref} \,. \tag{4.6}$$

We again emphasize that p_{ref} is usually atmospheric pressure.

4.1.2   Buoyancy in static fluids

Buoyancy is one of the earliest-studied of fluid phenomena due to its importance in ship building. Ancient Egyptians already understood basic concepts related to buoyancy, at least at a practical level, and were able to successfully construct barges for transporting various materials down the Nile River. Obviously, such applications are still very important today.

In this section we will provide a very brief introduction consisting of the statement of Archimedes' principle and then an example of applying it. We note that in these lectures we will not consider such important topics as stability of floating objects and buoyancy in flowing fluids. With respect to the latter, however, we comment that the equations of motion we have previously derived are fully capable of handling such phenomena if augmented with equations able to account for density changes in the fluid.

We begin with a formal definition of buoyancy in the context of the present treatment.

Definition 4.1 *The resultant fluid force acting on a submerged, or partially submerged, object is called the <u>buoyant force</u>.*

We remark that the objects in question need not necessarily be solid; in particular, fluid elements can experience buoyancy forces. As alluded to above, such forces are among the body forces already present in the Navier–Stokes equations. Furthermore, other forces might also be acting on the submerged body simultaneously, the most common being weight of the body due to gravitation.

Archimedes' Principle

We begin this subsection with a statement of Archimedes' principle.

Archimedes' Principle. *The buoyant force acting on a submerged, or partially submerged, object has a magnitude equal to the weight of fluid displaced by the object and a direction directly opposite the direction of local acceleration giving rise to body forces.*

In the most commonly-studied case, the acceleration is the result of a gravitational field, and it is clear that the buoyant force acting on a submerged object having volume V is

$$F_b = \rho_{fluid} V g \,. \tag{4.7}$$

In the case of a partially-submerged (or floating) object, only a fraction of the total volume corresponding to the percentage below the fluid surface should be used in the above formula for the buoyancy force.

We remark that the above statement of Archimedes' principle is somewhat more complete than that originally given by Archimedes in ancient Greece to permit its application in situations involving arbitrary acceleration fields, *e.g.*, such as those occurring in orbiting spacecraft when their station-keeping thrustors are activated.

Application of Archimedes' Principle

The following example will provide a simple illustration of how to apply the above-stated principle. It will be evident that little is required beyond making direct use of its contents.

EXAMPLE 4.4 We consider a cubical object with sides of length h that is floating in water in such a way that $\frac{1}{4}h$ of its vertical side is above the surface of the water, as indicated in Fig. 4.4. It is required to find the density of this cube.
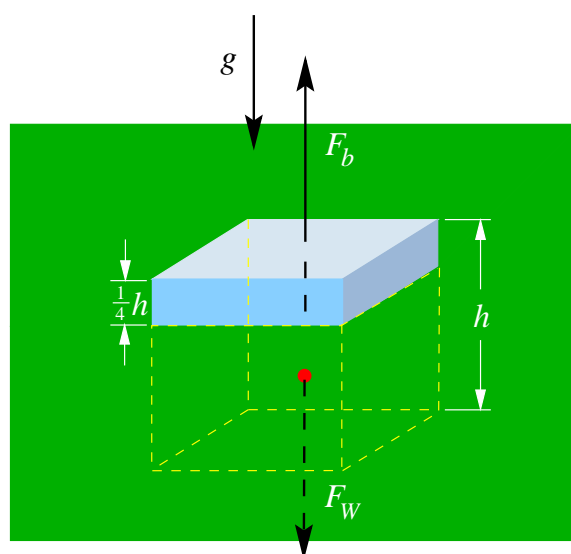
Figure 4.4: Application of Archimedes' principle to the case of a floating object.

From Archimedes' principle it follows directly that the buoyancy force must be

$$F_b = \rho_{water}\frac{3}{4}h^3 g\,,$$

and it must be pointing upward as indicated in the figure. The force due to the mass of the cube, *i.e.*, the weight, is given by

$$F_W = -\rho_{cube}h^3 g\,,$$

with the minus sign indicating the downward direction of the force. Now in static equilibrium (the cube floating as indicated), the forces acting on the cube must sum to zero. Hence,

$$F_b + F_W = 0 = \rho_{water}\frac{3}{4}h^3 g - \rho_{cube}h^3 g\,,$$

or

$$\rho_{cube} = \frac{3}{4}\rho_{water}\,,$$

the required result.

4.2 Bernoulli's Equation

Bernoulli's equation is one of the best-known and widely-used equations of elementary fluid mechanics. In the present section we will derive this equation from the N.–S. equations again emphasizing the ease with which numerous seemingly scattered results can be obtained once these equations are available. Following this derivation we will consider two main examples to highlight applications. The first of these will employ only Bernoulli's equation to analyze the working of a pitot tube for measuring air speed while the second will require a combination of Bernoulli's equation and the continuity equation derived in Chap. 3.

4.2.1 Derivation of Bernoulli's equation

As noted above, we will base our derivation of Bernoulli's equation on the N.–S. equations allowing us to very clearly identify the assumptions and approximations that must be made. Thus, we begin by again writing these equations. We will employ the 2-D form of the equations, but it will be clear as we proceed that the full 3-D set of equations would yield precisely the same result.

The 2-D, incompressible N.–S. equations can be expressed as

$$u_t + uu_x + vu_y = -\frac{1}{\rho}\,p_x + \nu(u_{xx} + u_{yy})\,, \tag{4.8a}$$

$$v_t + uv_x + vv_y = -\frac{1}{\rho}\,p_y + \nu(v_{xx} + v_{yy}) - g\,, \tag{4.8b}$$

where we have employed our usual notation for derivatives, and we are assuming that the only body force results from gravitational acceleration acting in the negative y direction. In addition to the incompressibility assumption embodied in this form of the N.–S. equations we need to assume that the flow being treated is inviscid. Recall from Chap. 2 that this implies that the effects of viscosity are negligible, and more specifically from Chap. 3 we would conclude that viscous forces can be considered to be small in comparison with the other forces represented by these equations, namely inertial, pressure and body forces. In turn, this implies that we will not be able to account for, or calculate, shear stresses in any flow to which we apply Bernoulli's equation, and furthermore, the no-slip condition will no longer be used.

Dropping the viscous terms in Eqs. (4.8) leads to

$$u_t + uu_x + vu_y = -\frac{1}{\rho}\,p_x\,, \tag{4.9a}$$

$$v_t + uv_x + vv_y = -\frac{1}{\rho}\,p_y - g\,, \tag{4.9b}$$

a system of equations known as the *Euler equations*. The compressible form of these equations is widely used in studies of high-speed aerodynamics.

The next assumptions we make are that the flows being treated are steady and irrotational. Recall that the second of these implies that $\nabla \times \boldsymbol{U} = 0$, which in 2D collapses to simply $u_y = v_x$. (We remark that irrotationality actually follows from the combination of inviscid and incompressible assumptions, provided the initial state of the flow is also irrotational; but the background needed to understand the reason for this is beyond the intended scope of these lectures, so we introduce this as an assumption.) With these simplifications the above equations can be expressed as

$$uu_x + vv_x = -\frac{1}{\rho}\,p_x\,,$$

$$uu_y + vv_y = -\frac{1}{\rho}\,p_y - g\,,$$

and application (in reverse) of the product rule for differentiation yields

$$\frac{\rho}{2}\left(u^2 + v^2\right)_x = -p_x\,, \tag{4.10a}$$

$$\frac{\rho}{2}\left(u^2 + v^2\right)_y = -p_y - \rho g\,. \tag{4.10b}$$

At this point we introduce some fairly common notation; namely, we write

$$U^2 = u^2 + v^2\,,$$

which is shorthand for $\boldsymbol{U} \cdot \boldsymbol{U}$, the square of the speed. Also, on the right-hand side of Eq. (4.10b) because ρ is constant by incompressibility, we can write

$$-p_y - \rho g = -\frac{\partial}{\partial y}(p + \rho g y) = -\frac{\partial}{\partial y}(p + \gamma y)$$

But we can employ the same construction in Eq. (4.10a) to obtain

$$-p_x = -\frac{\partial}{\partial x}(p + \rho g y) = -\frac{\partial}{\partial x}(p + \gamma y)$$

because the partial derivative of γy with respect to x is zero.

We now use these notations and rearrangements to write Eqs. (4.10) as

$$\frac{\partial}{\partial x}\left[\frac{\rho}{2}U^2 + p + \gamma y\right] = 0\,, \tag{4.11a}$$

$$\frac{\partial}{\partial y}\left[\frac{\rho}{2}U^2 + p + \gamma y\right] = 0\,, \tag{4.11b}$$

where we have again invoked incompressibility to move $\rho/2$ inside the partial derivatives.

It should be clear at this point that if we had considered the 3-D case, still keeping the gravity vector aligned with the negative y direction, we would have obtained an analogous result containing yet a third equation of exactly the same form as those given above, with a z-direction partial derivative. (But note that there is more to be done in this case at the time the irrotational assumption is used.)

Equations (4.11) are two very simple partial differential equations that, in principle, can be solved by merely integrating them. But a better way to interpret their consequences is to note that the first equation implies that $\frac{\rho}{2}U^2 + p + \gamma y$ is <u>independent of x</u> while the second equation implies the same for y. But this analysis is 2D; x and y are the <u>only</u> independent variables. Hence, it follows that this quantity must be a constant; *i.e.*,

$$\frac{\rho}{2}U^2 + p + \gamma y = C \equiv \text{const.} \tag{4.12}$$

throughout the flow field. This result can be written for every point in the flow field, but the constant C must always be the same. Thus, if we consider points 1 and 2 we have

$$\frac{\rho}{2}U_1^2 + p_1 + \gamma y_1 = C\,,$$

and

$$\frac{\rho}{2}U_2^2 + p_2 + \gamma y_2 = C\,.$$

But because C is the same in both equations, the left-hand sides must be equal, and we have

$$p_1 + \frac{\rho}{2}U_1^2 + \gamma y_1 = p_2 + \frac{\rho}{2}U_2^2 + \gamma y_2\,, \tag{4.13}$$

the well-known Bernoulli's equation.

There are a number of items that should be noted regarding this equation. First, it is worthwhile to summarize the assumptions that we made to produce it. These are: steady, incompressible, inviscid and irrotational flow. Associated with the last of these, we note that an alternative derivation can (and usually is) used in which the irrotational assumption is dropped and application of Eq. (4.13) is restricted to points on the same streamline. It is often stated that Bernoulli's equation can only be applied in this manner (*i.e.*, along a streamline), but if this were actually true it would be difficult to use this result in any but nearly trivial situations. (How do we know, *a priori*, where the streamlines go in a flowfield in order to pick points on them?) While the restriction to irrotational flows is stronger than would be desired, it makes fairly general application of Eq. (4.13) possible. Moreover, because we arrived at the same result as obtained with the assumption of streamline flow, we see that this assumption is not necessary for application of Bernoulli's equations. In addition, although we will not in these lectures develop the information needed to recognize this, in fact, once the steady, inviscid and incompressible assumptions (already employed in the "streamline" derivation of Bernoulli's equation) are invoked, irrotationality is actually a consequence and not an assumption, provided only that the initial flow that evolved to the steady state being considered is also irrotational. Thus, the assumption that Bernoulli's equation can only be applied along streamlines arises from a misunderstanding of what is actually needed to obtain the equation.

The next observation that should be made regarding Eq. (4.13) is that the terms γy_1 and γy_2 are essentially always neglected when considering flow of gases. These are equivalent to the hydrostatic terms discussed earlier where we concluded that they are usually small in gaseous flows. In such cases Bernoulli's equation takes the form

$$p_1 + \frac{\rho}{2}U_1^2 = p_2 + \frac{\rho}{2}U_2^2\,. \tag{4.14}$$

The same restrictions noted above apply to this form as well.

We recognize in Eqs. (4.13) and (4.14) a grouping of factors that we previously termed the dynamic pressure, and we earlier demonstrated that, indeed, it has the units of pressure. In this context we usually call p_1 and p_2 *static pressure*. It should be observed that these were the pressures originally appearing in the pressure-gradient terms of the N.–S. equations, so we now have an additional description of these. The sum of dynamic and static pressures appearing on both sides of Bernoulli's equation written between two points of a flow field is called the *total pressure*. (The same terminology is also applied to all three terms on each side of Eq. (4.13).) When no hydrostatic contribution is important, this is often referred to as *stagnation pressure*. One can think of this as the pressure required to bring the flow to rest from a given speed. In particular, if we have $U_1 > 0$ and stop the flow at point 2 so that $U_2 = 0$, then from Bernoulli's equation we have

$$p_2 = p_1 + \frac{\rho}{2}U_1^2\,,$$

with the right-hand side being the stagnation pressure.

The notion of stagnation pressure arises in the description of locations in a flow field where the flow speed becomes zero, as noted above. Such locations are called *stagnation points*; we have depicted such a point in Fig. 4.5 along with its associated streamline, termed the *stagnation streamline*.
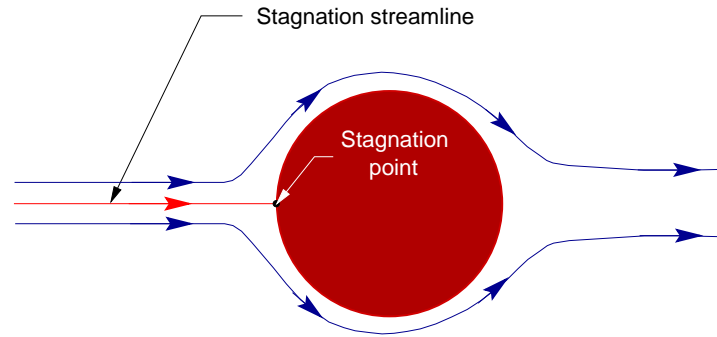
Figure 4.5: Stagnation point and stagnation streamline.

4.2.2   Example applications of Bernoulli's equation

In this section we will present two examples of employing Bernoulli's equation to solve practical problems. In the first we will analyze a device for measuring air speed of aircraft, and in the second we consider a simple system for transferring liquids between two containers without using a pump. Such systems often involve what is termed a syphon.

Analysis of a Pitot Tube

In this subsection we present an example problem associated with the analysis of a pitot tube via Bernoulli's equation.

EXAMPLE 4.5 In Fig. 4.6 we present a sketch of a pitot tube, a device as noted above which is used to measure air speed. This consists of two concentric cylinders, the inner one of which is open
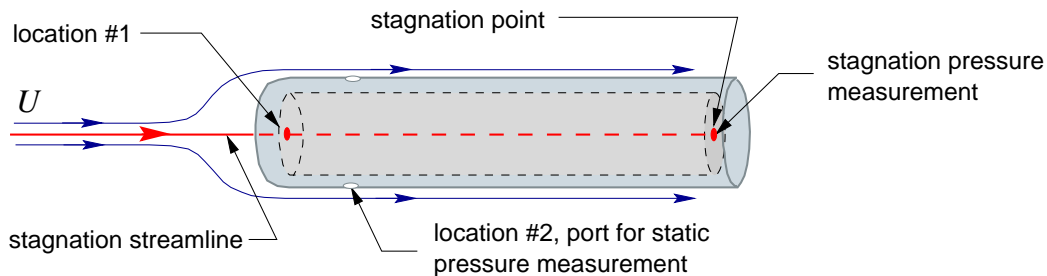
Figure 4.6: Sketch of pitot tube.

to oncoming air that stagnates in the cylinder. Thus, the stagnation pressure can be measured at the end of this inner cylinder. The outer cylinder is closed to the oncoming air but has several holes in its surface that permit measurement of static pressure from the flow going passed these holes. It is desired to find the flow speed U.

We first write Bernoulli's equation between the locations 1 and 2 indicated in the figure. For gases in which hydrostatic effects are usually negligible this takes the form of Eq. (4.14); *i.e.*,

$$p_1 + \frac{\rho}{2}U_1^2 = p_2 + \frac{\rho}{2}U_2^2\,.$$

Now, in the present case we can assume that the pressure at location 1 is essentially the stagnation pressure. This is on the stagnation streamline, and it is close to the entrance to the pitot tube.

(If this tube is small in diameter, the flow will be completely stagnant all the way to the tube entrance.) Furthermore, at any location where the pressure is the stagnation pressure the speed must be zero, by definition. Thus, in the above formula we can consider p_1 to be known; it is measured, say, with a pressure transducer, and $U_1 = 0$. Next, we observe that the streamline(s) passing the pitot tube outer cylinder where the static pressure is measured have started at locations where the speed is U, the desired unknown value. So, in the right-hand side of the above equation we take p_2 to be (measured) static pressure, and $U_2 = U$. This results in

$$p_1 = p_2 + \frac{\rho}{2}U^2\,,$$

which can be solved for the desired speed, U:

$$U = \sqrt{\frac{2(p_1 - p_2)}{\rho}}\,.$$

We remark that it is clear that we have had to use two different streamlines to obtain this result, a fact that is often ignored for this problem. But the results are correct provided we are willing to assume that the flow is irrotational. While this may not be completely accurate it provides a reasonable approximation in the present case. Moreover, it is also common practice to make automatic corrections to pitot tube readouts of speed to at least partially account for the approximate nature of the analysis.

Study of Flow in a Syphon

In this subsection we will consider a somewhat more elaborate example of the use of Bernoulli's equation, in fact, one that also requires application of the control-volume continuity equation, or actually just a simple formula for volume flow rate derived from this. In particular, we will analyze flow in a syphon, a device that can be used to transfer liquids between two containers without the use of a pump.

EXAMPLE 4.6 Figure 4.7 provides a schematic of a syphon being used to extract liquid from a tank using only the force of gravity. The heights y_2 and y_3 and areas A_1, A_2 and A_3 are assumed known with $A_2 = A_3$, and the pressure acting on the liquid surface in the tank, as well as that at the end of the hose draining into the bucket, is taken to be atmospheric; that is, $p_1 = p_3 = p_{atm}$. It is desired to determine speed of the liquid entering the bucket and the pressure in the hose at location 2. We will assume steady-state behavior, implying that the volume flow rate through the hose is small compared with the total volume of the tank; *i.e.*, the height of liquid in the tank does not change very rapidly.

It is easily seen from the continuity equation that $U_3 = U_2$ since the fluid is a liquid, and thus incompressible, and the corresponding areas are equal. Furthermore, again from the continuity equation, it must be the case that

$$U_2 A_2 = U_1 A_1\,.$$

We next observe that the figure implies $A_1 \gg A_2$, and it follows that $U_1 \ll U_2$. We now apply Bernoulli's equation. It should be recognized that to find the flow speed at location 2 via Bernoulli's equation it will be necessary to know the pressure at this location, and this must be found from the pressure at location 3 (known to be atmospheric) again via Bernoulli's equation and the fact, already noted, that the flow speeds are the same at these locations.
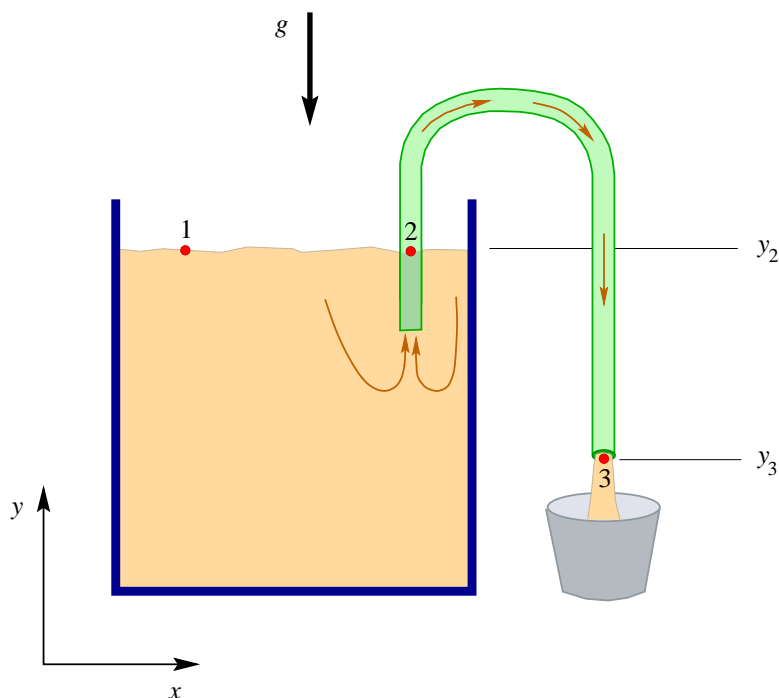
Figure 4.7: Schematic of flow in a syphon.

We begin by writing the equation between locations 1 and 2. By rearranging Eq. (4.13) we obtain the form

$$\frac{p_1}{\gamma} + \frac{U_1^2}{2g} + y_1 = \frac{p_2}{\gamma} + \frac{U_2^2}{2g} + y_2 \, ,$$

but we observe from the figure that $y_1 = y_2$, and we assume U_1 can be neglected. Since $p_1 = p_{atm}$, this results in

$$\frac{U_2^2}{2g} = \frac{p_{atm} - p_2}{\gamma} \, .$$

Next, we write Bernoulli's equation for the flow between locations 2 and 3:

$$\frac{p_2}{\gamma} + \frac{U_2^2}{2g} + y_2 = \frac{p_3}{\gamma} + \frac{U_3^2}{2g} + y_3 \, .$$

Now we have already indicated that $U_2 = U_3$, and with $p_3 = p_{atm}$ this reduces to

$$\frac{p_2 - p_{atm}}{\gamma} = y_3 - y_2 \, .$$

Combining this with the previous result yields

$$\frac{U_2^2}{2g} = y_2 - y_3 \, ,$$

and solving for U_2 gives

$$U_2 = \sqrt{2g(y_2 - y_3)} \, .$$

We can also obtain the expression for p_2 as

$$p_2 = p_{atm} + \gamma(y_3 - y_2)\,.$$

There are two observations to make regarding this solution. The first is that unless $y_2 > y_3$, *i.e.*, the liquid level in the tank is higher than the end of the hose, there is no real (as opposed to imaginary complex) solution to the equation for U_2, the speed of flow from the tank into the hose. Second, and this is related to the first, the pressure inside the hose at the tank liquid level must be lower than that outside the hose at the same level when liquid is flowing.

We conclude this section on Bernoulli's equation with several notes. First, it is possible to derive a time-dependent Bernoulli equation using essentially the same assumptions employed here, with the exception of steady flow, of course, and second, there is also a compressible Bernoulli's equation. Treatment of these must be left to more advanced classes in fluid dynamics. Finally, we mention that we will later in these lectures return to Bernoulli's equation, but then viewed as an energy equation (very much like those encountered in elementary thermodynamics classes) rather than as a momentum equation.

4.3   Control-Volume Momentum Equation

In Chap. 3 we provided a detailed derivation of the differential equations corresponding to pointwise momentum balance, the Navier–Stokes equations. We noted at that time that these equations are very difficult to solve analytically, and are only now beginning to be solved reliably via CFD. This lack of solutions motivated much effort along the lines we will briefly present in the current section, namely, control-volume momentum equations analogous to the control-volume continuity equation studied earlier. Prior to the wide use of CFD, this was one of the few analytical approaches available; but today there is much less need for it. We will, as a consequence, limit our treatment to this short section.

We will begin by deriving the general control-volume momentum equation by working backwards from the differential momentum balance, and we will then present one straightforward and interesting example.

4.3.1   Derivation of the control-volume momentum equation

Recall that the general differential form of the momentum balance derived earlier as Eq. (3.35) is

$$\rho\frac{D\boldsymbol{U}}{Dt} - \boldsymbol{F}_B - \nabla\cdot\boldsymbol{\mathcal{T}} = 0\,, \tag{4.15}$$

with $\boldsymbol{\mathcal{T}}$ given in Eq. (3.39). We should recall that Eq. (4.15) is a vector equation, and $\boldsymbol{\mathcal{T}}$ is a matrix (as noted earlier, usually termed a *tensor* in fluid dynamics). Our mathematical operations on this equation must reflect this.

Because Eq. (4.15) is valid at every point in a fluid, it follows that

$$\int_{\mathcal{R}(t)} \rho\frac{D\boldsymbol{U}}{Dt} - \boldsymbol{F}_B - \nabla\cdot\boldsymbol{\mathcal{T}}\,dV = 0\,, \tag{4.16}$$

for any region $\mathcal{R}(t)$. In particular, this equation holds for arbitrary control volumes of interest when analyzing practical engineering flow problems. Our task is to transform Eq. (4.16) into a more useful form for such calculations, just as we did earlier for the control-volume continuity equation.

We begin by recalling that as a consequence of Eq. (3.32) we have

$$\int_{\mathcal{R}(t)} \rho \frac{D\boldsymbol{U}}{Dt}\, dV = \frac{D}{Dt} \int_{\mathcal{R}(t)} \rho \boldsymbol{U}\, dV\,.$$

The right-hand side of this can be expressed as

$$\frac{D}{Dt} \int_{\mathcal{R}(t)} \rho \boldsymbol{U}\, dV = \int_{\mathcal{R}(t)} \frac{\partial}{\partial t} \rho \boldsymbol{U}\, dV + \int_{\mathcal{S}(t)} \rho \boldsymbol{U}\boldsymbol{U} \cdot \boldsymbol{n}\, dA$$

by means of the Reynolds transport theorem. We now apply the general transport theorem to the first term on the right-hand side to obtain

$$\begin{aligned}
\frac{D}{Dt} \int_{\mathcal{R}(t)} \rho \boldsymbol{U}\, dV &= \frac{d}{dt} \int_{\mathcal{R}(t)} \rho \boldsymbol{U}\, dV + \int_{\mathcal{S}(t)} \rho \boldsymbol{U}\boldsymbol{U} \cdot \boldsymbol{n}\, dA - \int_{\mathcal{S}(t)} \rho \boldsymbol{U}\boldsymbol{W} \cdot \boldsymbol{n}\, dA \\
&= \frac{d}{dt} \int_{\mathcal{R}(t)} \rho \boldsymbol{U}\, dV + \int_{\mathcal{S}(t)} \rho \boldsymbol{U}(\boldsymbol{U} - \boldsymbol{W}) \cdot \boldsymbol{n}\, dA\,.
\end{aligned}$$

We next observe that the surface integral in this expression can be analyzed in the same way as was done earlier for the control-volume continuity equation, with the result that momentum can flow only through entrances and exits. So it follows that

$$\int_{\mathcal{R}(t)} \rho \frac{D\boldsymbol{U}}{Dt}\, dV = \frac{d}{dt} \int_{\mathcal{R}(t)} \rho \boldsymbol{U}\, dV + \int_{\mathcal{S}_e(t)} \rho \boldsymbol{U}(\boldsymbol{U} - \boldsymbol{W}) \cdot \boldsymbol{n}\, dA\,. \tag{4.17}$$

As is usually the case, the body-force term in Eq. (4.16) is relatively easy to treat; it typically consists of gravitational acceleration, and we will not provide any further specific discussion.

The surface-force term requires more work. We can write this as

$$\int_{\mathcal{R}(t)} \nabla \cdot \boldsymbol{\mathcal{T}}\, dV = \int_{\mathcal{S}(t)} \boldsymbol{\mathcal{T}} \cdot \boldsymbol{n}\, dA = \int_{\mathcal{S}(t)} \boldsymbol{F}_S\, dA\,, \tag{4.18}$$

where the first equality comes from Gauss's theorem and the second from the mathematical representation of surface force given in Chap. 3.

This shows that we can rewrite Eq. (4.16) as

$$\frac{d}{dt} \int_{\mathcal{R}(t)} \rho \boldsymbol{U}\, dV + \int_{\mathcal{S}_e(t)} \rho \boldsymbol{U}(\boldsymbol{U} - \boldsymbol{W}) \cdot \boldsymbol{n}\, dA = \int_{\mathcal{R}(t)} \boldsymbol{F}_B\, dV + \int_{\mathcal{S}(t)} \boldsymbol{F}_S\, dA\,. \tag{4.19}$$

This equation embodies the following physical principle:

$$\left\{ \begin{array}{c} \text{time rate of change} \\ \text{of control-volume} \\ \text{momentum} \end{array} \right\} + \left\{ \begin{array}{c} \text{net flux of} \\ \text{momentum leaving} \\ \text{control volume} \end{array} \right\} = \left\{ \begin{array}{c} \text{body forces} \\ \text{acting on} \\ \text{control volume} \end{array} \right\} + \left\{ \begin{array}{c} \text{surface forces} \\ \text{acting on} \\ \text{control surface} \end{array} \right\}.$$

We remark that in most cases we attempt to define control volumes that are fixed in both space and time; moreover, the simple application to be considered below corresponds to a steady flow. In such cases, Eq. (4.19) simplifies to

$$\int_{\mathcal{S}_e} \rho \boldsymbol{U}\boldsymbol{U} \cdot \boldsymbol{n}\, dA = \int_{\mathcal{R}} \boldsymbol{F}_B\, dV + \int_{\mathcal{S}} \boldsymbol{F}_S\, dA\,. \tag{4.20}$$

Furthermore, as we have mentioned on several occasions, the body force is usually due to gravitational acceleration, so we have

$$\boldsymbol{F}_B = \rho \boldsymbol{g}\,,$$

and for inviscid flows as we will treat here the surface force consists only of pressure. This takes the form

$$\boldsymbol{F}_S = -\boldsymbol{n}p\,,$$

as can be easily deduced from Eq. (3.39). Combining these results leads to

$$\int_{\mathcal{S}_e} \rho \boldsymbol{U}\boldsymbol{U}\cdot\boldsymbol{n}\,dA = \int_{\mathcal{R}} \rho \boldsymbol{g}\,dV - \int_{\mathcal{S}} p\boldsymbol{n}\,dA\,. \tag{4.21}$$

We will employ this simplified form in the example of the next section.

4.3.2   Application of control-volume momentum equation

In this section we will apply the control-volume momentum equation to a problem of practical interest. We will first provide details of the problem, flow in a rapidly-expanding pipe, and derive its solution. Following this we will compare the results with those that are obtained by applying Bernoulli's equation to the same problem. We will see that for this case Bernoulli's equation fails to provide an adequate description of the flow, and we will discuss reasons for this.

Momentum Equation Applied to Rapidly-Expanding Pipe Flow

Flow in rapidly-expanding pipes and ducts is important in many areas of technology. Here we will present a simple analysis of such a flow based on the control-volume continuity and momentum equations. It is worthwhile to review the assumptions that have been imposed to achieve the forms of these to be used here. We are, as usual, taking the flow to be incompressible, and we also assume steady state. In such a case the control-volume continuity equation takes the form

$$\int_{\mathcal{S}_e} \boldsymbol{U}\cdot\boldsymbol{n}\,dA = 0\,.$$

Furthermore, we will assume the flow is inviscid and that there are no body forces acting upon it. Thus, the control-volume momentum equation (4.21) can be further simplified to

$$\int_{\mathcal{S}_e} \rho \boldsymbol{U}\boldsymbol{U}\cdot\boldsymbol{n}\,dA = -\int_{\mathcal{S}} p\boldsymbol{n}\,dA\,.$$

Of these assumptions only the neglect of viscosity poses a possible problem, but this has been done because treatment of viscous terms, even in a control-volume analysis, is quite burdensome.

EXAMPLE 4.7 A simplified version of the physical situation we are considering here is depicted in Fig. 4.8. Such flows occur in numerous applications, but especially in air-conditioning and ventilation systems, and in plumbing systems. As can be seen from the figure, which shows a plane going through the center of the pipe, the flow behind the point of expansion is quite complicated. In particular, it is seen to separate, recirculate and then reattach at a downstream location. This recirculation region is actually quite prominent in some flows, and as represented here would form a donut-shaped region around the inside of the expansion section of the pipe adjacent to the point
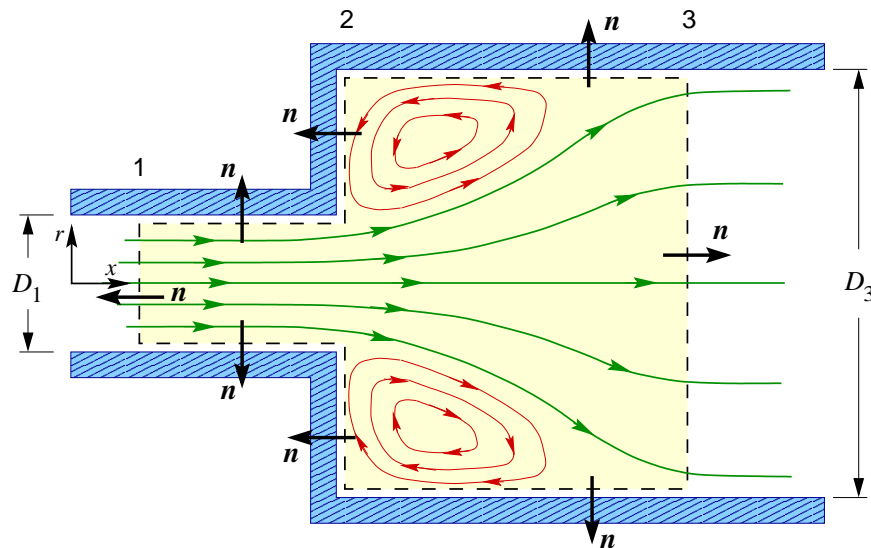
Figure 4.8: Flow through a rapidly-expanding pipe.

of expansion. It is important to recognize that these are mainly viscous effects, so our present analysis will not be able to account for all details.

Figure 4.8 also displays the control volume we will employ in the present analysis. This extends from location 1 upstream of the point of expansion, denoted as location 2, on downstream to location 3 and is fixed. In carrying out this calculation we will assume the flow is uniform at each cross section; *i.e.*, we take the pressure and velocity to be constant across each cross section. Then the flow field can vary only in the x direction, and this leads to only one nonzero velocity component, namely, the one in the x direction. We will denote this as u in what follows. The goal of this analysis is to predict the change in pressure of the flow resulting from rapid expansion of the pipe.

From the continuity equation we have

$$-u_1 A_1 + u_3 A_3 = -u_1 \frac{\pi D_1^2}{4} + u_3 \frac{\pi D_3^2}{4} = 0\,,$$

or

$$u_1 \frac{\pi D_1^2}{4} = u_3 \frac{\pi D_3^2}{4} \qquad \Rightarrow \qquad u_3 = u_1 \left(\frac{D_1}{D_3}\right)^2 .$$

Observe that the minus sign appearing in the first term of the first of these equations occurs because the flow direction at location 1 is positive, but the outward unit normal vector to the control volume at this location is in the negative x direction.

The integral momentum equation can now be written as

$$\int_{\mathcal{S}_e} \rho u^2 n_x dA = -\int_{\mathcal{S}} p\boldsymbol{n} dA\,.$$

where n_x denotes the x-direction component of the general control surface outward unit normal vector. Observe that this is the only nonzero component of this vector acting at the entrance and exit of the control volume. Also note that the control surface on which the pressure acts is the surface of the entire control volume—not simply that of entrances and exits. This is one

of the major differences between working with the control-volume momentum equation and the corresponding continuity equation.

We first evaluate the left-hand side integral, which contains contributions only from entrances and exits, to obtain

$$\int_{\mathcal{S}_e} \rho u^2 n_x dA = -\rho u_1^2 \frac{\pi D_1^2}{4} + \rho u_3^2 \frac{\pi D_3^2}{4}\,.$$

Similarly, evaluation of the right-hand side integral yields

$$-\int_{\mathcal{S}} p\boldsymbol{n} dA = p_1 \frac{\pi D_1^2}{4} + p_2 \frac{\pi}{4}\left(D_3^2 - D_1^2\right) - p_3 \frac{\pi D_3^2}{4}\,.$$

It should be noted that although pressure is acting on the lateral boundaries of the pipe, there is no contribution from this because such contributions cancel on opposite sides of the pipe across the diameter, *i.e.*, the outward normal directions are opposite, and since pressure is assumed constant in each cross section cancellation occurs.

We now equate these two results and divide by $\pi/4$ to obtain

$$\rho u_3^2 D_3^2 - \rho u_1^2 D_1^2 = p_1 D_1^2 + p_2 \left(D_3^2 - D_1^2\right) - p_3 D_3^2\,.$$

At this point we should recognize that the pressure difference we are seeking is that between pressures 1 and 3, so we need to eliminate p_2. There are several ways by means of which this can be done. One is to repeat the preceding analysis between points 1 and 2, and another is to apply Bernoulli's equation between these locations. (The assumptions with which we are currently working are consistent with application of Bernoulli's equation.) But the simplest approach is to note that in an inviscid incompressible flow there is no mechanism (no force) by which to cause a change in pressure if the velocity is constant, and it is clear from the continuity equation applied between locations 1 and 2 that this is the case. Hence, we set

$$p_2 = p_1\,.$$

With this simplification, the above becomes

$$\rho u_3^2 D_3^2 - \rho u_1^2 D_1^2 = (p_1 - p_3)D_3^2 \equiv \Delta p\, D_3^2\,,$$

or after rearrangement

$$\Delta p = \rho u_3^2 - \rho u_1^2 \left(\frac{D_1}{D_3}\right)^2\,.$$

We can now introduce the result obtained earlier from the continuity equation to express u_3 in terms of u_1 thus arriving at the desired result:

$$\Delta p = \rho u_1^2 \left[\left(\frac{D_1}{D_3}\right)^2 - 1\right]\left(\frac{D_1}{D_3}\right)^2\,. \tag{4.22}$$

From this we see that if the upstream velocity u_1 and the pipe diameters are known, it is possible to predict the pressure change through the expansion. Moreover, as we will see later in our analyses of pipe flow, *per se*, it is usually the case that the upstream velocity is known.

There are some things to note regarding the result given in Eq. (4.22). We see that since $D_1 < D_3$ it follows that $\Delta p < 0$, which in turn implies that $p_3 > p_1$. That is, the downstream pressure is <u>higher</u> than the upstream pressure. At first this may seem surprising and counterintuitive. How

could the flow move in the downstream direction if it is having to flow against a higher pressure? But one must first recognize that for incompressible flows the continuity equation forces the downstream flow to be slower than the upstream flow due to the increased downstream area. Hence, the flow momentum has decreased between locations 1 and 3, and for this to happen a force must be applied in the direction opposite the direction of motion of the fluid. In an inviscid flow the only mechanism for generating this force is an increase in the downstream pressure, as indicated in Eq. (4.22).

Bernoulli Equation Analysis of Rapidly-Expanding Pipe Flow

As we have already noted, the assumptions we utilized in the preceding analysis of flow in a rapidly-expanding pipe via the control-volume momentum equation are the same as those used to derive Bernoulli's equation. So it is worthwhile to repeat the analysis using the latter equation. We will assume the pipe diameters are not extremely large so that even for dense liquids the hydrostatic terms in Bernoulli's equation can be neglected (as the body-force terms were in the control-volume momentum equation). Then we can write Bernoulli's equation between locations 1 and 3 as

$$p_1 + \frac{\rho}{2}u_1^2 = p_3 + \frac{\rho}{2}u_3^2 .$$

We rearrange this as

$$p_1 - p_3 = \frac{\rho}{2}\left(u_3^2 - u_1^2\right) ,$$

and substitute the result relating u_3 to u_1 obtained earlier from the continuity equation to obtain

$$\Delta p = \frac{\rho}{2}u_1^2 \left[\left(\frac{D_1}{D_3}\right)^4 - 1\right] . \tag{4.23}$$

Comparison of this result from Bernoulli's equation with that obtained from the control-volume momentum equation given in Eq. (4.22) shows quite significant differences, despite the fact that the same basic physical assumptions have been employed in both analyses. In particular, we can calculate the difference between these as

$$
\begin{aligned}
\Delta p_M - \Delta p_B &= \rho u_1^2 \left\{\left[\left(\frac{D_1}{D_3}\right)^4 - \left(\frac{D_1}{D_3}\right)^2\right] - \frac{1}{2}\left[\left(\frac{D_1}{D_3}\right)^4 - 1\right]\right\} \\
&= \frac{1}{2}\rho u_1^2 \left[\left(\frac{D_1}{D_3}\right)^4 - 2\left(\frac{D_1}{D_3}\right)^2 + 1\right] \\
&= \frac{1}{2}\rho u_1^2 \left[1 - \left(\frac{D_1}{D_3}\right)^2\right]^2 ,
\end{aligned}
\tag{4.24}
$$

where the subscripts B and M respectively denote "Bernoulli" and "Momentum" equation pressure changes.

We first comment that experimental measurements quite strongly favor the control-volume momentum equation result—*i.e.*, Bernoulli's equation does not give the correct pressure change for this flow, even though it should be applicable and even more, we actually were able to apply it along a streamline in the present case. So, what has gone wrong?

Recall that we earlier noted the existence of prominent recirculation regions in the flow field immediately behind the expansion, as depicted in Fig. 4.8, and that these arise from viscous effects. While it is true that neither Bernoulli's equation nor the control-volume momentum equation in the

form employed here account for such effects, one of the main outcomes of these recirculating vortices is a reduced pressure very near the location of the expansion, and this pressure acts on the vertical part of the pipe at this expansion location. Bernoulli's equation does not even approximately account for this; it does not contain any use of the pressure at location 2; in particular, there is no account of the action of this pressure on the vertical part of the pipe expansion. On the other hand, this is explicitly taken into account by the control-volume momentum equation although ultimately the pressure at location 2 is set equal to that at location 1 (due to the inviscid assumption). But the important thing is that direct account is taken of the action of pressure on the vertical portion of pipe at the expansion location.

4.4   Classical Exact Solutions to N.–S. Equations

As we have previously indicated, there are very few exact solutions to the Navier–Stokes equations—it is sometimes claimed there are 87 known solutions, to a system of equations that represent all possible fluid phenomena within the confines of the continuum hypothesis. In this section we will derive two of the easiest and best-known of these exact solutions. These will correspond to what is known as Couette flow and plane Poiseiulle flow. In what follows we will devote a section to the treatment of each of these. Before doing this, for ease of reference, we again present the 3-D incompressible N.–S. equations.

$$u_x + v_y + w_z = 0 \,, \tag{4.25a}$$

$$u_t + u u_x + v u_y + w u_z = -\frac{1}{\rho} p_x + \nu \Delta u + \frac{1}{\rho} F_{B,1} \,, \tag{4.25b}$$

$$v_t + u v_x + v v_y + w v_z = -\frac{1}{\rho} p_y + \nu \Delta v + \frac{1}{\rho} F_{B,2} \,, \tag{4.25c}$$

$$w_t + u w_x + v w_y + w w_z = -\frac{1}{\rho} p_z + \nu \Delta w + \frac{1}{\rho} F_{B,3} \,. \tag{4.25d}$$

All notation is as used previously.

4.4.1   Couette flow

The simplest non-trivial exact solution to the N.–S. equations is known as *Couette flow*. This is flow between to infinite parallel plates spaced a distance h apart in the y direction, as depicted in Fig. 4.9. This is a shear-driven flow with the shearing force produced only by the motion of the upper plate traveling in the x direction at a constant speed U, provided we ignore all body forces. The reader should recognize this as the flow situation in which Newton's law of viscosity was introduced in Chap. 2 and recall that it is the no-slip condition of the fluid adjacent to the upper plate that leads to the viscous forces that ultimately produce fluid motion throughout the flow field.

We obtain the solution to this problem as follows. First, since U is constant and represents the only mechanism for inducing fluid motion, it is reasonable to assume that the flow is steady. Furthermore, because the plates are taken to be infinite in the x and z directions there is no reason to expect x and z dependence in any flow variables since there is no way to introduce boundary conditions that can lead to such dependences. The lack of x and z dependence reduces the continuity equation to
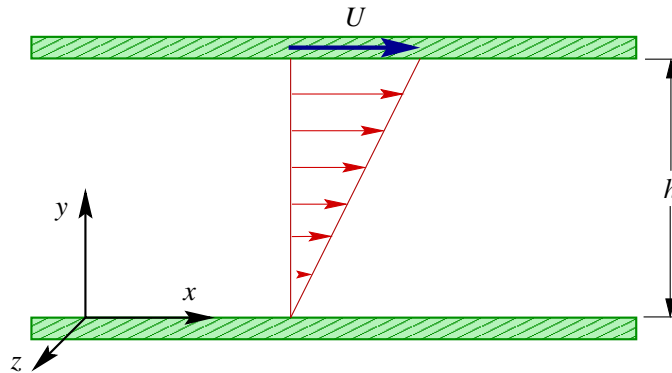
$$v_y = 0 \,,$$

Figure 4.9: Couette flow velocity profile.

as is clear from inspection of Eq. (4.25a). Thus, v is independent of y (as well as of x and z), and hence must be constant. But at the surface of either of the plates we must have $v = 0$ since the fluid cannot penetrate a solid surface; then, *e.g.*, $v(0) = 0$, which implies that $v \equiv 0$.

If we now consider the y-momentum equation (4.25c) in this light we see that all that remains is

$$p_y = 0 \, ,$$

and again because there is no x or z dependence we conclude that $p \equiv$ const.

Next we observe that lack of x and z dependence in w, along with the constancy of pressure just demonstrated, leads to the z-momentum equation taking the simple form

$$w_{yy} = 0 \, .$$

The boundary conditions appropriate for this equation are

$$w(0) = 0 \, , \qquad \text{and} \qquad w(h) = 0 \, ,$$

both of which arise from the no-slip condition and the fact that neither plate exhibits a z-direction component of motion. Then integration (twice) of the above second-order differential equation leads to

$$w(y) = c_1 y + c_2 \, ,$$

and application of the boundary conditions yields $c_1 = c_2 = 0$, implying that $w \equiv 0$.

To this point we have shown that both v and w are zero, and p is identically constant. We now make use of these results, along with the steady-state and x-independence assumptions to simplify the x-momentum equation (4.25b). It is clear that this equation is now simply

$$u_{yy} = 0 \, .$$

The corresponding boundary conditions arising from the no-slip condition applied at the bottom and top plates, respectively, are

$$u(0) = 0 \, , \qquad \text{and} \qquad u(h) = U \, .$$

Integration of the above equation leads to a result analogous to that obtained earlier for the z-momentum equation, namely,

$$u(y) = c_1 y + c_2 \, ,$$

and application of the boundary conditions shows that

$$c_2 = 0, \qquad \text{and} \qquad c_1 = \frac{U}{h}.$$

Thus, the Couette flow velocity profile takes the form

$$u(y) = \frac{U}{h}y, \tag{4.26}$$

exactly the same result we obtained from heuristic physical arguments when studying Newton's law of viscosity in Chap. 2.

We remark that despite the simplicity of this result it is very important and widely used. As we mentioned in Chap. 2 the case when h is small arises in the analysis of lubricating flows in bearings. Furthermore, this linear profile often provides a quite accurate approximation for flow near a solid boundary even in physical situations for which the complete velocity profile is far more complicated.

4.4.2   Plane Poiseiulle flow

The next exact solution to the N.–S. equations we consider is *plane Poiseiulle flow*. This is a pressure-driven flow in a duct of finite length L, but of infinite extent in the z direction, as depicted in Fig. 4.10. For the flow as shown we assume $p_1 > p_2$ and that pressure is constant in the y and z directions at each x location. We again start with Eqs. (4.25) and assume the flow to be
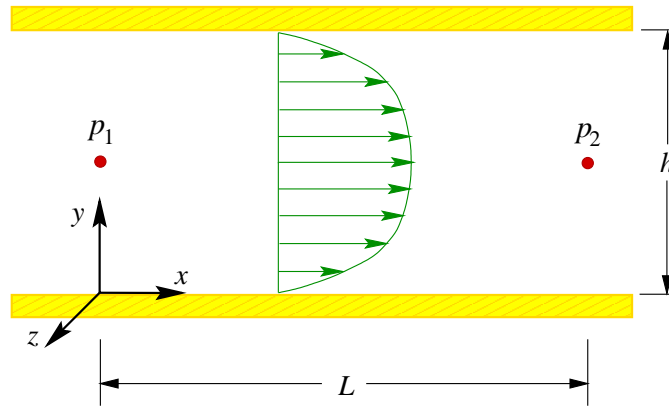
Figure 4.10: Plane Poiseiulle flow velocity profile.

steady, that body forces are negligible and that velocity does not change in the x direction. It is not obvious that this last assumption should hold because pressure is changing in the x direction; but it will be apparent that it leads to no physical or mathematical inconsistencies, and without the assumption it would not be possible to obtain a simple solution as we will do. We will examine this further when we study pipe flow in the next section.

We begin with arguments analogous to those used in the Couette flow analysis. In particular, since the flow varies only in the y direction, the continuity equation collapses to $v_y = 0$ from which it follows that $v \equiv 0$ must hold. The y-momentum equation, Eq. (4.25c), becomes simply

$$p_y = 0,$$

which implies that the pressure p does not depend on y.

Similarly, because w is zero at both the top and bottom plates, and the z-momentum equation can be reduced to $w_{yy} = 0$ by utilizing the preceding assumptions and results, it follows that $w \equiv 0$ also.

Now applying the steady-state assumption with $v = 0$ and $w = 0$ simplifies the x-momentum equation (4.25b) to

$$uu_x = -\frac{1}{\rho} p_x + \nu(u_{xx} + u_{yy}),$$

and with the assumption that the flow velocity does not vary in the x direction, we have $u_x = 0$. So the above becomes

$$u_{yy} = \frac{1}{\mu} p_x. \tag{4.27}$$

Next we note, since u is independent of x and z, that $u = u(y)$ only. This in turn implies from the form of Eq. (4.27) that p_x cannot depend on x and must therefore be constant. We can express this constant as

$$p_x = \frac{\Delta p}{L} = \frac{p_2 - p_1}{L}. \tag{4.28}$$

Then (4.27) becomes

$$u_{yy} = \frac{1}{\mu}\frac{\Delta p}{L}. \tag{4.29}$$

The boundary conditions to be provided for this equation arise from the no-slip condition on the upper and lower plates. Hence,

$$u(0) = 0, \qquad \text{and} \qquad u(h) = 0. \tag{4.30}$$

One integration of Eq. (4.29) yields

$$u_y = \frac{1}{\mu}\frac{\Delta p}{L}y + c_1,$$

and a second integration gives

$$u(y) = \frac{1}{2\mu}\frac{\Delta p}{L}y^2 + c_1 y + c_2.$$

Application of the first boundary condition in Eq. (4.30) shows that $c_2 = 0$, and from the second condition we obtain

$$0 = \frac{1}{2\mu}\frac{\Delta p}{L}h^2 + c_1 h,$$

which implies

$$c_1 = -\frac{1}{2\mu}\frac{\Delta p}{L}h.$$

Substitution of this into the above expression for $u(y)$ results in

$$u(y) = \frac{1}{2\mu}\frac{\Delta p}{L}y(y - h), \tag{4.31}$$

the plane Poiseiulle flow velocity profile. We observe that since the definition of Δp implies $\Delta p < 0$ always holds, it follows that $u(y) \geq 0$ as indicated in Fig. 4.10

We can also provide further analysis of the pressure. We noted earlier that p_x could not be a function of x. But this does not imply that p, itself, is independent of x. Indeed, the fact that $p_1 \neq p_2$ requires x dependence. We can integrate Eq. (4.28) to obtain

$$p(x) = \frac{\Delta p}{L}x + C\,,$$

and from the fact that

$$p(0) = p_1 = C\,,$$

we see that

$$p(x) = \frac{p_2 - p_1}{L}x + p_1\,. \tag{4.32}$$

This is simply a linear interpolation formula between the pressures p_1 and p_2 over the distance L.

4.5   Pipe Flow

Analysis of pipe flow is one of the most important practical problems in fluid engineering, and it provides yet another opportunity to obtain an exact solution to the Navier–Stokes equations, the Hagen–Poiseiulle flow. We will derive this solution in the present section of these notes. We begin with a physical description of the problem being considered and by doing this introduce some important terminology and notation, among these some basic elements of boundary-layer theory. Following this we present the formal solution of the N.–S. equations that provides the Hagen–Poiseiulle velocity profile for steady, fully-developed flow in a pipe of circular cross section, and then we use this to produce simple formulas useful in engineering calculations. In particular, we will see how to account for pressure losses due to skin-friction effects, thus providing a simple modification to Bernoulli's equation that makes it applicable to viscous flow problems. Then we extend this to situations involving pipes with arbitrary cross-sectional shapes and other geometric irregularities including expansions and contractions, bends, tees, *etc.*

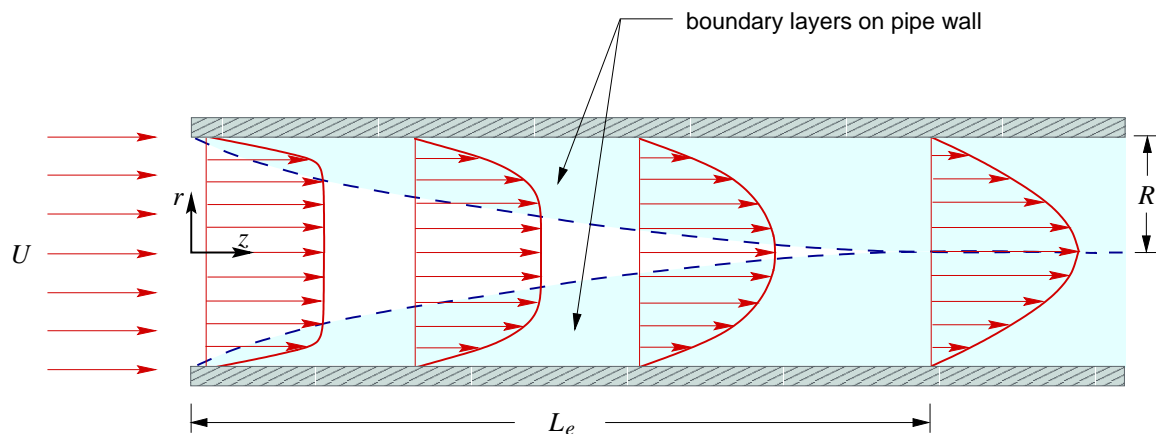### 4.5.1   Some terminology and basic physics of pipe flow

Figure 4.11: Steady, fully-developed flow in a pipe of circular cross section.

In this subsection we will consider some basic features of pipe flow that allow us to solve the
N.–S. equations for a rather special, but yet quite important, case corresponding to steady, fully-
developed flow in a pipe of circular cross section. We have schematically depicted this in Fig. 4.11.
What is apparent from the figure is a uniform velocity profile entering at the left end of the region
of pipe under consideration and then gradually evolving to a velocity profile that is much smoother
and, in fact, as we will later show is parabolic in the radial coordinate r. As indicated in the
figure, the distance over which this takes place is called the *entrance length*, denoted L_e, and this
corresponds to the merging of regions starting at the pipe walls within which the originally uniform
velocity adjusts from zero at the walls (imposed by the no-slip condition) to a free-stream velocity
ultimately set by mass conservation.

Elementary Boundary-Layer Theory

This region in which the flow adjusts from zero velocity at the wall to a relatively high free-
stream value is termed the *boundary layer*. The concept of a boundary layer is one of the most
important in all of viscous fluid dynamics, so we will at least briefly describe it here although a
complete treatment is well beyond the intended scope of the present lectures. We will first do this
in the context of external flow over a flat plate but then argue that the same ideas also apply to
the internal pipe flow under consideration here. Figure 4.12 presents the basic physical situation.
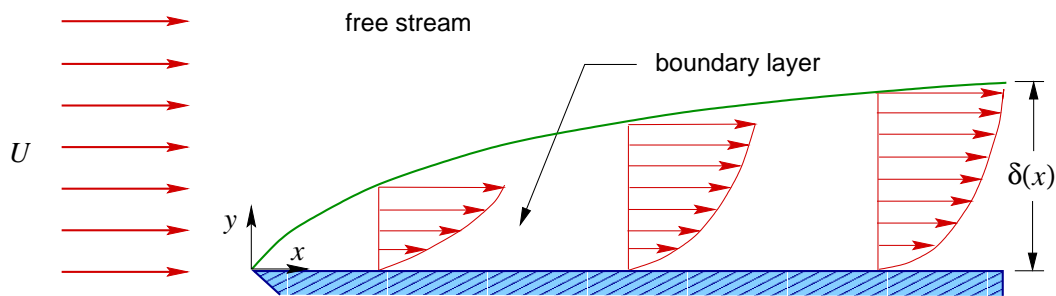
Figure 4.12: Steady, 2-D boundary-layer flow over a flat plate.

We will assume the flow is steady and that far from the surface of the plate it can be treated
as inviscid. Furthermore, due to the indicated form of the incoming uniform velocity profile of Fig.
4.12, it is reasonable to assume that the y velocity component is small in the free stream and thus
can be set to zero.

Then the x-momentum equation collapses to

$$uu_x = -\frac{1}{\rho}p_x\,,$$

but uniformity of the free-stream flow implies $u_x = 0$; hence, we conclude that far from the plate
the x-direction component of the pressure gradient is zero. We remark that it is possible to also
study cases in which flow in the streamwise direction is not uniform, and in these cases $p_x \neq 0$. In
fact, this will be the case for pipe flow considered here.

There are several key characterizations of boundary-layer flow, and we list these as follows:

i) streamwise diffusion of momentum (and any other transported quantity, temperature, for
     example) is small in comparison with diffusion in the wall-normal direction;

ii) the free-stream pressure is impressed on the solid surface beneath the boundary layer;

iii) the *boundary-layer thickness* δ in general scales as $1/\sqrt{Re}$, and in addition grows as $\sqrt{x}$.

The first of these allows us to neglect terms such as u_{xx} and v_{xx} in the momentum equations, which leads to the following system of partial differential equations for steady boundary-layer flow over a flat plate with zero free-stream pressure gradient:

$$
\begin{aligned}
u_x + v_y &= 0\,, & \text{(continuity)} \\
uu_x + vu_y &= \nu u_{yy}\,, & (x \text{ momentum}) \\
p_y &= 0\,. & (y \text{ momentum})
\end{aligned}
$$

The last of these implies item *ii)* in the above list, and item *iii)* is obtained from the overall boundary-layer scaling analysis that is beyond the scope of these lectures. We note that actually $p_y \sim 1/Re$, so the equation given here is valid only for very high Reynolds number. We also comment that there are numerous definitions of the boundary-layer thickness, but one that is widely used in elementary analyses is simply that δ is that height above the plate at which $u = 0.99U$.

Finally, we note that solution of the above system of partial differential equations is sometimes viewed as an exact solution to the N.–S. equations. Indeed, an early observation from experiments that the velocity profiles depicted in Fig. 4.12 are "geometrically similar" led to the notion of a *self-similar* boundary layer and use of a mathematical technique known as a *similarity transformation* to reduce the above PDEs to a single ordinary differential equation boundary-value problem. This resulting equation does <u>not</u> possess an exact solution, but it is so easily solved to arbitrarily high accuracy on a computer that the boundary-layer solution that results is often considered exact.

Further Discussion of Pipe Flow

We can now return to our discussion of flow in a circular pipe with a better understanding of what is occurring in the entrance region of the pipe. The preceding description of boundary-layer flow over a flat plate is applicable in a basic sense to this entrance flow until the boundary layers extend an appreciable distance out from the pipe walls. In particular, it is reasonable to expect that as long as the boundary-layer thickness satisfies $\delta \ll R$ the boundary-layer approximations given above will be valid.

In any case, we can now describe the entrance length in pipe flow as the required distance in the flow direction for the boundary layers from opposite sides of the pipe to merge. This distance cannot be predicted exactly, but many experiments have been conducted to determine it under various flow conditions. There are two important results to emphasize. First, for laminar flow it is known that

$$
L_e \simeq 0.06 D Re\,, \tag{4.33}
$$

where D is the pipe diameter, and for turbulent flow the entrance length can be anywhere in the range of 20 to 100 pipe diameters, with the following formula sometimes given:

$$
L_e = 4.4 D Re^{1/6}\,.
$$

We observe that in both laminar and turbulent flows one can define a dimensionless entrance length, L_e/D, that is simply a power of the Reynolds number.

Beyond this distance the flow is said to be *fully developed*. Fully-developed flow can be characterized by three main physical attributes:

i) boundary layers from opposite sides of the pipe have merged (and, hence, can no longer continue to grow);

ii) the streamwise velocity component satisfies $u_z = 0$;

iii) the radial (or in the case of, *e.g.*, square ducts, the wall-normal) component of velocity is zero, *i.e.*, $v = 0$.

These flow properties, especially the latter two, will be very important in the sequel as we attempt to solve the N.–S. equations for the problem of pipe flow.

4.5.2 The Hagen–Poiseiulle solution

We will now derive another exact solution to the N.–S. equations, subject to the following physical assumptions: steady, incompressible, axisymmetric, fully-developed, laminar flow. We will employ this, with some modifications based on experimental observations, to treat flows in pipes having irregularly-shaped cross sections, various fittings and changes in pipe diameter (through which the flow is no longer fully-developed), and turbulent flows (including parametrizations associated with different levels of surface roughness).

We begin with a statement of the governing equations, the Navier-Stokes equations in polar coordinates. We then provide a detailed treatment of the solution procedure, and we conclude the section with some discussions of the physics of the solution, including the derivation of mean and maximum velocities that will be of later use.

Governing Equations

The equations governing Hagen–Poiseiulle flow are the steady, incompressible N.–S. equations in cylindrical-polar coordinates, in the absence of body-force terms. We list these here as

$$\frac{\partial u}{\partial z} + \frac{1}{r}\frac{\partial}{\partial r}(rv) = 0\,, \qquad \text{(continuity)} \qquad (4.34\text{a})$$

$$\rho\left(u\frac{\partial u}{\partial z} + v\frac{\partial u}{\partial r}\right) = -\frac{\partial p}{\partial z} + \mu\left[\frac{\partial^2 u}{\partial z^2} + \frac{1}{r}\frac{\partial}{\partial r}\left(r\frac{\partial u}{\partial r}\right)\right]\,, \qquad (z\text{ momentum}) \qquad (4.34\text{b})$$

$$\rho\left(u\frac{\partial v}{\partial z} + v\frac{\partial v}{\partial r}\right) = -\frac{\partial p}{\partial r} + \mu\left[\frac{\partial^2 v}{\partial z^2} + \frac{1}{r}\frac{\partial}{\partial r}\left(r\frac{\partial v}{\partial r}\right)\right]\,. \qquad (r\text{ momentum}) \qquad (4.34\text{c})$$

Note that there are no θ-direction derivative terms due to the axisymmetric assumption imposed earlier.

If we invoke the fully-developed flow assumption so that $u_z = 0$ and $v = 0$, these equations can be readily reduced to

$$\frac{\partial u}{\partial z} = 0\,, \qquad (4.35\text{a})$$

$$\frac{\mu}{r}\frac{\partial}{\partial r}\left(r\frac{\partial u}{\partial r}\right) = \frac{\partial p}{\partial z}\,, \qquad (4.35\text{b})$$

$$\frac{\partial p}{\partial r} = 0\,. \qquad (4.35\text{c})$$

This system of equations holds for a physical situation similar to that depicted in Fig. 4.11, but only beyond the point where the boundary layers have merged, *i.e.*, beyond the entrance length L_e. Figure 4.13 displays the current situation.
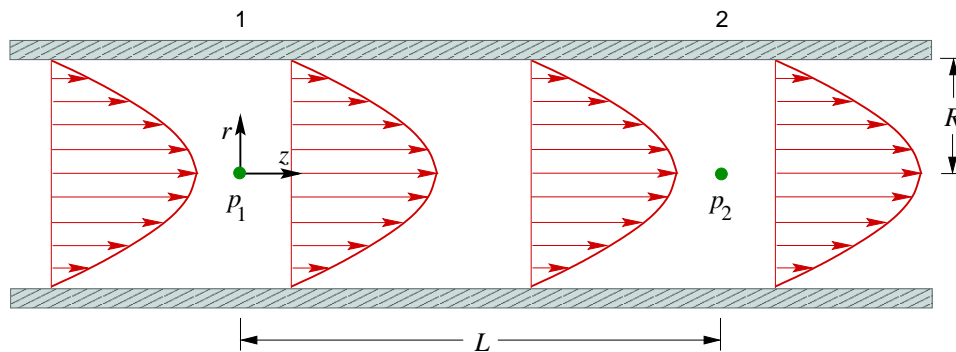
Figure 4.13: Steady, fully-developed pipe flow.

Solution Derivation

We begin by noting that there is no new information in the continuity equation (4.35a) since this merely expresses one of the requirements for fully-developed flow. Next, we observe from Eq. (4.35c) that pressure does not depend on the radial coordinate, or more formally,

$$p = C(z).$$

In particular, pressure can depend only on the z direction. (The reader should recall that we came to an analogous conclusion when studying plane Poiseiulle flow.) Differentiation of the above with respect to z gives

$$\frac{\partial p}{\partial z} = \frac{\partial C}{\partial z},$$

indicating that the z component of the pressure gradient can depend only on z.

Now from the fact that the flow is fully developed it follows that u can be a function only of r, implying that the left-hand side of Eq. (4.35b) can depend only on r. But we have just seen that the right-hand side, $\partial p / \partial z$, depends only on z. Thus, as was the case in plane Poiseiulle flow, this pressure gradient must be a constant, *i.e.*, a trivial function of z, and we set

$$\frac{\partial p}{\partial z} = -\frac{\Delta p}{L}, \tag{4.36}$$

just as we did in the planar case treated earlier. Here, $\Delta p \equiv p_1 - p_2$, with the minus sign being used for later notational convenience. Substitution of (4.36) into Eq. (4.35b) results in

$$\frac{\partial}{\partial r}\left(r\frac{\partial u}{\partial r}\right) = -\frac{\Delta p}{\mu L}r, \tag{4.37}$$

a second-order differential equation needing two boundary conditions in order to determine integration constants and produce a complete solution.

The first of these corresponds to the no-slip condition for a viscous flow, applied at the pipe wall $r = R$; that is,

$$u(R) = 0. \tag{4.38}$$

The second condition to be employed in the present case is less intuitive, but it is one that arises often when working with differential equations expressed in polar coordinate systems. Namely, we

require that the velocity remain bounded at $r = 0$, the center of the pipe. This is equivalent to imposing the formal mathematical condition

$$\left.\frac{\partial u}{\partial r}\right|_{r=0} = 0 \,. \tag{4.39}$$

We now integrate Eq. (4.37) to obtain

$$r\frac{\partial u}{\partial r} = -\frac{\Delta p}{2\mu L}\,r^2 + C_1 \,,$$

or

$$\frac{\partial u}{\partial r} = -\frac{\Delta p}{2\mu L}\,r + \frac{C_1}{r} \,. \tag{4.40}$$

Next we observe that at $r = 0$ this formula for the velocity derivative will become unbounded unless $C_1 = 0$. Thus, on physical grounds we should set $C_1 = 0$. But formally, we can apply the second boundary condition, given in Eq. (4.39) to show that indeed, if this condition is satisfied $C_1 = 0$ will hold, thus eliminating the unbounded term. (Note that if this term were retained a second integration, as will be performed next, would result in $u \sim \ln r$ which is unbounded as $r \to 0$.)

We can now integrate (4.40) with $C_1 = 0$ to obtain

$$u(r) = -\frac{\Delta p}{4\mu L}r^2 + C_2 \,, \tag{4.41}$$

and application of the no-slip condition contained in Eq. (4.38) gives

$$0 = -\frac{\Delta p R^2}{4\mu L} + C_2 \,,$$

or

$$C_2 = \frac{\Delta p R^2}{4\mu L} \,.$$

Finally, substitution of this back into Eq. (4.41) yields

$$u(r) = -\frac{\Delta p}{4\mu L}\left(r^2 - R^2\right) = \frac{\Delta p R^2}{4\mu L}\left[1 - \left(\frac{r}{R}\right)^2\right] \,, \tag{4.42}$$

the Hagen–Poiseiulle velocity profile for fully-developed flow in a pipe of circular cross section.

Some Physical Consequences of the Hagen–Poiseiulle Formula

We observe from the definition given earlier for Δp ($= p_1 - p_2$), that we expect $\Delta p > 0$ to hold; and we see that for this case the flow is indeed in the direction indicated in Fig. 4.13. Furthermore, it is clear from Eq. (4.42) that the variation of u with r is quadratic, and this is quite similar to the velocity profile found for plane Poiseiulle flow.

Two quantities of interest can be derived directly from the velocity profile obtained above. The first of these is the maximum velocity (actually speed in this case) which from the preceding figures we expect will occur on the centerline of the pipe, *i.e.*, at $r = 0$. In fact, we know from calculus that the maximum of a (twice-differentiable) function occurs at the location where the first derivative is zero and, simultaneously, the second derivative is negative.

From Eq. (4.42) we see that

$$\frac{\partial u}{\partial r} = -\frac{1}{2}\frac{\Delta p R^2}{\mu L} \cdot \frac{r}{R^2} \,,$$

and setting this to zero implies that $r = 0$, as expected. Furthermore, since $\Delta p > 0$ it is clear that the second derivative of u is uniformly negative implying that $r = 0$ is the location of the maximum of u. Then evaluation of Eq. (4.42) at $r = 0$ yields the maximum velocity

$$U_{max} = \frac{\Delta p R^2}{4\mu L} \,.$$
(4.43)

A second quantity of even more importance for later use is the average flow velocity, U_{avg}. We obtain this by integrating the Hagen–Poiseiulle profile over the cross section of the pipe and dividing by the area of the cross section. Thus, we have

$$
\begin{aligned}
U_{avg} &= \frac{1}{\pi R^2} \int_0^{2\pi} \int_0^R \frac{\Delta p R^2}{4\mu L} \left[1 - \left(\frac{r}{R} \right)^2 \right] r\,dr\,d\theta \\
&= \frac{\Delta p}{2\mu L} \int_0^R r - \frac{r^3}{R^2}\,dr \\
&= \frac{\Delta p}{2\mu L} \left[\frac{r^2}{2} - \frac{r^4}{4R^2} \right] \Big|_0^R \,.
\end{aligned}
$$

Thus, it follows that

$$U_{avg} = \frac{\Delta p R^2}{8\mu L} \,,$$
(4.44)

showing that in the case of a pipe of circular cross section the average flow speed is exactly one half the maximum speed for fully-developed flow.

Finally, we observe that we can use Eq. (4.40) written as

$$\mu \frac{\partial u}{\partial r} = -\frac{\Delta p}{2L} r$$

to calculate the shear stress at any point in the flow. In particular, we see that $\tau = 0$ onthe pipe centerline, and at the pipe wall we have

$$\tau_w = -\frac{\Delta p}{2L} R \,.$$

4.5.3   Practical Pipe Flow Analysis

In the practical analysis of piping systems the quantity of most importance is the pressure loss due to viscous effects along the length of the system, as well as additional pressure losses arising from other physics (that in some cases involve viscosity indirectly). The viscous losses are already embodied in the physics of the Hagen–Poiseiulle solution since Eq. (4.37) is actually a force balance needed to maintain fully-developed, steady flow. In particular, the viscous forces represented by the left-hand side of this equation must be balanced by the pressure forces given on the right-hand side. Thus, a pressure change Δp will occur over a distance L due to viscous action throughout the flow, but especially near the pipe walls. This change in pressure is a loss, and it must be balanced ultimately by a pump. Hence, analyses of the sort we will undertake in this section will provide information on how large a pump should be in order to move a specified fluid (with given density and viscosity) through a piping system.

We will begin the section with a rearrangement of the Hagen–Poiseiulle solution to express Δp in terms of Reynolds number and then obtain formulas for the friction factor in circular cross section

pipes, including effects of turbulence. We than introduce a modification of Bernoulli'sequation that permits account of viscosity to be included in an empirical way and quantify this with a physical parameter known as the head loss, which is then related to the friction factor. Following this we will treat so-called minor losses, consideration of which allows analyses of general geometric shapes in piping systems.

Friction Factors—Laminar and Turbulent

In this subsection we will provide details of obtaining friction factors for both laminar and turbulent pipe flows. In the latter case we will begin with a brief introduction to turbulent flow, *per se*, in order to elucidate the physics involved for that case.

The laminar case. We can rearrange Eq. (4.44) to obtain

$$
\begin{aligned}
\Delta p &= \frac{8\mu U_{avg} L}{R^2} \\
&= \frac{32\mu U_{avg} L}{D^2} \\
&= \frac{32\mu U_{avg}}{D}\left(\frac{L}{D}\right),
\end{aligned}
\tag{4.45}
$$

where we have introduced the pipe diameter D in place of the radius in the second step, and combined L and D to form an important dimensionless parameter in the third step.

Now to make the pressure difference dimensionless we divide by the dynamic pressure calculated in terms of the average velocity, U_{avg}. This leads to

$$
\frac{\Delta p}{\frac{1}{2}\rho U_{avg}^2} = \frac{32\mu U_{avg} L}{\frac{1}{2}\rho U_{avg}^2 D^2} = \frac{64\mu L}{\rho U_{avg} D^2}.
$$

Multiplication of this by D/L yields

$$
\frac{\Delta p}{\frac{1}{2}\rho U_{avg}^2}\frac{D}{L} = \frac{64\mu}{\rho U_{avg} D} = \frac{64}{Re}.
$$

We next observe from either Eq. (4.40) or (4.45) that Δp is proportional to the (average) shear stress ($\tau_{avg} \sim \mu U_{avg}/D$), and since as noted in Chap. 2 when we introduced the property of viscosity, this can be viewed as giving rise to an "internal friction," we now define a *friction factor*, f, in terms of the dimensionless pressure difference obtained above. We have

$$
f \equiv \frac{\Delta p}{\frac{1}{2}\rho U_{avg}^2}\frac{D}{L}.
\tag{4.46}
$$

This is called the *Darcy friction factor*, and for laminar flows we have

$$
f = \frac{64}{Re}.
\tag{4.47}
$$

It is worthwhile to note that there is another commonly-used result known as the *Fanning friction factor*, denoted c_f, and related to the Darcy friction factor by

$$
c_f = f/4.
\tag{4.48}
$$

From Eq. (4.47) we see that for laminar, fully-developed flows in pipes of circular cross section the friction factor depends only on the Reynolds number defined with a length scale equal to the pipe (inside) diameter and the cross-sectionally averaged velocity. Thus, for laminar flow the friction factor is easily computed, and we can then determine pressure loss from Eq. (4.46). The situation is somewhat more complicated for turbulent pipe flows for which values of friction factor must be obtained from experimental data. We will see in the sequel that f is a very important quantity for pipe flow analysis, so at this time we will provide further treatment of the turbulent case.

The turbulent case. We have to this point in these lectures avoided any detailed discussions of turbulent flow, noting only that turbulence as a phenomenon has been recognized for more than 500 years (recall Fig. 2.20), and that most flows encountered in engineering practice are turbulent. This is particularly true for pipe flows, so it is essential at this time to introduce a few very fundamental notions that will lead us to a better physical understanding of the friction factors, and hence the pressure losses, in such flows.

We begin by commenting that it has been theoretically known since 1971 that the Navier–Stokes equations are capable of exhibiting turbulent solutions—*i.e.*, solutions that fluctuate erratically in both space and time. In particular, in theory there is really no need for the statistical models that have dominated engineering practice since the beginning of the 20th Century because turbulence is *deterministic*, <u>not</u> <u>random</u>, and it is described by the N.–S. equations. Moreover, laboratory experiments commencing in the mid 1970s and continuing to the present have repeatedly supported the theory proposed in 1971; namely, the transition to turbulence takes place through a very short sequence (usually three to four) of distinct steps (recall Fig. 2.22). In this sense, the "turbulence problem" has been solved: the solution is the Navier–Stokes equations.

But from a practical engineering standpoint this is not of much help. Despite the tremendous advances in computing power and numerical solution techniques that have arisen during the last quarter of the 20th Century, we still are far from being able to simulate high-Reynolds number turbulent flows that arise on a routine basis in actual engineering problems. Furthermore, this is expected to be the case for at least the next 20 years unless true breakthroughs in computing hardware performance occur. This implies that in the near to intermediate future we will be forced to rely on considerable empiricism for our treatments of turbulent flow. It is the goal of the present subsection to provide an elementary introduction to this, specifically as it pertains to flow in pipes of circular cross section, for which voluminous amounts of experimental data exist.

It is worthwhile to first present a "way of viewing" turbulent pipe flow (and wall-bounded turbulent flows, in general) in terms of distinct physical regions within such flows. Figure 4.14 provides a simple schematic containing the essential features. To better understand the physics that occurs in each of the regions shown in this figure it is useful to consider a particular representation of the velocity field known as the *Reynolds decomposition*. This is given in 2D as

$$u(x, y, t) = \overline{u}(x, y) + u'(x, y, t), \tag{4.49}$$

for the x-component of velocity, with similar formulas for all other dependent variables. In Eq. (4.49) the bar (" $-$ ") denotes a time average, and prime (" $'$ ") indicates fluctuation about the time-averaged, mean quantity. Formally, the time average is defined as, *e.g.*, for the x-component of velocity,

$$\overline{u}(x, y) \equiv \lim_{T \to \infty} \frac{1}{T} \int_0^T u(x, y, t)\, dt. \tag{4.50}$$

At any particular spatial location, say (x, y), in a stationary flow (one having steady mean properties) the time-averaged and fluctuating quantities might appear as in Fig. 4.15.

Now the purpose of introducing the decomposition of Eq. (4.49) is to aid in explaining some
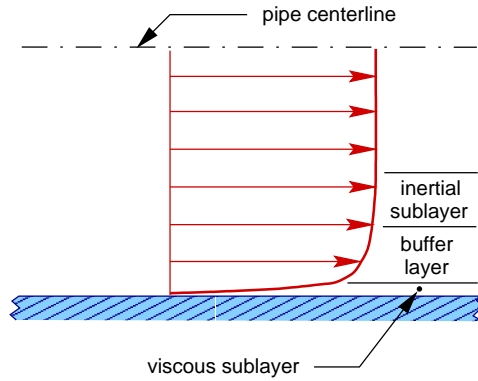
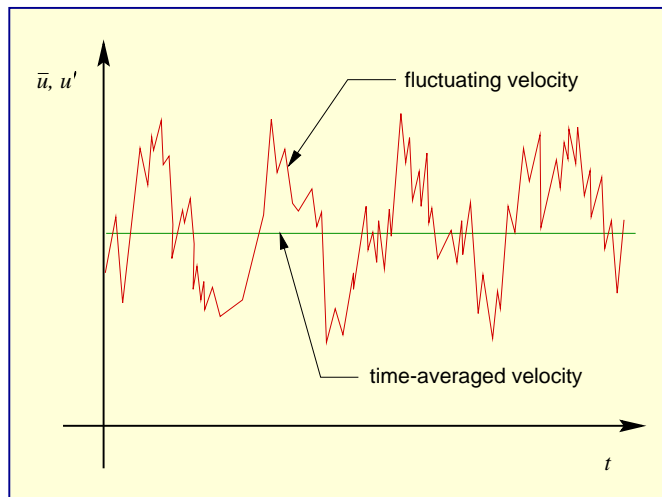Figure 4.14: Turbulent flow near a solid boundary.

Figure 4.15: Graphical depiction of components of Reynolds decomposition.

additional physics that occurs in turbulent flow, and which is not present in laminar flows. In particular, we consider the advective terms of the N.–S. equations, expressed for the 2-D x-momentum equation as

$$\left(u^2\right)_x + (uv)_y \,,$$

which follows from the divergence-free condition. For the second of these terms we can write

$$
\begin{aligned}
(uv)_y &= \left((\overline{u} + u')(\overline{v} + v')\right)_y \\
&= \left(\overline{u}\,\overline{v}\right)_y + \left(\overline{u}v'\right)_y + \left(u'\overline{v}\right)_y + \left(u'v'\right)_y \,,
\end{aligned}
\tag{4.51}
$$

with similar expressions available for all other inertial advection terms.

It can be shown using the definition of time average, Eq. (4.50), that $\overline{u'} = \overline{v'} = 0$ (an exercise we leave to the reader), so application of the averaging operator to both sides of Eq. (4.51), along with commuting averaging and differentiation, results in the simplification

$$\left(\overline{uv}\right)_y = \left(\overline{u}\,\overline{v}\right)_y + \left(\overline{u'v'}\right)_y \,.
\tag{4.52}$$

The second quantity on the right-hand side arises strictly from turbulent fluctuations and is of inertial origin, as are all the terms in Eq. (4.52). But if one recalls that in the derivation of the N.–S. equations <u>viscous</u> stresses, τ, appear in terms of the form, *e.g.*, $\partial\tau/\partial y$, it is natural to call quantities such as $\rho\overline{u'v'}$ *turbulent stresses*, or because they often arise as the result of a Reynolds decomposition, *Reynolds stresses*. Note that ρ must be inserted in the preceding expression for dimensional consistency with units of shear stress, but $\overline{u'v'}$ is often loosely termed a turbulent stress.

We can now return to Fig. 4.14 and describe the physics of each of the regions indicated there. The first of these is the *viscous sublayer*. This lies immediately adjacent to the solid wall, and in this region we expect velocities to be quite small due to the no-slip condition. Moreover, they increase roughly linearly coming away from the wall, similar to what occurs in Couette flow. Because of the low speed, turbulent fluctuations are small (sometimes, this layer is <u>incorrectly</u> termed the "laminar sublayer"), and they are readily damped by viscous forces. Thus, the <u>dominant</u> physics in this layer is the result of molecular viscosity—nonlinear inertial effects arising from $\overline{u'v'}$ are relatively small. As we move farther from the wall, into the *buffer layer* (sometimes called the "overlap region") the magnitude of turbulent fluctuations increases, and both molecular diffusion and turbulent stress terms are important aspects of the physics in this region, with the former decreasing in importance as we move farther from the wall. As we move yet further from the wall, into the *inertial sublayer*, effects of viscous diffusion become negligible, and only the turbulent stresses are important. Finally, an "outer layer" can be identified in which most of the flow energy is contained in motion on scales of the order of the pipe radius.

The motivation for the preceding discussions is to provide a rational framework for understanding the effects of surface roughness on turbulent friction factors. We have already indicated that even for laminar flow the friction factor is never zero, but in addition it does not depend on roughness of the pipe wall. In a turbulent flow wall roughness is a major factor, and the degree to which this is the case also depends on the Reynolds number. To see how this occurs we need to first recall one of the basic properties of boundary layers, *viz.*, their thickness decreases with increasing Re (recall that the boundary layer thickness is $\delta \sim 1/\sqrt{Re}$). From this we can expect that the boundary layer is relatively thick for laminar flows, corresponding to low Re, that the entire boundary layer acts as the viscous sublayer of a turbulent flow would and in particular, no matter how rough the pipe surface is, the mean "roughness height" will always lie within the highly viscous (molecular) shear stress dominated boundary layer.

As the Reynolds number is increased and transition to turbulence occurs, the boundary layer thins and so also does the thickness of the viscous sublayer. To some extent this has been quantified experimentally through the following formula:

$$\frac{u}{U_c} = \left(1 - \frac{r}{R}\right)^{1/n} .\tag{4.53}$$

Velocity profiles given by this formula for several values of the exponent n are provided in Fig. 4.16. The value of n used in Eq. (4.53) depends on the Reynolds number and increases from $n = 6$ at $Re \simeq 2{\times}10^4$ to $n = 10$ at $Re \simeq 3{\times}10^6$ in a nearly linear (on a semi-log plot) fashion. For moderate Re, $n = 7$ is widely used, almost independent of the actual value of Re.

In turn, this implies that as Re increases more of the rough edges of the surface are extending beyond the viscous sublayer and into the buffer and inertial layers (see Fig. 4.17) where the turbulent fluctuations are dominant. Because these are inertially driven the effect of their interactions with protrusions of the rough surface is to create a drag, thus significantly increasing the effective internal friction. In particular, one can envision the rough, irregular protrusions as locations where the flow actually stagnates creating locally-high "stagnation pressures," and thus slowing the flow.

Effectively, this leads to far more internal friction than does viscosity, so the result is considerable pressure loss and increased friction factor in comparison with laminar flow.

This interaction between the viscous sublayer and surface roughness suggests, simply on physical grounds, that the friction factor should be a function of Reynolds number and a dimensionless surface roughness, defined for pipe flow as ε/D, with ε being a mean roughness height. There are several ways in which this might be defined. Figure 4.17 displays one of these: the difference between mean values of protrusion maxima and protrusion minima.

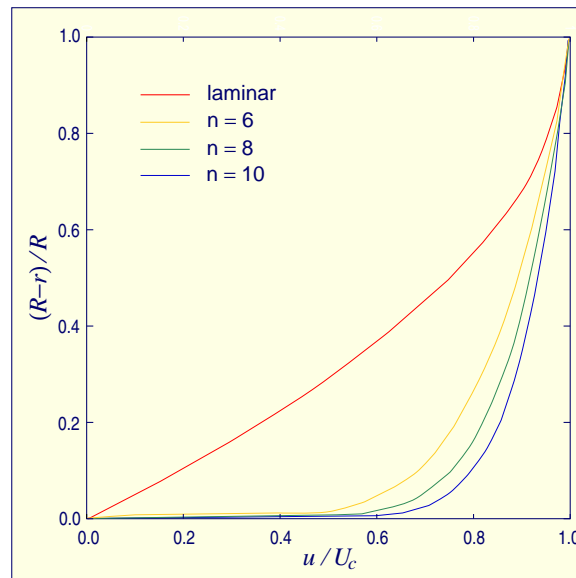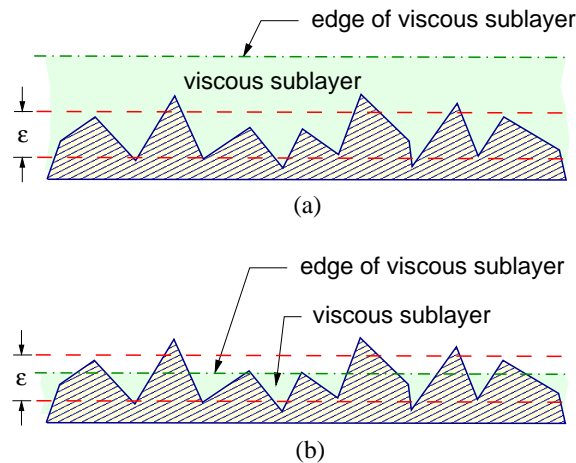Figure 4.16: Empirical turbulent pipe flow velocity profiles for different exponents in Eq. (4.53).

Figure 4.17: Comparison of surface roughness height with viscous sublayer thickness for (a) low Re, and (b) high Re.

Experimental data for friction factors have been collected for a wide range of dimensionless roughness heights and Reynolds numbers and have been summarized in the *Moody diagram* of Fig.

4.18. This diagram provides a log-log plot of friction factor over a wide range of Reynolds numbers and for numerous values of dimensionless surface roughness. There are a number of items to note regarding this plot. The first is that the laminar friction factor given in Eq. (4.47) appears in the left-hand side of the figure. We see from this that for pipe flow the laminar regime lasts only to $Re \simeq 2100$. Following this there is a range of Re up to $Re \simeq 4000$ over which the flow is a "mixture" of laminar and turbulent behavior. This typically consists of bursts of turbulence, often
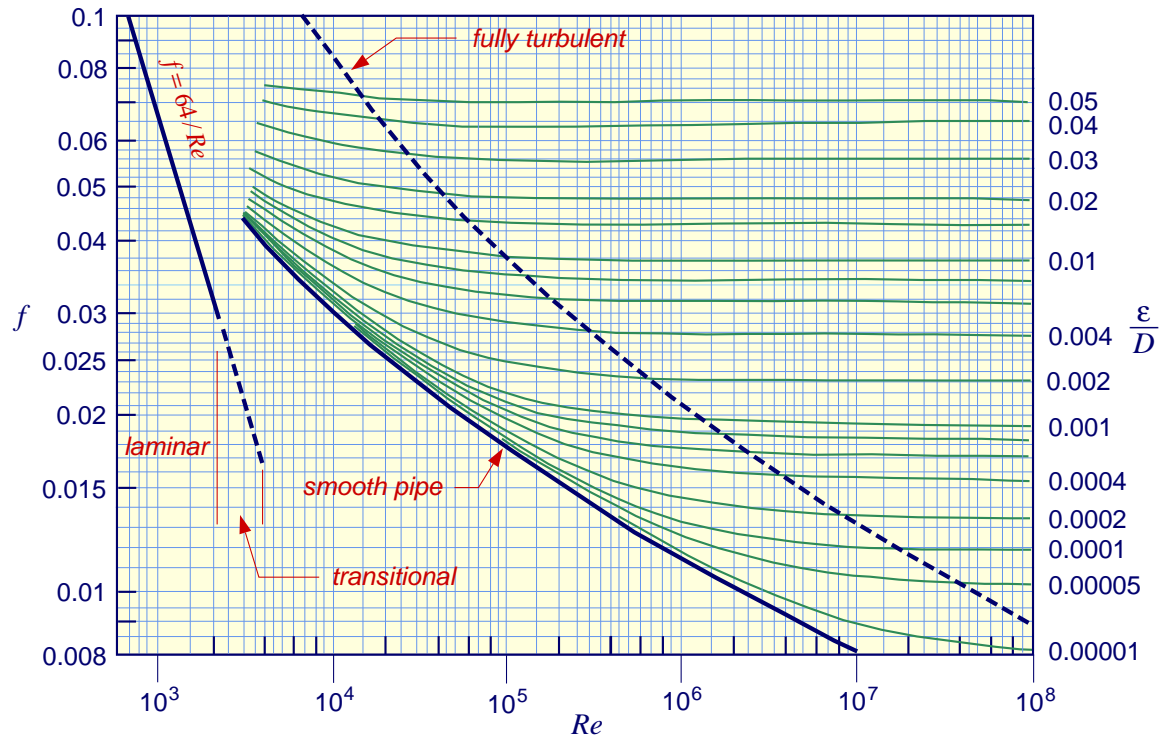

Figure 4.18: Moody diagram: friction factor *vs.* Reynolds number for various dimensionless surface roughnesses.

termed "puffs" and/or "slugs" appearing sporadically, persisting for a time as they are advected downstream, and ultimately decaying (due to viscous dissipation of their turbulent energy) only to be replaced by new puffs and/or slugs at a later time and different place. One way to study this activity in laboratory experiments is to measure a component (or components) of velocity as a function of time at a few locations in the flow field using, *e.g.*, laser-doppler velocimetry (LDV). The result of this might appear as in Fig. 4.19. Here we see periods of very erratic oscillation that last only a relatively short time before being replaced by an essentially steady signal. Then, later the complicated oscillations reappear, corresponding to the flow of a turbulent puff or slug past the measurement point. The ratio of the time during which the flow is turbulent to the total time is known as the *intermittency factor* and is one of the important quantifiers of turbulent flow.

The second feature to observe in the Moody diagram is a curve corresponding to turbulent flow in a smooth pipe. Pipes of this sort, sometimes termed "hydraulically smooth," are such that within the range of Reynolds numbers of practical importance the normalized surface roughness is so small that it never protrudes through the viscous sublayer. Thus, for any given Reynolds number in the turbulent flow regime a smooth pipe produces the smallest possible friction factor. Related to this is the dashed curve, labeled "fully turbulent," providing the locus of Re values
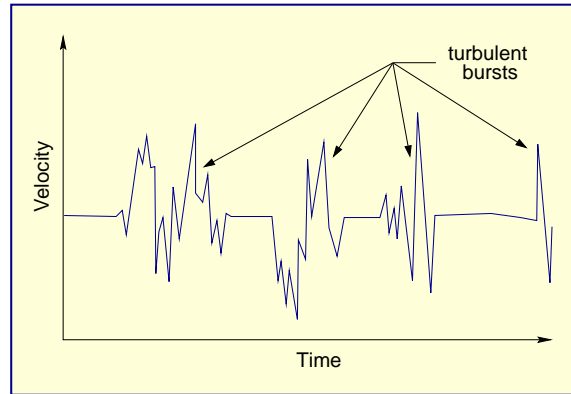
Figure 4.19: Time series of velocity component undergoing transitional flow behavior.

beyond which the viscous sublayer is so thin compared with each displayed value of ε/D that it has essentially no effect on the inertial behavior of the turbulent fluctuations; *viz.*, the friction factor shows almost no further change with increasing Reynolds number.

The next thing to note from the Moody diagram is the significant increase in friction factor following the transition to turbulence somewhat before $Re = 4000$, even for the case of a smooth pipe. (Note that this clearly shows that the viscous sublayer cannot be laminar.) It is clear from Fig. 4.16 that as Re increases (and n in Eq. (4.53) increases) the velocity gradient at the wall also increases, leading to increased shear stresses which in turn translate to increases in friction factor. But it must also be observed that in general, within each of the separate laminar and turbulent flow regimes, friction factor is a non-increasing function of Re. This occurs because increasing Re results in decreasing boundary-layer thickness, which in turn implies that less of the total flow field is subjected to high shear stresses (again, see Fig. 4.16). It is worthwhile to note that this implies the friction factor embodies more physics than simply the wall shear stress, τ_w, to which it is often related.

Finally, it is clear that in order to use the Moody diagram we must be able to obtain values of surface roughness. These have been measured and tabulated (and sometimes plotted) for an extensive range of materials used in piping systems. Table 4.1 provides some representative values.

Table 4.1   Surface roughness values for various engineering materials

PIPING MATERIAL	Roughness, ε (mm)
Cast iron	0.26
Commercial steel and wrought iron	0.045
Concrete	0.3–3.0
Drawn tubing	0.0015
Galvanized iron	0.15
Plastic (and glass)	0.0 (smooth)
Riveted steel	0.9–9.0

A note of caution is in order regarding the contents of this table. Namely, the values typically used are not actual measured ones, but are instead the result of data correlations constructed over

a range of measurements. They are sometimes referred to as "equivalent" roughnesses; it is useful to consider them as simply representative values.

There is one additional item associated with friction factors that we now address. The Moody diagram obviously contains a tremendous amount of information, but in the context of modern problem solving using digital computers it is very inconvenient to employ graphical techniques for determining such an important parameter as the friction factor. Indeed, this was actually recognized long before the advent of modern high-speed supercomputers, and a number of attempts have been made to correlate the data of the Moody diagram in a single formula. The most successful such expression is known as the Colebrook formula which takes the form

$$\frac{1}{\sqrt{f}} = -2\log_{10}\left(\frac{\varepsilon/D}{3.7} + \frac{2.51}{Re\sqrt{f}}\right). \tag{4.54}$$

This equation is valid for $4\times10^3 < Re < 10^8$, and within this range calculated values of friction factor differ from experimental results typically by no more than 15%.

Equation (4.54) is a nonlinear equation for the friction factor f, and it does not possess a closed-form solution. On the other hand, it can be readily solved via a numerical procedure known as "successive substitution," an instance of the general mathematical concept of *fixed-point iteration*. This can be carried out in the following way. First, for ease of notation we set

$$s = \frac{1}{\sqrt{f}}, \tag{4.55}$$

and

$$F(s) \equiv -2\log_{10}\left(\frac{\varepsilon/D}{3.7} + \frac{2.51}{Re}s\right). \tag{4.56}$$

Then from Eq. (4.54) we have

$$s = F(s), \tag{4.57}$$

so our task is to find s that satisfies this equation. That is, we need to find the value of s which when substituted into Eq. (4.56) will result again in s itself, *i.e.*, a "fixed point" of F. The procedure for doing this is straightforward. For specified values of Re and ε/D choose an initial estimate of s, call it s_0. Then carry out the following sequence of calculations:

$$
\begin{aligned}
s_1 &= F(s_0)\\
s_2 &= F(s_1)\\
&\vdots\\
s_m &= F(s_{m-1}), \qquad etc.,\\
&\vdots
\end{aligned}
$$

until $|s_m - s_{m-1}| < \epsilon$ with ϵ being a specified acceptable level of error. Once s has been obtained, the friction factor is calculated directly from Eq. (4.55); *i.e.*, $f = 1/s^2$.

It is easy to perform such calculations even on a hand-held calculator, and they are readily programmed for execution in a digital computer. Hence, obtaining reasonably accurate values of the friction factor is now very routine and essentially automatic. Furthermore, once we have obtained f, it turns out that we can approximate the corresponding turbulent velocity profile using Eq. (4.53) because it is known from experimental results that the exponent n of that equation is related to the friction factor by

$$n = \frac{1}{\sqrt{f}}, \tag{4.58}$$

which is precisely our parameter s employed to find f from the Colebrook formula.

Head Loss

The next step in the analysis of pipe flow requires development of a flow equation that is easy to use, and which at the same time can include the main parts of the basic physics. We recall that Bernoulli's equation is certainly very straightforward to apply, but it was derived on the basis of an inviscid assumption. We will now show how to modify this equation to account for not only viscous effects, but also turbulence, changes in pipe geometry and even the introduction of pumps and turbines into the flow system.

We begin by recalling the form of Bernoulli's equation given earlier in Eq. (4.13) and expressed here as

$$p_1 + \frac{1}{2}\rho U_1^2 + \rho g z_1 = p_2 + \frac{1}{2}\rho U_2^2 + \rho g z_2 \,. \tag{4.59}$$

The first thing to note is that this is formally an energy equation quite similar to that usually first encountered in elementary thermodynamics courses. In particular, we know from basic physics that kinetic energy is expressed as $\frac{1}{2}mU^2$, so the dynamic pressure $\frac{1}{2}\rho U^2$ is simply kinetic energy per unit volume; similarly, $\rho g z$ is potential energy per unit volume with z being the height above some fixed reference level. We have previously observed that static pressure must have the same units as dynamic pressure (we have often used the latter to scale the former), so it too represents energy per umit volume as is easily checked. (Recall that in thermodynamics this is associated with *flow work*, or *flow energy*, and is combined with internal energy of open flow systems to express the energy equation in terms of enthalpy. This will not be useful in the present context.)

We next divide Eq. (4.59) by the constant density ρ to obtain energy per unit mass, and then we add the internal energy per unit mass, u, to both sides of the equation:

$$\frac{p_1}{\rho} + \frac{1}{2}U_1^2 + g z_1 + u_1 = \frac{p_2}{\rho} + \frac{1}{2}U_2^2 + g z_1 + u_2 \,. \tag{4.60}$$

Now since each of these terms is associated with energy it is natural to express this as a change in energy between "outflow" and "inflow," namely

$$\Delta e = e_2 - e_1 \,,$$

where

$$e_i = \frac{p_i}{\rho} + \frac{1}{2}U_i^2 + g z_i + u_i \,, \qquad i = 1, 2 \,. \tag{4.61}$$

We next recall the first law of thermodynamics which we express as

$$Q_H - W = \Delta E \,, \tag{4.62}$$

where Q_H represents heat transferred to the system (to the fluid), and we use the "H" subscript to distinguish the notation from that used earlier for volumetric flowrate (Q). In Eq. (4.62) W is work done by the fluid. Thus, for our purposes it will be useful to express this as a combination of pump and turbine work, expressed as

$$W = W_T - W_P \tag{4.63}$$

since the fluid does work to rotate a turbine and has work imparted to it by a pump (or fan). Substitution of this into Eq. (4.62) yields

$$\Delta E = Q_H - W_T + W_P \,,$$

and division by mass m gives

$$\Delta e = \frac{Q_H}{m} - \frac{W_T}{m} + \frac{W_P}{m} \, ,$$

or

$$e_2 - e_1 = \frac{Q_H}{m} - \frac{W_T}{m} + \frac{W_P}{m} \, .$$

Then applying the forms of e_1 and e_2 from Eq. (4.61) and rearranging results in

$$\frac{p_1}{\rho} + \frac{1}{2}U_1^2 + gz_1 + \frac{W_P}{m} = \frac{p_2}{\rho} + \frac{1}{2}U_2^2 + gz_2 + \frac{W_T}{m} + (u_2 - u_1) - \frac{Q_H}{m} \, .$$

Finally, we divide this by the gravitational acceleration g (or possibly some other local acceleration), as appropriate, to obtain

$$\frac{p_1}{\gamma} + \frac{U_1^2}{2g} + z_1 + \frac{W_P}{mg} = \frac{p_2}{\gamma} + \frac{U_2^2}{2g} + z_2 + \frac{W_T}{mg} + \frac{1}{g}\left[(u_2 - u_1) - \frac{Q_H}{m}\right] \, . \qquad (4.64)$$

Here, as has been the case earlier, $\gamma = \rho g$ is the specific weight of the fluid under consideration.

At this point we can now introduce the terminology "head." This has long been used by hydraulics engineers as a measure of the height of fluid; *i.e.*, in a static fluid the height z is referred to as the *head*. But we also know from fluid statics that a change in height corresponds to a change in pressure, and from this we can now deduce the meaning of "head loss." In particular, note that all terms of Eq. (4.64) must have units of height, and consider the simplest case corresponding to fully-developed flow in a pipe at constant elevation z with no pumps or turbines, and no heat transfer. Thus, $z_1 = z_2$, $U_1 = U_2$ and $W_P = W_T = Q_H = 0$; Eq. (4.64) collapses to

$$\frac{p_1}{\gamma} - \frac{p_2}{\gamma} = \frac{1}{g}(u_2 - u_1) \, . \qquad (4.65)$$

We now need to investigate the physics that might lead to changes in the internal energy u.

We begin by recalling that the N.–S. equations which describe the motion of <u>all</u> fluid flows contain terms of the form, *e.g.*,

$$\mu \Delta u = \mu\left(\frac{\partial^2 u}{\partial x^2} + \frac{\partial^2 u}{\partial y^2} + \frac{\partial^2 u}{\partial z^2}\right) \, ,$$

in the x-momentum equation, with corresponding viscous terms in the other two momentum equations. We noted at the time the physics of such terms was discussed in Chap. 3 that they correspond to diffusion of momentum and thus, smoothing of the velocity field; moreover, we know from thermodynamics that diffusion results in entropy generation and a loss of usable energy. Indeed, a purely mathematical analysis of such terms shows that they lead to decay of the magnitude of the solution to equations in which they appear. Thus, as we have previously emphasized, the momentum equations are <u>balance</u> equations rather than conservation laws. But the question then arises, "where does the energy go?" since we know that overall (in a universal sense) energy is conserved.

The answer to this question is simple, although details of the precise physical mechanism are complicated. Namely, the action of viscosity in a fluid flow, in the course of mixing and smoothing that flow, converts some kinetic energy to <u>unusable</u> thermal energy and, again from thermodynamics, we know this results in a change (an increase in this case) of the internal energy u. We emphasize, however, that the viscous terms in the N.–S. equations in no way <u>explicitly</u> account for this energy loss. Recall that their form stems from Newton's law of viscosity, an <u>empirical</u> result, that produces the correct effect on momentum at macroscopic scales to account for energy

losses ocurring on microscopic scales. In this regard there is no contradiction with the continuum hypothesis.

We now associate this change of internal energy with the right-hand side of Eq. (4.65), and from this we see that there has been a loss in pressure between locations 1 and 2. Thus, in the terminology introduced at the beginning of this section there is a *head loss*, and we write this as

$$h_f = \frac{\Delta p}{\gamma} \,. \tag{4.66}$$

We earlier alluded to the fact that there are two distinct contributions to pressure loss, *i.e.*, head loss, in piping systems. The first of these is directly of viscous origin and thus can be associated with internal friction, justifying the preceding subscript f notation.

For this type of loss we have already determined Δp from the Hagen–Poiseiulle solution and related it to the friction factor; recall from Eq. (4.46), after some rearrangement, we have

$$\Delta p = \frac{1}{2}\rho U_{avg}^2 \frac{L}{D} f \,,$$

suggesting that head loss can be expressed in terms of the friction factor. Thus, substitution of the above into Eq. (4.66) yields

$$h_f = \frac{\frac{1}{2}\rho U_{avg}^2}{\rho g} \frac{L}{D} f \,,$$

or

$$h_f = f \frac{L}{D} \frac{U_{avg}^2}{2g} \,. \tag{4.67}$$

This is the well-known *Darcy–Weisbach formula* for frictional head loss.

It is important to recognize that up to this point in development of the head loss formula we have not specifically indicated whether the flow being considered was laminar or turbulent, except for the use of the laminar Hagen–Poiseiulle formula to obtain the pressure drop. This is because the friction factor f appearing in Eq. (4.67) is an empirical quantity that accounts for this somewhat automatically (recall the Moody diagram of Fig. 4.18). In particular, if U_{avg} is calculated consistently for a turbulent velocity profile and f is read from the Moody diagram (or calculated from the Colebrook formula, Eq. (4.54)) with a value of Re and appropriate surface roughness in the turbulent flow regime, the Darcy–Weisbach formula provides a correct head loss. But we remind the reader that there is additional physics in a turbulent flow that leads to larger friction factors, and thus larger head losses, compared with the laminar case, and this has been taken into account (empirically) through the surface roughness parameters needed for evaluation of the friction factor.

With this information in hand we can now express the modified Bernoulli's equation (energy equation), (4.64), as

$$\frac{p_1}{\gamma} + \alpha_1 \frac{U_1^2}{2g} + z_1 + h_P = \frac{p_2}{\gamma} + \alpha_2 \frac{U_2^2}{2g} + z_2 + h_T + h_f \,. \tag{4.68}$$

In this equation we have introduced the notation

$$h_P \equiv \frac{W_P}{mg} \tag{4.69}$$

corresponding to head gain provided by a pump, and

$$h_T \equiv \frac{W_T}{mg} \tag{4.70}$$

representing head loss in a turbine. It should also be noted that the heat transfer term of Eq. (4.64) has been omitted because we will not consider heat transfer in subsequent analyses.

Finally, we call attention to the factors α_i appearing in the kinetic energy terms. Recall that in the original formulation of Bernoulli's equation the entries for velocity were local (at specific points in the fluid), but now what is needed are representative values for entire pipe cross sections. The factors α_i are introduced to account for the fact that the velocity profiles in a pipe are nonuniform, and consequently the overall kinetic energy in a cross section must differ from that simply calculated from the average velocity. (The average of U^2 does not equal U^2 calculated with U_{avg}.)

In turbulent flows this difference is small. The boundary layer is thin due to the high Re, and the velocity profile is fairly flat (and hence, nearly uniform—recall Fig. 4.18). Thus, for turbulent flows $\alpha \simeq 1.05$ is a typical value, and as a consequence in many cases this correction is neglected; *i.e.*, $\alpha = 1$ is used. But for laminar flows the velocity profile is far from uniform, and it can be shown (analytically) that $\alpha = 2$. (We leave demonstration of this as an exercise for the reader.) So in this case a significant error can be introduced if this factor is ignored (and the kinetic energy happens to be an important contribution).

We have now accumulated sufficient information on practical pipe flow analysis to consider an example problem.

EXAMPLE 4.8 For the simple piping system shown in Fig. 4.20 it is required to find the pumping power and the diameter of the pump inlet that will produce a flow speed U_2 at location 2 that is double the flow speed U_1 at location 1. It is known that $p_1 = 3p_2$, and that p_2 is atmospheric
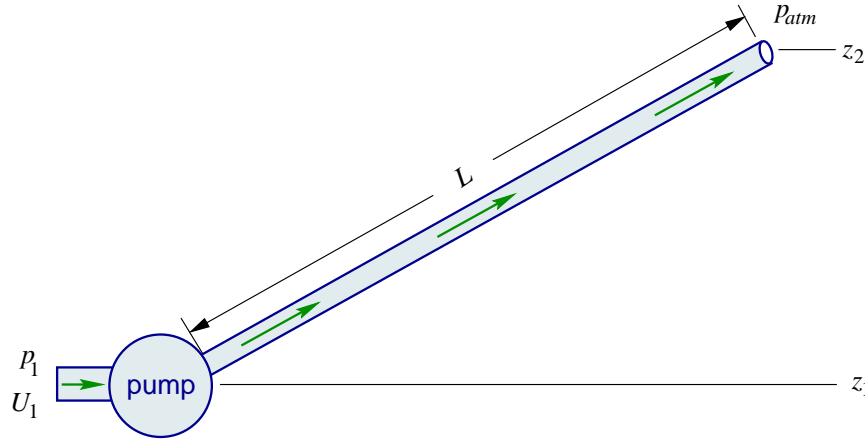

Figure 4.20: Simple piping system containing a pump.

pressure. Furthermore, the height z_1 is given, and $z_2 = 4z_1$. The fluid being transferred has known density ρ and viscosity μ. The pipe from the pump to location 2 is of circular cross section with known diameter D, and its length is given as $L \gg L_e$. Finally, the surface roughness of this pipe is given as ε. Two cases are to be considered: *i)* U_1 is sufficiently small that U_2 results in a Reynolds number such that $Re < 2100$; *ii)* the Reynolds number for U_1 is less than 2100, but that for U_2 is greater than 2100.

Clearly, the main equation we will use for this analysis is our modified Bernoulli equation (4.68). Since the physical situation does not include a turbine, but does have a pump, we write this equation as

$$\frac{p_1}{\gamma} + \alpha_1 \frac{U_1^2}{2g} + z_1 + h_P = \frac{p_2}{\gamma} + \alpha_2 \frac{U_2^2}{2g} + z_2 + h_f \,.$$

We next note that since pump power is required we use the definition of pump head given in Eq. (4.69) to obtain

$$W_P = mgh_P \qquad \Rightarrow \qquad \dot{W}_P = \dot{m}gh_P \, .$$

We begin by observing that since this is a steady-state situation the flow rate at location 2 must equal that at location 1, and

$$\dot{m}_2 = \rho U_2 A_2 = \rho(2U_1)\pi \frac{D_2^2}{4} \, .$$

Thus, we can solve for D_1, the required pipe diameter at the pump entrance, using

$$\dot{m}_1 = \dot{m}_2 \, ,$$

and

$$\rho U_1 \pi \frac{D_1^2}{4} = \rho U_1 \pi \frac{D_2^2}{2} \, .$$

Thus,

$$D_1^2 = 2D_2^2 \qquad \Rightarrow \qquad D_1 = \sqrt{2}D_2 \, .$$

This result holds for both cases of flow speeds to be considered.

We now specifically consider case *i)*. This corresponds to a situation in which the flow is laminar throughout the piping system (although almost certainly not inside the pump—but we do not consider internal details of this sort in these analyses). We can immediatedly deduce the friction factor to be used in the head loss formula from the expression for the Darcy friction factor. In particular, since the flow is laminar we need not be concerned with the level of pipe roughness. Hence,

$$f = \frac{64}{Re} \, ,$$

with

$$Re = \frac{\rho U_2 D_2}{\mu} = \frac{2\rho U_1 D_2}{\mu} \, .$$

In turn, we can now calculate the head loss associated with internal friction effects as

$$h_f = f \frac{L}{D} \frac{U_2^2}{2g} \, .$$

We are now ready to substitute all known quantities into the energy equation and solve for h_P, the required pump head. We note that we have assumed the length of pipe running from location 1 to the pump entrance is too short for friction losses to be significant, and we also make use of the fact that the flow is laminar throughout the piping system to set $\alpha_1 = \alpha_2 = 2$. Then Bernoulli's equation takes the form

$$\frac{3p_{atm}}{\gamma} + \frac{U_1^2}{g} + z_1 + h_P = \frac{p_{atm}}{\gamma} + \frac{4U_1^2}{g} + 4z_1 + h_f \, ,$$

which after combining various terms and solving for h_P leads to

$$h_P = \frac{3U_1^2}{g} - \frac{2p_{atm}}{\gamma} + 3z_1 + h_f \, .$$

Then the required pump power is obtained from

$$\dot{W}_P = \dot{m}gh_P \, ,$$

with $\dot{m}$ computed earlier as

$$\dot{m} = \rho U_1 \pi \frac{D_2^2}{2} \,.$$

We are now ready to analyze case *ii)*. This analysis differs from that just presented in two ways. First, because the flow in the pipe segment preceding the pump is still laminar, $\alpha_1 = 2$ as before. But now the turbulent flow in the section of pipe beyond the pump permits us to set $\alpha_2 \simeq 1$. The second main difference is that the friction factor f can no longer be directly calculated. It must either be obtained iteratively from the Colebrook formula, as discussed earlier, or it might be read from the Moody diagram. But once it has been determined, it can be applied in the same manner as in the laminar case. We will not provide these details here, leaving this as an exercise for the reader.

Head Loss Modification for Non-Circular Cross Sections

The Darcy–Weisbach formula, Eq. (4.67), holds only for pipes having circular cross section. But in engineering practice we often must deal with flow in square and rectangular ducts, sometimes even ducts with triangular cross sections; in fact, situations may arise in which geometry of the duct cross section may be very complicated. In this section we introduce a very straightforward approach to approximately handle these more difficult geometries.

We start by recalling the Darcy–Weisbach formula:

$$h_f = f \frac{L}{D} \frac{U_{avg}^2}{2g} \,.$$

The modification we introduce here involves simply replacing the pipe diameter D with an "equivalent diameter," termed the *hydraulic diameter* and denoted D_h, that at least partially accounts for effects arising from the non-circular cross section. The hydraulic diameter is defined as

$$D_h = \frac{4A}{P} \,, \tag{4.71}$$

where A is the cross-sectional area, and P is the "wetted perimeter" (around the cross section) of the duct. For example, for a duct having rectangular cross section with height h and width w, the hydraulic diameter is

$$D_h = \frac{4wh}{2(w + h)} \,.$$

Thus, to estimate the head loss for a duct of essentially arbitrary cross-sectional geometry, we use Eq. (4.71) to calculate the hydraulic diameter. Then we use this diameter in the Darcy–Weisbach formula, and in addition for calculating Re and surface roughness factor needed to find the friction factor f. That is, we use

$$Re_h = \frac{\rho U D_h}{\mu} \qquad \text{and} \qquad \frac{\varepsilon}{D_h} \,.$$

This approach works reasonably well for cross sections that do not deviate too much from circular; one can easily show that for a circular cross section $D_h = D$. But as the geometry departs significantly from circular, use of D_h as described leads to large errors. In particular, additional flow physics can arise even in not very complicated geometries if, *e.g.*, sharp corners are present. We will see some effects of this sort in the next subsection, but there they will be quantified only as they occur with respect to the streamwise direction. In the present context they may also influence

flow behavior in the cross stream direction, and this simply is not being taken into account by analyses such as discussed here.

<div align="center">

Minor Losses

</div>

We begin this section by again reminding the reader that all of the preceding analyses arose either directly, or indirectly through necessary empiricism, from the Hagen–Poiseiulle solution to the N.–S. equations. In particular, application of the preceding formulas requires an assumption of fully-developed flow. In the present section we will treat situations in which the flow cannot possibly be fully developed, and introduce formulas for additional head loss arising in such cases. It is worth noting that in systems having very long pipes, the head losses already treated are the main contributor to pressure drop, and are often called *major losses*. The losses we will treat in the present section are called *minor losses*, and they arise specifically from flow through pipe expansions and contractions, and through tees, bends, branches and various fittings such as valves. In almost all cases, these losses have been obtained empirically.

The form of the Darcy–Weisbach expression given above can be generalized to the case of minor losses by combining the two dimensionless factors f and L/D appearing in it into a single parameter usually denoted by K, and called the *loss coefficient*. Thus, the general formula for minor losses takes the form

$$h_m = K \frac{U_{avg}^2}{2g}, \tag{4.72}$$

with U_{avg} representing an average velocity usually just upstream of the region whose minor loss is to be estimated. The factor K is in general different for each physical flow situation and can seldom be predicted analytically. In what follows we will provide sketches corresponding to a number of different common flow devices along with tabulated values of K for each of these. In all cases the overall cross sections are circular, so in actual devices involving non-circular geometries it is necessary to employ hydraulic diameters in place of diameters, as appropriate, and subject to the same precautions noted earlier.

Finally, we note that the various forms of head losses are additive, and in general we can consider the complete head loss to be

$$h_L = h_f + h_m. \tag{4.73}$$

In turn, the term h_f appearing in the energy equation (4.68) should now be replaced with h_L.

In the following paragraphs we will treat several specific widely-encountered flow devices that contribute to minor losses, provide corresponding data for the loss coefficient K, and in some cases indicate the physics related to such flows.

Sharp-edged inlets. The first case of minor losses we consider is one that is often encountered in practice, that of flow in a sharp-edged inlet. This is shown schematically in Fig. 4.21. It is of interest to consider the physics of this case in some detail, first because it is analogous to a separated flow situation discussed in Chap. 2, and second because many of the other minor loss cases to be considered herein exhibit similar behaviors.

In this particular flow we consider the vertical wall to be of large extent compared with the size of the inlet. In this situation we can expect that some streamlines will flow essentially parallel to this wall as shown, and when they reach the sharp corner of the inlet they will be unable to make the abrupt turn into the inlet. As a result, such streamlines detach (separate) from the wall and later reattach farther downstream within the inlet. Starting at the point of separation is a recirculation region (also called a separation "bubble") containing flow that does not readily mix with the remaining unseparated incoming flow. This region acts as a physical blockage to
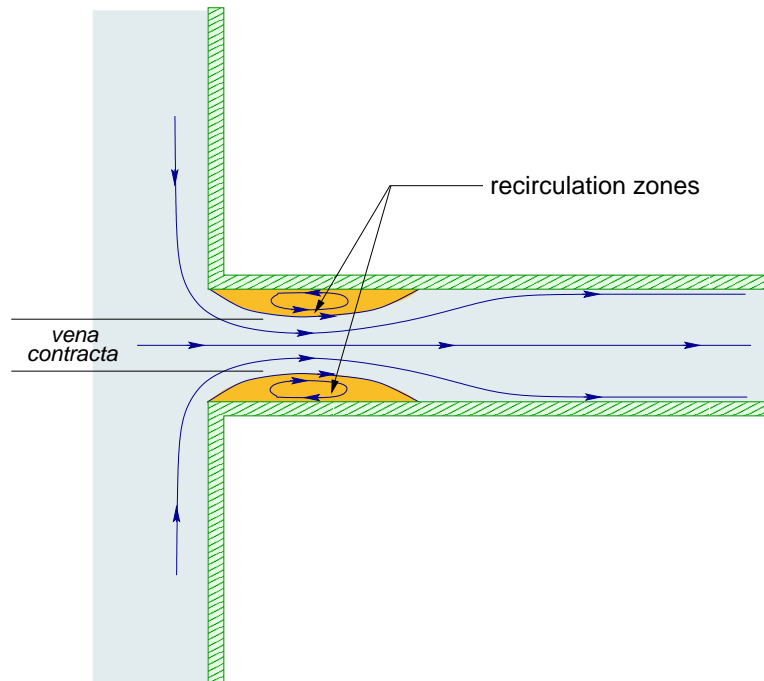
Figure 4.21: Flow through sharp-edged inlet.

the oncoming flow, effectively narrowing the flow passage (giving rise to the terminology *vena contracta*), increasing the flow speed, and thus decreasing the pressure—a head loss. It is also interesting to note that the extent of effective contraction of passage diameter can be greatly reduced simply by rounding the corners of the inlet, rather than using sharp edges. This can be seen in Table 4.2 which contains experimental data for the value of the loss coefficient K as a function of radius of curvature of the inlet edge normalized by the downstream diameter.

Table 4.2   Loss coefficient for different inlet radii of curvature

$\mathcal{R}/D$	K
0.0	0.5
0.02	0.28
0.06	0.15
≥ 0.15	0.04
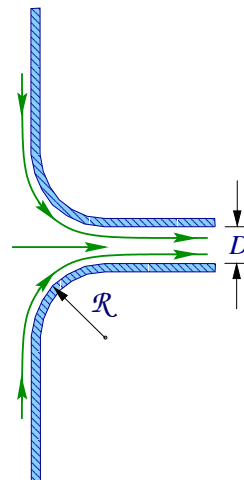
As the accompanying sketch implies, the amount of flow separation is decreased as the radius

of curvature of the corner increases, resulting in significant decrease in the extent of vena contracta and associated effective flow blockage.

Contracting pipes. Another often-encountered flow situation that can result in significant head loss is that of a contracting pipe or duct. A general depiction of such a configuration is presented in Fig. 4.22. It is clear that multiple recirculation zones are present. In the case of circular pipes
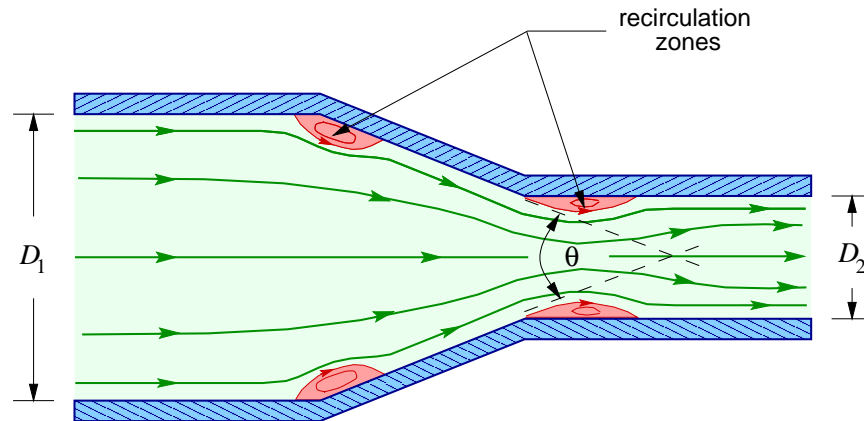

Figure 4.22: Flow in contracting pipe.

these wrap around the entire inner surface of the pipe, while for more general geometries they can take on very complicated shapes. In any case, they result in some effective blockage of the pipe or duct, and consequently additional head loss. It is reasonable to expect that as the angle θ becomes small, or as $D_2 \to D_1$, the size of the separated regions should decrease, and the loss factor will correspondingly be reduced. This is reflected to some extent in Table 4.3. In particular, we see for the case of $\theta = 60°$ that the value of K decreases as $D_2 \to D_1$, although in this rather mild situation no value of K is excessive.

Table 4.3   Loss coefficients for contracting pipes

D_2/D_1	K	
	$\theta = 60°$	$\theta = 180°$
0.2	0.08	0.49
0.4	0.07	0.42
0.6	0.06	0.32
0.8	0.05	0.18

The case of abrupt contraction ($\theta = 180°$) shows a much more dramatic effect as pipe diameters approach the same value. Namely, for the smallest downstream pipe (greatest amount of contraction), the value of K is 0.49; but this decreases to 0.18 when the pipe diameter ratio is 0.8. It is of interest to note that this case is essentially the same as that of a sharp-edged inlet, discussed above, with $D_1 \to \infty$. Furthermore, there is a reasonably-accurate empirical formula that represents this

case of a rapidly contracting pipe:

$$K \approx \frac{1}{2} \left[1 - \left(\frac{D_2}{D_1} \right)^2 \right] . \tag{4.74}$$

Rapidly-expanding pipes. The reader should recall that we earlier treated this example using the control-volume momentum equation, and then repeated the analysis using Bernoulli's equation to find that the results were considerably different. Figure 4.8 provides a detailed schematic; here we will repeat a few essential features in Fig. 4.23. We discussed details of the physics of this flow
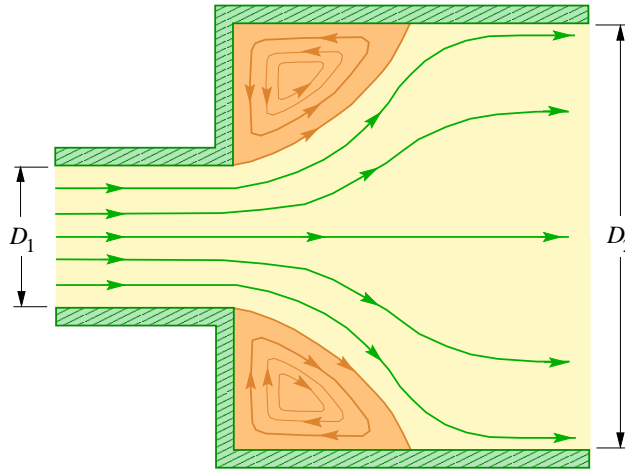

Figure 4.23: Flow in expanding pipe.

earlier, and the main thing to recall here is that laboratory measurements for these types of flows support the pressure-drop prediction of the control-volume momentum equation rather than that of Bernoulli's equation. We had earlier quantified the difference between these two pressure drops, and found this to be, in our current notation,

$$\Delta p_M - \Delta p_B = \frac{1}{2} \rho U_{avg}^2 \left[1 - \left(\frac{D_1}{D_2} \right)^2 \right]^2 . \tag{4.75}$$

Now recall in our modifications to Bernoulli's equation, that one of the main corrections is the head loss, consisting of major and minor contributions. If we argue that the pipe lengths are relatively short, we can ignore the major head loss, leaving only the minor loss. Our formula for this is Eq. (4.72):

$$h_m = K \frac{U_{avg}^2}{2g} .$$

Observe that division of Δp by ρg in Eq. (4.75) produces a quantity having units of length, the same as head loss; Thus, we set the right-hand side of (4.75) divided by ρg equal to minor head loss to obtain

$$h_m = \left[1 - \left(\frac{D_1}{D_2} \right)^2 \right]^2 \frac{U_{avg}^2}{2g} ,$$

and comparing this with the preceding equation shows that the loss coefficient for a rapidly-expanding pipe is

$$K = \left[1 - \left(\frac{D_1}{D_2} \right)^2 \right]^2 . \tag{4.76}$$

Elbows. As a final example of minor losses we consider flow in an elbow. Figure 4.24 depicts the qualitative features of the flow field in this case, and also provides a table of loss coefficient values

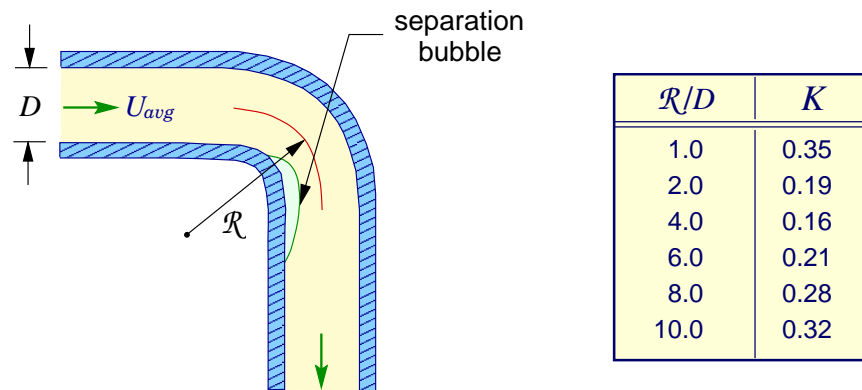| $\mathcal{R}/D$	K
1.0	0.35
2.0	0.19
4.0	0.16
6.0	0.21
8.0	0.28
10.0	0.32

Figure 4.24: Flow in pipe with 90° bend.

as a function of radius of curvature scaled with pipe diameter. An interesting feature of these values is their non-monotone behavior with respect to changes in radius of curvature. In particular, there appears to be a minimum in the loss coefficient near the normalized radius of curvature of 4. The flow in elbows is quite complicated. For very small radius of curvature the incoming flow is unable to make the turn at the bend, separates and in part stagnates against the opposite side of the pipe, raising the pressure and lowering the velocity. At the same time, a separation bubble forms below the bend, as indicated in Fig. 4.24, and in this region the pressure is relatively low. Specific details depend on the radius of curvature of the bend, as suggested by the entries in the above table.

We remark that there are many other cases of elbows, often called pipe bends. Data for corresponding loss coefficients can be found in many elementary fluid dynamics texts, and on the Internet. (Just enter "loss coefficient" in the search tool of any standard web browser.) Similarly, there are many other pipe fittings that we have not treated here, some of which we mentioned in introducing the present material. All are treated in the manner applied to those we have just considered. In particular, with the aid of basic geometric information associated with any particular fitting (*e.g.*, diameter, radius of curvature, contraction angle, *etc.*) we can find a value of loss coefficient K with the help of the appropriate table. Once this has been found we simply substitute it into Eq. (4.72) to compute the minor loss, h_m.

There is a final point to consider regarding minor losses. Although the notation we have employed herein is now fairly standard, occasionally a slightly different formulation is encountered. Namely, an "equivalent length," L_e, is defined such that the loss coefficient is given by

$$K = f \frac{L_e}{D} , \tag{4.77}$$

with f being the usual friction factor for a <u>straight</u> pipe of diameter D. Thus, if one knows K, then it is a direct calculation to obtain the equivalent length L_e. We note that L_e is not the same as the

entrance length discussed at the beginning of our treatment of pipe flow; the common notation is unfortunate.

   We conclude this section on pipe flow with a fairly extensive example demonstrating much of what has just been discussed regarding analyses utilizing the energy equation, friction factors and head loss.

EXAMPLE 4.9 Consider the liquid-propellant rocket engine fluid system depicted in Fig. 4.25. Assume all required geometric dimensions are known (including surface roughness heights), and all
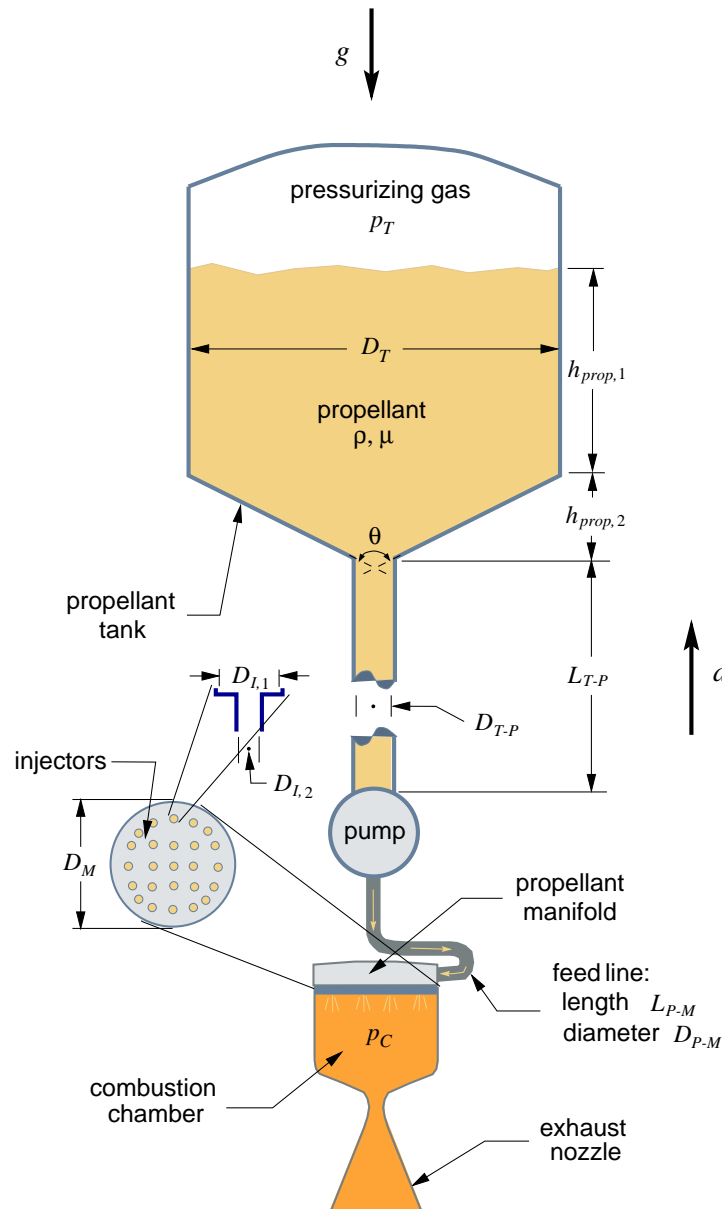

Figure 4.25: Liquid propellant rocket engine piping system.

devices possess circular cross sections. Assume further that the pressure in the combustion chamber, p_C, and that in the propellant tank ullage space (space occupied by gaseous pressurant above the

liquid propellant), p_T, are known and that the propellant mass flow rate into the combustion chamber, $\dot{m}_{prop}$, is given. It is required to find the pump power necessary to deliver the specified propellant flow rate under the given pressurization conditions.

We will perform a "quasi-steady" analysis; *i.e.*, we will use the steady-state formulas we have previously developed, but assume that these are applied only for a time sufficiently short that the main characteristics of the system do not change appreciably—for example, we will need to require that the vehicle and gravitational accelerations, a and g, respectively, remain constant. Likewise, we cannot permit the height of liquid in the tank to change significantly.

With these assumptions in place we can state the two basic equations connecting any two locations in the piping system as

$$\dot{m}_1 = \dot{m}_2\,,$$

and

$$\frac{p_1}{\gamma^*} + \alpha_1 \frac{U_1^2}{2g^*} + z_1 + h_P = \frac{p_2}{\gamma^*} + \alpha_2 \frac{U_2^2}{2g^*} + z_2 + h_L\,,$$

corresponding, respectively, to mass conservation and Bernoulli's equation. There are several things to observe regarding the form given for the Bernoulli equation. First, $\gamma^* = \rho g^*$, where g^* is the net acceleration experienced by the fluid: $g^* = g - a$. Second, we have included a term corresponding to pump head, and this will be the variable to be determined since pump power is directly related to this through Eq. (4.69). Finally, we have introduced a head loss term, h_L, that accounts for both major and minor losses in accordance with Eq. (4.73).

We begin by using conservation of mass to determine the flow speed $U_{T,1}$ in the upper portion of the propellant tank, above the variable-area region with height $h_{prop,2}$. We have

$$\dot{m}_{T,1} = \dot{m}_{prop}\,,$$

with the right-hand side given. Thus

$$\rho U_{T,1} \frac{\pi}{4} D_T^2 = \dot{m}_{prop}\,,$$

and

$$U_{T,1} = \frac{4\dot{m}_{prop}}{\rho \pi D_T^2}\,.$$

We observe that under our quasi-steady assumption, $U_{T,1}$ must be small. Similarly, we can express the flow velocity of propellant in the piping between the propellant tank and the pump as

$$U_{T\text{-}P} = \frac{4\dot{m}_{prop}}{\rho \pi D_{T\text{-}P}^2}\,,$$

and that in the feed line between the pump and the propellant manifold as

$$U_{P\text{-}M} = \frac{4\dot{m}_{prop}}{\rho \pi D_{P\text{-}M}^2}\,.$$

We next write Bernoulli's equation between the surface of the propellant in the tank and immediately upstream of the pump inlet:

$$\frac{p_T}{\gamma^*} + \frac{U_{T,1}^2}{2g^*} + (h_{prop,1} + h_{prop,2} + L_{T\text{-}P}) = \frac{p_P}{\gamma^*} + \frac{U_{T\text{-}P}}{2g^*} + h_L\,.$$

It is of interest to examine the rationale underlying choice of consecutive locations used in this equation. One might ask why we did not first consider flow between the surface of the liquid

propellant and the tank outlet. In fact, one might do that. But since the flow speed must be constant between the tank outlet and pump inlet (via mass conservation), it is more efficient to combine the two piping segments as we have done here. Rather generally, one should attempt to write the energy equation between successive constant-velocity regions.

In writing this expression we have assumed the flow is turbulent throughout (so $\alpha_1 = \alpha_2 \simeq 1$) despite the fact that $U_{T,1}$ must be small. The justification is that D_T is large, and as a consequence we expect

$$Re_T = \frac{\rho U_{T,1} D_T}{\mu}$$

to be greater than 2100. In addition, we are assuming the height of the pump above the injector location (our reference height) is small, so no terms associated with elevation appear in the right-hand side of this equation. Also, effects of the pump are <u>not</u> included in this portion of the calculation, so there is no term corresponding to pump head.

There are at this point two unknown quantities in the above energy equation: p_P, the pressure of the flow entering the pump, and the head loss h_L. All other terms are either part of the specified problem data, or they have already been calculated. We assume we will be able to calculate h_L, so we solve the equation for p_P in terms of the remaining quantities. This yields

$$\frac{p_P}{\gamma^*} = \frac{p_T}{\gamma^*} + \frac{1}{2g^*}\left(U_{T,1}^2 - U_{T\text{-}P}^2\right) + L_{sys} - h_L\,,$$

where

$$L_{sys} \equiv h_{prop,1} + h_{prop,2} + L_{T\text{-}P}\,.$$

We now recall that

$$h_L = h_f + h_m\,,$$

and note that there are two contributions to h_f, and one to h_m. In particular, if we view the propellant tank, itself, as a pipe of length $h_{prop,1}$ this provides one contribution to h_f, and the other comes from the pipe segment of length $L_{T\text{-}P}$ between the tank outlet and the pump. The minor loss contribution comes from the contraction at the bottom of the propellant tank.

We have already calculated the Reynolds number corresponding to flow in the upper part of the tank and assumed that it corresponds to turbulent flow. This implies that a surface roughness will be needed in order to find the friction factor required for the evaluation of h_f. From Table 4.1 we choose ε corresponding to riveted steel as an approximation to the roughness of the inside wall of the tank. Tank diameters for large launch vehicles are easily as large as two to three meters, so we see that even if the maximum value of ε is used, to be conservative, the equivalent dimensionless surface roughness ε_T/D_T will be relatively small, implying a fairly small value for f_T, the friction factor in the propellant tank. In any case, we now have all the data needed to either solve the Colebrook equation (4.54) or read f from the Moody diagram (Fig. 4.18). Thus, we can apply the Darcy–Weisbach formula, Eq. (4.67) to obtain

$$h_{f,T} = f_T \frac{h_{prop,1}}{D_T} \frac{U_{T,1}^2}{2g^*}\,.$$

The second major loss contribution is computed in a completely analogous way. First, the Reynolds number for this case is

$$Re_{T\text{-}P} = \frac{\rho U_{T\text{-}P} D_{T\text{-}P}}{\mu}\,,$$

and we would expect in this case that the pipe would be hydraulically smooth. Thus, the friction factor $f_{T\text{-}P}$ can be read directly from the Moody diagram in the turbulent flow regime, and the head loss is

$$h_{f,T\text{-}P} = f_{T\text{-}P} \frac{L_{T\text{-}P}}{D_{T\text{-}P}} \frac{U_{T\text{-}P}^2}{2g^*} \,.$$

We now calculate the minor loss. This requires a loss coefficient for a contracting pipe that can be read from tables parametrized by the angle θ and the inflow and outflow diameters D_T and $D_{T\text{-}P}$, respectively. This leads to a loss coefficient K_T from which we compute the minor head loss using

$$h_{m,T} = K_T \frac{U_{T,1}^2}{2g^*} \,.$$

Then the total head loss for this segment of the piping system is

$$h_L = h_{f,T} + h_{f,T\text{-}P} + h_{m,T} \,,$$

and we can now directly calculate the pressure at the pump inlet, p_P.

We next analyze the segment of the piping system running from the pump inlet to the manifold inlet. The energy equation for this case is

$$\frac{p_P}{\gamma^*} + \frac{U_{T\text{-}P}^2}{2g^*} + h_P = \frac{p_M}{\gamma^*} + \frac{U_{P\text{-}M}^2}{2g^*} + h_L \,,$$

where, as we noted before, we are assuming that the pump is at essentially the same elevation as the manifold. (This is generally a reasonable assumption for a typical rocket engine.) We have again also assumed turbulent flow so that $\alpha_1 = \alpha_2 \simeq 1$, and we observe that $U_{T\text{-}P}$ and $U_{P\text{-}M}$ are already known. Furthermore, we have already calculated p_P in the preceding step of the analysis, and the head loss term can be obtained as before. Thus, the unknowns are h_P, the required result of our overall analysis, and p_M, the manifold pressure.

As was the case in treating the first two pipe segments, the head loss term is easily calculated; so we will formally solve the above equation for h_P, the desired result, and evaluate h_L. Following this we will determine p_M to complete the analysis.

Thus, we write the above energy equation in the form

$$h_P = \frac{1}{\gamma^*} \left(p_M - p_P \right) + \frac{1}{2g^*} \left(U_{P\text{-}M}^2 - U_{T\text{-}P}^2 \right) + h_L \,.$$

In the current pipe segment there is one contribution to major losses and two minor losses. We will again assume turbulent flow in a hydraulically-smooth pipe. The Reynolds number in the present case is

$$Re_{P\text{-}M} = \frac{\rho U_{P\text{-}M} D_{P\text{-}M}}{\mu} \,,$$

and for a smooth pipe we can immediately read the friction factor from the Moody diagram. We express this as $f_{P\text{-}M}$ and write the major head loss from the Darcy–Weisbach formula as

$$h_{f,P\text{-}M} = f_{P\text{-}M} \frac{L_{P\text{-}M}}{D_{P\text{-}M}} \frac{U_{P\text{-}M}^2}{2g^*} \,.$$

The minor losses in the piping between the pump and the manifold arise from two bends: one of 90° and one of 180°. We denote the loss factors for these (obtained from tables, assuming the

radii of curvature are given) as $K_{P\text{-}M,90}$ and $K_{P\text{-}M,180}$, respectively. Then the combined head loss for this entire segment of pipe is

$$
\begin{aligned}
h_L &= h_f + h_m \\
&= \left(f_{P\text{-}M} \frac{L_{P\text{-}M}}{D_{P\text{-}M}} + K_{P\text{-}M,90} + K_{P\text{-}M,180} \right) \frac{U_{P\text{-}M}^2}{2g^*} \, .
\end{aligned}
$$

We now turn to determination of the manifold pressure p_M, the only remaining unknown needed to completely prescribe the required pump head. We will calculate p_M by writing Bernoulli's equation between the manifold and the combustion chamber. This takes the form

$$
\frac{p_M}{\gamma^*} + \frac{U_{P\text{-}M}^2}{2g^*} = \frac{p_C}{\gamma^*} + \frac{U_{I,2}^2}{2g^*} + h_L \, .
$$

We have again assumed turbulent flow and set $\alpha_1 = \alpha_2 = 1$, and we view the entire manifold as being at the same elevation. We recall that the combustion chamber pressure p_C is given, but we need to find the flow velocity $U_{I,2}$, and the head loss. In the present case we can assume there are no major losses because the injectors are quite short; indeed, we would expect that the flow within them never becomes fully developed. This will be accounted for by assuming the minor losses arise from the sharp-edged entrances to the injectors as depicted in Fig. 4.25.

We begin this part of the analysis by finding $U_{I,2}$ via mass conservation. We assume there are N_I injectors each having a diameter $D_{I,2}$ at the end exiting into the combustion chamber. The total flow rate of all injectors must equal $\dot{m}_{prop}$. Thus, conservation of mass implies

$$
N_I \rho U_{I,2} \frac{\pi}{4} D_{I,2}^2 = \dot{m}_{prop} \, ,
$$

so we find

$$
U_{I,2} = \frac{4 \dot{m}_{prop}}{\rho N_I \pi D_{I,2}^2} \, .
$$

Furthermore, we can find the velocity at the entrance of the injector, again from mass conservation, to be

$$
U_{I,1} = U_{I,2} \left(\frac{D_{I,2}}{D_{I,1}} \right)^2 \, .
$$

We now treat each of these injectors as a rapidly-contracting pipe for which we have an approximate loss coefficient given in Eq. (4.74) as

$$
K_I \approx \frac{1}{2} \left[1 - \left(\frac{D_{I,2}}{D_{I,1}} \right)^2 \right] \, ,
$$

and the corresponding minor head loss is

$$
h_{m,I} = K_I \frac{U_{I,1}^2}{2g^*} \, .
$$

But there are N_I such injectors, so we have

$$
h_L = N_I h_{m,I} = N_I K_I \frac{U_{I,1}^2}{2g^*} \, .
$$

We can now solve the Bernoulli equation for p_M:

$$\frac{p_M}{\gamma^*} = \frac{p_C}{\gamma^*} + \frac{1}{2g^*}\left(U_{I,2}^2 - U_{P\text{-}M}^2\right) + h_L\,.$$

This, in turn, completes the determination of h_P, and from this we can directly calculate the required pump power using

$$\dot{W}_P = \dot{m}_{prop}g^*h_P\,.$$

4.6 Summary

We conclude this chapter by recalling that we have applied the equations of fluid motion, the Navier–Stokes equations derived in Chap. 3, to successively more difficult problems as we have proceeded through the lectures. We began with an essentially trivial derivation of the equation of fluid statics—trivial in the context of the N.–S. equations because by definition (of fluid statics) the velocity is identically zero, and the equations collapse to a very simple form. Nevertheless, the resulting equation has a number of useful applications, including analysis of various pressure measurement devices such as barometers and manometers.

We next employed the N.–S. equations to derive Bernoulli's equation, one of the best-known and widely-used results of elementary fluid dynamics. We applied this in the analysis of the pitot tube used to measure airspeed, and to study flow in a simple gravity-driven fluid transport system.

The next step up in difficulty involved derivation of two classical <u>exact</u> solutions to the N.–S. equations in planar geometry: Couette and plane Poiseiulle flows. Following this we began the study of pipe flow by first considering the basic physics of boundary layers and their association with entrance length and fully-developed flow in a pipe with circular cross section. We then derived an exact solution to the N.–S. equations for this case, the Hagen–Poiseiulle solution. Use of this led to a relationship between pressure changes over a length L of pipe, and a friction factor associated with viscous effects.

Following this we made modifications to Bernoulli's equation to permit its application to pipe flow. Specifically, we noted that this equation is actually an energy equation, and we related pressure losses (termed "head losses") to changes in internal energy resulting from conversion of useful kinetic energy to unusable thermal energy due to entropy production during diffusion of momentum—which is mediated by viscosity. Hence, these head losses were associated with internal friction, and related to a friction factor. Further generalizations of Bernoulli's equation permitted treatment of pumps and turbines and account of turbulence.

Finally, we generalized treatment of head losses arising from internal friction to the case of so-called minor losses allowing empirical analysis of pressure losses in various practical flow devices such as contracting and expanding pipes, tees, bends, *etc.* This permits analysis of quite complex piping systems in an efficient, though only approximate, manner. But it must be emphasized that all of these practical techniques have their roots in the Navier–Stokes equations, once again underscoring the universality of these equations in the context of describing the motion of fluids.